Using Eye Movements to Quantify Human Sensation of Linear Translation: A Potential Test of Changes Induced by Adaptation to Spaceflight

by

Karla Anne Polutchko

BS, Tufts University, College of Engineering, 1991

Submitted to the Department of Aeronautics and Astronautics
in Partial Fulfillment of
the Requirements for the Degree of

MASTER OF SCIENCE

in

AERONAUTICS AND ASTRONAUTICS

at the

MASSACHUSETTS INSTITUTE OF TECHNOLOGY

Cambridge, Massachusetts
June, 1993

Signature of Author _____
Department of Aeronautics and Astronautics
May 7, 1993

Certified by _____
Dr. Daniel M. Merfeld
Thesis Supervisor
Research Scientist and Lecturer

Certified by _____
Dr. Charles M. Oman
Director, Man-Vehicle Laboratory
Senior Research Engineer

Accepted by _____
Professor Harold Y. Wachman
Chairman, Department Graduate Committee

USING EYE MOVEMENTS TO QUANTIFY HUMAN SENSATION OF LINEAR TRANSLATION: A POTENTIAL TEST OF CHANGES INDUCED BY ADAPTATION TO SPACEFLIGHT

by
Karla Anne Polutchko

Submitted to the Department of Aeronautics and Astronautics
in Partial Fulfillment of the Requirements for the
Degree of Master of Science
in Aeronautics and Astronautics

ABSTRACT

Astronauts tested on a linear sled have subjectively reported greater translation postflight than preflight. To develop a test to quantify these findings, experiments were performed to test the ability of subjects to visually track a hidden target while translating. The magnitudes and directions of the eye movement data were used to obtain a threshold level of linear acceleration that humans can detect on earth, to measure differences in perception to directional stimuli, to measure the dependence of eye movement responses on trial duration, and finally to quantify changes following adaptation to a linear motion visual adaptation paradigm.

Two hidden target pursuit experiments were performed: fixed displacement and fixed duration. Each test was run in two subject orientations: upright with acceleration along the inter-aural direction (y-axis) and supine with acceleration along the longitudinal direction (z-axis). Subjects were instructed to visually track an imagined target fixed in space while they were linearly accelerated in "damped position steps" of displacement (single cycles of sine acceleration). Eye movements were recorded using scleral search coils except for the y-axis fixed displacement test, for which electrooculography (EOG) was used. The fixed displacement test (8.82 or 18.20 cm) utilized G-levels between 0.001 and 0.020 G and durations between 1.68 and 9.35 seconds. The fixed duration test (1.0 or 2.5 seconds) used displacements between 5 and 40 cm with G-levels between 0.005 and 0.256 G. Five to eight subjects were tested in each experiment.

Threshold levels for perception of direction of linear translation, determined from eye movement responses, depended on the individual but averaged to approximately 0.003 G in the y-axis and 0.006 G in the z-axis.

Subjects exhibited a significant bias in the magnitude of their eye movements toward headward translation in the z-axis, but did not consistently give similar subjective reports. The asymmetry was in the direction opposite the vertical optokinetic nystagmus (OKN), optokinetic afternystagmus (OKAN), and angular vestibulo-ocular reflex (AVOR) eye movement asymmetries previously shown. In the y-axis, no clear significant directional bias was apparent in the eye movements or subjective responses.

In the fixed displacement experiment, subjects' eye movement and subjective response gains were significantly larger during the 8.82 cm trials than the 18.20 cm trials in both sled orientations. Although a significant correlation existed between eye movements and

head displacement in the y-axis fixed duration experiment, subjects overcompensated for small displacements and undercompensated for larger displacements in both subject orientations, which supports the similar result from the fixed displacement test.

Eye movement and subjective responses were larger for 2.5 second trials than 1.0 second trials during y-axis translation. This indicates a dependence of eye movements and perception of translation upon trial duration. The same result was not significant in the z-axis.

No significant differences emerged between the pre- and post-linear adaptation experiments. Fatigue may have masked some of the adaptation, but more likely, other factors inhibited the adaptation process. Since this experiment was the first attempt to alter visual responses to linear stimulation, the important experimental conditions to needed produce adaptation had not been defined. Therefore, the lack of significant adaptation observed using the current paradigm does not show that linear adaptation is not possible, rather it provides a basis for future research.

These results indicate that the voluntary saccadic eye movements evoked by the hidden target pursuit task can be used to quantify subjective translation. Extension of the hidden target pursuit experiment to quantify changes due to adaptation to micro-gravity may provide further understanding of the effects of spaceflight on sensory neural processing, as well as the role of gravity in perception of body movement.

Thesis Supervisor: Daniel M. Merfeld
Research Scientist and Lecturer

ACKNOWLEDGMENTS

To the people who have made these past two years both challenging and amusing. You've walked with me to the depths of hell and taken me high above the rooftops. Most impressively, you've seen me through the accumulation of this thesis, which I could not have done without any of you.

To Larry Young for bringing me into the Man-Vehicle Laboratory. Somehow I feel like I have missed a part of the MVL experience without you here, but I appreciate the opportunity you provided for me. To Chuck Oman, for picking up where Larry left off and providing guidance with my job search. To Jim, Sherry, Beverly, and Kim, I thank you for your daily support, laughs and nourishment. You've given this place a true sense of family.

To Dan, my friend and my advisor. Congratulations on your first thesis signing. I'm honored to have been the first. Thanks for your trust. Hopefully, I'll see the highlight of this Spacelab experience before I go.

To Jock, Dava and Keoki, three of the best officemates I could have asked for. You each have added something special to my life that I will never forget. Jock, for your sodameister title and my sister's misfortune (just kidding); Dava, for your unbridled enthusiasm in everything you do; and Keoki, for opening my eyes to the art of glass and twisties and for being such an awesome friend throughout. I truly appreciate your companionship, your support, and your goofy ways that have kept me smiling. Thanks.

To Corrie, for strapping me in the sled and feeding me Clinton propaganda. To Juan, for always feeling guilty when I asked you to the Border. To Ted, for threatening Chuck's life if he didn't sign my thesis and move on to yours. I'm convinced that is how I got out of here. To Scott, for actually learning the sled software so you could help me hack through it. To Winfried, for saving us all from LabTech Notebook. To Valerie, for your smiling face (I miss you). To Michele, for starting as a great UROP and progressing into a pretty cool friend. To Ted Carpenter-Smith, for your wacky sense of humor and your unbelievable sense of direction. Good luck to all of you.

Thank you to Laura and Maureen for reminding me of the world outside of MIT (from a five year old's perspective).

To JR. If anyone has been here to experience the brunt of this thesis, it has been you. Thank you for understanding me the past several months, and waiting patiently by my side. I wouldn't have made it without you.

To Mom, Dad, Bob, Diane, Carol, and Dukee. Thank you for your undying love and support. You've let me be the "baby" when I needed to, but have inspired me to be the person that I am. I am the luckiest person in the world to have a family as wonderful as you.

This research was supported by NASA grant NAG2-445.

CONTENTS

FIGURES

TABLES

1. INTRODUCTION

The human body receives redundant information from several sensory mechanisms including the visual, auditory, tactile, proprioceptive, and vestibular systems. The interaction of the sensory cues from these mechanisms contributes to a person's control of balance and posture, spatial orientation, gaze stabilization, and motion perception. This experiment is primarily concerned with the perception of linear motion as measured by the otolith organs, which are the portion of the vestibular system stimulated by gravity and linear acceleration. On earth, gravity pulls on the otoliths, causing the brain to constantly appraise the position of the head and body with respect to gravity. This contributes to a person's ability to decide whether she is tilting to the left or to the right. The visual system also provides such cues from a person's environment that interact with and complement the other sensory systems, providing a comprehensive "view" of the surrounding environment and the position of the human body in it. This sensory interaction is evident in the eye movements that compensate for motions of the body in an attempt to stabilize the visual environment on the retina (Baloh et al, 1988; Buizza et al, 1979; Israel et al, 1989; Oman, 1982). Without such sensory interactions, a person walking down the street would perceive her visual surroundings as bouncing up and down.

A problem arises when the various sensory inputs conflict with each other, as occurs in microgravity. The visual system sends normal signals to the brain, while the vestibular system, which is accustomed to sensing gravity in one-G, sends a signal that does not complement the visual signal. The brain does not know which sensory input to believe or respond to, the visual stimuli or the vestibular stimuli, and for a time will try to follow both. This conflict of sensory inputs has been proposed to contribute to the onset of space motion sickness, and thus has instigated a myriad of interesting questions for

research in sensory processing in microgravity. (Oman, 1982) After several days of spaceflight, the human body shows signs of adaptation produced by some reorganization of the central nervous system's processing of sensory information. As it will be used throughout this thesis, an clear definition of adaptation is necessary. Robert Welch appropriately describes adaptation as "a semipermanent change of perception or perceptual-motor coordination that serves to reduce or eliminate a registered discrepancy between or within sensory modalities or the errors in behavior induced by this discrepancy." (Welch, 1978) In microgravity, a discrepancy exists between the sensory information from the visual and vestibular systems, and the central nervous system reorganizes to interpret this discrepancy, leading to changes in a person's control of balance and posture, spatial orientation, gaze stabilization, and motion perception.

The focus of the current study is to further develop our understanding of the processing of linear acceleration stimuli as it contributes to the perception of linear translation. Many astronauts on return to earth subjectively report translation greater than reported during preflight base-line data collections. One crew member even reported translation postflight larger than that allowed by the test apparatus. The present experiments were designed to develop a test to study these reports quantitatively, in the hope that it will be used as a preflight/postflight test for future shuttle missions.

"For the most part, everyday perception is fully developed, very accurate, and served by a redundancy of cues. Consequently, in order to increase our understanding of this capacity it has become a common strategy to interfere with its operation." (Welch, 1978) To interfere with the normal operation of motion perception, a one-G linear adaptation experiment is used to test whether humans are capable of short term adaptation due to a sensory conflict between the visual and otolith portion of the vestibular system. The sensory conflict is produced by changing the "normal" relationship between head

movement and movement of the visual scenery. To date, no experiments have been performed testing short term, nor long term adaptation, using linear acceleration. Numerous studies with humans and animals have been performed using rotational stimulation and altered visual stimulation to produce a sensory conflict between the visual and vestibular systems. (Baker, et al., 1986; Demer, et al., 1989; Gonshor and Melvill Jones, 1976; Harrison, et al., 1986; Lisberger, 1988; Miles and Eighmy, 1990; Shelhamer, et al., 1992; Snyder and King, 1988) Likewise, several spaceflight experiments have shown changes in response after long term adaptation to microgravity in both humans and animals. (Arrott, et al., 1986; Cohen, et al., 1992; Correia, et al., 1992; Kozlovskaya, et al., 1984; Oman, 1982; Oman, et al., 1988; Young, 1982; Young, et al., 1966; Young, et al., 1986) In microgravity, there is no gravity force stimulating the otolithic membranes to indicate bodily orientation as in the one-G environment of earth, but the visual system is functioning normally. Although there is some evidence to the contrary, the semicircular canals are generally unaffected by weightlessness, as it is the otoliths that sense the gravitational force. This means that at least some of the adaptation that occurs in spaceflight occurs in the pathways leading from the otolith organs. The adaptation portion of this experiment, therefore, is an attempt to repeat the type of adaptation protocols used for the short term angular adaptation studies, but using linear stimulation to develop a deeper understanding of the adaptation that occurs during spaceflight.

1.1. Motivation

The experiments described in the following pages were performed to develop a test to quantify a person's perception of linear translation using voluntary saccadic eye movements. Once this goal is achieved, the magnitude and direction data can be used to obtain a threshold level of linear acceleration that a human can detect on earth, to measure differences in perception to directional stimuli, to measure the dependence of

perception following adaptation to spaceflight or other sensory conflicts established in one-G.

1.2. Thesis Organization

Chapter two gives an introduction to the issues and problems in question, including a discussion of the physiology of the end organs under study and the related research that motivated this research. Chapter three gives a description of the test apparatus, the experimental protocols, and the data analysis techniques used in the current experiments. Chapter four provides a detailed description of the results of the experiments and some discussion of their implications. Chapter five draws conclusions from the results where possible and gives ideas for future exploration.

Since the experiments described in this thesis were performed in two different subject orientations (Y-axis and Z-axis) that will be referred to throughout, the terminology used to define the coordinate system (X, Y, and Z-axes) is summarized here. Y-axis motion of the subject refers to inter-aural (rightward/leftward) acceleration, Z-axis motion refers to rostro-caudal (headward/footward) acceleration, and X-axis motion of the subject refers to occipito-nasal (front/back) acceleration. In the Y-axis experiments performed in this thesis, subjects were seated with their head upright (erect), whereas the Z-axis experiments were performed with the subject supine. All accelerations were performed along the earth-horizontal axis.

As stated above, the purpose of these experiments was to develop a test to quantify a person's perception of translation so that changes in that perception following spaceflight can be detected. Therefore, several experiments were performed to establish that these tests can quantify the perception of translation using voluntary saccadic eye movements. Once the tests were developed, a subsequent experiment was performed "using" the tests

Once the tests were developed, a subsequent experiment was performed "using" the tests to detect changes in perception following an earth based linear adaptation paradigm. To maintain proper organization, where appropriate, chapters of this thesis will be divided into two sections: *Hidden Target Pursuit* describing the initial experiments and *Linear Adaptation* describing the adaptation experiment that applies the Hidden Target Pursuit Tests.

2. BACKGROUND

2.1. Anatomy and Physiology

The human systems relevant to the perception of bodily motion are primarily the visual, vestibular, and auditory systems, and to a limited extent, the proprioceptive and somatosensory systems. In the experiments described in this thesis, which quantify human perception of linear translation, significant steps were taken (discussed in METHODS) to isolate the vestibular system, by minimizing if not eliminating stimulation of the other systems. With no auditory or visual cues indicating motion, no head rotation, and no differential movement of parts of the body, detection of linear motion is primarily dependent upon the sensitivity of the otoliths to linear acceleration stimuli and the sensitivity of the somatosensory system to pressure changes on the body surface, which are minimal at low stimulus frequencies. Therefore, the primary end organs described here will be those contained in the inner ear, or labyrinth, including the semicircular canals and the otolith organs. (Figure 2.1.)

2.1.1. Semicircular Canals

Humans have three orthogonal semicircular canals (SCC) in each vestibule that are filled with a viscous fluid called endolymph. When the head rotates in any direction, the inertia of the endolymph in one or more of the semicircular ducts causes the fluid to remain stationary while the ducts themselves rotate. This causes relative fluid flow in the ducts in the direction opposite to the rotation of the head. The fluid bends the cupula, a gelatinous mass obstructing the fluid flow in each canal. Hundreds of sensory hair cells located beneath the cupula in the crista are stimulated by the cupula deformation. As a result of the near orthogonality of the three canals, the system is capable of sensing and transducing angular acceleration about every axis in space. The semicircular canals

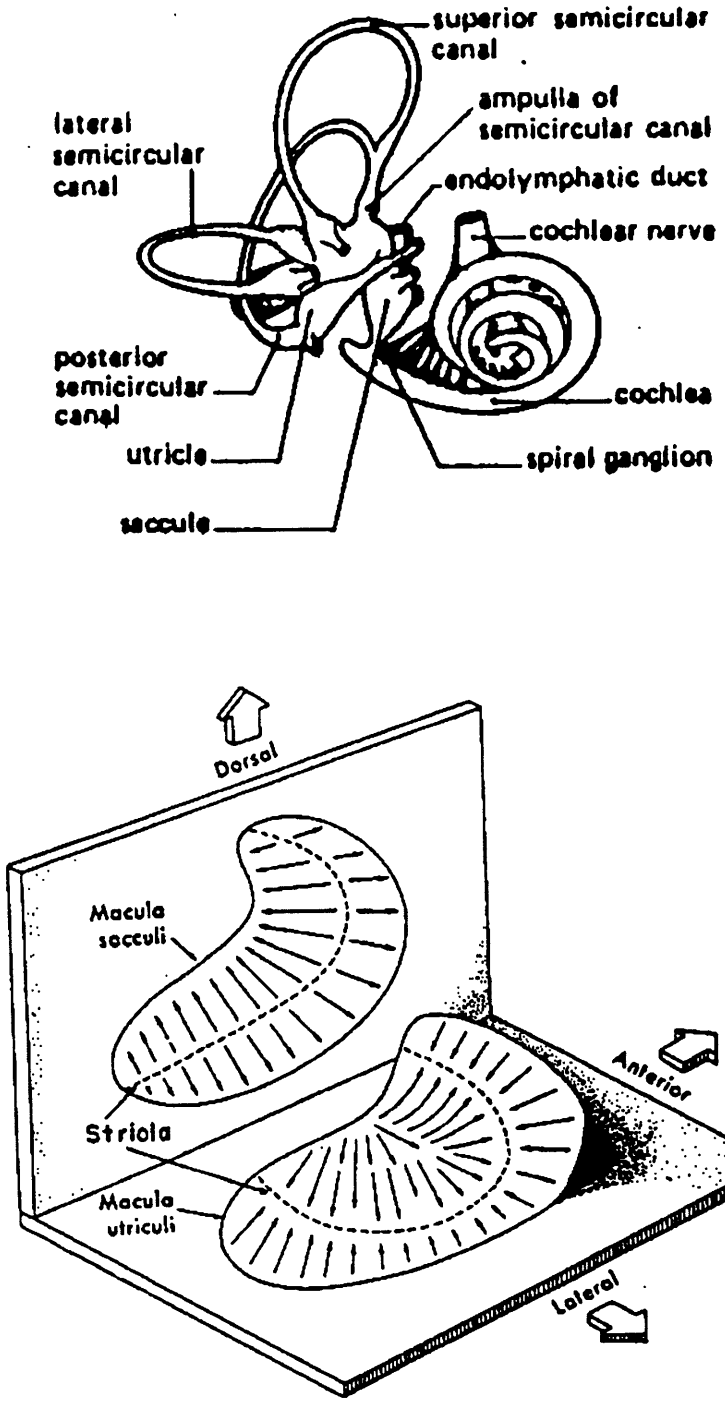

Figure 2.1. Schematic drawings of the human vestibular system. Orientation of the utricular and saccular otoliths.

(SCC) respond to rotational acceleration stimuli with a damped exponential response, meaning that their output more accurately indicates angular velocity than angular acceleration for most frequencies of natural head movements. The time constant of the cupula itself is not known, but the firing rates of the primary afferents (nerve cells) carrying this information have an exponential decay response with a time constant of approximately five to six seconds in squirrel monkeys. Therefore, during prolonged rotation the sensation of rotation decays as the cupula returns to its normal position (Benson, 1982; Wilson and Melvill Jones, 1979).

2.1.2. Otolith Organs

Although the semicircular canals are highly effective in sensing angular accelerations, they are relatively insensitive to orientation of the head with respect to gravity (Young, 1982). Therefore, the sensing of linear acceleration and gravity is performed by two other specialized organs, the utricular and the saccular otoliths. The otoliths are the principal non-visual determinants of static orientation with respect to the vertical. They act in conjunction with the vertical semicircular canals to signal changes in orientation with respect to gravity and initiate corrective postural responses. Each otolith organ is formed by a specialized region of the inside wall of the membranous labyrinth, and is made up of several thousand mechanoreceptive hair cells, covered by a layer of calcite crystals (otoconia). The utricular otolith is located on the floor of the utricular sac tilted approximately 20° up from the horizontal, and the saccular otolith is located mainly in a vertical plane. The arrangement of the otoliths is not symmetric with respect to the X- and Z-axes, but is relatively symmetric along the Y-axis. Fernandez et al. (1972) determined through the direction specificity of hair cell orientation and the separate recordings of primary afferent neurons from saccular and utricular maculae of monkeys that head erect horizontal and vertical movements with respect to gravity predominantly stimulate the utricular and saccular end organs respectively. The saccular otolith is also

important for sensing motion when a person is accelerated while in the supine position (head tilted 90° from head erect).

The stimulus for the otolith receptor cells is a displacement of the sensory hairs, or cilia, caused by movements of the otoconial mass under the influence of the shear-directed force of gravity or linear accelerations. The input to the otoliths is equal to the vector sum of gravity (g) minus linear acceleration (a), as shown in Figure 2.2 below. Therefore, the gravitoinertial force is rotated in the direction of motion through the arctan of a/g and its magnitude is increased to $(a^2 + g^2)^{1/2}$ during one-G horizontal linear motion and during head tilt. Along a vertical track, the magnitude of force is changed to (g + a) or (g - a) for downward or upward motions respectively. The otolith responses, and therefore the eye movements driven by them, cannot distinguish between the inertial force to due acceleration and the force of gravity. This ambiguity in the use of otolith information for static orientation, i.e., distinguishing between linear acceleration and head tilt with respect to gravity, is normally solved by interpreting the otolith signals based on other sensory information (Young, 1982).

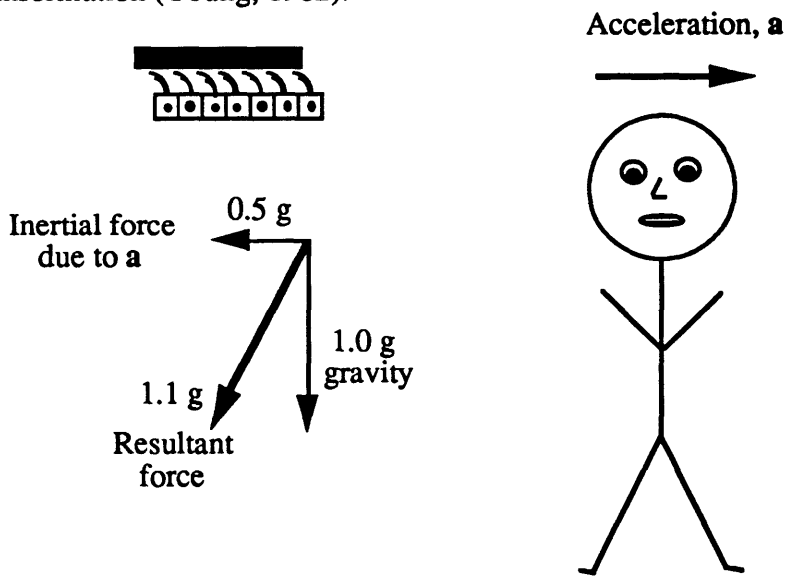

Figure 2.2. Representation of the vector sum of the gravity and linear acceleration vectors which constitute the input to the otoliths.

At low frequencies a substantial phase lead exists in the perception of linear translation, while as the frequency increases the phase lag between the stimulus velocity and the perceived velocity also increases (Young, 1982). This low frequency phase lead and high frequency phase lag are consistent with a transfer function relating the perception of linear velocity to the actual horizontal linear velocity given by:

$$\frac{V_{Perceived}}{V_{Actual}} = \frac{1.5(s+0.076)}{(s+0.19)(s+1.5)}$$

The only direct measurements of otolith displacements during oscillation, taken by deVries in the fish, indicate an extremely fast reacting system with dominant time constants of the order of 0.005 seconds (Young, 1983). Direct recording of first order afferent units from utricular and saccular maculae showed substantial sensitivity up to at least 2.0 Hz (Young, 1982). From their experimental data, Mah et al. (1989) believe that the perceptual bandwidth is greater than 3.0 Hz (the bandwidth of their study). For brief periods of linear acceleration lasting less than five seconds, the effective time to detect the acceleration decreases with increasing acceleration level. Changes in linear velocity less than approximately 22 cm/s are likely to go undetected in the horizontal plane, as will be discussed further in relation to the threshold tests performed by previous experimenters.

2.1.3. Eye Movements

Nystagmus, alternating fast and slow eye movements, can be caused by rotation or linear translation of the subject or movement of the subject's visual field. The compensatory slow phases move the eyes in the same direction as the relative visual field movement, while the fast phases, or saccades, reset the eyes in the opposite direction. During rotation in the dark, the vestibular nystagmus and the sensation of rotation decay with a

similar long time constant as the vestibular nucleus (VN) firing rate, approximately 12 seconds (Henn, et al., 1980). If such a constant velocity rotation is maintained in the dark for a minimum of approximately thirty seconds, the deceleration while stopping will stimulate the SCCs much like an acceleration in the opposite direction. The response, therefore, will be similar to the one when rotation began but in the opposite direction.

Optokinetic nystagmus (OKN) is the nystagmus produced when the peripheral visual field rotates around the subject's head without vestibular stimulation. OKN has an initial rapid rise in slow phase velocity (SPV) and then a slow rise to maximum velocity close to the speed of the visual field (Henn, et al., 1980). The initial rapid rise is presumably due to a direct optokinetic pathway from the visual parts of the brain to the oculomotor nuclei. Thus, the visual information is combined with the vestibular information at a very early stage in the brain. Interestingly, the slow OKN rise and vestibular nystagmus decay time constants are approximately the same when the head is rotated with a velocity step (Henn, et al., 1980). Therefore, the combined effect during rotation in the light is that the vestibular nuclei units in question accurately reflect that the subject is continuously rotating.

Linear VOR, an eye movement response evoked by linear motion, is poorly characterized, and the results from experimental studies of the LVOR are weak and variable. However, it is needed for stability during natural behavior which includes frequencies of motion between 0.5 and 5.0 Hz. A slightly more robust response is seen at stimuli greater than 1.0 Hz, a range that exceeds the operating limits of the visual following mechanism (Paige and Tomko, 1991). Regarding the utility of having similar otolith responses for two different types of head movements, Paige and Tomko (1991) proposed that the otoliths are able to distinguish between linear acceleration and head tilt by a central mechanism that segregates the LVOR into two frequency selective processes:

low frequency stimulation associated with head tilt and derived from a low pass filtered otolith input, and high frequency stimulation associated with head translation and derived from a high pass filtered otolith input. This hypothesis, however, implies that the central processing of the otolith signals is different from that in canal driven angular VOR (AVOR) pathways.

2.1.4. Pathways

Semicircular canal and otolith organ afference travel within the 8th cranial nerve to relay neurons in the brain stem and cerebellum, where it combines with other sensory neural inputs. Lisberger (1988) suggested the following overview of the Vestibulo-ocular Reflex (VOR), which has been identified anatomically with the semicircular canals and is believed to be true, but not identified, for the otoliths. (Figure 2.3) VOR pathways in the brain stem and cerebellum transform the amplitude and dynamics of the input to provide commands for motor output. Image motion (retinal slip) results if the transformations are wrong. Retinal slip is the speed with which a pattern moves over the retina, which equals the difference between pattern velocity and eye velocity in space. Image motion is fed back for immediate visual guidance of eye movement and for motor learning to slowly recalibrate the VOR pathways. The Vestibulo-ocular Reflex (VOR) helps stabilize visual images on the retina by generating eye movements that counteract, or compensate for head movements. These slow compensatory eye movements alternate with rapid reset movements yielding a saw-tooth position profile called nystagmus. The following diagram summarizes this process.

The vestibular nucleus (VN), located in the brain stem, is a dense area of nerve cells that receives the primary afferents, processes the information and, along with other targets, sends it to the oculomotor nuclei. The visual system also transmits important

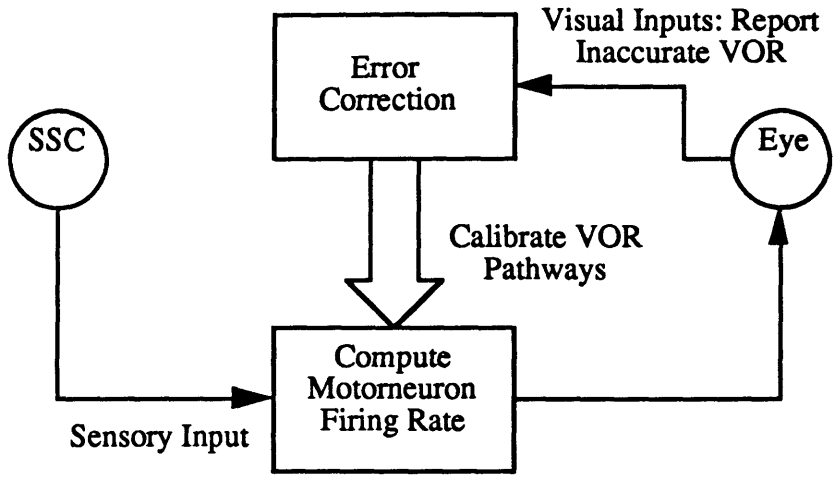

Figure 2.3. Overview of vestibulo-ocular pathways from the semicircular canals. (Lisberger, 1988)

information, sensed primarily in the peripheral visual field, to the vestibular nucleus (VN). The oculomotor nuclei are also located in the brain stem and send the efferent signals to the oculomotor muscles that move the eyes. The firing rates of these efferents signals have an exponential decay response. The time constant of the decay in the vestibular nucleus is longer than the time constant of the primary afferents traveling from the semicircular canals -- approximately twelve seconds versus five seconds. Since the neurons in the vestibular nucleus have a prolonged firing rate relative to the afferents, this increase in time constant is sometimes referred to as "velocity storage."

The slow phase of linear nystagmus is produced primarily by direct stimulation of the otolith maculae and is organized through a linear Vestibulo-ocular Reflex (VOR) similar to that of the angular VOR pathways (Buizza, et al., 1981). The model of the linear VOR shown in Figure 2.3 was derived from the classical models of the angular VOR by changing only the dynamics of the input mechanical receptor. According to some theoretical and experimental results reported in the literature (reviewed by Buizza, et al. 1981) the time constant of the leaky integrator (T_I) in darkness is larger than 10 seconds

and the otolith dynamics can be described in a simplified form by a first order transfer function with a time constant, T_O:

$$\frac{\Theta_E}{Y} = \frac{-K_o K_E T_I s^2}{(1+sT_o)(1+sT_I)} = \frac{-K_o K_E s}{(1+sT_o)}$$

where K_F (gain of the Medial Longitudinal Fasciculus pathway) = 0.2, T_I (time constant of leaky integrator) = $1/K_L \geq 10$ seconds, T_E = 0.2 seconds, T_O (time constant of otolith periphery) = 0.25 seconds, and $K_O K_E \approx 2$ deg/m. These values are provided for completeness and will not be discussed further. Further description of their origin and their significance can be found in Buizza, et al. (1981).

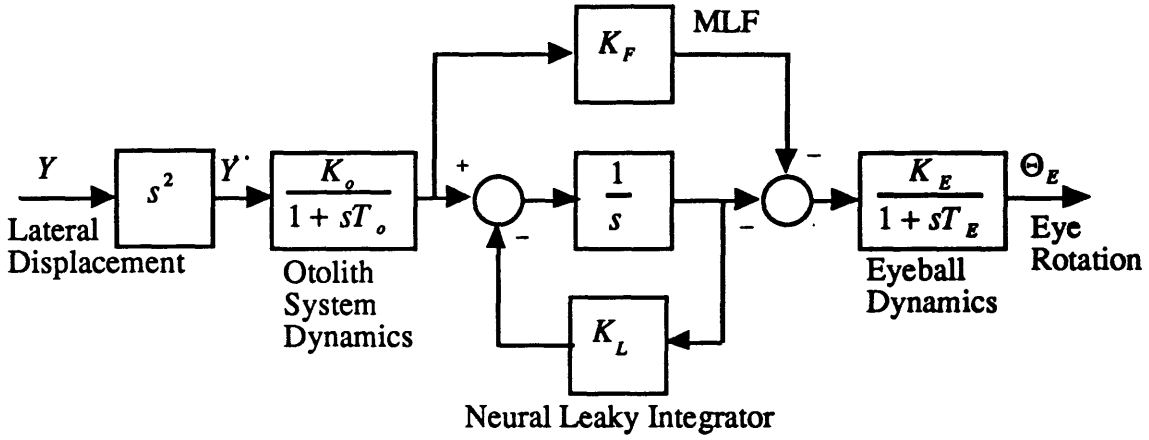

Figure 2.3. Model of Linear Vestibular-ocular Reflex (LVOR) from Buizza, et al. (1981).

Some of the same neurons in the vestibular nucleus (VN) that respond to SCC stimulation also respond to motion of the peripheral visual field in the opposite direction (Henn, et al., 1980). For example, if head rotation to the right excites a neuron in the vestibular nucleus (VN), then peripheral visual field rotation to the left will also excite that neuron. These two processes are complementary, since in the light head rotation to the right would produce a relative motion of the visual field to the left.

2.1.5. Eye Movement Asymmetries

Several experiments have been performed to study the dynamics of vertical nystagmus, in particular, in both humans and animals (Baloh, et al., 1983; Matsuo and Cohen, 1984; Böhmer and Baloh, 1991). The dynamics of horizontal and vertical slow eye movements were studied during vestibular stimulation, pursuit tasks, optokinetic stimulation, and visual-vestibular interaction while subjects were oriented either upright (head erect) or with their head tilted 90° (right and left) and rotated in the yaw axis (Baloh, et al., 1983). The following asymmetries in the dynamics of vertical eye movements were discovered: 1) the mean time constant of the post-rotatory nystagmus (PRN) with upward slow phases was consistently longer than the mean time constant of the PRN with downward slow phases; 2) vertical optokinetic afternystagmus (OKAN) --nystagmus in the opposite direction of the OKN following cessation of the optokinetic stimuli-- only occurred when the optokinetic stimulus moved upward; 3) upward pursuit was better than downward pursuit; and 4) upward slow phases of vestibular nystagmus were poorly inhibited with fixation while downward slow phases were normally inhibited (Baloh, et al., 1983).

Vertical optokinetic nystagmus (OKN) was found to be asymmetrical in the monkey when induced with the animals lying on their sides in a 90° roll position (Matsuo and Cohen, 1984). Downward OKN (slow phases up) increased proportionally with stimulus velocity at close to unity gain to about 60°/s, while upward OKN (slow phases down) increased to only about 40°/s. In addition, upward and downward optokinetic afternystagmus (OKAN) were asymmetrical. Upward OKAN was weak or absent, while downward OKAN was stronger, implying that the stored activity related to the slow phase velocity contributes little to the production of upward OKN. Furthermore, there was no slow rise to steady state in the slow phase velocity during upward OKN, rather it rose to its peak velocity at the onset of the stimulus. The lack of stored information may

be responsible for the differences in regularity, gain, and frequency between the upward and downward OKN. During vertical vestibular nystagmus, the velocity of the monkeys' initial upward and downward slow phases was approximately symmetric, but the vertical VOR was asymmetric. The downward nystagmus had a higher frequency and lasted longer than the upward nystagmus. The time constant of the upward nystagmus was approximately 8 seconds, while that of the downward nystagmus was approximately 15 seconds (similar to horizontal). As with the optokinetic nystagmus, the stored activity related to the slow phase velocity makes a smaller contribution to upward than downward or horizontal nystagmus (Baloh, et al., 1983).

More recent experiments have studied vertical optokinetic nystagmus (OKN) and optokinetic afternystagmus (OKAN) while subjects were oriented in both the head erect and the lateral side position to evaluate the up-down asymmetry of these responses (Böhmer and Baloh, 1991). Contrary to many of the previous experiments, no consistent up-down asymmetry was found in the vertical OKN, but the OKAN was asymmetric (up slow phase velocity > down slow phase velocity). Thus, asymmetries in human vertical optokinetic nystagmus are inconsistent, with a tendency toward higher gain with slow phase up than slow phase down. Regarding OKAN, the data suggest that vertical OKAN in humans can be described as the discharge of two oppositely directed storage mechanisms: one with a shorter time constant in the direction of the prior OKN, and the other with a longer time constant in the reverse direction. An upward optokinetic stimulus results in greater velocity storage in the first system than in the second so that the OKAN is in the direction of the optokinetic stimulus, while downward optokinetic stimuli activate the second system more than the first, resulting in reversed OKAN (Böhmer and Baloh, 1991).

2.2. Threshold Experiments

Otolith function is more difficult to assess than semicircular canal function because stimulation of the maculae does not elicit well defined and easily recorded nystagmus. One approach for studying otolith processing is through perceptual techniques such as the threshold for detection. The linear motion detection system has an effective detection threshold of approximately 0.005 G, although it can be described as a signal-in-noise detection process (Mah, et al., 1989). The signal must be great enough to produce a noticeable difference above the biological noise in the system. Experimental artifacts (noise) such as acoustic noise, distraction, fatigue, number of stimulus cycles, and the test procedure can significantly affect the determination of threshold. Gundry (1976) demonstrated that perceptual thresholds were raised by approximately forty percent in roll vection when subjects were distracted by a task such as mental arithmetic or vehicle steering.

Four general types of otolith stimuli have been used to study thresholds: 1) controlled translation oscillations relative to a given axis of the head, 2) 'sustained' (duration limited by 32 foot track) linear acceleration relative to some axis of the head on an earth-horizontal or vertical linear track, 3) sustained linear acceleration relative to some axis of the head produced by a centrifuge, 4) sustained gravitational force relative to some axis of the head produced by a tilt device (Guedry, 1974). Although often used, oscillatory motion is not the optimal procedure for determining threshold because only the threshold of motion detection can be accurately determined, not the threshold for direction detection. 'Sustained' linear acceleration provides the least contaminated procedure for measuring thresholds for linear acceleration because it contains no rotary stimuli. However, a constant stimulus value can be maintained for only short durations as the velocity of the signal becomes too large. Since the threshold experiments in the current

study are performed on a linear accelerator, stimulus modes 1) and 2) from above are most relevant and will be reviewed here.

Table 2.1, copied from Benson, et al. (1986), summarizes the data from previous experiments on thresholds for detection of linear motion in the horizontal plane acting in the X, Y and Z-axes of the head. The thresholds are stated as the maximal acceleration of the stimuli producing the response and range from 0.018 m/s^2 (0.002 G) on a parallel swing in the X-axis to 0.154 m/s^2 (0.0157 G) during single cycles of sine acceleration in the Z-axis.

Table 2.1. Summary of data on threshold for detection of low frequency linear motion stimuli in the horizontal plane acting in the X, Y, and Z axes of the head. (Benson, et al., 1986)

		Threshold (m/s^2)				
Stimulus	freq. (Hz)	X	Y	Z	N	Source
Parallel Swing	0.4	0.018	0.019	0.021	?	Walsh (1961)
	0.4	-	0.038	0.053	6	Walsh (1961)
	0.29	0.045	0.035	0.053	12	Greven et al. (1974)
Continuous Oscillation	0.3	0.025	0.032	0.070	6	Benson et al. (1984)
Step Acceleration	-	0.059	-	0.098	3	Meiry (1965)
Single Acceleration Sinusoid	0.3	0.063	0.057	0.154	24	Benson et al. (1986)

Walsh (1961) performed an experiment to isolate the primary receptors involved in the detection of linear acceleration (reviewed by Gundry, 1978). Subjects without otolith function had thresholds of detection of linear oscillation between 0.016 and 0.023 G, which are significantly higher than for subjects with full otolith function. As a comparison, subjects without somatic sensation (with high spinal cord injuries) were studied and found to have thresholds between 0.0035 and 0.008 G, which are very similar to the normal population. These results suggest that the otoliths are the primary receptors

involved in detection of linear acceleration at the test frequency, 0.4 Hz. It is unknown whether at higher frequencies the somatic sensation has more of an influence.

Using a 32 foot long horizontal track, Meiry (1965) imposed different magnitude accelerations to determine how long accelerations must be sustained to yield 75% correct detection judgments. Thresholds of 10 cm/sec^2 for acceleration along the Z-axis and 6 cm/sec^2 for Y-axis acceleration were determined using latency times. Theoretically, response latency is the time required for a given magnitude stimulus to produce threshold deflections of the otoliths. He inferred that the difference in threshold is due to the angle of imposed acceleration relative to the average utricular shear plane (Meiry, 1965).

A similar experiment using vertical accelerations ranging from 0.005 to 0.06 G was performed to test for thresholds of detection of acceleration along the subject's z-axis with the head erect (Melvill Jones and Young, 1978). Subjects were instructed to indicate their direction of acceleration, and the latency of the subjects' response was measured. To avoid any jerk at the start of the acceleration, the accelerations were presented at a random time interval after the cabin was moving at 0.61 m/s. Detection of the stimulus was determined by attainment of a given velocity (21.6 ±2.65 cm/sec) rather than the magnitude of the acceleration. Thus, if detection is attributable to the otoliths, then the neural processes must act as integrating accelerometers, similar to the semicircular canals, for short-duration stimuli (Melvill Jones and Young, 1978).

The time-to-detect varied inversely with the size of the step of acceleration, allowing a velocity constant to be calculated for each subject using the following relation:

$$V = A \times TTD$$

where **A** = acceleration and **TTD** = time-to-detect. Re-analysis of previous data with inter-aural (Y-axis) acceleration with the head erect and supine elicited the same

relationship, with velocity constants equal to 22.6 ±1.28 cm/sec and 32.4 ±1.96 cm/sec, respectively. As mentioned in the discussion of anatomy and physiology of the vestibular system, Fernandez et al. (1972) determined that with the head erect, horizontal and vertical movements predominantly stimulate the utricular and saccular end organs respectively. The striking similarities between the different experimental data indicate that the thresholds of predominantly utricular (horizontal acceleration) stimulation and saccular (vertical acceleration) stimulation with the head erect were similar. With the head supine, the saccular threshold is approximately 1.5 times greater. Fernandez and Goldberg (1976) also discovered that saccular-dependent vestibular primary afferents responding to +Z (upwards re head) and -Z force vectors have similar steady state discharges when the head is erect, but the same population has significantly different values when supine. Melvill Jones and Young interpreted this finding in support of their own conclusions regarding the lower sensitivity when the body's Z-axis was horizontal. If the differential firing rate between +Z and -Z constitutes the meaningful signal, a change of that signal caused by an acceleration would constitute a smaller portion of the static differential signal with the Z-axis horizontal than vertical. According to Weber's Principle, the threshold would be associated with a larger stimulus when the Z-axis was horizontal (Melvill Jones and Young, 1978).

The design of the experiment discussed above using earth vertical accelerations along the subjects' z-axis permitted investigation of effects due to practice, up-going versus down-going accelerations, and increasing versus decreasing levels of vibration. Although actual data comparing these effects is not presented in their paper, it is important to note that an absence of any asymmetry was reported between upward and downward trials during Z-axis accelerations when the head was erect. Likewise, neither practice nor the direction of the vibration level produced statistically significant effects either (Melvill Jones and Young, 1978).

There is some question whether the axis of the imposed linear motion affects the threshold for detection. During linear experiments performed in the vertical axis with respect to the earth, the resultant acceleration vector is only a change in magnitude (acceleration + gravity), whereas in the horizontal axis the stimulus produces a change in the magnitude and direction of the resultant vector. Contrarily, Guedry (1974) argued that the magnitude of the imposed acceleration, rather than the magnitude of the resultant, is relevant to determination of the threshold, implying that for both horizontal and vertical accelerations the threshold can be described by the magnitude of linear acceleration applied to the subject. If this argument were true, any bias due to the gravitational force would be rejected. In comparing the axis of motion with respect to the subject, not with respect to the earth, Z-axis thresholds and response latencies have been reported to be slightly higher than for the X- or Y-axes. (Gundry, 1978)

Another threshold experiment was performed on a linear accelerator in the X-axis using a cosine acceleration wave (Mah, et al., 1989). The subjects were instructed to signal when they perceived the acceleration. A 21 second delay between each trial was used for the subject to report her confidence level and for the experimenters to give feedback for motivational purposes. The stimulus frequencies ranged from 0.2 to 3.0 Hz. A two interval forced choice method was used to determine each subject's threshold. The results indicate that the perceptual process is dominated by an integrative mechanism at frequencies greater than 0.5 Hz, and potentially at lower frequencies. When comparing the thresholds at different stimulus frequencies, a higher sensitivity (lower threshold) was observed at 1.0 Hz. Otherwise, thresholds were similar across frequency levels. This indicates that the thresholds do not exhibit a large sensitivity to the rate of change of acceleration (jerk).

Comparing thresholds of different subject orientations, subjects tend to have a higher threshold in the Z-axis (supine) than in the X- or Y-axes (upright) (Benson, 1984). The higher Z-axis thresholds may exist because in everyday life the acceleration of gravity acts in the plane of the saccular otoliths and the dominant head accelerations that accompany locomotion activities are in the Z-axis. The CNS, therefore, may employ a lower 'gain' in relaying saccular information than afference from the utricular maculae. Neurophysiological evidence supports a higher Z-axis threshold, since the sensitivity of neurons signaling the X- and Y-axes acceleration is approximately 30% greater than those responding to Z-axis acceleration (Benson, 1984).

2.3. Target Pursuit

Several experimenters have studied the human's perception of linear acceleration. The experiments most directly related to the present research were performed by Israël and Berthoz (1989). Due to their relevance to the current experiments, they will be discussed first and the experiments prior to them will be discussed subsequently.

Subjects were linearly accelerated using "damped position steps" and "sine wave" trajectories while being instructed to fixate on the location of a memorized or imaginary target (Israël and Berthoz, 1989). During sinusoidal and step-like motion, a combination of smooth compensatory eye movements and compensatory saccades allowed the subjects to track the memorized target. The mean "vestibular-saccadic" (VS) gain during sinusoidal motion, which was defined as the ratio of overall eye movement peak-peak versus head displacement, was 1.52 +/- 0.80, showing an overestimation of head displacement. During step-like head displacements in darkness, similar to the current study, the Linear VOR mean gain values, defined as the ratio of slow phase cumulated peak-to-peak amplitude versus head displacement amplitude, were very small. Subjects, therefore, depended primarily on saccades to track the target. However, they were still

able to stabilize their gaze with a mean VS gain of 1.01 +/- 0.70. The evidence supports that an approximate estimation of head displacement can be derived from the linear acceleration measured by the otoliths. However, since the gain of the linear VOR is by itself extremely small regardless of the memorized or imagined target distance from the head, the information for the estimation is also fed into the saccadic system. Therefore, as proposed previously by Buizza et al. (1979), adequate control of eye movements during linear acceleration is the result of a cooperation of the linear VOR together with other oculomotor subsystems.

A similar step-like experiment was performed to test for a person's ability to memorize her estimation of displacement after a variable delay time (Israël and Berthoz, 1989). Rather than tracking the target during the sled motion, the subject was instructed to make a saccade back to the target once the sled had stopped. The varying time delay (between 5 and 50 seconds) between the end of the sled motion and the instant the subject was to make the saccade had no significant effect on the subjects' performance. In addition, no significant difference was found between the two step-like paradigms in the subjects' ability to calculate the target position.

The two experiments discussed above were preceded by several experiments that examined the otolithic contribution to eye movements using a similar paradigm but with acoustic targets (Buizza, et al., 1979). Relative motion between the target and subject was produced by either oscillating a target in front of a stationary subject or by sinusoidally oscillating the subject with the target fixed in space. Subjects were asked to track the acoustic target during the relative target movement. Tracking of an imagined or acoustic target in the absence of other sensory inputs was accomplished mainly by saccades. If the relative motion of the target took place during subject acceleration in the frontal plane, the subject would track the target using smooth eye movements. Whether

this effect is due to better performances of a central reconstruction of target velocity in the presence of otolithic information or to an increase of LVOR gain produced by the presence of a real or imaginary target is still an open question.

According to the perceptual feedback hypothesis (Yasui, 1973; Young, 1977), smooth pursuit (SP) eye movements are produced whenever the CNS has enough sensory information for a velocity reference signal to be reconstructed centrally. The observation that subjects did not use smooth eye movements to track the oscillating acoustic target while they were stationary implies that the acoustic information is not enough for such a central reconstruction of the velocity reference signal. When additional information is present smooth pursuit eye movements can be produced.

The characteristics of eye movements elicited by the presentation of acoustic targets were also examined during both ramps and sinusoidal relative displacements (Zambarbieri, et al., 1981). In these studies, the subjects were seated in a fixed position while the target moved. The reaction time of the saccadic responses evoked by target presentation was defined as the total time required for acquiring the target position information, making a decision, programming, and executing a response. In comparing visual to acoustic targets, acoustic targets required a longer latency before the first saccade. This may be due to more time needed for determining the target position and making a decision. There was also a decrease in the acoustic latency with larger target eccentricity, which was attributed to greater uncertainty with the smaller signal.

2.4. Adaptation

Throughout normal development the Vestibulo-ocular Reflex (VOR) is an ever-changing system -- one that continually changes its characteristics to maintain stable retinal images as circumstances require. Miles and Eighmy (1980) use the word 'plastic' to describe the

system -- meaning it is a system that is modifiable and has the ability to retain the modified state without reinforcement (like head immobilization or blind folding). Several different experiments have investigated the neural changes that occur following a period of some stimuli combination producing a conflict of signals in the brain. These conflicting stimuli force the brain to reinterpret the signals and alter its response to stabilize the image on the retina. The 'adaptation' stimuli range from short- or long-term ground-based sensory conflicts developed for experimental purposes to zero-G experiments where the sensory conflict is a consequence of being in space.

2.4.1. One-G Adaptation to Angular Acceleration

Short-term adaptive changes in the human Vestibulo-ocular Reflex arc have been examined using a horizontal sinusoidal rotational stimulus of 1/6 Hz and 60°/s angular velocity amplitude (Gonshor and Melvill Jones, 1976). Each subject underwent eleven two minute runs of the stimulus in the dark on three consecutive days, with a 3-minute rest period between runs. During eight of the two minute daily runs the subject attempted a reversed visual tracking task by means of mirrors. VOR was measured during the first, sixth, and eleventh trials conducted in the dark. VOR gain was reduced significantly ($P < 0.001$) and can be attributed solely to the 14 minutes of reversed visual tracking attempted during the 50 minute daily experiment. In addition, the pre-test control gain was lower on day 3 than on day 1, indicating a small cumulative effect from beginning to end of the three day experiment. The following conclusion was made: the reversed visual tracking task induced VOR attenuation due solely to the antagonistic visual stimulus. The attenuation represented an adaptive change in the VOR induced by retinal image slip. A control experiment showed that the repeated vestibular stimulus would not itself induce a significant response decline, therefore, isolating the effects due to the discrepancy between vestibular and visual sensory inputs from those due to potential habituative attenuation.

The following mechanisms were proposed as plausible causes of the adaptive changes in the VOR: 1) Unsuccessful optokinetic tracking would lead to relative image slip on the retina. Afferent retinal discharge would cause VOR modification in an attempt to null that discharge resulting in an attenuation of VOR gain. 2) Since the optokinetic stimulus induces an overt oculomotor drive, an efferent copy of this drive (opposite to the vestibular one) might be responsible for changing the VOR. 3) Mismatch between extraocular muscle afferent discharge and the concurrent vestibulo-ocular drive could cause the VOR modification (Gonshor and Melvill Jones, 1976).

Plastic changes in VOR of humans have also been studied after long-term optical reversal of vision during free head movements using head mounted dove prism goggles (Gonshor and Melvill Jones, 1976). VOR was measured using a sinusoidal rotational stimulus in the dark identical to the short-term adaptation experiment discussed above. All four of the subjects tested showed substantial reduction of VOR gain during the first two days of vision reversal and continued to decrease until reaching a plateau of 25 percent of the normal in five to seven days. In the second week of vision reversal, large changes of phase developed in the VOR, lagging as much as 130°. Subsequently, the phase stabilized at this value while the gain climbed to about 50 percent of its normal control value. After return to normal vision, recovery of VOR gain began almost immediately but took several days to reach completion. Thus, free head movement with vision-reversal prisms produced a similar effect as the strictly sinusoidal movements employed in the earlier experiments. The daily level of VOR attenuation remained intact each night, whereas during the short term experiment subjects returned to approximately normal vision after each daily experiment. Since the alteration of reflex function only occurred in the presence of a mismatched visual stimulus and always in a manner to

correct that mismatch, these changes were truly adaptive to the requirements of retinal image stabilization during head movement (Gonshor and Melvill Jones, 1975).

A neurological mechanism that may be responsible for the changes observed in the gain and phase is shown in Figure 2.4 (Gonshor and Melvill Jones, 1975). Primary vestibular afferents from the canals (B) innervate the vestibular nuclei through direct projections that are excitatory to second order vestibular neurons. Primary vestibular afferents also innervate the vestibular cerebellum which through Purkinje cell projections (C) inhibit the vestibular neurons projecting to the oculomotor nuclei (D). When B>C, i.e., when the excitatory function of the primary vestibular afferents exceeds the inhibitory function, there would be a normal response in D. As the effectiveness in C increases, the VOR gain would progressively decline until B=C and overall gain would become zero. When C>B, i.e., the vestibular neurons are inhibited more than excited, the net effect would be reversal of the signal in D, relative to the afferent input generated by the rotational stimulation of the canal. Since this explanation would not account for the complex phase changes observed, a simple 'lead' term with a single time constant of about 1 second was introduced to channel C. The change in phase and the interdependence of gain and phase would then be accounted for. This mechanism explains how the visual tracking system might be capable of modifying the VOR (Gonshor and Melvill Jones, 1975).

Humans can also adjust their VOR gain dependent on a situational context (Shelhamer, et al., 1992). Subjects were sinusoidally rotated (0.2 Hz and 30°/s) for two hours on a rotating chair inside an OKN drum that either counterrotated or moved with the chair at ten minute intervals. By altering the viewing angle during the different drum configurations, the subjects were able to store a lower VOR gain (6 percent lower) while looking 20° down and a higher gain (8 percent higher) while looking 20° up. VOR was tested using step displacements before and after the adaptation paradigm. The results

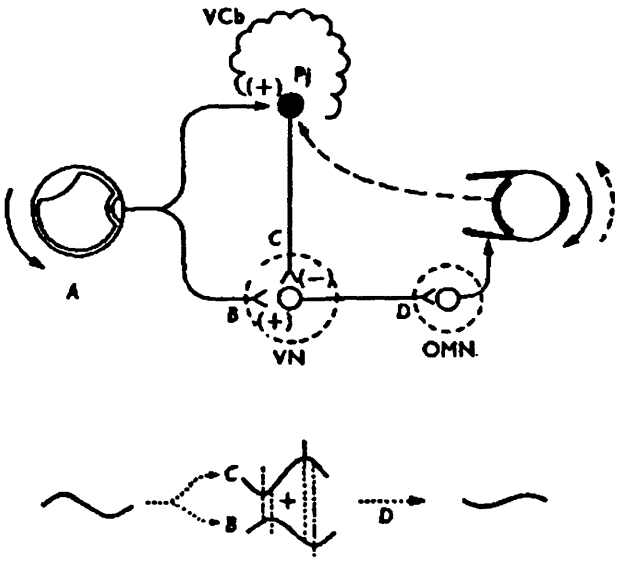

Figure 2.4. Schematic diagram of a neural network capable of producing the complex changes of gain and phase observed in experiments performed by Gonshor and Melvill Jones (1975). A = primary afferent input, B = synaptic input to vestibular neurons (VN) via brainstem pathway, C = synaptic input to vestibular neurons (VN) via brainstem cerebellar pathway, D = projection from VN to oculomotor neurons (OMN), Pj = Purkinje cells in the vestibulo cerebellum (VCb). Dashed pathway indicates the visual influence on Pj in VCb. The figure and the notation described above was extracted from Gonshor and Melvill Jones (1975) to help illustrate the proposed mechanism.

showed that humans can learn to store two VOR gains simultaneously and depending on the context can switch from one to another.

Spectacles to miniaturize and magnify the visual inputs have been used to elicit motor learning in rhesus monkeys (Lisberger, 1988). After several days of passive head turns in darkness with the x2 spectacles, VOR gains reached as high as 1.8. Similarly with 0.25 spectacles the gain of the VOR decreased as low as 0.3. In agreement with the Gonshor and Melvill Jones data (1976), motor learning did not occur during either head turns in the dark or during image motion when the head is stationary, indicating that the site of modification must also be a site of convergence for visual and vestibular inputs that guide learning. Lisberger suggested that there are modified and unmodified parallel VOR

pathways. The unmodified pathways have the shortest latency and are driven by phasic afferents, while the modified pathways have a longer latency and are driven by tonic afferents. This would suggest that the tonic response would be more likely to be modified during motor learning than the phasic response. The following model (Figure 2.5) was proposed for learning simple motor skills, including alteration of the VOR (Lisberger, 1988).

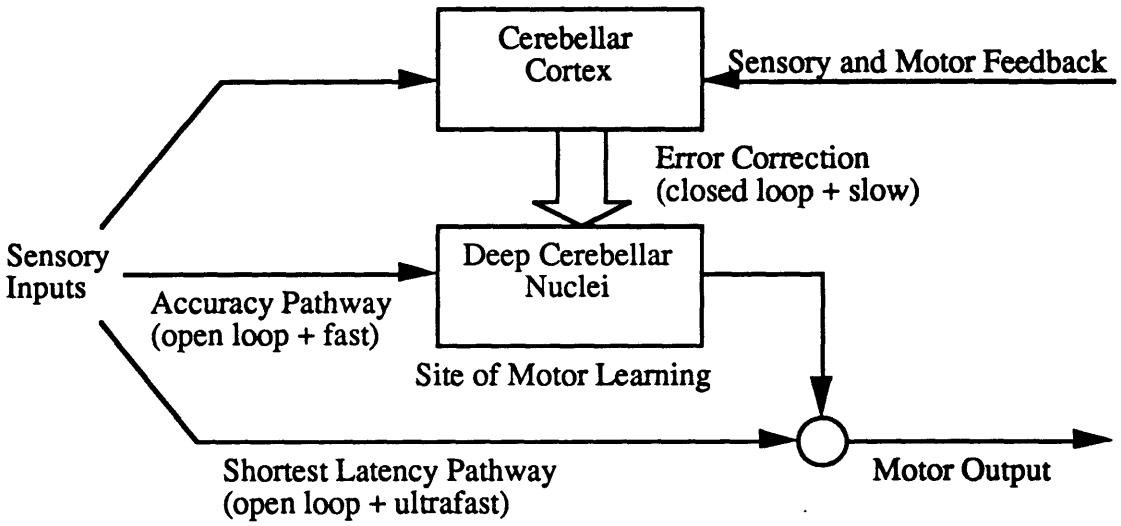

Figure 2.5. Lisberger's (1988) model for motor learning.

Additional experiments testing long-term adaptive changes in primate VOR have been performed using several different types of optical devices during active head turns, including: telescopic spectacles (magnification 2.0 and 0.5), fixed field spectacles that fix the field of view with respect to head, and dove prism spectacles providing left/right reversal (Miles and Eighmy, 1980). The first two optical devices required adaptive changes in gain alone, which occurred exponentially up to 75 percent. No phase changes were necessary for compensation. Recovery after removal of the spectacles also proceeded exponentially but at a more rapid pace than the initial adaptation. The rate of acquisition was similar from one animal to another and for repeated exposures. The data

supports previous conclusions that some retinal slip is necessary for adaptation to occur. An important aspect of VOR is its open loop mode of operation, and the visual system closes the loop. The animals' VOR was assessed by passively oscillating them about the vertical axis at 0.1 - 1.0 Hz and ±5° to ±35°. A caloric test was performed while the animals were in the adapted state to see if the adapted VOR was only present during head turns. The slow phase velocity during the caloric test, however, was consistently greater than normal when the animal was in the high-gain state. The mean ratio of high-gain/normal equaled 2.15 during the caloric and 2.03 during passive head turns. Contrary to the telescopic optical devices, reversing prisms require a 180° phase change for perfect compensation. Attenuated compensatory eye movements were observed, but little phase change occurred with active head movements alone. Subsequently, forced oscillations of 0.2 Hz and ±30° for five to six hours for five weeks produced more attenuation of gain and an increase in phase lag (Miles and Eighmy, 1980).

Eye velocity has been studied during the first two seconds of the vertical VOR elicited from cats placed on their sides (90° roll position) and rotated about an earth vertical axis (Snyder and King, 1988). To increase the VOR gain, each cat was oscillated for four to seven hours at 0.20 Hz and ±15 °/sec amplitude while the illuminated surround counterrotated. An identical protocol was used to decrease the VOR gain, except the surround rotated in phase with head velocity. VOR was tested using velocity steps of 10, 20, 40 or 80 °/sec and sinusoids of ±15°/sec at 0.02, 0.05, 0.2, and 0.5 Hz. The effects of adaptation were greatest at the adaptation frequency (0.20 Hz). For both high and low gain adaptation, the percentage change in plateau velocity was approximately two times the percentage change in peak velocity, supporting Lisberger's idea that the tonic response is more likely to be modified during motor learning than the phasic response. In addition, the VOR gain adaptation was symmetric and the VOR latency was unchanged by adaptation (Synder and King, 1988).

2.4.2. Adaptation to Microgravity

Experimenters have hypothesized that weightlessness leads to an inhibition of otolith derived spatial orientation information, and that the central nervous system eventually may adapt to weightlessness, and thus, reinterpret otolith information (Arrott et al., 1986; Oman, 1982). The resting discharge of the otoliths will be different from that on earth and during head movements the otoliths will be stimulated in an atypical manner. Although many of the results from microgravity experiments have been inconsistent, the weight of evidence points to an elevation and increased variability of the threshold of linear acceleration in the first few days following space-flight.

Thresholds for perception have been used to measure adaptation to microgravity (Benson, 1984). In flight, thresholds for detection of motion were raised by a factor of 1.5 - 4.3. Fourteen hours after landing of Spacelab-1 (SL-1), the Red Crew still had significantly raised thresholds in the X- and Y-axes. Thresholds returned to the preflight baseline within twenty-four hours. The Blue Crew had significantly lowered thresholds on postflight day one. Because of the variability of the results and the limited amount of data it is difficult to draw conclusions. The increased threshold during flight could be attributed to (1) the lowering of the 'gain' of the end organ by efferent control or (2) modification (sensory rearrangement) within the central nervous system (Benson, 1984). Following the D-1 flight, tests performed on a linear accelerator on the first and second day yielded thresholds that were significantly raised ($p<0.01$) above the values obtained preflight for all axes of acceleration (Benson, 1984). Although a change in the excitability of the otoliths in microgravity cannot be excluded, it is more probable that this decreased sensitivity is a manifestation of a central adaptive mechanism in which the "weighting" of gravireceptor information is reduced. (Benson, 1982)

A battery of pre- and postflight experiments were performed on Spacelab Mission 1 (SL-1) as well as in-flight experiments on the D-1 mission to investigate adaptation to weightlessness and readaptation to one-G (Young, et al., 1986). The experiments were based on the "sensory reinterpretation hypothesis," which includes the following components: 1) utricular otolith afferent signals are reinterpreted as indicating head translation rather than tilt, 2) sensitivity of reflex responses to footward acceleration is reduced, and 3) increased weighting is given to visual and tactile cues in orientation perception and posture control. The basic question that remains is how the sensory motor system reorganizes to account for the environmentally imposed change in the sensory information.

The input to the otoliths can be compared to the path followed by a pendulum (Young, et al., 1986). On earth, a non-accelerating body is subject to gravity alone, and the pendulum points toward the vertical. In orbital flight, a body not accelerating relative to the spacecraft experiences linear acceleration, A, equal to gravity as the object free falls around the earth, producing no specific force on the otoliths except during head movements. In one G lower frequency components of the otolith signals have been linked to the direction of the head relative to gravity, whereas higher frequency signals reflect head tilt and linear acceleration. In space static head orientation does not influence otolith organ afferent activity. Each head movement, therefore, produces a specific force stimulus which can swing in direction, even without a head tilt. Young, et al. hypothesized that the otolith signals are either inhibited, reducing their influence on posture, eye movements and spatial orientation, and decreasing the ability to sense linear acceleration, or are reinterpreted as the central nervous system learns that the afferent signals now code only linear acceleration.

The experiments of specific relevance to this thesis were performed pre-and postflight on a linear accelerator modeled after the MIT sled used in the current experiments. First, using a joystick subjects seated in complete darkness were instructed to indicate their direction of acceleration during a series of accelerations between 0.001 G and 0.08 G, similar to the experiments performed by Young and Melvill Jones (1978) described previously with the Threshold experiments. Each crew member's threshold level and a mean time-to-detect were calculated from this data. As before, the time-to-detect varied inversely with the size of the step of acceleration, allowing a velocity constant to be calculated for each subject. No dramatic changes in threshold, time to detect, or velocity constant were observed preflight to in-flight (D-1) nor preflight to postflight (D-1 and SL-1). The primary change observed was an increase in variability postflight.

During the second test, the Closed Loop Otolith Assessment Test (CLOAT), subjects were asked to null the motion of the sled using a joystick as they were accelerated with a pseudo-random sled signal. Postflight six out of nine crew members in the y-axis and two out of three crew members in the z-axis were "temporarily more capable of sensing and reacting to linear acceleration more effectively than preflight" as long as they did not have to stabilize their trunk with respect to gravity. (Young, et al., 1986) This indicates that postflight subjects are able to control translation better, but cannot control tilt.

The gain of the horizontal angular VOR of two rhesus monkey was measured 15 and 18 hours following 14 days of spaceflight and found to be approximately the same as preflight measurements (Cohen, et al., 1992). Latency, rising time constant, steady-state eye velocity and phase modulation during off-vertical axis rotation (OVAR) were also similar to preflight. Changes were observed in the amplitude of modulation of otolith related components of nystagmus induced by OVAR and in the ability to discharge stored

activity by tilt dumping. This suggests that adaptation to microgravity caused alteration in the way the central nervous system processes otolith input.

Controversial data exist as to whether the gain of yaw VOR is affected by altered states of gravity (Cohen, et al., 1992). Until recently on Spacelab Life Sciences-1 (Oman and Balkwill, 1992), data from NASA and ESA spaceflights did not show any change in compensatory yaw eye movements evoked by voluntary head movements (Oman and Young, 1988). However, Kozlovskaya, et al. (1984) did see an increase in gain of the horizontal VOR during active head movements in monkeys and humans in-flight and postflight.

As described above, a significant portion of data exist related to the adaptation of the neural pathways governing both the angular and linear Vestibulo-ocular Reflex. No preflight/postflight tests, however, have been able to quantify the human's perception of linear translation as the experiments described in this thesis aim to do. In addition, although several experimenters have attempted to alter the angular VOR pathways using conflicting visual and vestibular stimuli in one G, no experimenters have attempted to alter the LVOR pathways in the same manner. This thesis is an attempt to investigate these unstudied issues.

3. METHODS

The following chapter is divided into three sections which describe the methodology used to meet the objectives of this thesis as stated in Chapter 1, that is, to develop a test that quantifies the human perception of linear translation using voluntary saccadic eye movements. The three sections are experiment design and procedure, experimental apparatus, and data analysis.

3.1. Experiment Design and Procedure

3.1.1. Hidden Target Pursuit

All of the experiments to be described here were performed on a linear accelerator (sled) located in the Man-Vehicle Laboratory at the Massachusetts Institute of Technology. Two different hidden target pursuit experiments were performed independently: 1) the fixed displacement test, where the amplitude of the sled motion was fixed at either 8.82 or 18.20 cm, and 2) the fixed duration test, where the duration of the sled trial was fixed at either 1.0 or 2.5 seconds. Each test was run in two different subject orientations: upright with acceleration along the inter-aural direction (y-axis) and supine with acceleration along the longitudinal direction (z-axis). Four basic hidden target pursuit experiments were run and they will be referred to by the following names throughout this thesis: y-axis fixed-displacement, y-axis fixed-duration, z-axis fixed-displacement, and z-axis fixed-duration. In all four experiments, subjects were instructed to visually track an imagined target fixed in space while they were linearly accelerated using a "damped position step" displacement.

3.1.1.1. Fixed-Displacement Test

The protocols for the y-axis and z-axis tests are identical. However, since the target is 50 cm from the subject in the y-axis and 52 cm from the subject in the z-axis, the two different axis require slightly different eye movements for perfect compensation. The sled displacement was fixed at just two values (8.82 cm and 18.20 cm), which for perfect compensation would require eye movements of 10 and 20 degrees respectively in the y-axis and 9.6 and 19.3 degrees in the z-axis. Throughout both the y- and z-axis fixed displacement experiments, these two different displacements will be referred to as the "10 degree" and "20 degree" cases.

In the y-axis, each subject was run through two separate (30 - 45 minute) sessions on two different days within the same week to complete all of the required trials. In each session the subject was tested with forty trials consisting of ten randomly varied peak acceleration levels (1.35 milliG, 1.82 milliG, 2.46 milliG, 3.31 milliG, 4.47 milliG, 6.03 milliG, 8.14 milliG, 10.99 milliG, 14.82 milliG, 20.0 milliG), two directions (left and right), and the two displacement amplitudes (8.82 cm and 18.20 cm). In two data sessions, this protocol yielded a total of eighty trials for each subject with two trials for each test condition.

The z-axis fixed-displacement test was similar to the y-axis test, and was first run using electrooculography (EOG) to measure eye movements. However, because of the asymmetry, increased signal noise level, and increased variability associated with vertical EOG measurements, this data was rejected and the experiment was redone using search coils. Identical motion profiles were used in the z-axis, except that the lowest two acceleration levels (1.4 milliG and 1.8 milliG) were excluded to yield a single half-hour session. Therefore, each subject was tested during only one session including thirty-two unique trials, each repeated twice for a total of sixty-four trials. The two lowest

accelerations were chosen as the conditions to delete since the threshold for detection of linear acceleration is higher than that in the y-axis (Benson, 1989). Therefore, the conditions could be removed without eliminating the sub-threshold portion of the test range.

3.1.1.2. Fixed-Duration Test

The fixed-duration tests, in both the y-axis and the z-axis, were performed to further investigate the dependence of displacement estimation on trial duration and distance. The experimental set-up was identical to the fixed-displacement tests. The protocol was modified slightly to hold the duration of the trial, or the frequency of the sinusoidal acceleration constant. Two different trial durations were tested: 1.0 sec and 2.5 sec (1.0 Hz and 0.4 Hz). The sled was moved eight different displacements ranging from 5 cm to 40 cm. Due to the relationship of the acceleration, displacement, and trial duration (Equation 3.1), the acceleration was allowed to vary with the fixed trial durations and distances. The sled displacements and trial durations were chosen so that all of the accelerations were above the average subject's threshold of 5 milliG (Mah, et al., 1989). This experiment, therefore, was not a threshold experiment as the fixed displacement test, rather it was a means of further investigating the role of trial duration in the process of displacement estimation.

3.1.1.3. Sled Motion Stimuli

The motion stimuli for all experiments were damped position steps (single cycles of sine acceleration). The motion parameters are related by the following equation:

$$t^2 = \frac{2\pi d}{A} \tag{3.1}$$

where t = duration of trial (seconds), A = peak acceleration (cm/s^2), and d = sled displacement (cm). Figure 3.1 shows a the acceleration, velocity, and position traces to illustrate the sled motion.

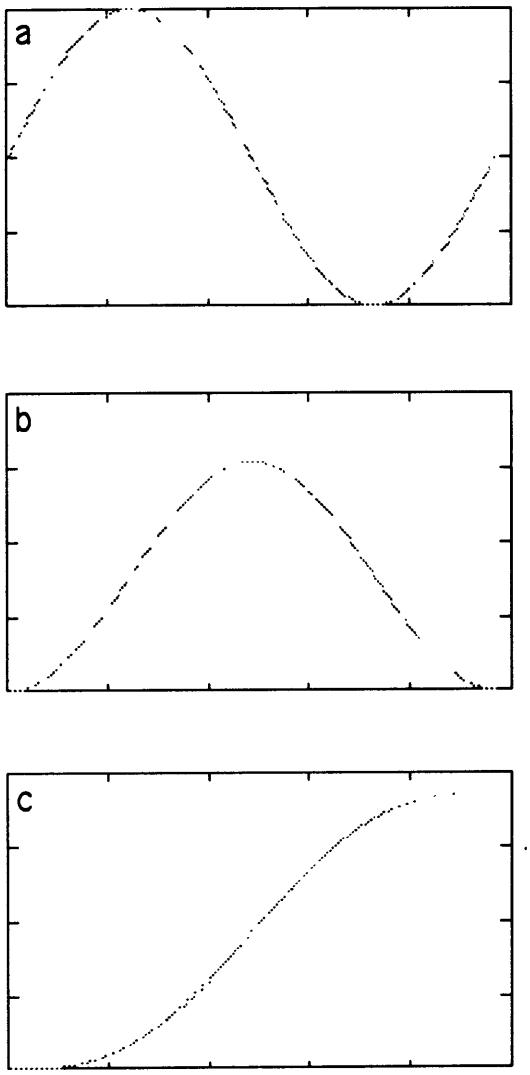

Figure 3.1. Sled motion stimulus: (a) acceleration, (b) velocity, and (c) position.

Each trial proceeded as follows: 1) The subject was asked to fixate on the red light emitting diode at eye level 50 cm (z-axis: 52 cm) from the subject's eye. For this protocol it was important that the target be in the same position in front of the subject before and

after each trial. Therefore, the subject was made to believe that the target was fixed to the earth even though it was actually fixed to the sled. 2) The Target Pursuit Shade run by a DC motor dropped down between the subject and the target to hide the target from view. 3) One second later the sled motion began. The subject was asked to track the "earth-fixed target" (LED) throughout the sled motion even though it was not visible. 4) When the sled had stopped, the experimenter asked the subject to give a subjective response as to which direction the sled moved (e.g., left/right) and how confident they were with their answer using the following scale: 1 = very confident, 2 = somewhat confident, 3 = not confident. 5) With the Target Pursuit Shade still in its lowered position, the sled was then moved back to the center with a 5 milliG damped position step profile. 6) Once the sled was back to the center, the shade was raised and the subject could see the target and prepare for the next trial. Figure 3.2 graphically illustrates the sequence of events described above for an individual trial.

3.1.2. Linear Adaptation Test

The linear adaptation experiment consisted of three pre- and post-adaptation protocols that tested for changes caused by a thirty minute earth based stimulus combination designed to produce a conflict between the visual and vestibular sensory inputs. The three pre- and post-adaptation tests included a fixed displacement Hidden Target Pursuit test, a linear VOR test, and an angular VOR test. Identical testing conditions were performed pre- and post-adaptation. First, the subject was tested on the rotating chair for angular VOR evoked by a sinusoidal stimulus. Next, the subject was moved onto the linear sled and tested using the Hidden Target Pursuit protocol in the y-axis. The optokinetic stimulus was then mounted onto the sled and several linear VOR trials were performed. This identical sequence was performed post-adaptation in reverse order (i.e., 1. LVOR, 2. Hidden Target Pursuit, 3. Rotating Chair)

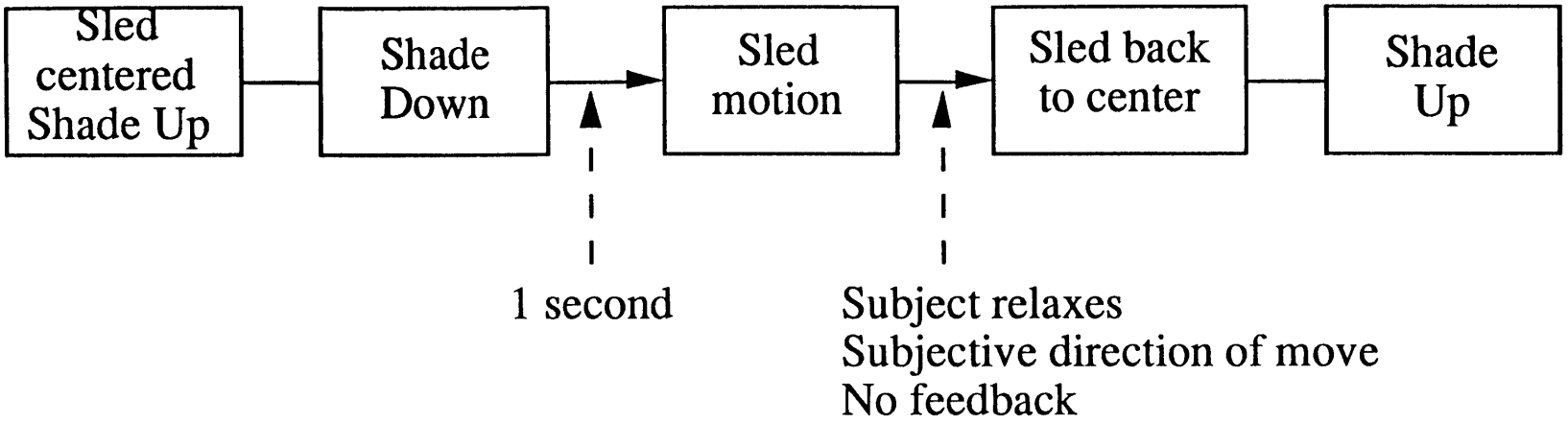

Figure 3.2. Graphical representation of the sequence of events during a trial in the Hidden Target Pursuit Experiment.

3.1.2.1. The Adaptation Protocol

This section describes the stimulus used during the thirty minute adaptation portion of the experiment which was designed to produce a sensory conflict. The subject was seated in the sled in the y-axis upright identical to the subject position during the pre- and post-adaptation experiments. Two fluorescent lights shined toward the visual stimulus to provide enough illumination for the subject to adequately see the moving black and yellow stripes in the dark room. The sled computer linked the optokinetic stimulus and sled so that the visual pattern moved twice the distance that the sled moved and in the compensatory direction relative to the subject. This stimulus combination was designed to evoke a visual response twice that normally experienced. The subject was given a linear joystick with which she simultaneously controlled the sled and optokinetic stimulus. Full deflection of the joystick produced ±10 Volts, which was sent to the sled and optokinetic controllers. No computer generated signal was input to the system. Therefore, the only signal the sled and optokinetic motors received was from the subject's joystick deflections. The combination was valid except at very high frequency maneuvers where the optokinetic stimulus lagged the sled movement slightly. Analyses of the frequency spectrum of each subject's adaptation sessions indicate the range of frequencies each subject injected. Subjects were asked to look straight ahead at the center of the striped optokinetic stimulus and notice each stripe as it moved past their eyes. This active protocol was chosen over a passive sinusoidal or pseudo-random stimulus to keep the subject alert and allow the subject to experiment in her own manner.

Each subject experienced five, five-minute segments of the adaptation protocol. In between each five-minute session a one to two minute break was taken where the subjects were permitted to relax their eyes by shutting them, but the room remained dark and the only visual stimulus was the stationary stripes in front of them. During these one minute breaks the experimenter would question the subject on motion sickness symptoms and

other illusions. A scale from 1-20 was used to indicate motion sickness symptoms, where 1 was normal and 20 was vomiting. If a subject felt signs of extreme motion sickness, the break was extended until the subject felt well enough to begin again to ensure that the subject was able to concentrate on the stripes during the five minute adaptation segments. Only one subject (MB) needed additional time between segments to quell her motion sickness symptoms. Between the fourth and fifth adaptation segment MB took a four minute break.

3.1.2.2. Hidden Target Pursuit Protocol

The Hidden Target Pursuit protocol used during pre- and post-adaptation was similar to the Fixed-Displacement Test, where the subject was accelerated using damped-position step profiles of equal length. The displacement amplitude was held constant at 18.20 cm, which if perfectly compensated for would require eye movements of 20 degrees. Each subject was tested on 32 trials (16 unique) of eight randomly varied peak acceleration levels (2.46 milliG, 3.31 milliG, 4.47 milliG, 6.03 milliG, 8.14 milliG, 10.99 milliG, 14.82 milliG, 20.0 milliG) in two directions (left and right). Each trial was repeated to increase the number of trials of each condition. The subjects' task during this portion of the Linear Adaptation experiment was identical to the preliminary Hidden Target Pursuit experiments, namely to visually track the earth fixed target even though it was not visible during the sled motion.

3.1.2.3. Linear VOR Protocol

The linear VOR portion of the pre- and post-adaptation session included three trials testing the gain of the slow phase velocity of the horizontal eye movements. During the first trial the subject was seated in the sled in complete darkness. The sled stimulus included eight cycles of a sinusoidal velocity stimulation with a frequency of 0.25 Hz and acceleration of 0.4 G. The second trial consisted of only the optokinetic stimulus while

the sled remained stationary. The optokinetic stimulus moved in a sinusoidal profile with a frequency of 0.25 Hz and the same peak linear velocity moved by the sled in trial #1 but 180° out of phase (i.e., in the compensatory direction). The third trial combined trial #1 and trial #2 to test the visual vestibular interaction (VVI).

During the first run in the dark, the subject was asked to keep her eyes open and to imagine the optokinetic stimulus used in the other trials. This was an attempt to control the vergence of the subjects' eyes during the trial. Mendoza (1993) tested this procedure to control vergence and found that while imagining the striped pattern while in the dark subjects verged their eyes similar to trials where the optokinetic stimulus was visible. During the two trials using the optokinetic stimulus (OK alone and OK+Sled), the subject was asked to look straight ahead and notice each stripe as it passed by. During all of the linear VOR trials the subject was asked trivia questions to occupy the subject and maintain mental alertness.

3.1.2.4. Angular VOR Protocol

Each subject was tested with a set of two identical trials on the rotating chair both pre- and post-adaptation. The trials consisted of ten cycles of sinusoidal stimulation with a peak velocity of 60 degrees per second and a frequency of 0.25 Hz. The subject was seated in a dark room with a black cloth mask covering her eyes. The subject was asked to look generally straight ahead and to try to keep her eyes from wandering in the darkness. The subjects were asked trivia questions throughout the trials. Before and after the two trials an eye movement calibration was performed by having the subject alternate his gaze between three dots centered on the wall in front of him. Eye movements were measured during this portion of the experiment using electrooculography (EOGs).

3.1.3. Subjects

The subjects in all of the experiments were student volunteers in, or indirectly associated with, the Man-Vehicle Laboratory at MIT. All subjects were informed of the potential risks involved in the experiment and gave written consent to be a subject (see Human Use Statement in Appendix). Subjects volunteered for all tests and were not paid for their time.

In the y-axis fixed-displacement test, eight subjects (six males and two females) ranging between the ages of nineteen and forty-five years old were tested on the MIT Laboratory Sled. These subjects are labeled with the following subject codes: BP, JM, KP, LF, LH, SS, TL, and WT. Each of the subjects was tested during two identical sessions on two different days of the same week, once in the morning and once in the afternoon.

The z-axis fixed-displacement test was originally run on eight subjects using electrooculography. However, because of the variability and the lack of reliability of vertical eye movement measurements with EOG the test was repeated using scleral search coils. Because of the higher level of reliability using coils, only six subjects (3 males and 3 females) between the ages of twenty-two and thirty were run in the z-axis fixed-displacement test and will be referred to throughout with the following subject codes: CL, JM, KJ, KP, RZ, and TC. Using coils for eye measurement necessitated fewer calibrations and down time required to adjust the EOG bias, thus more trials could be included in each session. Therefore, each subject was run only once.

In the y-axis fixed duration test, five subjects (2 males and 3 females) between twenty-one and fifty years old were each run once through the experimental protocol. The subjects were given the following letter codes: GS, TC, JM, CL, and MB.

Six subjects (3 males and 3 females), between the ages of nineteen and fifty, were run in the z-axis fixed duration test. Each subject was run once through the test session. The subjects were labeled with the following subject codes: JR, AA, GS, MB, SS, and KP.

Four subjects (2 males and 2 females), between the ages of nineteen and thirty-five were run in the linear adaptation experiment. The subjects will be referred to as: DM, MB, CL, and KJ.

Table 3.1. Summary of Subject Participation.

Subject		Y-axis		Z-axis		Y-axis
Code	Gender	Fixed Displace-ment	Fixed Duration	Fixed Displace-ment	Fixed Duration	Adapta-tion
AA	M				√	
BP	M	√				
CL	F		√	√		√
DM	M					√
GS	F		√		√	
JM	M	√	√	√		
JR	M				√	
KJ	M			√		√
KP	F	√		√	√	
LF	F	√				
LH	M	√				
MB	F		√		√	√
RZ	F			√		
SS	M	√			√	
TC	M			√		
TL	M	√	√			
WT	M	√				

Table 3.1 summarize the subject participation in the different experiments. As is evident from the letter codes, several subjects were run in multiple experiments (CL, GS, JM, KP, MB, SS, and TL). Thirteen of the seventeen subjects had been subjects in other experiments on the linear accelerator prior to the first Hidden Target Pursuit experiment. The experiments were performed in the order they appear in Table 4.1 (Y-axis fixed

displacement, Y-axis fixed duration, Z-axis fixed displacement, Z-axis fixed duration, and Y-axis linear adaptation). The experiments were separated by at least one month time for all subjects, except KP who was a subject in both Z-axis experiments within one week.

3.2. Experimental Apparatus

3.2.1. Sled

The primary piece of equipment used in this experiment was the Massachusetts Institute of Technology linear acceleration sled located in the Man-Vehicle Laboratory. The sled consists of an aluminum cart supported on four meter long parallel rails by a set of four circulating bearings in pillow blocks. Mounted on top of the cart is a chair in which the subject is securely strapped with a five strap restraint system and with their head fixed in a chair mounted helmet.

3.2.1.1. Driver

The sled is driven by an electric motor that is controlled by a dedicated 386 based PC. The control program, written in C++ by Robert Grimes of Payload Systems Inc. and maintained and modified by the author of this thesis, is a menu driven routine that allows the user to create and output a series of velocity commands, called *trajectories*, to the motor controller that drives the sled. The output from the sled computer is actually a series of voltage commands sent at a rate of 100 commands per second. Currently, the sled is capable of generating seven different types of *trajectories* that control the sled motion: 1) constant velocity, 2) sinusoidal velocity, 3) sum of sines (pseudo-random), 4) square acceleration (step), 5) modified square acceleration step (uses two different accelerations), 6) velocity step, and 7) damped-position step (single cycle of sine acceleration). Trajectories (4) through (7) were designed and implemented by the author for use during the current experiments (7) and the experiments to be performed as

preflight/postflight tests on the SpaceLab Life Sciences-2 Shuttle mission and are documented in Appendix F. Similar *trajectories* can also be generated for an auxiliary output channel to control any sled accessory, or piece of equipment that needs to be computer controlled (windowshade, lights, optokinetic stimulus, etc.).

The sled program links the sled and auxiliary *trajectories* together to create *profiles*. Each *profile,* which can contain either a sled or an auxiliary *trajectory* or both, makes up one trial in the experiment. The *profiles* can be grouped together in any sequence into a *protocol.* The user can then pick individual trials (*profiles*) from the *protocol* by selecting it with a mouse, or the user can run the series of *profiles* contained within the protocol file. This increases the speed with which trials can be run, by allowing the experimenter to set up an entire experimental session (*protocol*) before the subject enters the sled. The system is capable of accelerations up to approximately 0.9 g, while the minimum frequency of the stimulus (i.e., the maximum duration of one cycle) is limited by the length of the track (4 meters) and the particular type of *trajectory* (described above).

3.2.1.2. Helmet

In vestibular experiments, it is extremely important to limit head motion relative to the sled motion stimuli. If the head is not properly fixed, the motion stimuli will be contaminated by head motion relative to the sled, which could affect the eye movement responses as well as a subject's perceptions of motion. Likewise, acoustic noise from the sled motor and bearings could provide motion cues to the subject. Therefore, an effective head fixation and noise cancellation system is imperative to isolate the biological systems of interest, namely, the vestibular and visual systems, and to meet the goals of these experiments. The primary design criteria were to rigidly fix the subject's head to the sled, eliminate or mask all acoustic cues from the sled motion, provide open communication

between the subject and the experimenter, and maintain subject comfort for a minimum of thirty minutes. Therefore, a head fixation system was developed for use during these experiments and future sled experiments in the Man-Vehicle Laboratory which integrates a new helmet, a communication system, a noise cancellation system, and a white noise generator.

Before entering the sled, the subject puts on a David Clark flight helmet which consists of a soft mesh and leather helmet that snaps into a hard plastic covering. A chin strap holds the helmet in place on the subjects head. Two eight by three inch inflatable pads were fit between the soft mesh and hard plastic portions of the helmet to reduce head movements. A wood frame with a formed piece of dense Styrofoam inside is bolted to the back side of the chair. Velcro covers the inside surface of the Styrofoam and mating velcro covers the surface of the hard portion of the helmet. As the subject enters the sled, she fits the helmet into the Velcro covered molded Styrofoam, thereby fixing her head to the sled. To exit from the sled, the subject keeps the helmet on and simply pulls the helmet loose from the Velcro covered Styrofoam frame. Once off the sled the subject can remove the helmet.

3.2.1.2.1. Noise Cancellation

Bose, Inc. donated two active noise cancellation headsets to the Man-Vehicle Laboratory for use on all sled experiments. The headset was attached inside the David Clark helmet described above. In addition to the high quality active noise cancellation, wide band noise was pumped through the headphones to further mask any noise generated by the sled motor, cables or bearings. These precautions were taken to remove auditory cues providing directional or magnitude information. The noise level was adjusted for each subject to a comfortable level which minimized detection of any surrounding noise. Despite the precautions, some very low frequency sound was detectable through the Bose

active nose cancellation and the additional noise mask during some sled trials. Fortunately, at the low accelerations used in these experiments, the level of sound was minimal, and did not give any indication of direction or magnitude of movement.

3.2.1.2.2. Communication

In conjunction with the two headsets, Bose, Inc. also donated a communication system which allows two way communication between the subject and experimenter throughout the test session. This facilitates communication of subjective responses from the test subjects after each trial rather than waiting until the end of the experimental session. The wide band noise used to mask the sled noise is mixed into the communication channels such that the subject can hear the masking noise at all times, regardless of whether someone is speaking.

3.2.1.3. Lighting

During all of the Hidden Target Pursuit experiments the lights in the room remained off for the entire test session. The sled chair was enclosed with an opaque black cloth, minus a 32 cm by 20 cm window which allowed the subject to view the target. Significant care was taken to seal all light leaks to the room that might provide visual cues of movement to the subject. While the sled was moving an opaque black window shade dropped down in front of the window to block the target and any other light from the subject. To further inhibit external light cues from reaching the subject, two small fluorescent lights were placed inside the sled facing toward the subject, but outside the subject's normal field of view. These fluorescent lights remained on throughout the experiment, including during the calibrations to maintain a constant light level within the sled, to eliminate the chance of dark adaptation, and to minimize EOG gain changes when EOG was used for eye movement measurements. The subjects were asked to report if any light other than the

target or the fluorescent lights were visible. If such a report was made, the experimenter stopped the current trial and further darkened the area surrounding the subject.

A few changes were made to the lighting arrangement during the linear VOR portion of the adaptation experiment. During the first trial, the fluorescent lights inside of the sled were extinguished and a black opaque shroud covered the entire sled to block all exterior lights from the subject. During the optokinetic (OK) and the optokinetic+sled (OK+Sled) trials, and the adaptation paradigm, the subject needed to be able to see the striped optokinetic stimulus. The black cloth covering the front of the sled was removed so that the optokinetic stimulus would fill the subject's full field of view. The side cloths remained on the sled to block out extraneous lights from the subject's peripheral vision. The fluorescent lights used in the Hidden Target Pursuit test were turned 180° to face away from the subject towards the optokinetic stimulus to allow adequate illumination of the optokinetic (OK) pattern. All other room lights remained off during the entire experiment.

3.2.2. Visual Target

During the Hidden Target Pursuit Experiments a visual target made up of a dim red light emitting diode (LED) mounted on a black wooden rod was centered in front of the sled 50 cm from the subject's eyes in the y-axis experiments and 52 cm from the subject's eyes in the z-axis experiments. The position of the target could be adjusted to align with the eyes of each subject in both axes. Since the sled does not have positional feedback control, it was not possible to quickly position the sled directly in front of the target after each trial. To compensate for this problem, the target was fixed to the frame of the sled cart and, without the subject's knowledge, moved with the sled during each trial. All subjects believed that the target was fixed to the earth at all times, and only one subject reported any difficulty performing the task.

3.2.3. Target Pursuit Shade

To hide the target during the all movements of the sled a black opaque windowshade (referred to as the *Target Pursuit Shade* or *windowshade*) was lowered between the subject and the target. The shade was connected via cables and pulleys to a flywheel attached to a DC motor. The power supply used to run the motor was connected to the auxiliary output channel of the 386 PC so that the movement of the shade could be controlled and synchronized with the sled motion. The shade used was a household windowshade with the stopping mechanism removed. The spring was wound to a desired stiffness to pull against the tension in the cables caused by the motor. This configuration was used to keep the shade from swaying during sled motion. Figure 3.3. shows a schematic of the general setup of the sled, target, and windowshade used for the Hidden Target Pursuit experiments.

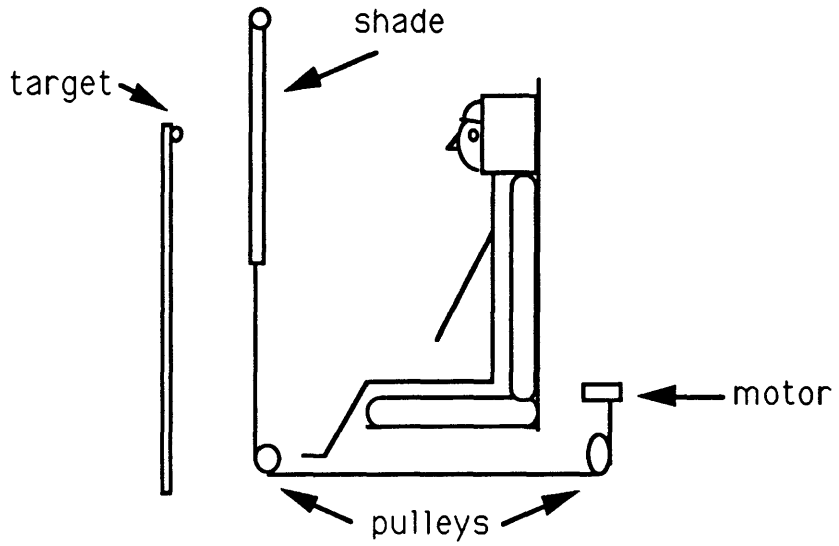

Figure 3.3. Schematic drawing of Hidden Target Pursuit setup.

3.2.4. Optokinetic (OK) Stimulus

For the linear VOR trials and the adaptation paradigm, an 86 cm x 86 cm (177 cm circumference) optokinetic (OK) stimulus was attached to the sled. The OK stimulus was approximately 71 cm (28 in) in front of the subject's eyes and completely filled the subject's field of view. The visual stimulus was striped with 36 alternating black and yellow stripes, each approximately 4.9 cm wide. At this distance each stripe subtends 3.9° and the optokinetic stimulus itself subtends 50° by 50°.

3.2.5. Rotating Chair

The rotating chair located in the Man-Vehicle Laboratory at MIT was used for the angular VOR trials pre- and post-adaptation. The chair consists of a modified 'dentist chair' driven by a stepper motor. The chair is run from a menu driven program on a dedicated 286 based PC. The subject is strapped into the chair by a standard lap belt, the lights in the room are extinguished, and a black cloth mask is placed over the subjects eyes to eliminate any visual cues cause by light leaks from the computers. Horizontal and vertical EOG, and chair tachometer data were collected on an Macintosh IIci (Apple Computers, Inc., Cupertino, CA), using LabView 2 (National Instruments, Austin, TX) data acquisition software. EOG signals were automatically adjusted to stay within $\pm$10 volts.

3.2.6. Eye Movement Measurement Systems

3.2.6.1. Electrooculography

In the first Hidden Target Pursuit experiment, the y-axis fixed-displacement test, horizontal and vertical eye movements were measured using an Electrooculography (EOG) system that consists of one electrode placed just off the outer corner of each eye on the subject's temples, one above and one below the left eye, and a ground electrode placed in the center of the forehead. The EOG system utilizes the differences in polarity

between the cornea and retina of the eyes. The cornea of the human eye has a positive polarity relative to the retina. When the eyes point straight ahead, the potential difference measured differentially between the electrodes is zero. As the eyes move left or right the differential measurement of the electrodes changes. The EOG electrodes were applied to the subjects face 30 minutes prior to testing to help stabilize the electrodes and to ensure better performance. A calibration of the EOG signal output was performed periodically throughout the experiment (discussed below).

3.2.6.2. Scleral Search Coils

The scleral search coil (Skalar, Inc., the Netherlands) is an insulated copper wire embedded in a silicone rubber ring worn on the surface of the sclera of the subject's eye. The subject's head is restrained close to the center of four large Helmholtz coils which produce a spatially constant magnetic flux in the test region. The magnetic field generator and phase detection electronics were manufactured by C-N-C Engineering (Seattle, WA). As the eye and search coil turn together, the magnetic flux through the coil changes, which induces a measurable current. The search coils are more accurate than electrooculography (EOG), especially for vertical eye position measurements, but they add several constraints to the experiment as well. Most importantly, to prevent a scleral abrasion, the search coils should not be worn for more than thirty minutes. This limits the amount of time available for an experimental session. Fortunately, the increased accuracy of the search coils necessitates fewer trials and fewer calibrations.

When preparing to use the search coil the following procedure was followed. The impedance was measured to be between 19 and 21 Ohms. (If the coil wire is broken at any point the impedance will measure in units of mega Ohms.) The coil system was powered at least thirty minutes before use. Once the system warmed up, the coil to be used in the experiment was taped to a calibration gimbal which was mounted within the

field coils. The coil output was set to zero when the coil was centered at zero degrees horizontally and vertically. The coil was then calibrated for horizontal and vertical rotations so that 10° of eye movement equaled approximately 350 A/D units. Once calibrated, the gimbal was removed from within the coil frame, the eye coil was released from the gimbal and was soaked for several hours in CibaVision® AOSEPT® disinfectant/neutralization solution. Prior to insertion into the subjects eye the annulus was rinsed thoroughly in a stream of saline solution and the impedance across the leads was again measured.

Once the subject was seated in the sled chair within the field coils, the subject's right eye was anesthetized using a topical 0.5% solution of proparacaine HCl (Ophthetic®). The search coil was inserted under the subject's eyelid so that the ring was aligned on the eye and the coil lead exited the eye at the medial (nasal) corner of the eye. The lead was taped to the subject's forehead, the helmet, and then to the sled frame to prevent it from moving within the coil field causing signal noise or from interfering with the subject's vision. Once in the subjects eye, the signal output was again set to zero as the subject looked at the center dot of a calibration device directly in front of her. A calibration was then performed with the coil in the subject's eye (described below). The subjects were informed that additional anesthetic was available if the eye coil was uncomfortable at any time during the test session.

Following a test session, the search coil was immediately removed from the subject's eye and placed into the disinfectant solution. Each subject was given drops of sterile saline once the coil was removed to soothe the eye and help return the scleral pH to normal.

3.2.6.3. Calibration

Every eighth trial and at the beginning and end of each experimental session a calibration run was performed as a control for EOG comparisons. For all experiments using search coils for eye measurements, a calibration was performed at the beginning and end of the experimental session only. Because of the accuracy of the coils and the absence of signal drift, it was not necessary to take calibrations every eight trials. The black Target Pursuit Shade used to shield the target from the subject during actual trials in the Hidden Target Pursuit experiments was also used for the calibration. The shade would drop down three quarters of the way so that the five calibration dots were visible to the subject. The center dot was located in the center of the field of view in front of the subject. The other four dots were placed on the shade above, below, to the left and to the right of the center dot at a distance that translates to a 10 degree eye movement. During a calibration trial the subject is asked to look to the Center-Right-Center-Left-Center-Up-Center-Down-Center as the eye movements are recorded. Once the calibration is over, the shade moves back up to the starting position, enabling the subject to view the visual target (LED), and prepare for the trial to begin. During actual trials, the shade would drop down far enough that the calibration dots were hidden from the subject by the black shroud surrounding the sled.

3.3. Data Analysis

Four channels of data were collected at 200 Hz for each experiment and recorded on a Compaq 386 computer : sled velocity or sled position, windowshade motor output or optokinetic stimulus velocity, and horizontal and vertical eye position (EOG or coils). Eye position data was using LabTech Notebook for the first two experiments (y-axis fixed displacement and fixed duration). The data was transferred to a Macintosh using MacLink (DataViz, Trumbull, CT) and was then converted to MatLab (Mathworks, Inc., Needham, MA) format using a conversion program called *Convert* (Balkwill, 1992).

A data collection routine written by Dr. W. Teiwes was used instead of LabTech Notebook for subsequent experiments (z-axis fixed displacement and fixed duration and linear adaptation). The switch to the new program was made because of the increase in speed, the ability to view the data being recorded on the computer display, and the ability to store the data directly in MatLab format rather than in binary format.

3.3.1. Hidden Target Pursuit

3.3.1.1. Eye Position Analysis

Horizontal and/or vertical eye movement calibration factors were calculated to convert the A/D units to degrees of eye movements for each subject using a MatLab script called *Calibrate* (Balkwill, 1992) . This script calls other MatLab scripts called *Three_Point* and *Pick_Regions* which allow the subject to manually pick three regions off of the plot of the eye position data: positive deflection, negative deflection, and center. The mean value across the specified interval was used as the number corresponding to a 10° deflection of the eye, or any other amplitude specified by the user. The calibration factor, in degrees per unit, was calculated as the ratio of the difference in angular displacements specified by the user to the difference in digital units. This is a simple linear fit to the data which has been shown to be valid for eye movements less than approximately 30 degrees. (Balkwill, 1992)

Using these calibration factors for each subject, the horizontal and/or vertical eye position data was analyzed using a MatLab script called *Target_Pursuit.* Working on the same philosophy as *Calibrate,* this script enables the user to manually pick points off of a plot by calling a modified version of M. D. Balkwill's *Three_Point* script called *Two_Point* which in turn calls a modified version of *Pick_Regions. Pick_Regions* allows the user to zoom in on a particular part of the plot, for example on one trial as shown in Figure 3.4.

The user selects an area of approximately one second before the sled moves where the eyes are fixating on the target, shown in Figure 3.4. *Target_Pursuit* averages the amplitude of the points in that region. Next the user selects a flat region of the eye position signal once the sled and eyes have stopped. *Target_Pursuit* again averages the amplitude of the points in that region and subtracts the pre-trial mean from it, yielding the total amplitude and direction of the eye movement. The direction of the eye movement is compared to the direction of the sled motion to determine whether the subject's eye movement response was in the correct (compensatory) direction.

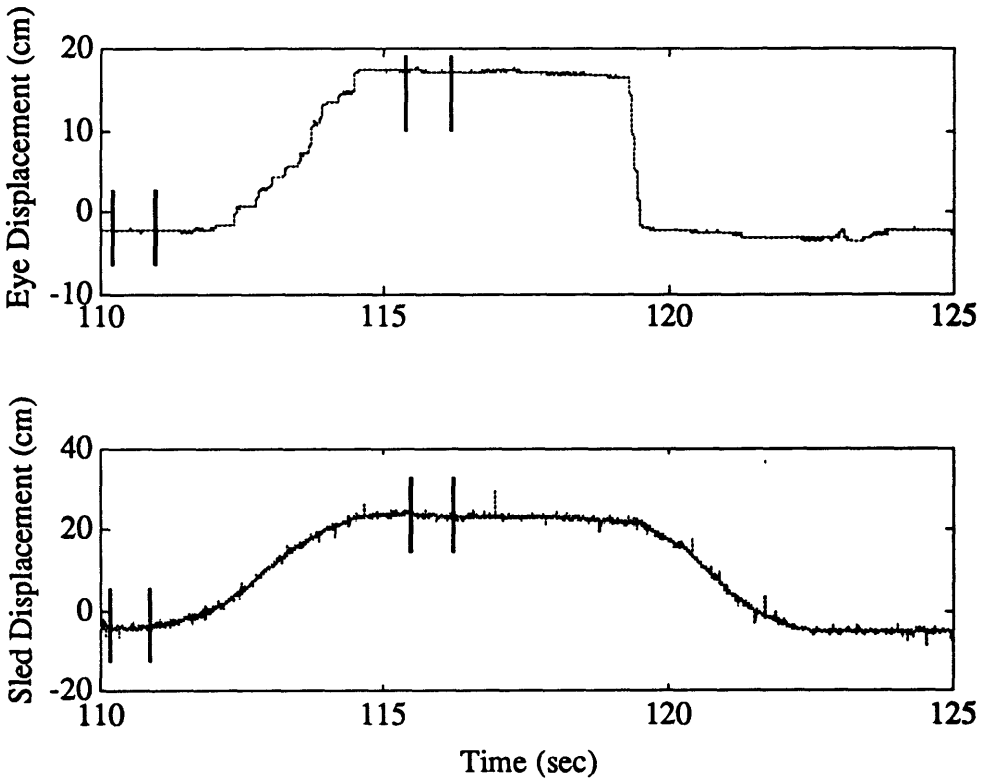

Figure 3.4. Example of analysis of raw eye movement and sled position signals during in the Hidden Target Pursuit Experiment.

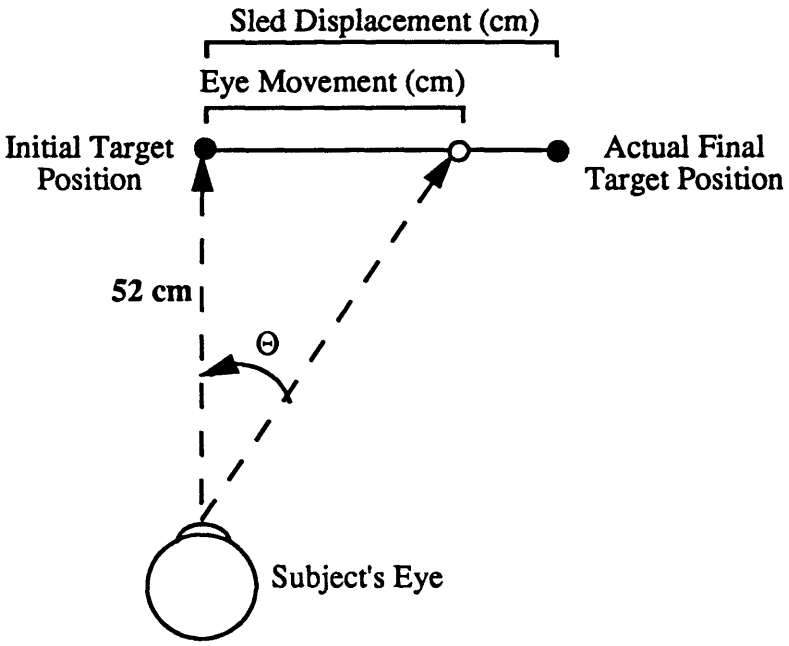

Figure 3.5. Relative eye movement corresponding to the displacement of the sled with the target fixed in space. In this example, the subject undercompensated for the z-axis (target distance 52 cm) sled displacement.

Since the subjects were asked to compensate for linear displacement while tracking the target, eye movements were evaluated in centimeters. The eye displacements calculated correspond to the projection of the line of sight of the subject on a line parallel to the direction of displacement, running through the target position (50 or 52 cm). For example, in the y-axis experiments an eye movement of 1 cm corresponds to an eye rotation of Arctan(1/50) = 1.15° (Arctan(1/52)=1.10° in the z-axis).

In the example shown in the Figure 3.5, the eye movement undercompensated for the relative target motion, i.e. the subject perceived less motion than actually occurred. The eye movement in centimeters is calculated as follows:

$$Eye_i = 52 \times \tan^{-1}(\Theta_i) \qquad (3.2)$$

For purposes of comparison between the different trial conditions, all eye movements were normalized by the displacement of the sled. In the z-axis and adaptation Hidden Target Pursuit experiments the normalized eye movement was found by dividing the eye movement in centimeters by the sled displacement in centimeters for that particular trial (Equation 3.3).

$$\text{Gain}_i = \frac{\text{Eye}_i}{\text{Sled}_i} \tag{3.3}$$

This was necessary to account for slight discrepancies between the commanded sled displacement and the actual distance it moved. This normalization leads to a more accurate depiction of the subject's response to the sled displacement. Section 3.3.1.3. describes how the sled displacement is calculated. In the two y-axis Hidden Target Pursuit experiments, since only the sled velocity signal was measured, it was not possible to accurately calculate the actual sled displacement. Therefore, the eye movements were normalized using the commanded sled displacement which is somewhat less accurate compared to the normalization in the z-axis and adaptation experiments. However, the variability in the sled position signal calculated in the z-axis and linear adaptation experiments was less than ±10% of the commanded sled displacement. This variability is significantly smaller than the variability of a subject's response from one trial to another, which is closer to 30 or 40%.

3.3.1.2. Statistical Analysis

All eye movement magnitudes and directions were stored in spreadsheet format using Systat 5.2., a statistical package used for all subsequent statistical analysis and summary plots. For the fixed-displacement Hidden Target Pursuit experiments (both y- and z-axes), plots were made of the mean and standard error of the normalized eye displacements at each G-level, as shown in Figure 3.6 for subject BP. Threshold levels for detection of linear acceleration were chosen from observation of the means and standard errors at each G-level for each subject according to the following rule: *An*

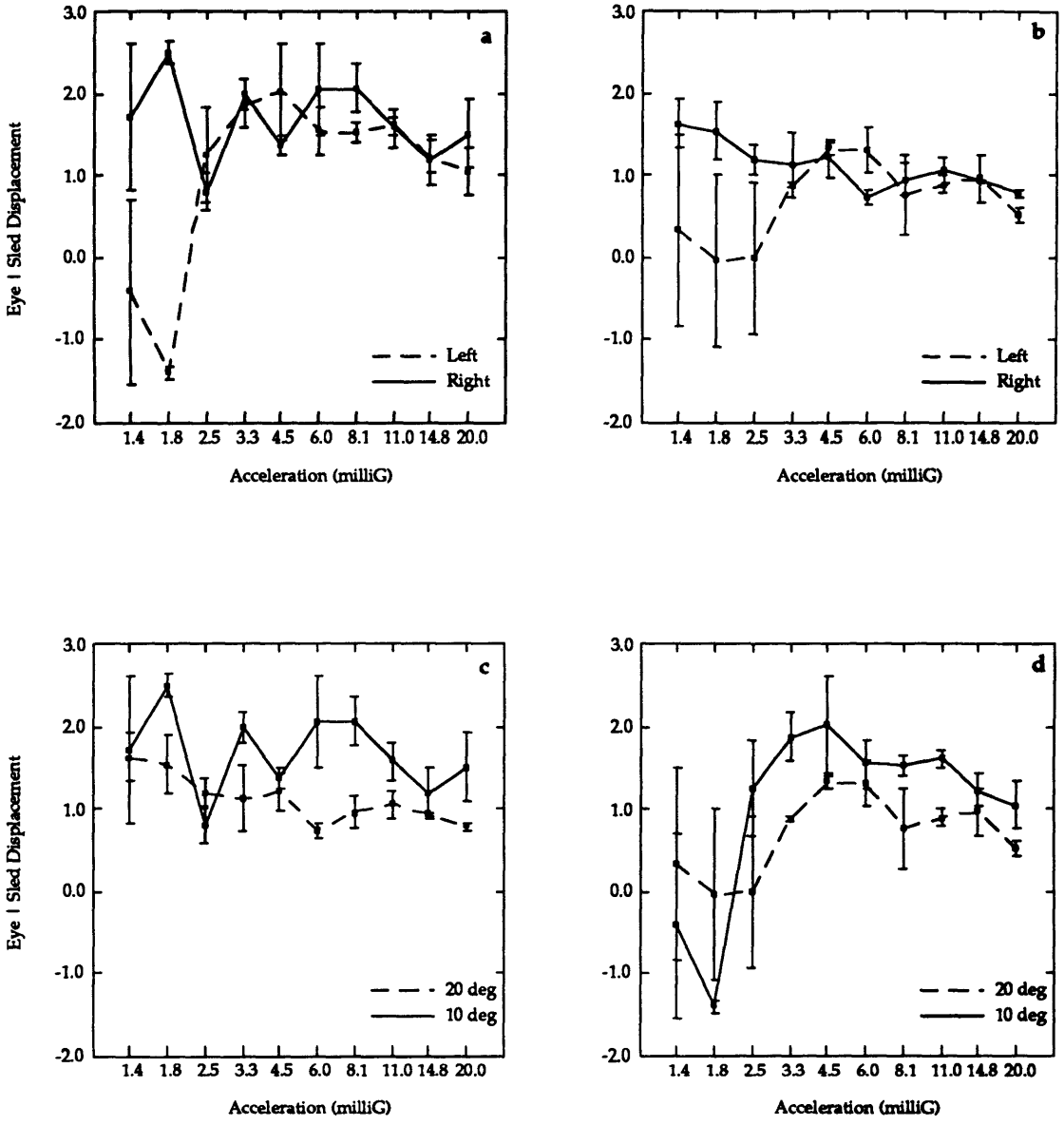

Figure 3.6. Y-Axis Fixed Displacement eye movement data for subject BP. a) 10 degree trials comparing leftward and rightward trials, (b) 20 degree trials comparing leftward to rightward trials, (c) rightward trials comparing 10 and 20 degree trials, (d) leftward trials comparing 10 and 20 degree trials. Error bars signify standard error.

individual's threshold level is the lowest of two or more consecutive accelerations tested whose mean normalized eye movement response is statistically greater than zero. Such a complex definition of threshold is needed to account for the within subject variability between acceleration levels that precludes defining the threshold as simply the lowest acceleration significantly different from zero. In the example shown in Figure 3.6, the threshold levels were calculated to be 1.8 milliG in the 10 degree rightward trials (solid line in figure **a**), 3.3 milliG in the 10 degree leftward trials (dotted line in figure **a**), less than 1.4 milliG in the 20 degree rightward trials (solid line in figure **b**), and 3.3 milliG in the 20 degree leftward trials (dotted line in figure **b**).

Mathematical differences between the mean normalized eye movements of trials toward the right (head) and trials toward the left (foot) were calculated using the following formula:

$$\mathbf{Diff_{R\text{-}L}} = \left[\Sigma \frac{\mathbf{Eye_i}}{\mathbf{Sled_i}}\right]_{\mathbf{R}} - \left[\Sigma \frac{\mathbf{Eye_i}}{\mathbf{Sled_i}}\right]_{\mathbf{L}} \qquad (3.4)$$

These differences were plotted versus sled acceleration with error bars indicating the standard error of the differences for each subject to graphically depict any consistent asymmetry in subjects' responses as shown in Figure 3.7 for subject BP in the Y-axis Fixed Displacement test. The standard error of the differences is calculated by applying the Pythagorean theorem as follows:

$$\mathbf{SE^2_{R\text{-}L} = SE^2_R + SE^2_L} \qquad (3.5)$$

where SE is the standard error of the mean of the normalized eye movements and is calculated by:

$$\mathbf{SE_X} = \sqrt{\frac{\frac{1}{n-1}\sum_{i=1}^{n}(x_i - \bar{x})^2}{n}} = \frac{\mathbf{Standard\ Deviation}}{\sqrt{n}} \qquad (3.6)$$

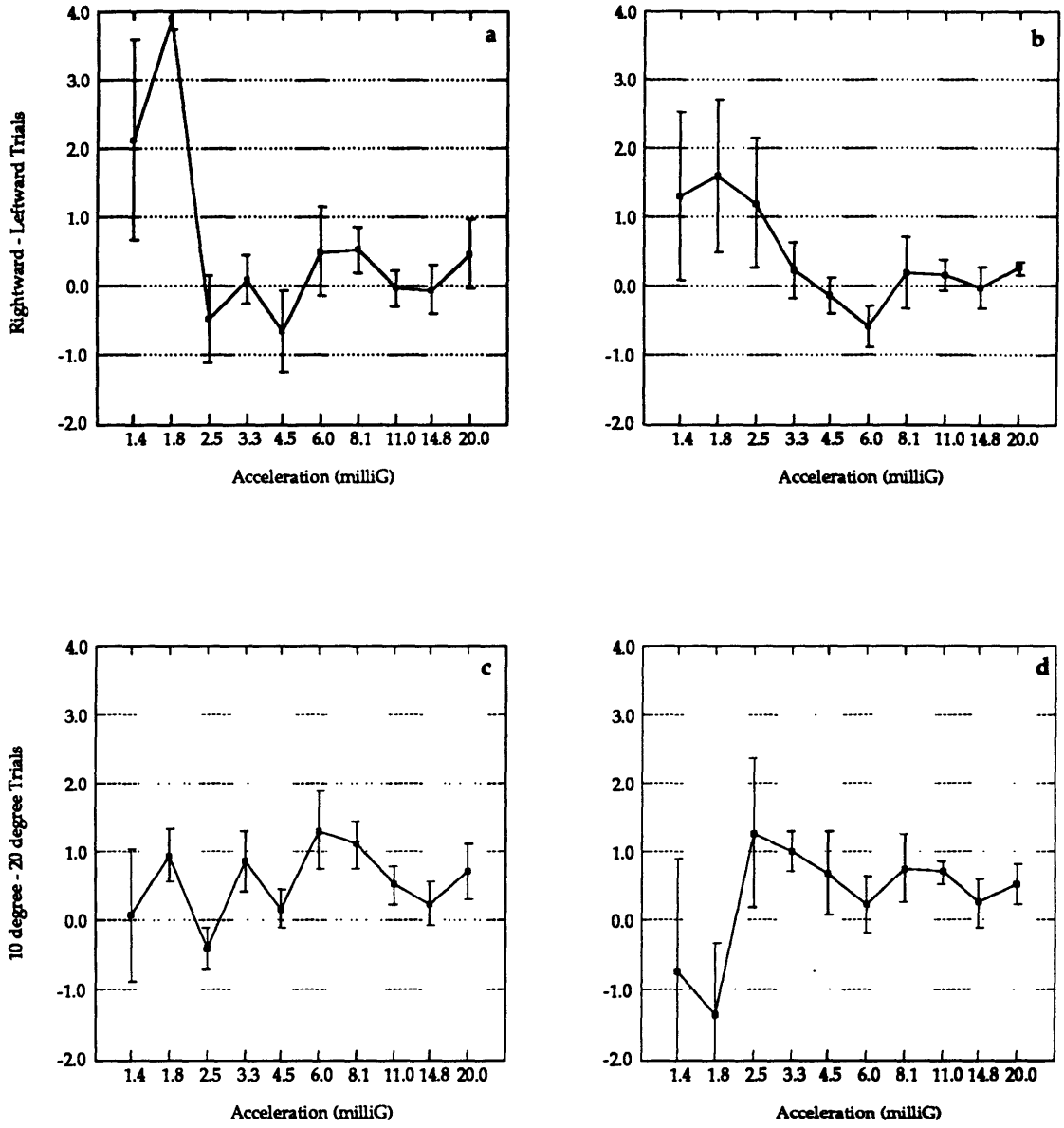

Figure 3.7. Y-Axis Fixed Displacement difference plots for subject BP. (a) difference between rightward and leftward 10 degree trials, (b) difference between rightward and leftward 20 degree trials, (c) difference between 10 and 20 degree rightward trials, (d) difference between 10 and 20 degree leftward trials. Error bars indicate standard error of the difference.

A Chi Squared (χ^2) Test was performed to statistically test whether the difference between the two conditions was significant. The null hypothesis was that the mean response to the headward trials and footward trials was symmetric. The χ^2 statistic for each subject is the sum of the squares of the quotients of the calculated difference and the standard error of that difference for each acceleration level as follows:

$$\chi^2 = \sum_{j=1}^{a} \left(\frac{\mathbf{Diff}_{(R-L)_j}}{\mathbf{SE}_{(R-L)_j}} \right)^2 \qquad (3.7)$$

A similar χ^2 analysis was performed to test for a response difference to the 10 and 20 degree trials. When normalized to the sled displacements, the responses should be similar under the null hypothesis. The difference between the mean normalized responses to each displacement was calculated and plotted versus sled acceleration. The χ^2 test was performed to test if the difference between the two conditions was significant.

The significance of the χ^2 for each subject is determined by looking up the value calculated in equation 3.7 in a table of critical χ^2 values for the appropriate number of degrees of freedom (Bernard and Rosner, 1990). Since the subjects are unable to accurately or reliably determine their direction or magnitude of translation below threshold, the below and above threshold measurements were analyzed separately. (Responses below threshold are potentially from a different population than the responses above threshold.) The somewhat arbitrary 'rule' described above for determining a subject's threshold for detection of linear translation was chosen to be robust and consistent, potentially at the expense of precision in the determination of the threshold value. Therefore, we report a χ^2 test of all eight (z-axis) or ten (y-axis) acceleration levels. Two additional χ^2 tests are also calculated for each subject, one above threshold

and one below threshold. The method of choosing the break point between the below- and above-threshold χ^2 tests is also somewhat arbitrary because the threshold level might be different for the two conditions in the comparison (i.e., headward versus footward). For simplicity, the higher of the two threshold levels was chosen as the overall threshold. Therefore, whereas the above-threshold χ^2 test includes only above threshold data, the below-threshold test, including all acceleration levels below the higher of the two thresholds, includes data that was above-threshold in one condition, but not the other. That is, data from two potentially different population sets are grouped together in the below-threshold χ^2 test. All three χ^2 values are tabulated for comparison.

The p-values associated with the χ^2 statistical test are two-tailed. Therefore, a statistically significant χ^2 value is ambiguous, and its interpretation requires further examination of the data. In fact, the deviations show trends not yet analyzed that undermine the assumptions underlying the χ^2-test. It is common for the difference between two conditions to be significant according to the χ^2 because the difference is significantly greater than zero at a some accelerations and less than zero at others. In such a case, no significant difference can be deduced.

For the fixed-duration Hidden Target Pursuit experiments (both y- and z-axes), raw eye movement amplitudes were plotted versus sled displacement. The results were analyzed via linear regression analysis similar to that of Israël and Berthoz (1989) to investigate dependence of estimation of translation on trial duration. The data were split into four general conditions each with sled displacement as the independent variable: 1.0 second trials to the right (head), 1.0 second trials to the left (foot), 2.5 second trials to the right (head), and 2.5 second trials toward the left (foot). Regression analysis was performed on the regression line for the 1.0 second trials and the 2.5 second trials to test whether each slope was significantly different from a slope of 1.0, 0.0 or significantly different from

one another. The results of this analysis are tabulated and discussed in the Results chapter (Chapter 4).

In addition to the regression analysis, means and standard errors of the normalized eye movements were calculated and plotted versus sled displacement to emulate the analysis performed during the fixed displacement experiments where the normalized eye movements were plotted versus sled acceleration. Mathematical differences between the normalized eye movement data from the 1.0 second and 2.5 second trials were calculated and plotted versus sled displacement with error bars indicating the standard error of their differences. A χ^2 test was performed to test whether the 1.0 and 2.5 second trials were significantly different, indicating a dependence of the eye movement response on trial duration. Likewise, the mathematical differences between the Rightward (Headward) and Leftward (Footward) normalized data were plotted to show whether a directional asymmetry in response existed. A similar χ^2 was performed. A threshold level was not determined in the analysis of either the y- or z-axis fixed duration experiments because, based on the results from the Fixed Displacement test, the trials in these experiments are above threshold for the majority of the subjects. Therefore, only one χ^2 test was performed across all sled displacements for each subject.

3.3.1.3. Sled Profile Analysis

In the analysis of the y-axis fixed displacement and y-axis fixed duration experiments the sled velocity signal was used to signify the start and end of each trial. The sled velocity signal was chosen because of its high signal to noise ratio. The other sled signals, sled position and acceleration, have higher noise levels. However, after analysis of the data from the y-axis experiments, it became obvious that sled position should be recorded because of small sled displacement errors that often occurred (error < 10%). More

accurate analysis is enabled by comparing the eye movement with the actual sled displacement.

For subsequent experiments the sled position signal was amplified, filtered through a low pass filter with a break frequency of 40 Hz and 20 dB gain, saved on the data collection Compaq computer, and subsequently used to signify the beginning and end of each trial. Further analysis was performed on the sled position signal to actually measure the sled displacement rather than assuming the sled displacement was exactly that commanded.

The sled position signal was calibrated by manually moving the sled to previously measured marks on the track 10 and 20 cm to either side of the center. A sled calibration factor was calculated using the same MatLab script *Calibrate* as used to calculate the eye movement calibration factors to convert the A/D units to centimeters. The calibration factor in centimeters per unit was calculated as the ratio of the difference in linear displacement specified by the user to the difference in digital units. The amplitudes of the sled displacements were calculated using the same *Target_Pursuit* MatLab script that was used to analyze the magnitude of the eye movements. *Target_Pursuit* allows the user to input the calibration factor and then for each trial pick a region of points before the sled moved and then again after the sled stopped. The difference between the two values equals the amplitude that the sled moved in centimeters.

As discussed above, the sled displacement was used to normalize the eye movement for each sled trial. Since the sled position signal was not taken during the y-axis experiments, the commanded sled position was used to normalize the eye movement response for each trial. For example, in the y-axis fixed displacement test the magnitude of the eye movement response was divided by either 8.82 cm or 18.20 cm for the 10 or 20° trials respectively. The responses in the fixed duration experiment were normalized

by dividing by the commanded displacement: 5, 10, 15, 20, 25, 30, 35, or 40 cm. This may lead to some variability in the data. In the z-axis, where the position signal was directly available, the difference between the commanded and measured sled position was less than 10% (worst case was ± 4cm at the largest displacement) of the commanded sled signal. Considering that the scatter of the eye movements at each sled displacement is approximately ±15 cm, ±4 cm is relatively small.

Although the sled position signal was measured during the y-axis adaptation experiment, a sled calibration was not performed. It was assumed that the calibration factors calculated in the z-axis experiments would be the same for the y-axis. However, based on the analysis of the measured sled displacements this assumption is not true for a number of reasons. 1) The sled displacements calculated are on average 6 cm greater in the adaptation experiment than in the z-axis fixed displacement test. 2) Response gains of eye movement divided by the measured sled displacement average to less than 1.0 in the adaptation experiment. In the previous y- and z-axis experiments most subjects had a gain of 1.0 or greater. Taken by itself, the pre-adaptation Hidden Target Pursuit trials are identical to those previous experiments and one would expect similar responses. These analyses do not affect the comparative analysis between the subject's relative responses pre-adaptation and post-adaptation, which was the prime focus of these experiments. However, since a calibration was not actually performed, no discussion can be made about the magnitude of the subjects' responses, for example, whether they over or under compensated for the sled displacement.

3.3.1.4. Subjective Response Analysis

Subjective responses following every trial were recorded by the experimenter and stored with the eye movement data. The directional responses were used to calculate percentages of subjective correct responses that are tabulated in the Results section.

Inspection of these tables are used to further interpret the quantitative eye movement data in determining each subject's threshold for detection of linear acceleration (fixed displacement tests), directional asymmetries (primarily z-axis), and differences due to trial duration (fixed duration tests). Subjective response thresholds were determined similarly to the eye movement threshold calculations using the following rule: *the subjective response threshold is the lowest of two consecutive acceleration levels where the subject chose the correct direction in at least 75% of the trials.*

For all but the y-axis fixed-displacement test each subject was asked to give a subjective estimate to how far she translated in addition to the directional response. Subjects were given the option of responding in any unit of linear measurement they were comfortable using. Subsequently, all subjective responses were converted to centimeters. Averages were calculated at each G-level for each subject (similar to the eye movement data). These plots were used to evaluate the correlation of subjective responses to the magnitude of the corresponding eye movements as the subject tracks the target, as well as to determine if any subjective asymmetries exist.

3.3.2. Linear and Angular VOR Experiments

Four channels were simultaneously sampled during the Linear VOR experiments on the sled, each at 200 Hz: sled velocity, linear OK stimulus velocity, and horizontal and vertical eye position. The time series were saved directly in MatLab format ready for analysis. During the rotating chair trials, three channels were simultaneously sampled at 200 Hz each: chair velocity, and horizontal and vertical eye position. The LabView data acquisition program used during the rotating chair trials saved these time series in three binary files per trial. These binary files were converted to MatLab format using a modified C program called *Convert* (Balkwill, 1992). Once in MatLab format the horizontal eye position data from each experiment (linear and angular VOR) were

analyzed similarly using a number of MatLab scripts originally written by M. D. Balkwill and then modified by J. Christie and J. C. Mendoza and several frequency analysis scripts. Since the Angular and Linear VOR experiments were performed such that the expected response was in the horizontal eye movements , the vertical eye position data was not quantitatively analyzed and will not be discussed in this thesis. In addition, the first four seconds of each trial were not analyzed due to vestibular-induced transients caused by the sudden acceleration of the sled or chair motion which may produce sinusoidal eye movements different from those after the stimulus has reached steady-state.

The algorithm used to calculate the Slow Phase Velocity based on the eye position data is called *NysA v. 1.4* (Nystagmus Analysis). *NysA* is a set of MatLab scripts which were implemented by several previous members of the MIT Man-Vehicle Laboratory (Massoumnia, 1983; Merfeld, 1990; Balkwill, 1992). A user's manual and further description of the *NysA* algorithm can be found in Balkwill (1992). The algorithm first scales the horizontal and vertical eye position data, differentiates it twice using finite impulse response (FIR) digital filters, and calculates eye velocity and eye acceleration along each axis. The fast phase detection algorithm uses the magnitude of the two-dimensional acceleration vector to locate and remove the majority of the saccades from the velocity signal. By adding the acceleration vectors from each axis, it estimates the absolute magnitude of the acceleration as a function of time. Fast phases are located when the magnitude of the total acceleration exceeds two standard deviations from the mean. Interpolations of the velocity are made based on the velocity at the beginning of the saccade.

The automated fast phase removal algorithm correctly detects approximately 90-95% of the saccades in the slow phase velocity signal. Manual editing is used to identify and

remove any remaining saccades from the slow phase velocity signal. It is performed using a version of the original *NysA edit_spv* which was revised by J. Christie and called *edit_spv_dual*. The procedure displays the eye position, velocity, and slow phase velocity to the user. Fast phases that were missed by the automatic saccade removal algorithm can be removed and any incorrect interpolations may be removed or modified. The beginning and end points of the undetected saccades are selected by the operator. The saccade is replaced by a first order interpolation between the two endpoints, as opposed to the inferior zero-order interpolations made during the automatic desaccading process. Although the first-order interpolations are superior, to minimize the operator bias introduced during manual editing of the slow phase velocity, only obvious missed saccades were edited from the signal unless gross over interpolations were made by the automatic algorithm.

After calculating the slow phase velocity (SPV) of the eye movements a frequency analysis is performed to determine if it has oscillations at the frequency of the stimulus or its harmonics. Each cycle analyzed is fit with a combination of a sine and cosine at the desired frequency which define the vector of the response. The method Least Squares is used to perform the frequency analysis. Four frequencies, the stimulus frequency and its first three higher harmonics (2nd, 3rd, and 4th), and a DC component are simultaneously analyzed using a MatLab script called *freq_analysis*. A more thorough explanation of the frequency analysis methods is located in Mendoza (1993). *freq_analysis*, written by J. Christie and J. Mendoza generates polar plots of the sine and cosine amplitudes for qualitative analysis. Each polar plot shows the eight cycles and the mean resultant vector. The convention maintained throughout the analysis is that a phase difference of 180° indicates that the response was in the compensatory direction relative to the sled (velocity 180° out of phase with respect to the sled) or optokinetic stimulus (velocity in-phase with the OK stimulus velocity).

After calculation of the magnitude and phase information for each of the three test conditions pre- and post-adaptation, statistical analysis is used to test whether the responses are significantly different from zero and to compare the pre-adaptation responses to the post-adaptation responses.

As the output of the frequency analysis has two components, the sine and cosine representing the magnitude and phase information, a multivariate statistical method was employed. This was done by extending the concept of the univariate confidence intervals determined by a t-test to a multivariate confidence area determined by the Hotelling's T^2 distribution. (Mendoza, 1993). The confidence region of the mean μ of a **p**-dimensional normal population is obtained from the following equation:

$$P\left[n(\overline{X}-\mu)' (S)^{-1}(\overline{X}-\mu) \leq \frac{(n-1)p}{(n-p)} F_{p,n-p}(\alpha) \right] = 1-\alpha \qquad (3.8)$$

where **n** is the number of samples, **p** is the number of parameters, $\overline{X}$ is the mean of the data, **S** is the covariance matrix of the given data, and **F** is the value of the F statistic for the appropriate number of degrees of freedom. The points satisfying this equation define an ellipse centered at the mean of the data, $\overline{X}$. The ellipses were generated using the MatLab scripts *Mult_Sbj* and *Conf_Sbj* (Mendoza, 1993). Figure 3.8 contains an overview of the main elements in the data analysis pathway for the VOR experiments and printouts of the primary analysis programs and scripts are located in the appendix.

3.3.3. Adaptation Frequency Analysis

During the adaptation paradigm the sled velocity channel was collected at a sampling rate of 200 Hz. The MatLab script called *Adaptation* written by the author utilized the Fast-

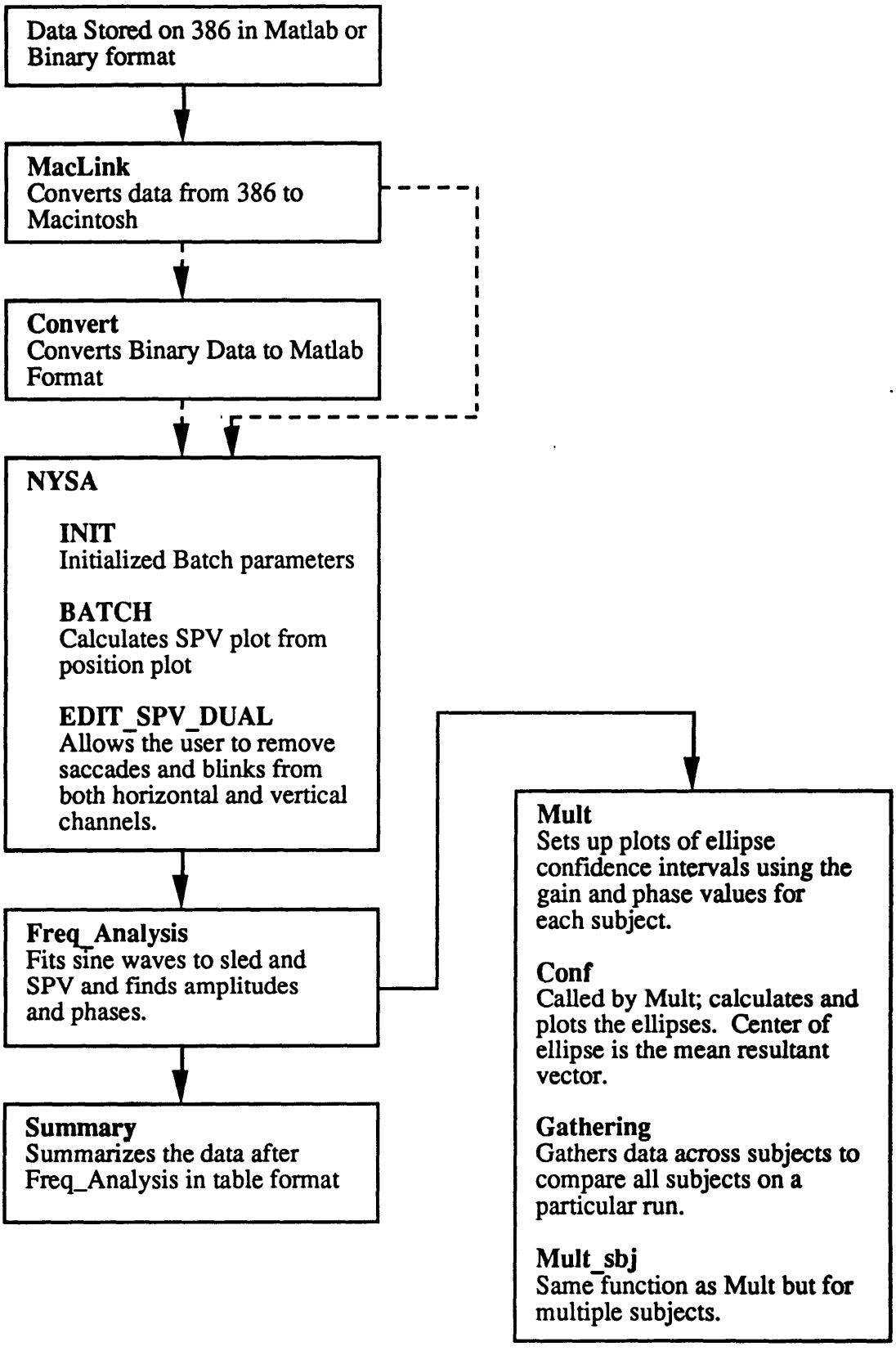

Figure 3.8. Summary of linear and angular VOR data analysis.

Fourier Transform (FFT) function in MatLab to attain a power spectral density function of the sled velocity signal. Analysis of each subjects' adaptation paradigm may provide some explanations for the type of adaptation or lack of adaptive responses in each of the post-adaptation experiments.

In MatLab, the function FFT(X) is the discrete Fourier transform of vector X. If the length of X is a power of two, a fast radix-2 fast-Fourier transform algorithm is used. If the length of X is not a power of two, a slower non-power-of-two algorithm is employed. Therefore, to decrease the processing time the first step in performing this analysis was to reduce or enlarge the data set to be a length that is a power of two. MatLab allows the user to do this by defining the number of points in the vector to be analyzed. FFT(X,N) is the N-point FFT, padded with zeros if X has less than N points and truncated if it has more. The majority of the files containing the sled velocity signal from the adaptation paradigm are approximately 60020 points corresponding to the five minute session sampled at 200 Hz. If the subject were to hit the safety break located at the end of the track during the five minute session, a new file was started. Thus, a few trials exist with a smaller number of points. The power of two closest to 60020 is 2^{16} points = 65536. This means the data was padded with approximately 5516 points. After taking the fast-Fourier transform (FFT), the power spectral density provides a measurement of the energy at the various frequencies. The power spectral density is found by multiplying the resultant of the FFT by its complex conjugate. One can then plot the power spectral density function versus frequency to view the primary frequencies of the sled velocity signal.

4. RESULTS

The following chapter is divided into two major sections: Hidden Target Pursuit and Adaptation. Each section is further divided by the experiments performed. As significant differences exist between subjects, averaging responses across subjects would be difficult to interpret statistically. Therefore, one subject most representative of the subject pool in each experiment will be analyzed in depth to lead the reader through the analysis process and the results gathered from it. The results from the other subjects for each experiment will be discussed, compared, and contrasted with the representative subject, and associated summary plots and tables can be found in the appendices. In addition, at the end of each sub-section, a summary plot is given averaging the eye movement responses to the particular experiment conditions to provides an overall qualitative understanding of the subjects' responses.

4.1. Hidden Target Pursuit

This section presents the results from the magnitudes and directions of the horizontal (y-axis experiments) and vertical (z-axis experiments) eye movements during the fixed displacement and fixed duration hidden target pursuit experiments. The y-axis experiments were run primarily to replicate and further investigate previous experiments run by Israël and Berthoz (1989) and Buizza, et al (1979). The results from those previous studies will be compared to the current data in the Discussion section. Similar target pursuit experiments have never before been performed along the z-axis. The description of the results for each sled orientation (y-upright and z-supine) will follow the outlines given in Table 4.1 for the fixed displacement and Table 4.2 for the fixed duration experiments. They are provided here as a "road map" to aid the reader through the subsections. In each experiment four conditions are compared: two directions of sled

displacement (right/left or up/down) and either two displacement amplitudes (fixed displacement test) or two trial durations (fixed duration test).

Table 4.1 Organization of the discussion of the fixed displacement experimental results.

1) Mean eye movement gains (eye displacement/sled displacement) are plotted versus sled acceleration and discussed for each of the four conditions.
2) Threshold levels for perception of linear translation are calculated and discussed.
3) Differences between the test conditions are plotted versus sled acceleration.
4) χ^2 statistics are used to test for significant differences between the four conditions.
5) Discussion of directional asymmetry (for all accelerations, above threshold accelerations, and below threshold accelerations)
6) Discussion of differences between 10 and 20 degree trials (for all accelerations, above threshold accelerations, and below threshold accelerations)
7) Discussion of subjective correct response data.
8) Mean subjective response gains (subjective displacement/sled displacement) are plotted versus sled acceleration and discussed for each of the four conditions. (z-axis only)
9) χ^2 statistics are used on subjective responses to test for significant differences between the four conditions. (z-axis only)
10) Discussion of subjective directional asymmetry. (z-axis only)
11) Discussion of subjective differences between 10 and 20 degree trials. (z-axis only)
12) Brief discussion of other subjects.
13) Plots and discussion of mean normalized eye movements (gain) for all subjects averaged together.

Table 4.2. Organization of the discussion of the fixed duration experimental results.

1) Scatter plots of the eye movement data.
2) Linear regression analysis comparing the 1.0 and 2.5 second trials.
3) Mean eye movement gains (eye displacement/sled displacement) are plotted versus sled displacement and discussed for each of the four conditions.
4) Differences between the test conditions are plotted versus sled displacement.
5) χ^2 statistics are used to test for significant differences between the four conditions.
6) Discussion of directional asymmetry.
7) Discussion of differences between trial durations.
8) Discussion of subjective correct response data.
9) Scatter plot comparing subjective estimates of translation to eye movements.
10) Mean subjective response gains (subjective response/sled displacement) are plotted and discussed for each of the four conditions.
11) χ^2 statistics are used on the subjective responses to test for significant differences between the four conditions.
12) Discussion of subjective directional asymmetry.
13) Discussion of subjective differences between the 1.0 and 2.5 second trials.
14) Brief discussion about other subjects.
15) Plots and discussion of mean normalized eye movements (gain) for all subjects averaged together.

In all of the Hidden Target Pursuit experiments the eye movements evoked by the damped position step sled profile while the subject visually tracked the hidden target usually often a combination of compensatory smooth pursuit and compensatory saccades (fast phases). Figure 4.1 shows a typical time series of the raw horizontal eye movement data (upper trace) for a trial in the hidden target pursuit experiments. The eye began to follow the hidden target shortly after the sled motion started and reached the maximum amplitude just before the sled motion stopped. The particular time series shown is a trial in the y-axis with a sled acceleration of 4.5 milliG and a commanded displacement of 18.20 cm, however it is also typical of trials in the z-axis. The bottom trace is the sled position signal which was measured during the adaptation experiment and both z-axis experiments, but not during the y-axis experiments where sled velocity was collected.

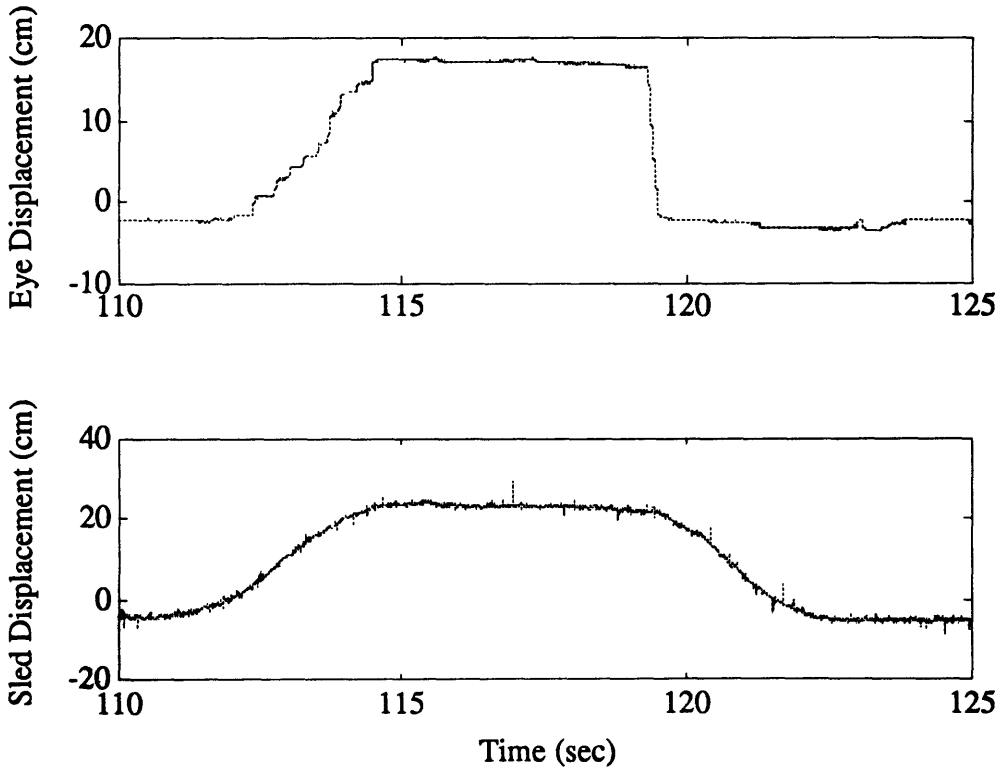

Figure 4.1. Typical trial for the hidden target pursuit experiment. The eye movement trace has been inverted for comparison. While tracking the imaginary target the eyes move in the opposite direction from the sled.

4.1.1. Y-Axis Experiments

Overall, during the Y-axis experiments subjects were able to track the target moderately well. No consistent directional asymmetry was found in the eye movement responses. The overall threshold level for detection of direction was approximately 3.0 milliG. Inconclusive evidence shows that eye movements tend to depend on trial duration, with larger eye movements occurring during longer trial durations. Normalized eye movement and subjective response gains were larger during the 10 degree trials than the 20 degree trials, indicating overcompensation of the smaller sled displacements. The following will describe the details of the two hidden target pursuit experiments in the Y-axis.

4.1.1.1. Fixed Displacement Test

As stated in the Methods section, the relationship between mean eye movement amplitudes and sled acceleration was analyzed through statistical methods and observational strategies. Figure 4.2 shows four plots of the normalized (eye displacement/sled displacement) means and standard errors for subject BP during the y-axis fixed displacement target pursuit experiment. The four plots compare the mean eye movement response at each acceleration level for the four different trial conditions. The first two plots separate the data into (a) 10 degree and (b) 20 degree trials comparing the subject's responses to sled displacements to the left and right. The third and fourth plots in Figure 4.2 separate the (c) rightward trials from the (d) leftward trials to compare the response to the 10 and 20 degree (8.82 and 18.20 cm) sled displacements. Similar plots for the other seven subjects are included in Appendix A. The eye movement responses have been normalized by dividing the amplitude of the eye movement in centimeters by the commanded sled displacement in centimeters to produce a measure of overall gain similar to Israel and Berthoz's 'Vestibular Saccadic' gain (1989). If the subject were to perfectly compensate for the sled displacement, the normalized value would be 1.0. If the subject were to over- or under-compensate for the sled movement, the normalized value

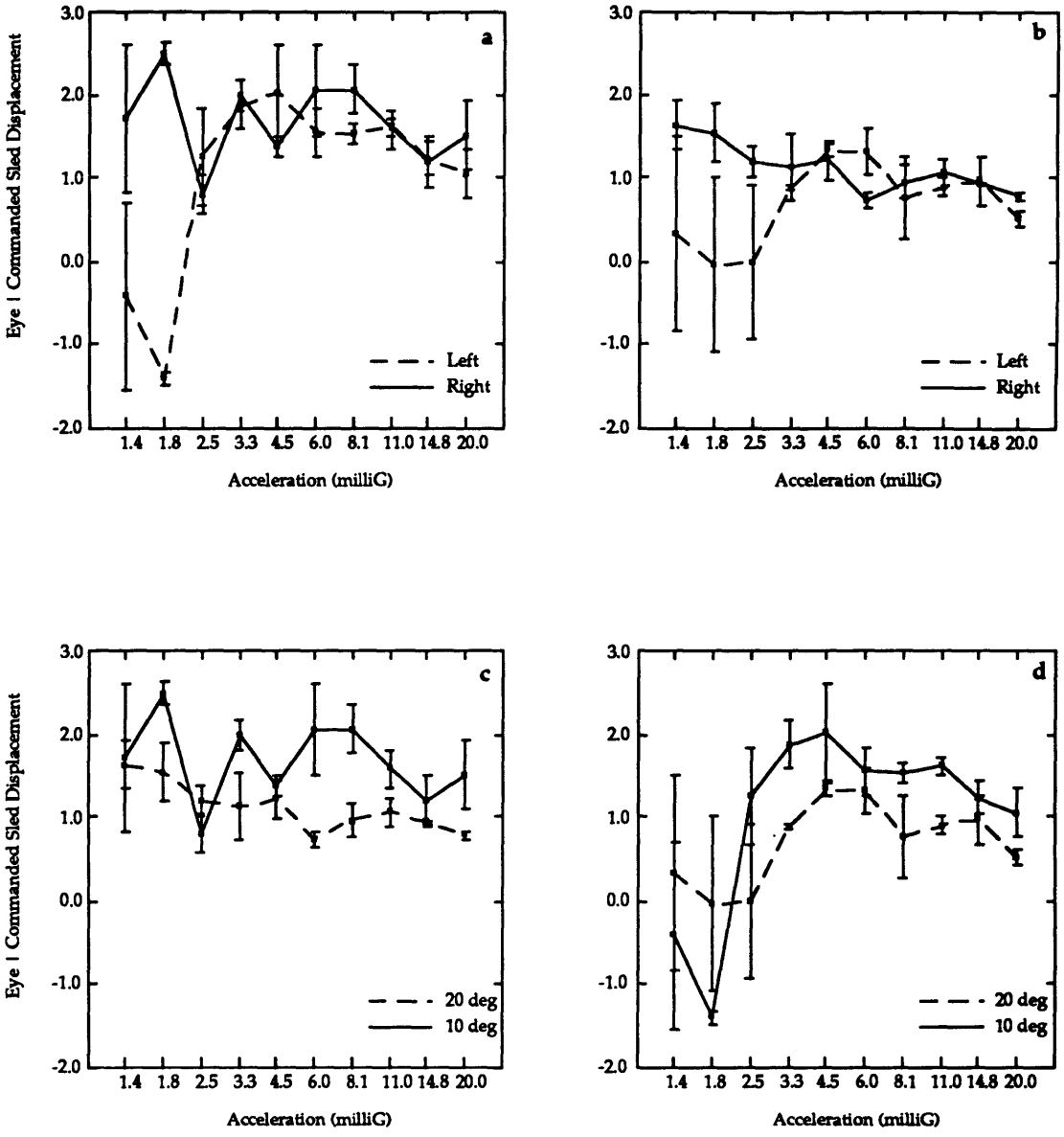

Figure 4.2. Y-Axis Fixed Displacement eye movement data for subject BP. a) 10 degree trials comparing leftward and rightward trials, (b) 20 degree trials comparing leftward to rightward trials, (c) rightward trials comparing 10 and 20 degree trials, (d) leftward trials comparing 10 and 20 degree trials. Error bars signify standard error.

would be greater or less than 1.0, respectively. As stated in the Methods section, eye movements were measured using electrooculography (EOG) in the y-axis fixed displacement experiment, which adds to the signal variation but should not have an effect on the average response.

As expected, the variance of the mean responses at the lower G-levels (below threshold) was higher than that of the higher G-levels for subject BP. A smaller mean (closer to zero or negative) and higher variance indicate that the subject sometimes responded with eye movements in the incorrect direction. Threshold levels for detection of linear acceleration were chosen based on the 'rule' described in the METHODS section, namely *the lowest of two or more consecutive accelerations where the mean eye displacement is significantly different from zero.* Table 4.4 and Table 4.5 show the threshold level for perception calculated for each subject in each of the four test conditions. One would expect that at an acceleration level below a person's threshold the mean response of many trials would average to approximately zero, confirming that the probability of 'guessing' the correct direction is fifty percent. With only two data points at each acceleration level in each condition, an average response of zero is rarely observed. However, the variances are usually high.

Table 4.3. Summary of eye movement threshold levels for each subject during each test condition.

Subject	10 degree trials RIGHT	10 degree trials LEFT	20 degree trials RIGHT	20 degree trials LEFT
BP	1.8	3.3	< 1.4	3.3
JM	1.8	6.0	< 1.4	6.0
KP	6.0	3.3	< 1.4	3.3
LF	< 1.4	2.5	< 1.4	< 1.4
LH	3.3	3.3	< 1.4	6.0
SS	1.8	< 1.4	2.5	< 1.4
TL	< 1.4	6.0	3.3	4.5
WT	1.8	1.8	< 1.4	< 1.4

Except at the two lowest acceleration levels (< 2.5 milliG) subject BP displayed no left/right asymmetry in the 10 degree trials. An independent student t-test was performed on the mean normalized eye movement responses at each acceleration to test for a difference between displacements toward the subject's right and left. Subject BP showed a significant left/right difference at only one acceleration level in the 10 degree cases (1.8 milliG). At 1.8 milliG, he responded in the wrong direction for both leftward trials and in the correct direction for both rightward trials, meaning he moved his eyes left in all four trials. In the 20 degree trials his mean response to rightward trials was larger than the left at the lower accelerations, but the variability was so high that no statistical difference was determined. Above threshold he showed no left/right asymmetry, and similar left/right symmetries were observed in the other seven subjects. However, to confirm that no asymmetry exists, a χ^2 test was performed on the differences between the rightward and leftward trials across all acceleration levels. Comparing the 10 and 20 degree trials, it is evident from the high gains in Figure 4.2 (c) and (d) that subject BP overcompensated for the 10 degree trials in both directions, yet he accurately compensated for the 20 degree trials variation at the low accelerations.

Figure 4.3 shows plots of the differences between subject BP's rightward and leftward trials and 10 and 20 degree trials. These difference plots make any significant disparity between the conditions under examination more visible. In Figure 4.3 (a) it is clear that BP responded asymmetrically at the lowest two accelerations, favoring sled displacements toward his right. At higher accelerations, however, the difference plot varies insignificantly around zero, indicating no asymmetry. Table 4.4 and 4.5 summarize the results from the χ^2 tests performed on all acceleration levels simultaneously, on accelerations above threshold, and on accelerations below threshold. A distinction is made between sub- and super-threshold accelerations because they could be interpreted as belonging to two different populations as discussed in the Methods

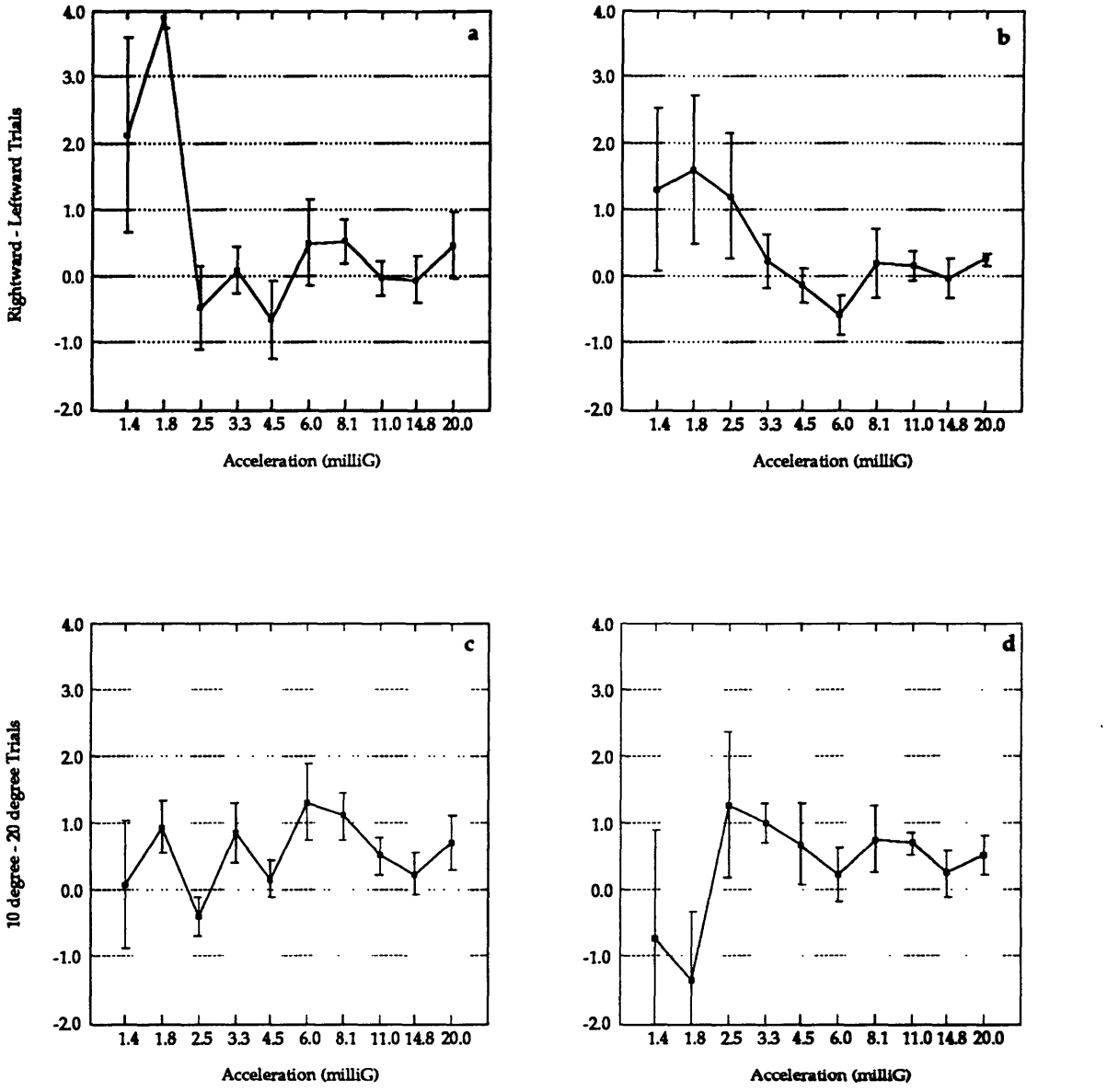

Figure 4.3. Y-Axis Fixed Displacement difference plots for subject BP. (a) difference between rightward and leftward 10 degree trials, (b) difference between rightward and leftward 20 degree trials, (c) difference between 10 and 20 degree rightward trials, (d) difference between 10 and 20 degree leftward trials. Error bars indicate standard error of the difference.

Table 4.4. Y-axis Fixed Displacement test summary of χ^2 tests of right/left asymmetry for all subjects. • = < 0.001, √ = < 0.005, † = < 0.025, Δ = < 0.05.

Subj.	Right - Left Difference Test	N	χ^2: 10° trials	Trend	P	N	χ^2: 20° trials	Trend	P
BP	All Accelerations	10	569.360	var.	•	10	18.411	var.	Δ
	Above Threshold	7	5.461			7	13.515		
	Below Threshold	3	563.897	R>L	•	3	4.896		
JM	All Accelerations	4	516.580	R>L	•	8	54.785	R>L	•
	Above Threshold	2	507.511			5	36.061	R>L	•
	Below Threshold	2	9.069			3	18.724	R>L	•
KP	All Accelerations	5	21.216	R>L	†	10	78.825	R>L	•
	Above Threshold	4	20.592	R>L	•	7	37.474	var.	•
	Below Threshold	1	0.624			3	41.351	R>L	•
LF	All Accelerations	6	14.469	var.	†	2	5.400		
	Above Threshold	3	13.163	var.	√	2	5.400		
	Below Threshold	3	1.306			0	0.0		
LH	All Accelerations	10	18.172	var.	•	7	184.148	var.	•
	Above Threshold	8	3.429			4	163.198	L>R	•
	Below Threshold	1	14.743	R>L	•	3	20.95	R>L	•
SS	All Accelerations	10	19.295	var.	Δ	10	19.044	var.	Δ
	Above Threshold	9	18.041	var.	Δ	8	14.405		
	Below Threshold	1	1.254			2	4.639		
TL	All Accelerations	10	14.782			10	59.833	L>R	•
	Above Threshold	5	6.482			6	57.86	L>R	•
	Below Threshold	5	8.3			4	1.973		
WT	All Accelerations	10	39.648	var.	•	10	155.576	var.	•
	Above Threshold	7	39.485	var.	•	10	155.576	var.	•
	Below Threshold	1	0.163			10	0.0		

section. The P-values associated with the χ^2 statistical test are two-tailed. Therefore, a statistically significant χ^2 value is ambiguous, and its interpretation requires further examination of the data to determine the direction of the trend (which condition is greater) or even if a trend exists. It is common for the difference between two conditions to be significant according to the χ^2 because the difference is significantly greater than zero at some accelerations and less than zero at others. In such a case, no significant trend can be deduced.

Table 4.5. Y-axis Fixed Displacement test summary of χ^2 tests of difference between the 10 and 20 degree trial s. • = < 0.001, √ = < 0.005, † = < 0.025, Δ = < 0.05.

Subj.	10° - 20° Difference Test	N	χ^2: Right trials	Trend	P	N	χ^2: Left trials	Trend	P
BP	All Accelerations	10	33.766	10>20	•	10	41.095	10>20	•
	Above Threshold	9	33.759	10>20	•	7	37.828	10>20	•
	Below Threshold	1	0.007			3	3.267		
JM	All Accelerations	6	138.592	10>20	•	6	14.154	var.	Δ
	Above Threshold	6	138.592	10>20	•	3	8.547	var.	Δ
	Below Threshold	0	0.0			3	5.607		
KP	All Accelerations	10	11.392			10	33.846	10>20	•
	Above Threshold	5	8.814			7	30.795	10>20	•
	Below Threshold	5	2.578			3	3.051		
LF	All Accelerations	2	286.819	10>20	•	4	72.359	10>20	•
	Above Threshold	2	286.819	10>20	•	4	72.359	10>20	•
	Below Threshold	0	0.0			0			
LH	All Accelerations	6	171.503	10>20	•	6	27.158	10>20	•
	Above Threshold	3	158.635	10>20	•	3	22.694	10>20	•
	Below Threshold	3	12.868	10>20	Δ	3	4.464		
SS	All Accelerations	10	102.037	10>20	•	10	438.739	10>20	•
	Above Threshold	8	92.843	10>20	•	10	438.739	10>20	•
	Below Threshold	2	9.194	10>20	†	0	0.0		
TL	All Accelerations	10	68.544	10>20	•	10	39.362	var.	•
	Above Threshold	7	57.234	10>20	•	5	38.915	10>20	•
	Below Threshold	3	11.31		†	5	0.447		
WT	All Accelerations	10	192.812	10>20	•	10	65.195	10>20	•
	Above Threshold	9	192.676	10>20	•	9	64.701	10>20	•
	Below Threshold	1	0.136			1	0.494		

The χ^2 analysis confirms BP's right/left asymmetry below threshold during the 10 degree trials. His responses were symmetric at all other acceleration levels for both the 10 and 20 degree trials. The χ^2 value calculated across all accelerations was also significant during the 10 degree trials because of the large sub-threshold χ^2 values. This exemplifies the importance of separating the above and below threshold accelerations in the χ^2 analysis.

In Figure 4.3 (c) and (d) it is apparent that subject BP's normalized responses to the 10 degree trials was greater than that of the 20 degree trials. The χ^2 values shown in Table 4.5 confirm the difference is significant in both the rightward and leftward sled accelerations. In both directions the difference is most significant above threshold.

Subjective correct response threshold data support the previous results, with a few exceptions, following a rule similar to that used with the eye movement data. As defined in the Methods section, *the subjective response threshold is the lowest of two consecutive acceleration levels where the subject chose the correct direction in at least 75% of the trials*. Table 4.6 summarizes the percent of correct responses for each subject at each acceleration level. The asterisks indicate the threshold acceleration level based on the above rule for each subject. Subject BP's subjective responses are an example of the correlation between the subjective and quantitative data typical of most of the other subjects. His threshold determined from eye movements was less than 1.4 milliG for the trials to the right and between 2.5 and 3.3 for trials to the left (see Table 4.3), which correspond to the subjective thresholds shown in Table 4.6.

The following is a brief description of the results from the other seven subjects. The summary plots and tables similar to those that were presented for subject BP are included in Appendix A.

Subject JM and KP responded similarly to BP, with small mean amplitudes and high variance at low acceleration levels and larger mean amplitudes (overcompensation in some cases) and smaller variances at higher accelerations. For these three subjects a clear transition was visible on the plots indicating the threshold level.

Table 4.6. Summary of subjective percent correct responses for each subject at each acceleration level.

Subj.	Cond	1.4	1.8	2.5	3.3	4.5	6.0	8.1	11.0	14.8	20.0
BP	Right	100*	100	100	100	100	75	100	100	100	100
	Left	50	25	75*	100	100	100	100	100	100	100
JM	Right	100*	75	100	100	75	100	100	100	100	100
	Left	75	50	75*	100	100	100	100	100	100	100
KP	Right	75*	100	75	75	100	100	100	100	100	100
	Left	25	75	50	100*	100	100	100	100	100	100
LF	Right	50	100*	100	100	100	100	100	100	100	100
	Left	100*	100	100	100	100	100	100	100	100	100
LH	Right	100*	100	50	100	100	100	100	100	100	75
	Left	0	75	25	75*	75	75	100	100	100	75
SS	Right	100*	100	75	100	100	100	100	100	100	100
	Left	75*	75	75	100	100	100	100	100	100	100
TL	Right	100*	100	100	100	100	100	100	100	100	100
	Left	100*	100	100	100	100	100	100	100	100	100
WT	Right	75*	100	100	100	100	100	100	100	100	75
	Left	100*	75	100	50	100	100	100	100	100	100

Four of the eight subjects had asymmetric eye movements. Three subjects favored rightward sled displacements during one or both of the sled displacements (BP, KP, JM). As described above, BP showed a significant trend toward rightward eye movements below threshold in the 10 degree cases. Otherwise, his responses were symmetric. Subject KP's response in both the 10 and 20 degree trials was approximately symmetric, but at the two lowest acceleration levels in the 20 degree trials she responded correctly during both rightward displacement and incorrectly during leftward displacements, producing a significant difference. JM's eye movement response was asymmetric in both the 10 and 20 degree trials, with larger responses during rightward displacements. His data is difficult to interpret because several acceleration levels have only one data point in each direction due to experimental circumstances. In the 20 degree trials, 8 of the 10 acceleration levels can be used in the analysis, so the asymmetric result is more believable.

One subject responded with an asymmetry favoring leftward trials (TL). Subject TL showed no consistent right/left asymmetry in the 10 degree trials, but in the 20 degree cases, his mean eye movements were slightly larger to the left than to the right across most accelerations. This asymmetry is opposite from the subjects discussed above that showed a rightward asymmetry in the same conditions.

Four of the eight subjects responded with either no significant directional asymmetry or one that varies across accelerations (SS, WT, LF, LH). SS showed no right/left asymmetry in the 10 degree cases. At the lowest accelerations in the 20 degree cases, he responded as if all of the displacements were to his left, but the χ^2 value was not significant. WT showed no consistent right/left asymmetry in either the 10 or 20 degree cases. As with subject JM, interpretation of the differences in LF's responses was difficult because of missing data points. Although not significant, it appears that in the 20 degree trials she used larger eye movements during trials to her right, but no asymmetry was apparent in the 10 degree trials. Subject LH showed no consistent right/left asymmetry in the 10 degree cases. At the lowest acceleration (1.4 milliG) in the 20 degree cases he responded with leftward eye movements, as if the sled was moving to the right for all four trials. However, at the higher acceleration levels, the right/left asymmetry reversed as his response to trials to the left was greater than in trials to the right. The most unusual point was at the 20 milliG level where subject LH gave an incorrect directional response in half of the 10 degree trials. In the subject debriefing, the subject responded that the trials were "too quick to figure out which direction I was moving."

Overall, subjects did not accurately discriminate between the two different sled displacements. KP was one of very few subjects to accurately compensate for the 10 and

20 degree trials. The mean gain of her response (eye/sled displacement) for both conditions was approximately 1.0, except at two mid-range sled accelerations where her gain in the 10 degree trials was significantly larger than in the 20 degree trials.

The other seven subjects had consistent differences between the gain of their eye movement responses during 10 and 20 degree trials. For subject JM, the same difficulty with missing data points was encountered. However, he tended to overcompensate for the 10 degree trials slightly more than the 20 degree trials. Subject LF responded similar to BP, KP, and JM, but with much larger overcompensation (higher gain). Many of LF's eye movements during the 10 degree trials were up to four times the sled displacement, and approximately two times the 20 degree sled displacements (18.20 cm). LH also significantly overcompensated for both sled displacements. At accelerations in the middle of the range, he overcompensated by as much as four times the 10 degree sled displacements, and by approximately twice the sled displacement during the 20 degree cases. At the low and very high accelerations LH showed large variances and variable mean amplitudes across acceleration levels. Subject WT also overestimated his displacement by two to four times the distance moved, especially at the lower acceleration levels. He consistently overcompensated for 10 degree trials more than the 20 degree trials. SS and TL also tended to overcompensate for the 10 degree trials, especially at the lower accelerations. SS was more accurate during the 20 degree cases (gain of 1.0), while TL undercompensated for the 20 degree trials to his right, and overcompensated for leftward translations, which supports his asymmetry toward leftward trials.

4.1.1.1.1. Summary of Y-axis Fixed Displacement Test

In summary, several subjects had slightly asymmetric responses at some accelerations, but no consistent pattern existed across subjects. A significant difference exists between

the subjects' responses to the two different sled displacements. In the extreme the two different sled displacements were treated approximately the same, leading to an overall normalized gain for the 10 degree trials approximately twice that of the 20 degree trials.

Figure 4.4 shows the comparison of the normalized responses to the four test conditions for all subjects. Quantitative conclusions may be inappropriate because of inter-subject variability. However, it provides an overall qualitative understanding of the subjects' responses to changes in acceleration, including a comparison between the 10 and 20 degree and the rightward and leftward trials.

The average normalized eye movement gain for all subjects was approximately 2.0 for the 10 degree trials indicating an overcompensation of approximately two times the sled displacement. The gain for the 20 degree trials was approximately 1.0 during the leftward trials and slightly larger during trials to the right. Both plots (c) and (d) clearly depict the differences in eye movement gains during the 10 and 20 degree trials. Because the normalized eye movement responses to the two different displacements were quite different, they were kept separate throughout the analysis.

In the Y-Axis experiments, subjects were not asked to verbally report their perceived magnitude of translation. Therefore, it is unknown whether the observed overcompensation accurately reflects a perception of larger displacement than actually attained. However, following the test session during the subject's debriefing, many of the subjects, including subject LF and LH, reported moving as far as two meters during some trials (maximum displacement was 18.20 cm). Reports such as these prompted the experimenter to ask for subjective reports of translation in subsequent experiments.

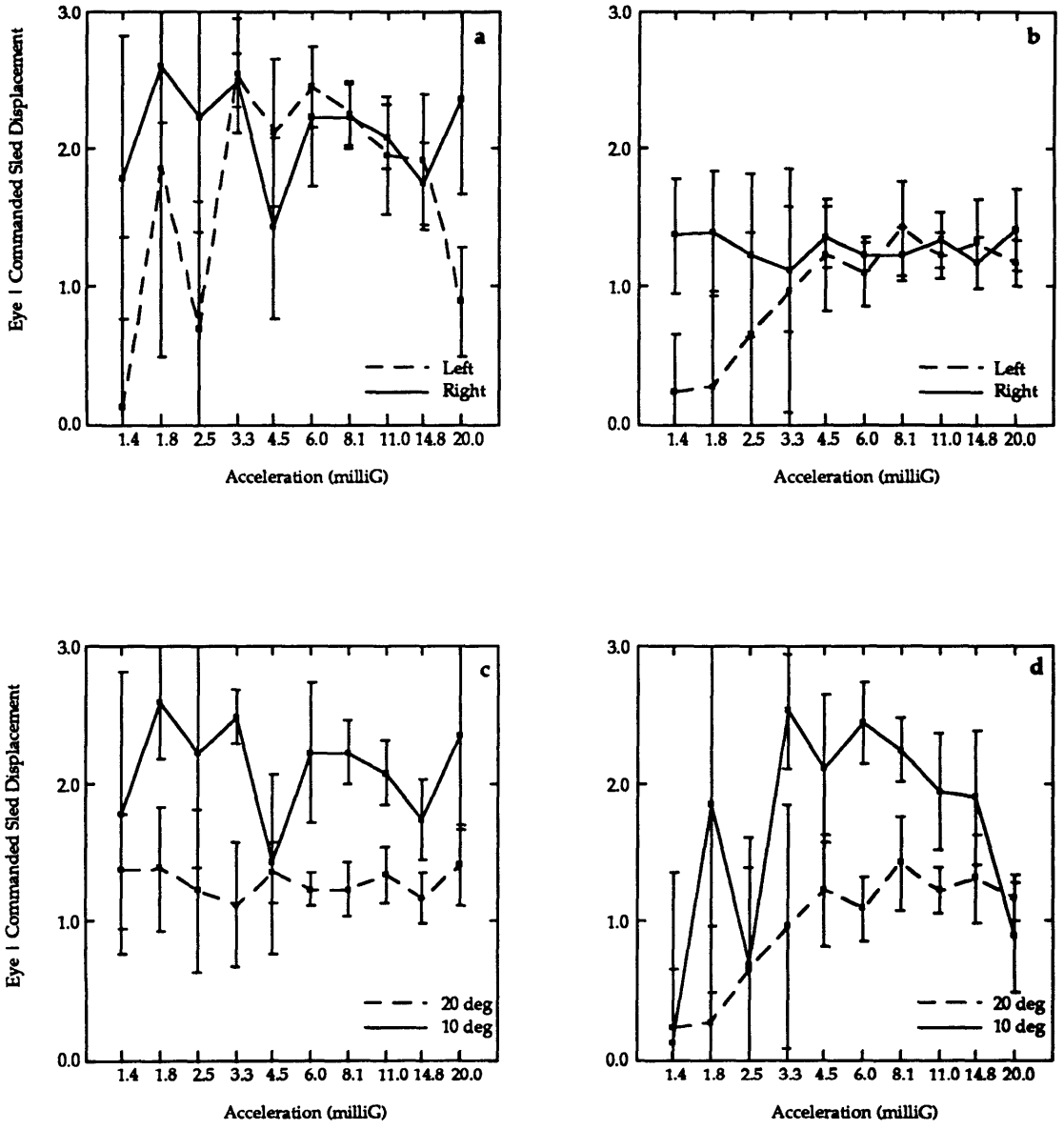

Figure 4.4. Y-Axis Fixed Displacement eye movement data for all subjects. a) 10 degree trials comparing leftward and rightward trials, (b) 20 degree trials comparing leftward to rightward trials, (c) rightward trials comparing 10 and 20 degree trials, (d) leftward trials comparing 10 and 20 degree trials. Error bars signify standard error.

4.1.1.2. Fixed Duration Test

As many of the subjects reported that they perceived that they were moving farther during trials of longer duration, another set of experiments was run to test the relationship between eye movement responses and trial duration. As stated in the Methods, linear regression of the data elicit how well a subject's eye movement response correspond to the distance the sled traveled. These data allow us to test two different observations: 1) whether a difference exists in the responses for two different trial durations and 2) whether the subjects are able to accurately track the hidden target. Thresholds for perception of acceleration were not considered in these experiments since the lowest acceleration tested (5 milliG) was above the threshold level for most of the subjects as shown in the Y-axis Fixed Displacement test. Since trial duration is proportional to the inverse of the acceleration, the longer trials (2.5 seconds) have lower accelerations. Incorrect responses were made more often during the 2.5 second trials where the accelerations are closer to the threshold level for perception of acceleration. Therefore, the incorrect responses were eliminated from the linear regression analysis so that the negative values would not falsely skew the comparisons between the conditions being tested (i.e., 1.0 second versus 2.5 second trials).

Scatter plots of eye movements are shown in Figure 4.5 for a representative subject (subject MB) for comparison to those made by Israël and Berthoz (1989). Similar plots are shown for the other four subjects in Appendix B. Linear regression lines are drawn on the plots to indicate the slope of the data. A slope of 1.0 would indicate that the subject accurately estimated the distance the sled moved by tracking the hidden target with her eyes. Subject MB responded in the correct direction for all displacements tested, as indicated by the lack of negative values on the plot in Figure 4.5.

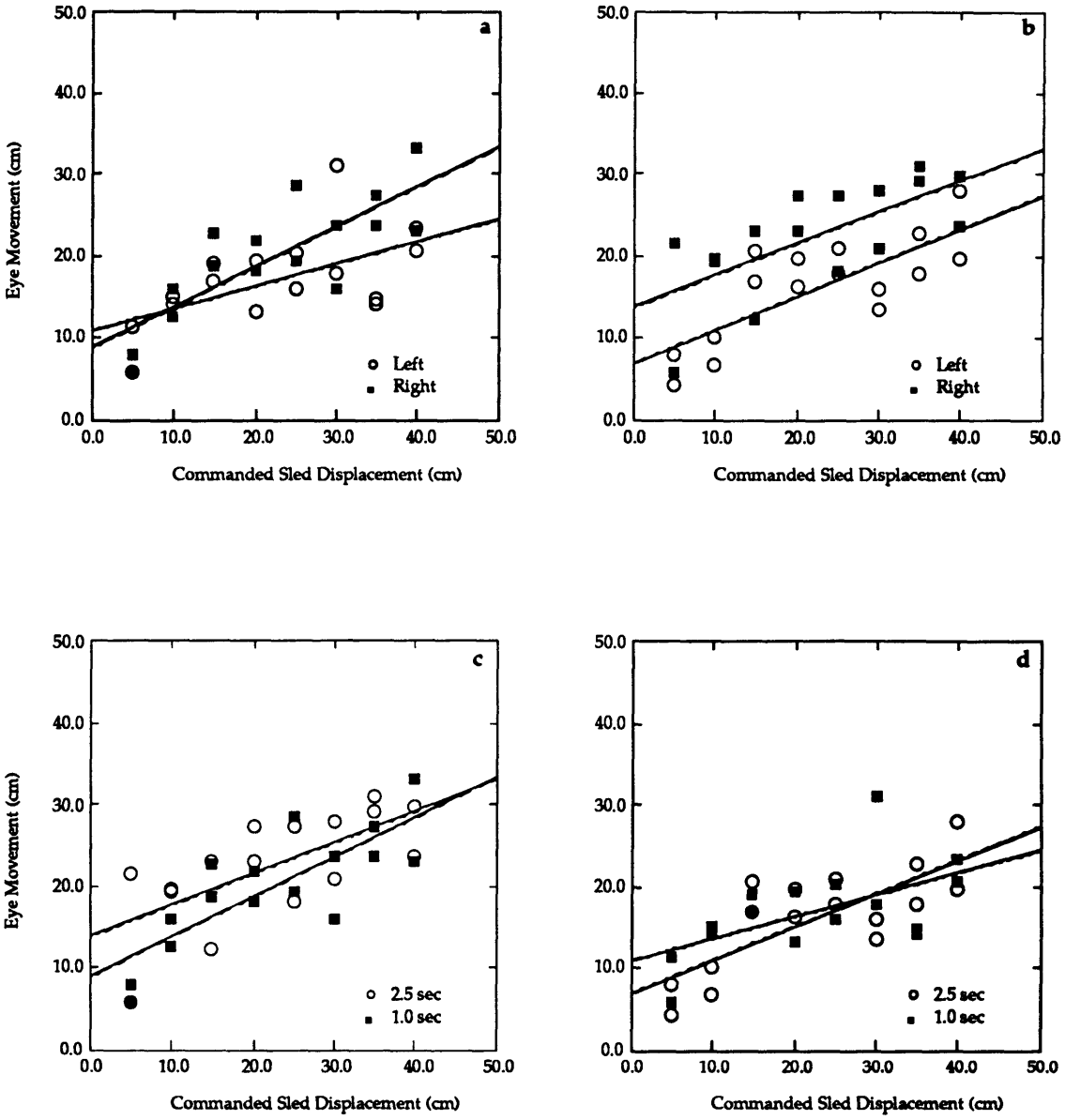

Figure 4.5. Y-Axis Fixed Duration eye movement data comparing 1.0 sec trials and 2.5 sec trials for subject MB. (a) 1.0 second trials comparing leftward and rightward trials, (b) 2.5 second trials comparing leftward to rightward trials, (c) rightward trials comparing 1.0 and 2.5 second trials, (d) leftward trials comparing 1.0 and 2.5 second trials. Error bars signify standard error.

Table 4.7 shows the "regression coefficients", or the "slopes" of the lines relating eye displacement to sled displacement for the 1.0 second trials and the 2.5 second trials, indicating how well each subject estimated the sled displacement. The following three rows provide the p-values describing whether each regression coefficient is significantly different from a slope of 0.0 (no dependence on distance), 1.0 (accurate compensation), or the slope of the trial with the other duration.

Table 4.7. Summary of linear regression analysis for all subjects.

Subject	Test	1.0 second	2.5 second
CL	Regression Coeff.	0.231	0.584
	P-Value H_0: B=0.0	0.004	0.000
	P-Value H_0: B=1.0	0.000	0.000
	P-Value H_0: $B_1=B_2$	0.001	
GS	Regression Coeff.	0.302	0.389
	P-Value H_0: B=0.0	0.026	0.111
	P-Value H_0: B=1.0	0.000	0.018
	P-Value H_0: $B_1=B_2$	0.708	
JM	Regression Coeff.	0.554	0.300
	P-Value H_0: B=0.0	0.000	0.050
	P-Value H_0: B=1.0	0.000	0.000
	P-Value H_0: $B_1=B_2$	0.093	
MB	Regression Coeff.	0.381	0.400
	P-Value H_0: B=0.0	0.000	0.000
	P-Value H_0: B=1.0	0.000	0.000
	P-Value H_0: $B_1=B_2$	0.830	
TC	Regression Coeff.	0.290	0.378
	P-Value H_0: B=0.0	0.000	0.000
	P-Value H_0: B=1.0	0.000	0.000
	P-Value H_0: $B_1=B_2$	0.294	

The slopes of the 1.0 and 2.5 second regression lines are very similar for subject MB, as was typical for the majority of the subjects. Both are significantly greater than 0.0, indicating a positive correlation between the eye displacement and sled displacement (larger eye movements were made with larger sled displacements). However, the

coefficients for both trial durations are also significantly less than 1.0, which indicates inaccurate compensation. MB overcompensated for sled displacements less than 25 cm, and undercompensated for larger sled displacements, resulting in a very flat regression line. This result was true for all five subjects.

The method of linear regression shown above was chosen to allow direct comparison to previous experiments performed by Israël and Berthoz (1989). The high amount of scatter at each sled displacement indicates that MB was not consistent in her responses at each displacement. For instance, at each sled displacement the scatter of subject MB's responses was approximately 15 cm. Therefore, the fit of the regression line had large errors associated with it, making statistical comparisons between regression lines less powerful. A second analysis method was chosen to make more accurate comparisons between the different conditions for each subject. Similar to the fixed displacement experiment, mean eye movement amplitudes and standard errors were calculated for each sled displacement. Figure 4.6 shows four plots of the normalized mean eye displacement versus sled displacement comparing the different test conditions for subject MB: (a) 1.0 second trials comparing right and left, (b) 2.5 second trials comparing right and left, (c) rightward trials comparing the 1.0 and 2.5 second trials, and finally the (d) leftward trials comparing the 1.0 and 2.5 second trials.

The first thing to notice about the four plots in Figure 4.6 is the relatively small error bars compared to the four plots shown in Figure 4.2 for the y-axis fixed displacement experiment. The smaller error is primarily attributable to the use of scleral search coils for eye movement measurements as opposed to EOG.

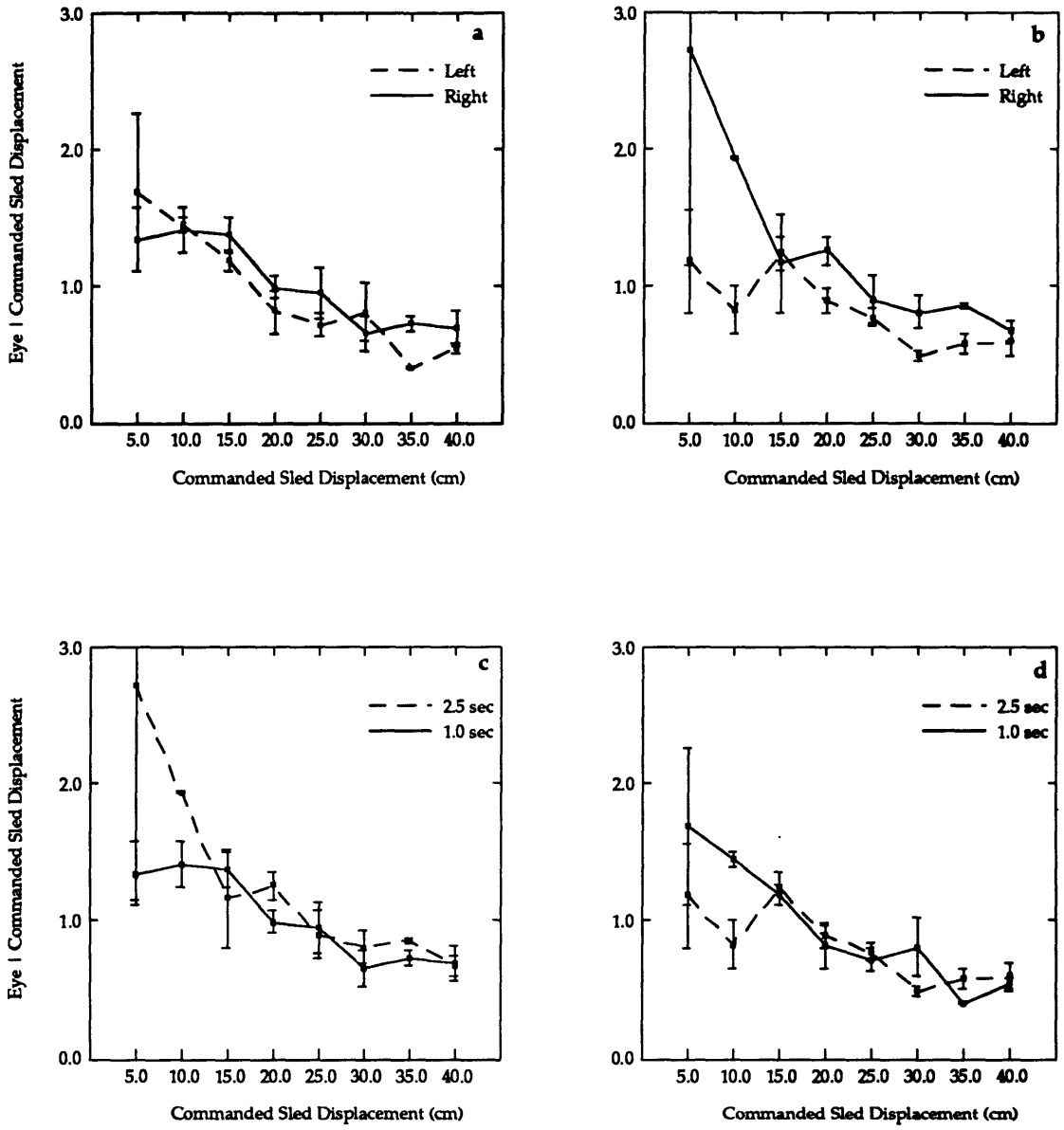

Figure 4.6. Y-Axis Fixed Duration mean normalized eye movements for subject MB. (a) 1.0 second trials comparing leftward and rightward trials, (b) 2.5 second trials comparing leftward to rightward trials, (c) rightward trials comparing 1.0 and 2.5 second trials, (d) leftward trials comparing 1.0 and 2.5 second trials. Error bars signify standard error.

The most interesting result from Figure 4.6 is the downward trend of the normalized eye movements. As the sled displacement increased, subject MB's normalized eye movement response (gain) decreased. Thus, she overcompensated for the smaller sled displacements and undercompensated for the larger displacements, as was also apparent by the slopes of less than 1.0 in the regression plot of Figure 4.5.

Further simplification of the plots in Figure 4.6 and statistical analysis of the data was performed similar to that of the Y-axis Fixed Displacement test to investigate any significant differences between the four test conditions. The mathematical difference between the responses for each test condition was calculated and then plotted versus sled displacement as shown in Figure 4.7. MB exhibited slightly larger eye movements in trials to the right than to the left in the 2.5 second trials and at one sled displacement in the 1.0 second trials. Otherwise the plots appear to vary around a line at zero. Similar observation of 4.7 (c) and (d) shows that MB responded with slightly greater eye movements in the 2.5 second trials than in the 1.0 second trials to the right, but showed no consistent difference dependent upon the duration in the trials to the left.

For statistical purposes a χ^2 test was performed on each difference curve to determine whether the calculated difference between the two trial durations was significant. Table 4.8 summarizes the results from the χ^2 test for all subjects. The p-value gives the probability that the difference between the two conditions was due to chance alone. The last column describes from observation of the difference plots the direction of the trend if one exists.

Subject MB displayed a significant right/left asymmetry in her eye movement response to both the 1.0 and 2.5 second trials, favoring trials to the right. In regards to the dependence of eye movements on trial duration, subject MB responded with larger eye

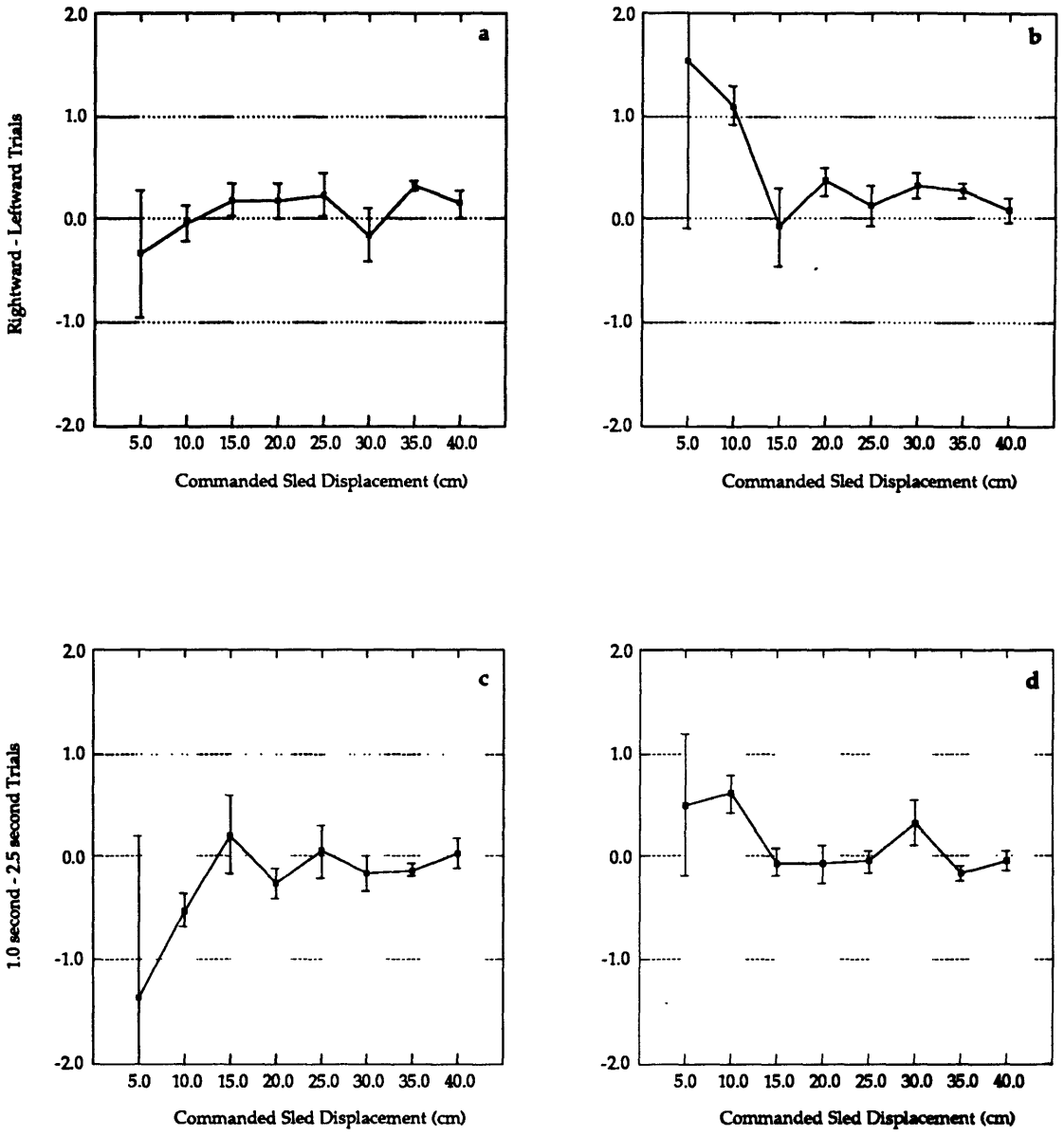

Figure 4.7. Y-Axis Fixed Duration plots of the differences in the mean normalized eye movements for the four conditions tested for subject MB. (a) 1.0 second trials comparing leftward and rightward trials, (b) 2.5 second trials comparing leftward to rightward trials, (c) rightward trials comparing 1.0 and 2.5 second trials, (d) leftward trials comparing 1.0 and 2.5 second trials. Error bars signify standard error of the difference.

Table 4.8. Summary of χ^2 statistical analysis for all subjects in the Y-axis Fixed Duration test. • = <0.001, √ = <0.005, † = <0.025, Δ = <0.05, blank = not significant.

Subj.	Difference Test	N	χ^2	P	Sign. Trend
CL	1 s trials: Right - Left	8	13.258		
	2.5 s trials: Right - Left	8	30.183	•	variable
	Right trials: 1s - 2.5s	8	53.833	•	2.5s > 1.0s(var.)
	Left trials: 1s - 2.5s	8	135.169	•	2.5s > 1.0s
GS	1 s trials: Right - Left				
	2.5 s trials: Right - Left				
	Right trials: 1s - 2.5s				
	Left trials: 1s - 2.5s				
JM	1 s trials: Right - Left	8	37.275	•	Left > Right
	2.5 s trials: Right - Left	8	17.283	Δ	variable
	Right trials: 1s - 2.5s	8	27.655	•	2.5s > 1.0s
	Left trials: 1s - 2.5s	8	6.567		
MB	1 s trials: Right - Left	8	44.513	•	Right > Left
	2.5 s trials: Right - Left	8	69.301	•	Right > Left
	Right trials: 1s - 2.5s	8	20.649	†	2.5s > 1.0s
	Left trials: 1s - 2.5s	8	20.279	†	1.0s > 2.5s(var.)
TC	1 s trials: Right - Left	8	100.494	•	Left > Right
	2.5 s trials: Right - Left	8	216.037	•	Left > Right
	Right trials: 1s - 2.5s	8	14.979		
	Left trials: 1s - 2.5s	8	75.365	•	2.5s > 1.0s

movements during the 2.5 second trials than the 1.0 second trials during rightward sled motion , but the same result was not significant during motion to the left. This result is not supported by the regression analysis shown previously in Table 4.7 for subject MB, as the regression coefficients for the two trial durations were not significantly different from one another.

Subjective correct response data could be used to determine if subjects responded correctly more frequently to trials to the left or right or during 1.0 second or 2.5 second trials. As shown in Table 4.9 however, MB answered in the correct direction for all trials. Therefore, the left/right asymmetry shown in the χ^2 analysis above was due entirely to differences in the magnitudes of her eye movements, not incorrect perceptual responses.

Table 4.9. Percent of correct subjective responses for all subjects during the Y-axis Fixed Duration test.

Subj.	Cond	5	10	15	20	25	30	35	40
CL	Right	75	75	100	100	75	100	100	50
	Left	75	100	100	100	100	100	100	100
GS	Right	100	100	100	100	100	100	100	100
	Left	100	100	100	100	100	100	100	100
JM	Right	100	100	75	100	100	100	100	100
	Left	75	100	100	100	100	100	100	100
MB	Right	100	100	100	100	100	100	100	100
	Left	100	100	100	100	100	100	100	100
TC	Right	100	100	100	100	100	100	100	100
	Left	100	100	100	100	100	100	100	100

Analysis of the subjective estimates of translation can also be used to more fully understand the quantitative eye movement data. Figure 4.8 shows that subject MB subjectively overcompensated for the larger sled displacements, effectively raising the slope of the regression line close to 1.0 as we would expect during accurate compensation. Although the slope of the regression line is closer to 1.0, the subjective data contains a large amount of scatter at each sled displacement similar to the eye movement data, indicating a large error associated with the fit of the regression line.

An analysis similar to that performed for the eye movement data was performed on the subjective data to test whether the differences between the test conditions are significant. Although the same procedure was employed, for brevity only the plots of the mean normalized responses to the four conditions are given in Figure 4.9. The difference plots have been excluded.

A χ^2 test was performed to test whether the differences between the plots shown are statistically significant. The summary statistics from the χ^2 test are shown in Table 4.10. In the 1.0 second trials the difference between MB's subjective responses during

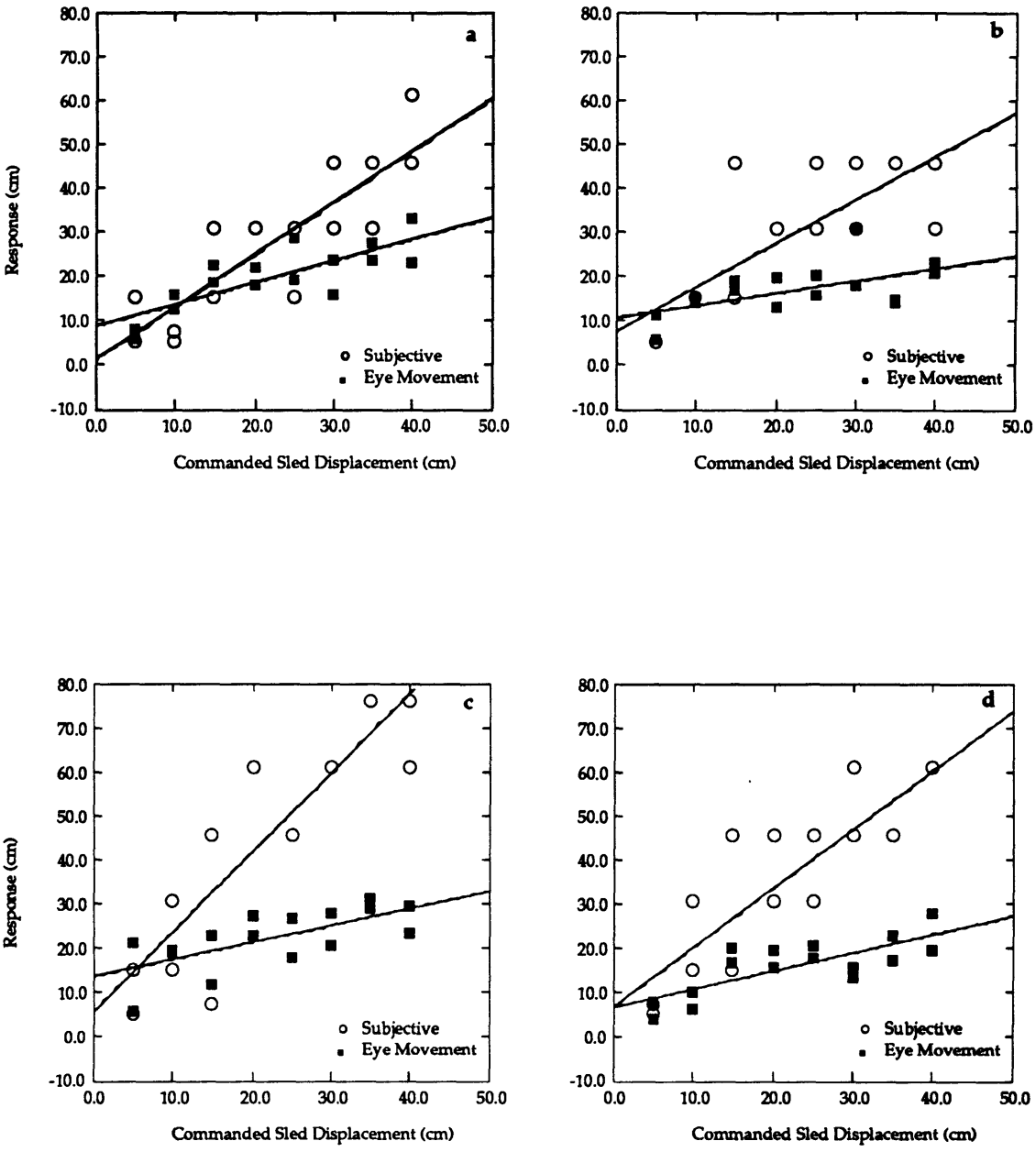

Figure 4.8. Comparison of subjective response and magnitude of eye movements for subject MB. (a) 1.0 second rightward trials, (b) 1.0 second leftward trials, (c) 2.5 second rightward trials, (d) 2.5 second leftward trials.

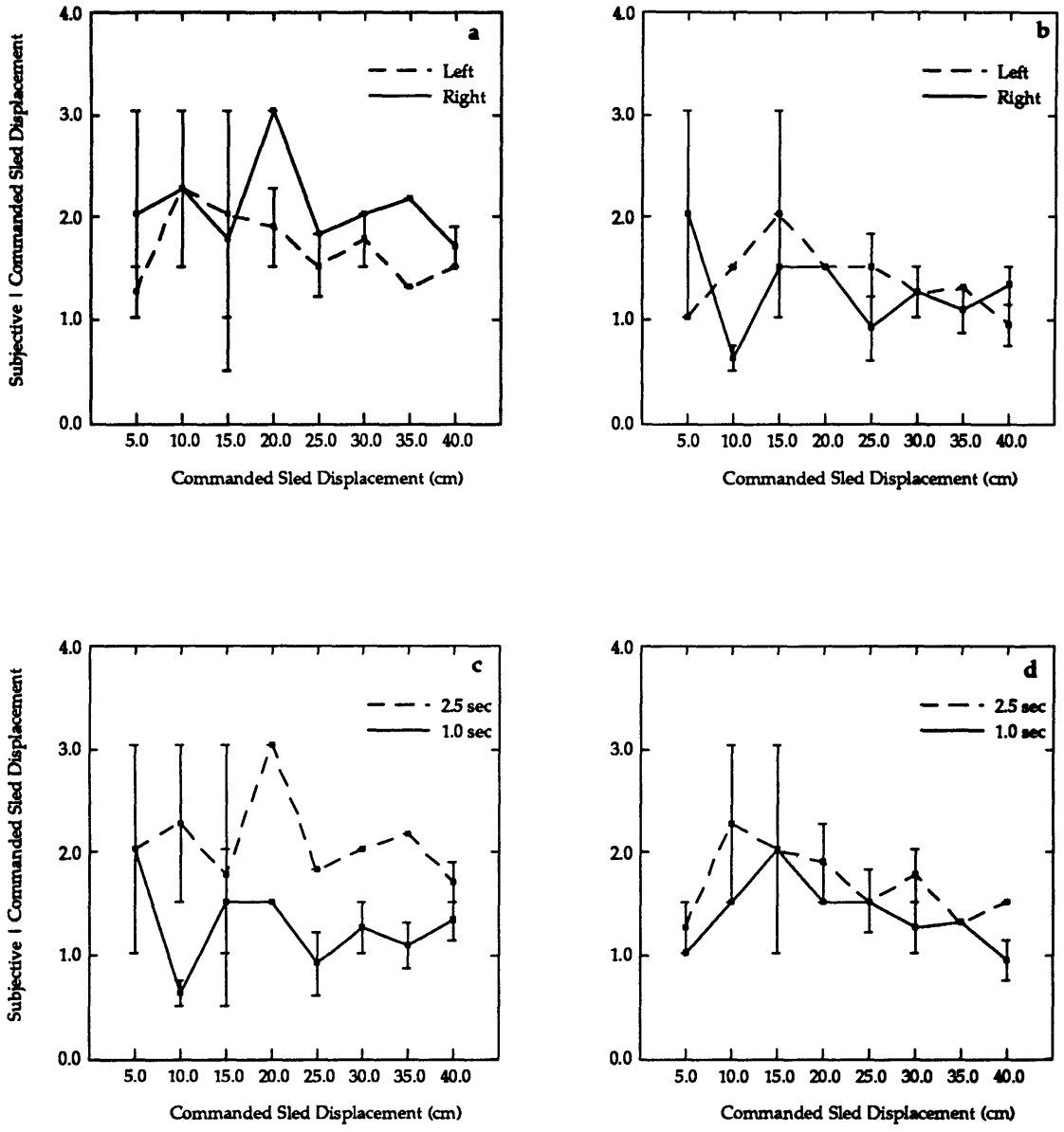

Figure 4.9. Mean normalized subjective responses for subject MB. (a) difference between rightward and leftward 1.0 second trials, (b) difference between rightward and leftward 2.5 second trials, (c) difference between 1.0 and 2.5 second rightward trials, and (d) difference between 1.0 and 2.5 second leftward trials. Error bars indicate the standard error of the difference.

rightward trials and leftward trials was somewhat variable with some bias toward the leftward trials. Whereas in the 2.5 second trials, her subjective responses were slightly biased toward the rightward displacements, but was not statistically significant (Table 4.8). These responses are not consistent with her eye movement responses, where she demonstrated a significant bias towards rightward trials in both the 1.0 and 2.5 second trials. In both the rightward and leftward trials MB gave a subjective report of moving farther during the 2.5 second trials, but the bias was only significant in the rightward trials. This agrees with the results from her eye movement responses.

Table 4.10. Summary of χ^2 statistical analysis for the subjective responses of all subjects in the Y-axis Fixed Duration test. • = <0.001, √ = <0.005, † = <0.025, Δ = <0.05, blank = not significant.

Subj.	Difference Test	N	χ^2	P	Trend
CL	1 s trials: Right - Left	7	5.725		
	2.5 s trials: Right - Left	8	5.645		
	Right trials: 1s - 2.5s	7	36.549	•	2.5s > 1.0s
	Left trials: 1s - 2.5s	8	26.523	•	2.5s > 1.0s
GS	1 s trials: Right - Left				
	2.5 s trials: Right - Left				
	Right trials: 1s - 2.5s				
	Left trials: 1s - 2.5s				
JM	1 s trials: Right - Left	4	4.999		
	2.5 s trials: Right - Left	6	1.421		
	Right trials: 1s - 2.5s	5	4.002		
	Left trials: 1s - 2.5s	7	4.421		
MB	1 s trials: Right - Left	7	55.908	•	Left > Right
	2.5 s trials: Right - Left	7	12.548		
	Right trials: 1s - 2.5s	7	49.513	•	2.5s > 1.0s
	Left trials: 1s - 2.5s	6	12.953		
TC	1 s trials: Right - Left	5	12.989		
	2.5 s trials: Right - Left	6	6.247		
	Right trials: 1s - 2.5s	5	13.000	†	2.5s > 1.0s
	Left trials: 1s - 2.5s	6	4.058		

The following is a brief description of the results from the other four subjects. The summary plots and tables similar to those shown for subject MB are included in Appendix B.

Subject CL, JM, and TC's normalized mean eye movement response plots exhibit downward trends as sled displacement increases, rather than a gain of 1.0, indicating that they did not accurately discriminate between the different sled displacements. TC's eye movement gain at the large sled displacements was only approximately 0.5. The low gain indicates that he was underestimating his displacement at the larger displacements. The downward trend in most of the other subjects was caused by overestimation of the small displacements and correct compensation for the larger displacements.

Subject CL and JM each responded in the incorrect direction in a few of the 2.5 second duration trials. No consistent directional asymmetry existed in their subjective correct responses. CL also showed no consistent right/left asymmetric trend in her eye movements nor in her subjective estimates of translation. JM responded with a bias in his eye movements toward leftward translation in the 1.0 second trials, but was symmetric in the 2.5 second trials. His subjective responses to the four test conditions (1.0 sec rightward, 1.0 sec leftward, 2.5 sec rightward, 2.5 sec leftward) were not significantly different from each other. TC responded with a bias in his eye movements towards trials to the left at larger sled displacements, however his subjective responses were relatively unbiased.

Comparing the 1.0 and 2.5 second trial durations, subject CL responded with larger eye movements during the 2.5 second trials than during the 1.0 second trials. The slope of her 2.5 second trials was also significantly greater than that of the 1.0 second trials, indicating that she discriminated between the sled displacements better during the 2.5 second trials. Opposite of CL, the slope of JM's 1.0 second regression line was significantly greater than that of the 2.5 second trials. The χ^2 test of his mean response, however, revealed larger eye movements during the longer trials. Because of

experimental circumstances, no repeat trials were performed for subject GS. Therefore, a χ^2 analysis comparing the four different conditions was not possible. However, by not separating the rightward and leftward trials, the regression coefficients of the 1.0 and 2.5 second trials are almost identical and neither was significantly different from 0.0, indicating that her eye movements were not significantly correlated with changes in sled displacement. TC responded with larger eye movements and larger subjective responses during 2.5 second trials than 1.0 second trials.

4.1.1.2.1. Summary of Y-axis Fixed Duration Test

To summarize, Figure 4.10 shows the average normalized eye movement responses for all subjects in the four y-axis fixed duration test conditions. Quantitative conclusions may be inappropriate because of inter-subject variability. However, it provides an overall qualitative understanding of the subjects' responses to changes in acceleration, including a comparison between the 1.0 and 2.5 second and the rightward and leftward trials. The downward trend of the normalized eye movement responses as sled displacement increases indicates that subjects overcompensated for the smaller displacements (gain of approximately 2.0) and correctly compensated for the larger sled displacements (gain of approximately 1.0). This is also evident in the slopes of the regression lines for each subject. Therefore, although a significant correlation exists between eye movements and sled displacement, overall subjects did not accurately compensate for the different sled displacements.

All five subjects responded with slightly larger mean eye movements during the 2.5 second trials. The difference was significant for each subject in either the leftward or rightward trials, but not both. Four of the five subjects (all except JM) also had slightly larger regression coefficients during the 2.5 second trials, although only in one subject

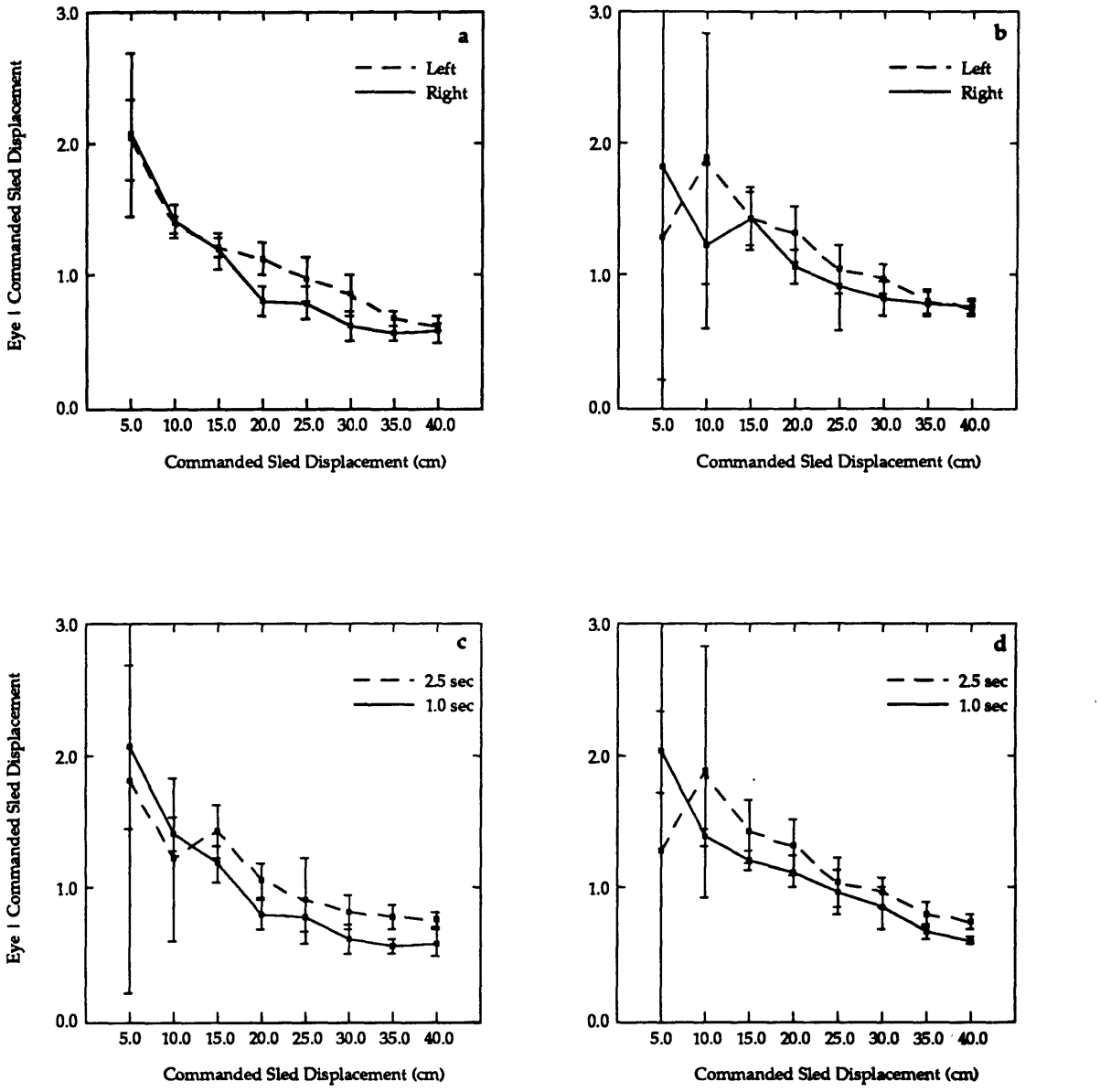

Figure 4.10. Y-Axis Fixed Duration mean normalized eye movements for all subjects. (a) 1.0 second trials comparing leftward and rightward trials, (b) 2.5 second trials comparing leftward to rightward trials, (c) rightward trials comparing 1.0 and 2.5 second trials, (d) leftward trials comparing 1.0 and 2.5 second trials. Error bars signify standard error.

was the difference significant. Thus, each subject's eye movement response indicates some dependence upon trial duration.

Although several of the subjects showed a directional asymmetry in their eye movements and/or their subjective responses, no consistent trend seems to exist across subjects. Since the results from the quantitative measurements (eye movements) were often different from that of the subjective measurements, it does not appear that eye movements accurately quantify the perception of translation.

4.1.2. Z-Axis Experiments

In the Z-axis, subjects had more difficulty accurately tracking the hidden target. Some subjects showed greater variability in their eye movements in the z-axis experiments compared to the subjects in the y-axis, as well as higher threshold levels for perception of translation (average 0.006 G). The majority of the subjects tested in either z-axis test responded with an asymmetry favoring trials moving towards their head, requiring downward eye movements. The headward/footward eye movement asymmetry is larger at small sled displacements and gradually decays as sled displacement increases, however, it this is not consistently supported by the subjective estimates of translation. As in the y-axis experiments, subjects consistently overcompensated for the 10 degree trials and approximately compensated correctly for the 20 degree trials. These results are discussed in detail below.

4.1.2.1. Fixed Displacement Test

Mean normalized eye movement responses are plotted versus acceleration in Figure 4.11 for subject KJ as representative of the subjects tested. The eye movement responses were normalized by dividing by the distance the sled traveled during the particular trial, which

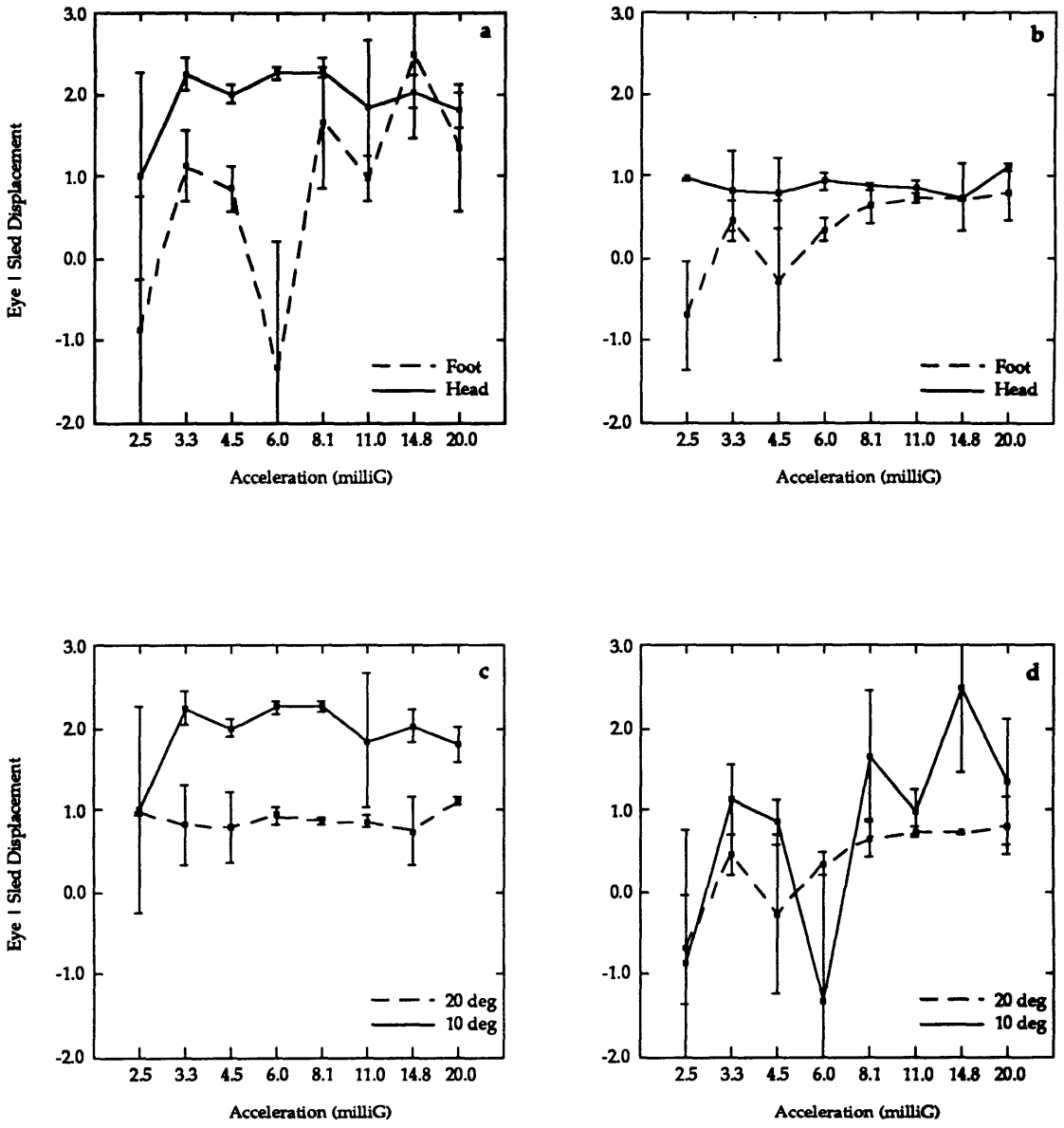

Figure 4.11. Z-Axis Fixed Displacement normalized eye movement data for subject KJ. (a) headward and footward 10 degree trials, (b) headward and footward 20 degree trials, (c) 10 and 20 degree headward trials, (d) 10 and 20 degree footward trials. Error bars signify standard error.

was calculated from the measured sled position signal. This is more accurate than the y-axis experiment analysis where the eye movements were normalized by the commanded sled displacement (8.82 or 18.20 cm). This more accurate normalization was chosen after the asymmetry was observed between the upward and downward eye movements to make certain that it was not an artifact induced by an asymmetry in the motion stimulation. The four plots in Figure 4.11 compare the mean eye movement response at each acceleration level for the four different trial conditions. The first two plots separate the data into (a) 10 degree trials and (b) 20 degree trials and compare the eye movement responses to headward and footward sled displacements. The third and fourth plots separate the (a) headward trials from the (b) footward trials and compare the responses to the 10 and 20 degree trials. Similar plots for the other five subjects are included in Appendix C.

At most acceleration levels, KJ's mean normalized eye movements were greater during sled displacements toward his head. Independent t-tests were performed on the difference between the upward and downward mean responses at each acceleration. The asymmetry was not statistically significant at any individual acceleration level, but the plots reveal an asymmetric trend across the range of accelerations. Subject KJ's asymmetric response was most apparent at the lower and middle acceleration levels. At the two or three highest accelerations his response was almost symmetric. During the 10 degree trials, the average gain of his eye movements when moving toward his head was close to 2.0, while during the footward trials his gain was closer to zero and sometimes negative (average = 0.78). In the 20 degree cases his mean gain for headward trials was approximately 1.0, while his gain during the footward trials was slightly larger than 0.5, again indicating that he undercompensated for sled motion toward his feet.

KJ also showed a significant difference between his response to the 10 and 20 degree trials. He significantly overcompensated for the 10 degree trials. His gain was approximately twice that of the 20 degree trials, indicating that the two different sled displacements yielded similar responses.

Thresholds were determined using the same criteria as was used in the y-axis fixed displacement test (i.e., the lowest of two consecutive acceleration levels that the mean eye movement response is significantly different from zero). Table 4.8 gives the eye movement threshold level for each subject in each of the four test conditions. One would expect that below a person's threshold the mean response of many trials would average to approximately zero, confirming that the probability of 'guessing' the correct direction is fifty percent. With only two data points at each acceleration in each condition the variances are usually very high.

Table 4.11. Summary of eye movement threshold levels for each subject in each test condition in the z-axis fixed displacement test.

Subject	10 degree trials HEADWARD	10 degree trials FOOTWARD	20 degree trials HEADWARD	20 degree trials FOOTWARD
CL	6.0	6.0	11.0	6.0
JM	3.3	8.1	4.5	11.0
KJ	3.3	3.3	6.0	8.1
KP	< 2.5	< 2.5	< 2.5	8.1
RZ	14.8	8.1	4.5	< 2.5
TC	4.5	4.5	< 2.5	3.3

To statistically evaluate the differences in the eye movement responses to the four sled conditions apparent in Figure 4.11 (10 degree up, 10 degree down, 20 degree up, and 20 degree down) a χ^2 analysis was performed across all acceleration levels. To illustrate the process, the mathematical differences between subject KJ's headward and footward trials and 10 and 20 degree trials are shown in Figure 4.12.

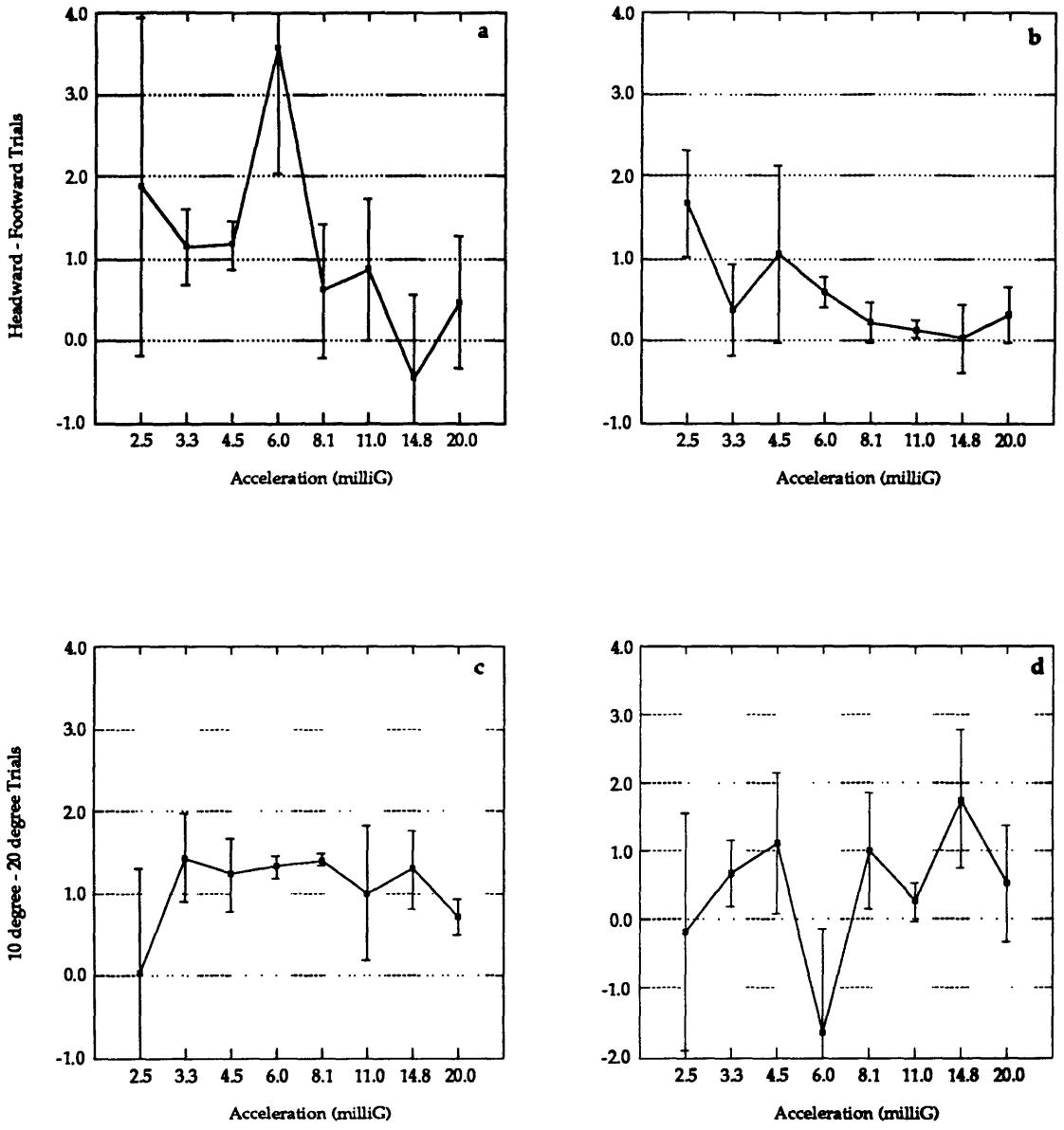

Figure 4.12. Differences in the mean normalized eye movement responses for subject KJ. (a) 10 degree trials comparing headward and footward trials, (b) 20 degree trials comparing headward to footward trials, (c) headward trials comparing 10 and 20 degree trials, (d) footward trials comparing 10 and 20 degree trials. Error bars signify standard error of the difference.

The plots of the differences between the responses to the different test conditions make any significant disparity between them more visible. In Figure 4.12 (a) and (b) it is clear that at the lower and middle accelerations KJ responded asymmetrically, favoring sled displacements toward his head. As the acceleration increased, however, the difference curve tended toward zero, indicating little or no asymmetry. Likewise, a difference of 1.0 is evident between the 10 and 20 degree cases across most accelerations. Table 4.9 summarizes the results from the χ^2 tests performed on all acceleration levels simultaneously, on accelerations above threshold, and on accelerations below threshold. As in the y-axis experiment, a distinction is made between the responses above and below the threshold acceleration because they could belong to two different populations. However, since the threshold value is selected somewhat arbitrarily using the rule described in the Methods section, a χ^2 of the full range of accelerations was also performed. The χ^2 statistic only tests if the response is different from zero. Therefore, a significant χ^2 value requires further review of the data to determine the direction of the trend (which condition is greater) or even if a trend exists.

As confirmed by these statistical tests, subject KJ had a significant asymmetric trend in his eye movement response across acceleration levels favoring headward sled displacements. The χ^2 test also confirmed the significant difference between KJ's normalized responses to the 10 and 20 degree trials across all acceleration levels. Since KJ's threshold value was so low in the 10 degree trials, the differences between his responses were significant in the above threshold χ^2 tests, but were not significant below threshold, as that test included only one acceleration. In the 20 degree trials KJ showed significantly greater eye movement responses to headward trials below threshold, as well as across all acceleration levels.

Table 4.9. Summary of χ^2 tests for (a) headward/footward asymmetry and (b) differences between 10 and 20 degree trials for all subjects. • = <0.001, √ = <0.005, † = <0.025, Δ = <0.05, blank = not significant.

Subj.	Up - Down Difference Test	N	χ^2: 10° trials	Trend	P	N	χ^2: 20° trials	Trend	P
CL	All Accelerations	8	190.749	U>D	•	8	76.104	U>D	•
	Above Threshold	5	122.560	U>D	•	3	68.269	U>D	•
	Below Threshold	3	68.189	U>D	•	5	7.835		
JM	All Accelerations	8	90.341	U>D	•	8	109.660	U>D	•
	Above Threshold	4	71.470	U>D	•	3	1.312		
	Below Threshold	4	18.872	U>D	•	5	108.347	U>D	•
KJ	All Accelerations	8	28.846	U>D	•	8	22.329	U>D	√
	Above Threshold	7	28.019	U>D	•	4	3.446		
	Below Threshold	1	0.827			4	18.883	U>D	†
KP	All Accelerations	8	59.663	U>D	•	8	4.508		
	Above Threshold	8	59.663	U>D	•	4	1.600		
	Below Threshold	0				4	2.908		
RZ	All Accelerations	8	227.550	var.	•	8	16.297	var.	Δ
	Above Threshold	2	0.382			6	11.282	U>D	Δ
	Below Threshold	6	227.168	var.	•	2	5.015		
TC	All Accelerations	6	242.978	U>D	•	8	10.477	U>D	Δ
	Above Threshold	6	242.978	U>D	•	7	8.912		
	Below Threshold	0				0			

(b)

Subj.	10° - 20° Difference Test	N	χ^2: Up trials	Trend	P	N	χ^2: Down trials	Trend	P
CL	All Accelerations	8	138.357	10>20	•	8	332.624	10>20	•
	Above Threshold	3	125.169	10>20	•	5	7.445		
	Below Threshold	5	13.188	10>20	†	3	325.180	10>20	•
JM	All Accelerations	8	230.200	10>20	•	8	169.924	var.	•
	Above Threshold	6	225.097	10>20	•	3	42.645	10>20	•
	Below Threshold	2	5.103			5	127.279	var.	•
KJ	All Accelerations	8	515.538	10>20	•	8	10.079	10>20	√
	Above Threshold	7	515.537	10>20	•	4	5.303		
	Below Threshold	1	0.001			4	4.776		
KP	All Accelerations	8	118.084	10>20	•	8	14.859		
	Above Threshold	8	118.084	10>20	•	4	6.920		
	Below Threshold	0	0.0			4	7.940		
RZ	All Accelerations	8	33.557	10>20	•	8	254.884	var.	Δ
	Above Threshold	2	10.826	var.	†	4	13.420	10>20	Δ
	Below Threshold	6	22.731	var.	•	4	241.464	var.	•
TC	All Accelerations	7	309.693	10>20	•	7	47.346	10>20	Δ
	Above Threshold	6	309.150	10>20	•	6	45.853	10>20	Δ
	Below Threshold	1	0.543			1	1.494		

Subjective correct response threshold data provide further insight into the subjects perceptions of translation. As defined in the Methods section, *the subjective response threshold is the lowest of two consecutive acceleration levels where the subject chose the correct direction in at least 75% of the trials.* Table 4.10 summarizes the percent correct response for each subject at each acceleration level. The asterisks indicate the threshold acceleration level based on the above rule for each subject. Subject KJ's subjective response thresholds (Table 4.10) do not directly relate to the thresholds previously determined from his eye movements (Table 4.8), since he responded in the correct direction during most of the trials. The high variability in his eye movements, therefore, caused his sub-threshold means to be insignificantly different from zero. It appears that at the lowest acceleration level where he may have been 'guessing' which direction he moved, he responded more frequently with downward eye movements, indicating he perceived motion toward his head more frequently than toward his feet. However, across all other acceleration levels the difference between the mean headward and footward responses was solely due to the magnitude of the eye movements.

Table 4.10. Summary of percent correct subjective responses for each subject at each acceleration level.

Subj.	Sled	2.5	3.3	4.5	6.0	8.1	11.0	14.8	20.0	total
CL	Up	75	50	25	100*	75	100	100	100	78.125
	Down	50	50	50	100*	100	100	100	100	81.250
JM	Up	75*	75	100	100	100	100	100	100	93.750
	Down	0	0	50	50	75*	100	100	100	59.375
KJ	Up	75*	100	100	100	100	100	100	100	96.875
	Down	50	100*	100	75	100	100	100	100	90.625
KP	Up	100*	100	100	100	100	100	100	100	100.00
	Down	75*	100	75	75	100	100	100	100	90.625
RZ	Up	25	75	50	100*	75	75	100	100	75.000
	Down	100*	100	100	100	100	100	100	100	100.00
TC	Up	75*	75	100	75	75	100	100	100	87.500
	Down	75*	75	100	100	100	100	100	100	93.750

An analysis similar to that performed for the eye movement data was performed on the subjective estimates of translation to test whether differences in eye movements between the four test conditions are perceptual. Although the same procedure was employed (as described in the Methods chapter), for brevity only the plots of the mean subjective responses are shown in Figure 4.13. The difference plots have been omitted. Figure 4.13 indicates that KJ subjectively overestimated his translation by as much as a factor of ten in all test conditions, but showed larger subjective gains in the 10 degree trials than the 20 degree trials. Although his subjective responses are variable, they also appear to be slightly biased toward footward displacements in figures (a) and (b).

A χ^2 test was performed to test the null hypothesis that the difference is significant. The summary statistics from the χ^2 test are shown in Table 4.11. In the 10 degree trials the difference between KJ's subjective responses during headward and footward trials was somewhat variable with some bias toward the footward trials. In the 20 degree trials his subjective responses varied insignificantly around zero. These responses are inconsistent with his eye movement responses, where he demonstrated a significant bias towards headward trials in both the 10 and 20 degree trials. In both the headward and footward trials, KJ's normalized subjective report supported that he overcompensated for the 10 degree trials and undercompensated for the 20 degree trials, i.e., a significant difference exists between the two normalized mean responses. This agrees with the results from his eye movement responses.

The following is a brief description of the results from the other five subjects. The summary plots and tables similar to those that were presented for subject KJ are included in Appendix C.

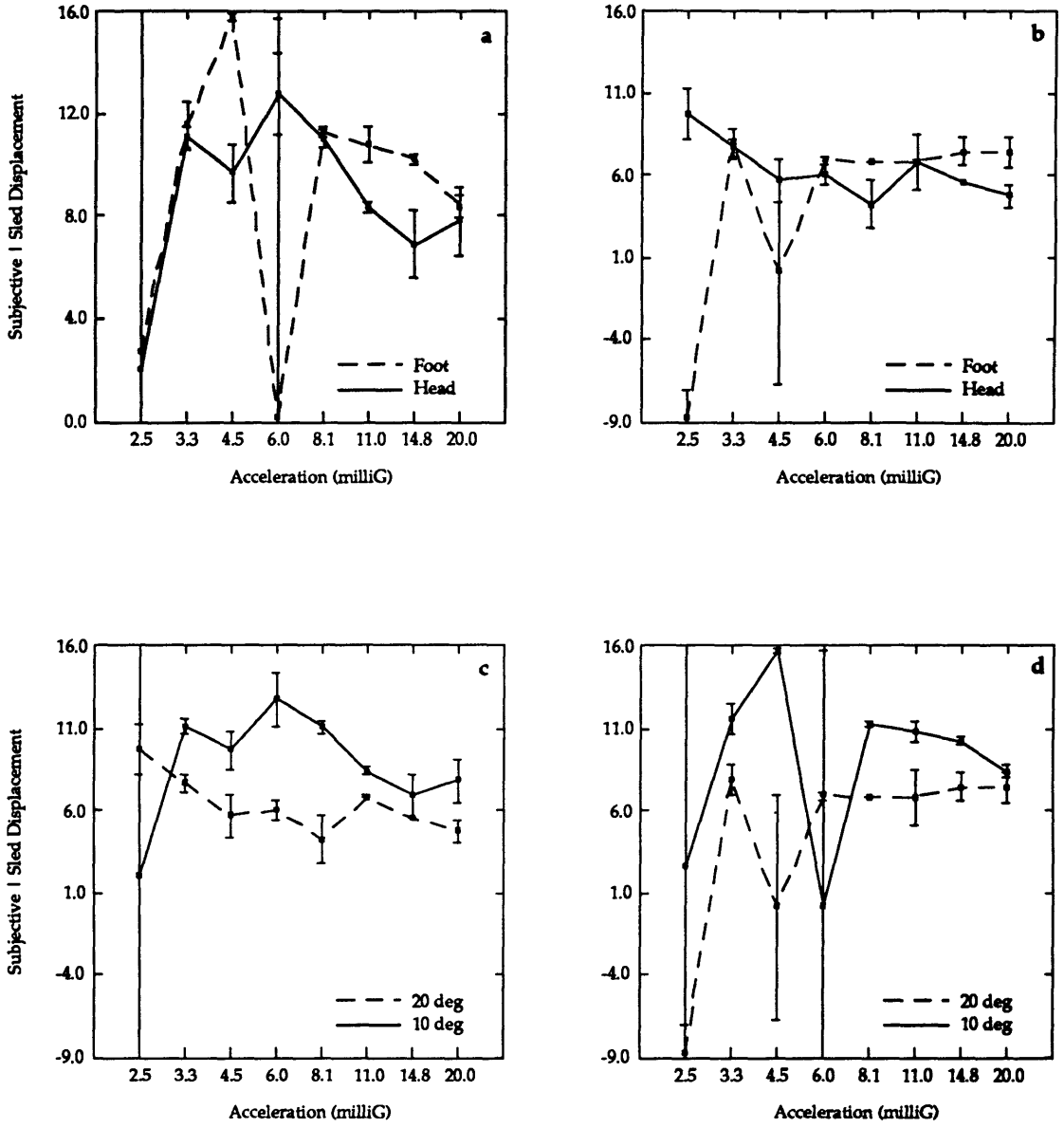

Figure 4.13. Mean normalized subjective responses for subject KJ. (a) headward and footward 10 degree trials, (b) headward and footward 20 degree trials, (c) 10 and 20 degree headward trials, and (d) 10 and 20 degree footward trials. Error bars indicate the standard error of the mean difference.

Table 4.11. Summary of χ^2 test of the subjective responses for all subjects . (a) test of up/down asymmetry and (b) test of difference between the 10 and 20 degree trial s. • = < 0.001, √ = < 0.005, † = < 0.025, Δ = < 0.05.

(a)

Subj.	Up - Down Difference Test	N	χ^2: 10° trials	Trend	P	N	χ^2: 20° trials	Trend	P
CL	All Accelerations	7	25.074	var.	•	8	33.051	var.	•
	Above Threshold	5	15.149	var.	Δ	3	28.554	var.	•
	Below Threshold	2	9.925	D>U	Δ	5	4.497		
JM	All Accelerations	8	105.392	var.	•	8	161.222	U>D	•
	Above Threshold	4	9.774	D>U	Δ	3	61.229	D>U	•
	Below Threshold	4	95.618	U>D	•	5	99.993	U>D	•
KJ	All Accelerations	8	45.966	D>U	•	7	74.240	var.	•
	Above Threshold	7	45.965	D>U	•	3	9.404	D>U	†
	Below Threshold	1	0.001			4	64.836	var.	•
KP	All Accelerations	8	33.495	var.	•	8	13.202		
	Above Threshold	8	33.495	var.	•	4	11.781	var.	†
	Below Threshold	0	0.0			4	1.421		
RZ	All Accelerations	7	27.798	var.	•	6	5.447		
	Above Threshold	2	21.919	var.	•	5	0.235		
	Below Threshold	5	5.879			1	5.212		
TC	All Accelerations	5	7.659			4	6.566		
	Above Threshold	5	7.659			3	1.354		
	Below Threshold	0	0.0			1	5.212		

(b)

Subj.	10° - 20° Difference Test	N	χ^2: Up trials	Trend	P	N	χ^2: Down trials	Trend	P
CL	All Accelerations	7	184.566	var.	•	8	3246.05	10>20	•
	Above Threshold	3	164.813	10>20	•	5	57.344	10>20	•
	Below Threshold	4	14.753	var.	Δ	3	3188.71	10>20	•
JM	All Accelerations	8	27.149	10>20	•	8	36.980	10>20	•
	Above Threshold	6	2.88			3	4.404		
	Below Threshold	2	4.269			5	32.576	var.	•
KJ	All Accelerations	7	121.918	10>20	•	8	508.432	10>20	•
	Above Threshold	4	91.848	10>20	•	4	495.006	10>20	•
	Below Threshold	3	30.07	10>20	•	4	13.426	10>20	Δ
KP	All Accelerations	8	497.183	10>20	•	8	90.852	10>20	•
	Above Threshold	8	497.183	10>20	•	4	79.05	10>20	•
	Below Threshold	0	0.0			4	11.802	10>20	Δ
RZ	All Accelerations	6	3.718			8	31.960	10>20	•
	Above Threshold	1	0.819			5	30.408	10>20	•
	Below Threshold	5	2.899			3	1.552		
TC	All Accelerations	3	33.936	var.	•	6	8.819		
	Above Threshold	2	33.935	var.	•	5	3.066		
	Below Threshold	1	0.001			1	5.753		

At low levels of acceleration five of the six subjects (all except RZ) exhibited smaller mean eye movements during footward sled motion toward than during headward trials. The subjective correct response data in Table 4.10 shows that half of the subjects responded incorrectly more often during footward trials while others simply used smaller eye movements during footward trials. Above threshold, subjects RZ, TC, JM, and CL continued to undercompensate for footward sled displacements, while approximately compensating correctly, or slightly overcompensating for sled motion toward their head. Above and below threshold subject KP also significantly overcompensated for sled displacements toward her head, however she compensated correctly for sled displacements toward her feet.

If the eye movement response is related to the subjects' perception of translation, these results would imply that the subjects may perceive that they moved farther when moving toward their heads. The distinct headward/footward asymmetry that was evident in the eye movement responses, however, is not obvious in the subjective responses. Only one subject, JM, had a consistent bias in his subjective responses toward headward trials in both the 10 and 20 degree cases, and he was the only subject with any significant bias in the 20 degree trials. KP responded with a bias toward headward displacements in the 10 degree trials, but CL, RZ and KJ responded subjectively as moving farther during footward trials. This is opposite the trends in their eye movements.

A statistically significant difference also exists between the eye movement responses to the two different sled displacements in all six subjects. Like subject KJ, subjects overestimated the 10 degree trials significantly more than the 20 degree trials. The difference between the 10 and 20 degree trials was also evident in the subjective response data, as subjects significantly overestimated their displacement during the 10 degree trials. Because the normalized eye movement responses and the subjective responses to

these two different displacements were different from each other, they were kept separate throughout the analysis.

4.1.2.1.1. Summary of Z-axis Fixed Displacement Test

Although significant variation exists between subjects, Figure 4.14 compares the normalized 10 and 20 degree trials and the normalized headward and footward trials for all subjects combined. Quantitative conclusions from this plot may be inappropriate because of the inter-subject variability. However, it provides an overall qualitative understanding of the subjects' responses to changes in acceleration, including a summary of the differences statistically shown above and shown previously for subject KJ . The relatively constant eye movement gain across acceleration levels shown in Figure 4.14 indicates that changes in acceleration do not significantly change the amplitude of the eye displacement.

The trends described for each individual subject are supported by the plots of all subjects averaged together. The responses to headward trials are greater than those to footward trials across all accelerations in both the 10 and 20 degree trials. As shown in figures (a) and (b) the asymmetric eye movement response is most significant at the low accelerations, but continues to exist at the high accelerations. Subject estimates of translation do not consistently support the eye movement asymmetry. In fact, many subjects' estimates of translation were greater during downward trials. Since the subjective and eye movement responses do not coincide, it does not appear that the eye movements accurately quantify the perception of translation.

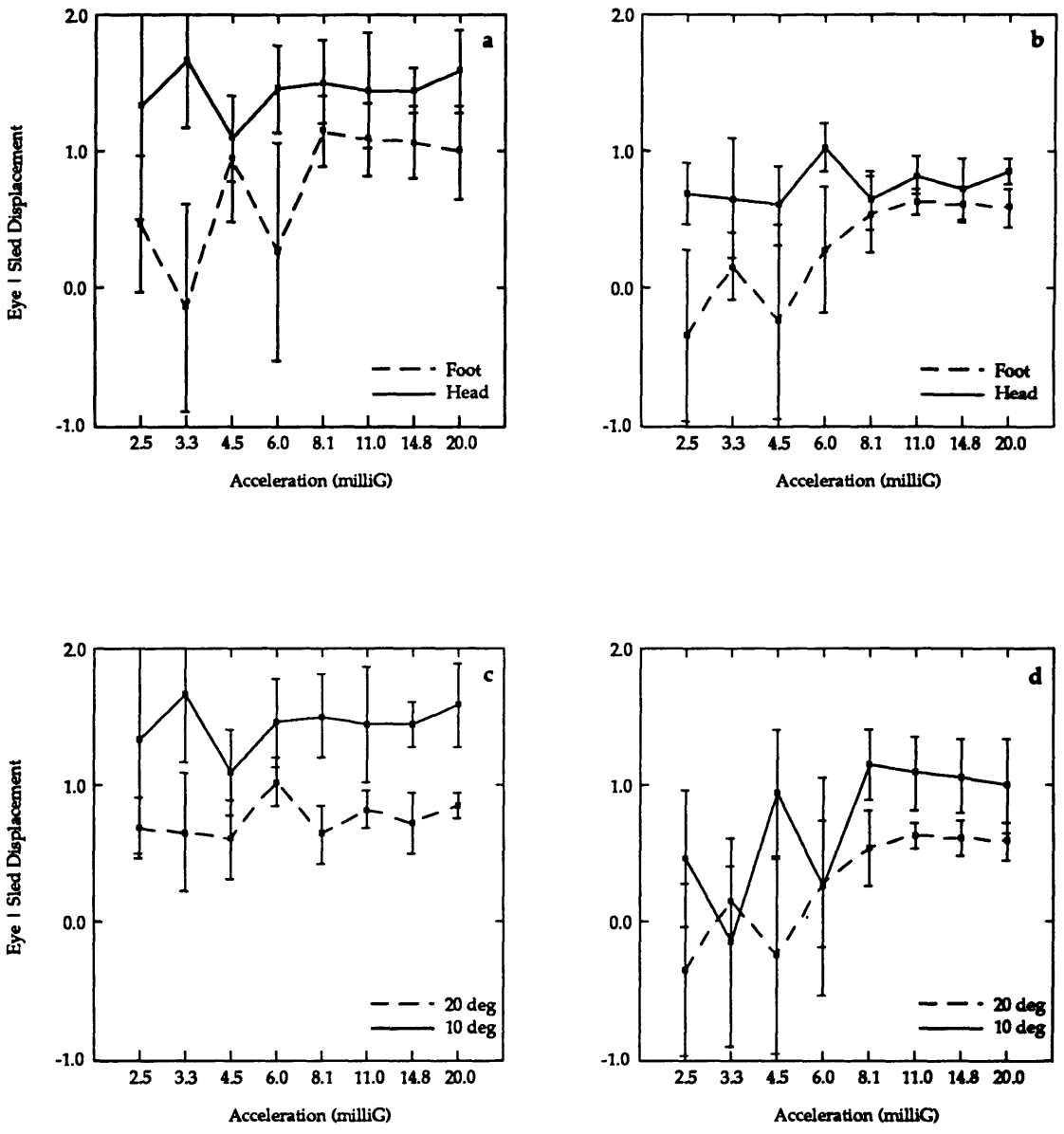

Figure 4.14. Z-Axis Fixed Displacement normalized eye movement data for all subjects. (a) headward and footward 10 degree trials, (b) headward and footward 20 degree trials, (c) 10 and 20 degree headward trials, (d) 10 and 20 degree footward trials. Error bars signify standard error.

The difference between the 10 and 20 degree trials is particularly evident in the headward trials (c), but also exists in the footward trials (d). The difference between the two displacements exists across all accelerations, and is primarily cause by undercompensation of the 20 degree trials and slight overcompensation of the 10 degree trials. Subjective estimates of translation support the differences between the two displacement amplitudes across all subjects.

In the y-axis experiments, the fixed duration test was justified by subjective reports that the responses depended on the duration of the trial. The subjects' eye movements in the fixed displacement test did not coincide with their subjective reports, but in the fixed duration test the 2.5 second trials were significantly greater than the 1.0 second trials for half of the subjects. In the z-axis fixed displacement experiment discussed above, one subject of six (KP) responded with eye movements that decreased with increasing acceleration in both the 10 and 20 degree cases. The result indicates that she was overestimating the displacement of the sled at low accelerations (large trial durations) and correctly compensating for the sled displacement at larger accelerations (smaller trial durations). Her response suggests that her perception of the distance traveled was dependent upon the duration of the trial. Thus, to further investigate this potential effect, and to complete the battery of Hidden Target Pursuit experiments, the fixed duration experiment was performed in the z-axis.

4.1.2.2. Fixed Duration Test

As stated in the Methods, linear regression of the data determine how well a subject's eye movement response correspond to the distance traveled by the sled. The subjects in the z-axis fixed duration test were not able to track the hidden target very accurately. Post-hoc tests determined whether significant differences existed between different linear regression lines. Scatter plots of the eye movement responses are shown in Figure 4.15

for subject MB for comparison to those made by Israël and Berthoz (1989). (Similar plots are shown for the other four subjects in Appendix D.) Each point on the plot is the response to one trial. Linear regression lines are drawn on the plot to indicate the slope of the data for each trial duration in each sled direction. A slope of 1.0 would indicate that the subject was able to discriminate between the different sled displacements by tracking the hidden target with her eyes.

Thresholds for perception of acceleration were not considered in these experiments since only the lowest acceleration tested (5 milliG) was near or below the threshold level for most of the subjects, as shown in the Z-axis Fixed Displacement test (second lowest acceleration was 10 milliG). Since trial duration is proportional to the inverse of the acceleration, the trials with the longer duration (2.5 seconds) have lower accelerations. Therefore, incorrect responses were made more often during the 2.5 second trials where the accelerations were closer to the threshold level for perception. The incorrect responses were eliminated from the linear regression analysis (results shown in Table 4.12) so that the negative values would not falsely skew the comparisons between the conditions being tested (i.e., 1.0 versus 2.5 second trials).

Table 4.12 shows the regression coefficients (slopes) for the 1.0 second headward and footward trials and the 2.5 second headward and footward trials, indicating how well the subjects' eye movements compensated for translation during each condition. The following four rows in the table provide the p-values describing whether the slope of each line is significantly different from 0.0 (no dependence on distance), 1.0 (accurate compensation), the slope of the trials in the same direction with the other duration, and the slope of the trials with the same duration but opposite direction.

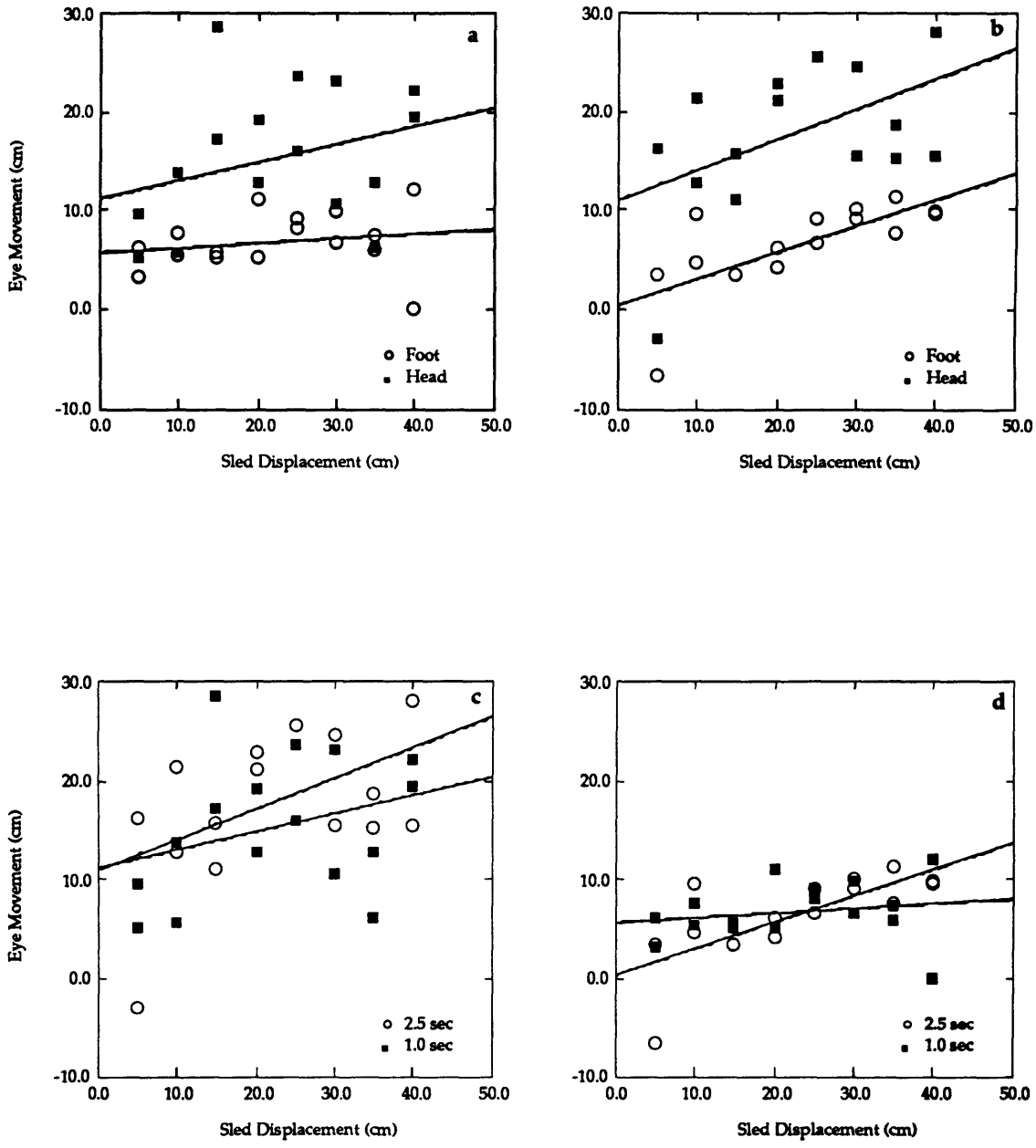

Figure 4.15. Scatter plot of the Z-Axis Fixed Duration eye movement data comparing 1.0 and 2.5 second trials for subject MB. (a) 1.0 second trials comparing headward and footward trials, (b) 2.5 second trials comparing headward and footward trials, (c) headward trials comparing 1.0 and 2.5 second trials, (d) footward trials comparing 1.0 and 2.5 second trials. Error bars signify standard error.

Table 4.12. Z-axis Fixed Duration summary of linear regression analysis for all subjects.

Subj.	Test	1.0sec Up	1.0sec Down	2.5sec Up	2.5sec Down
JR	Regression Coeff.	0.174	0.087	0.307	0.584
	P-Value H_0: B=0.0	0.351	0.187	0.064	0.000
	P-Value H_0: B=1.0	0.000	0.000	0.000	0.000
	P-Value H_0: $B_1=B_2$	UP trials: 0.399		DOWN trials: 0.730	
	P-Value H_0: $B_u=B_d$	1.0 sec trials: 0.186		2.5 sec trials: 0.009	
AA	Regression Coeff.	0.179	0.247	0.178	0.324
	P-Value H_0: B=0.0	0.125	0.009	0.414	0.002
	P-Value H_0: B=1.0	0.000	0.000	0.002	0.000
	P-Value H_0: $B_1=B_2$	UP trials: 0.998		DOWN trials: 0.371	
	P-Value H_0: $B_u=B_d$	1.0 sec trials: 0.414		2.5 sec trials: 0.102	
GS	Regression Coeff.	0.217	-0.085	0.064	0.558
	P-Value H_0: B=0.0	0.052	0.834	0.717	0.002
	P-Value H_0: B=1.0	0.000	0.023	0.000	0.008
	P-Value H_0: $B_1=B_2$	UP trials: 0.395		DOWN trials: 0.001	
	P-Value H_0: $B_u=B_d$	1.0 sec trials: 0.465		2.5 sec trials: 0.004	
MB	Regression Coeff.	0.166	0.038	0.272	0.249
	P-Value H_0: B=0.0	0.214	0.541	0.049	0.002
	P-Value H_0: B=1.0	0.000	0.000	0.000	0.000
	P-Value H_0: $B_1=B_2$	UP trials: 0.416		DOWN trials: 0.006	
	P-Value H_0: $B_u=B_d$	1.0 sec trials: 0.055		2.5 sec trials: 0.722	
SS	Regression Coeff.	0.317	0.519	-0.331	0.576
	P-Value H_0: B=0.0	0.332	0.318	0.325	0.239
	P-Value H_0: B=1.0	0.048	0.354	0.001	0.381
	P-Value H_0: $B_1=B_2$	UP trials: 0.066		DOWN trials: 0.904	
	P-Value H_0: $B_u=B_d$	1.0 sec trials: 0.693		2.5 sec trials: 0.073	
KP	Regression Coeff.	0.219	0.277	0.376	0.739
	P-Value H_0: B=0.0	0.041	0.002	0.294	0.018
	P-Value H_0: B=1.0	0.000	0.000	0.092	0.361
	P-Value H_0: $B_1=B_2$	UP trials: 0.656		DOWN trials: 0.117	
	P-Value H_0: $B_u=B_d$	1.0 sec trials: 0.428		2.5 sec trials: 0.211	

It is evident from the slopes of the regression lines for subject MB (between 0.038 and 0.272) that she was not able to accurately compensate for her translation with eye movements over the range of sled displacements presented. She tended to overestimate for the small displacements and underestimate for the larger displacements, producing a large amount of scatter of the data and a very flat regression line. This agrees with the

results from the fixed displacement experiments where the subjects' eye movements during the 20 degree trials were not consistently twice the magnitude of the 10 degree trials, as they should have been for perfect compensation. Not surprisingly, the slope of MB's regression lines were significantly different from a slope of 1.0 in all four test conditions. In the 1.0 second trials, the regression coefficients were not significantly different from 0.0. A slightly greater correlation existed between her eye movements and sled displacement in the 2.5 second trials, evidenced by a slope that is significantly greater than zero. The difference between the slopes of the 1.0 and 2.5 second trials was only significant in the downward trials, as shown in the second to last row of MB's regression data in Table 4.12.

The last row of the regression table for MB shows that she demonstrated a significant difference between headward and footward 1.0 second trials, and no asymmetry in the 2.5 second trials. The asymmetry supports the asymmetric results from the Z-axis fixed displacement test. However, because of the large amount of scatter in the data around the regression lines, regression analysis may not be the most accurate method to evaluate the differences.

To confirm or refute the results from the regression analysis, a second analysis method, similar to the χ^2 test used in the previous experiments was employed. The first step in the analysis is to produce plots of the mean eye movement response at each sled displacement. Figure 4.16 shows such plots for subject MB.

Similar to her response in the Y-axis Fixed Duration test, MB's normalized means have a downward trend as sled displacement increases. The amplitude of her eye movements did not change significantly with sled displacement, as was also apparent by the very flat slope in the regression plot of Figure 4.15. Further simplification of the plots in Figure

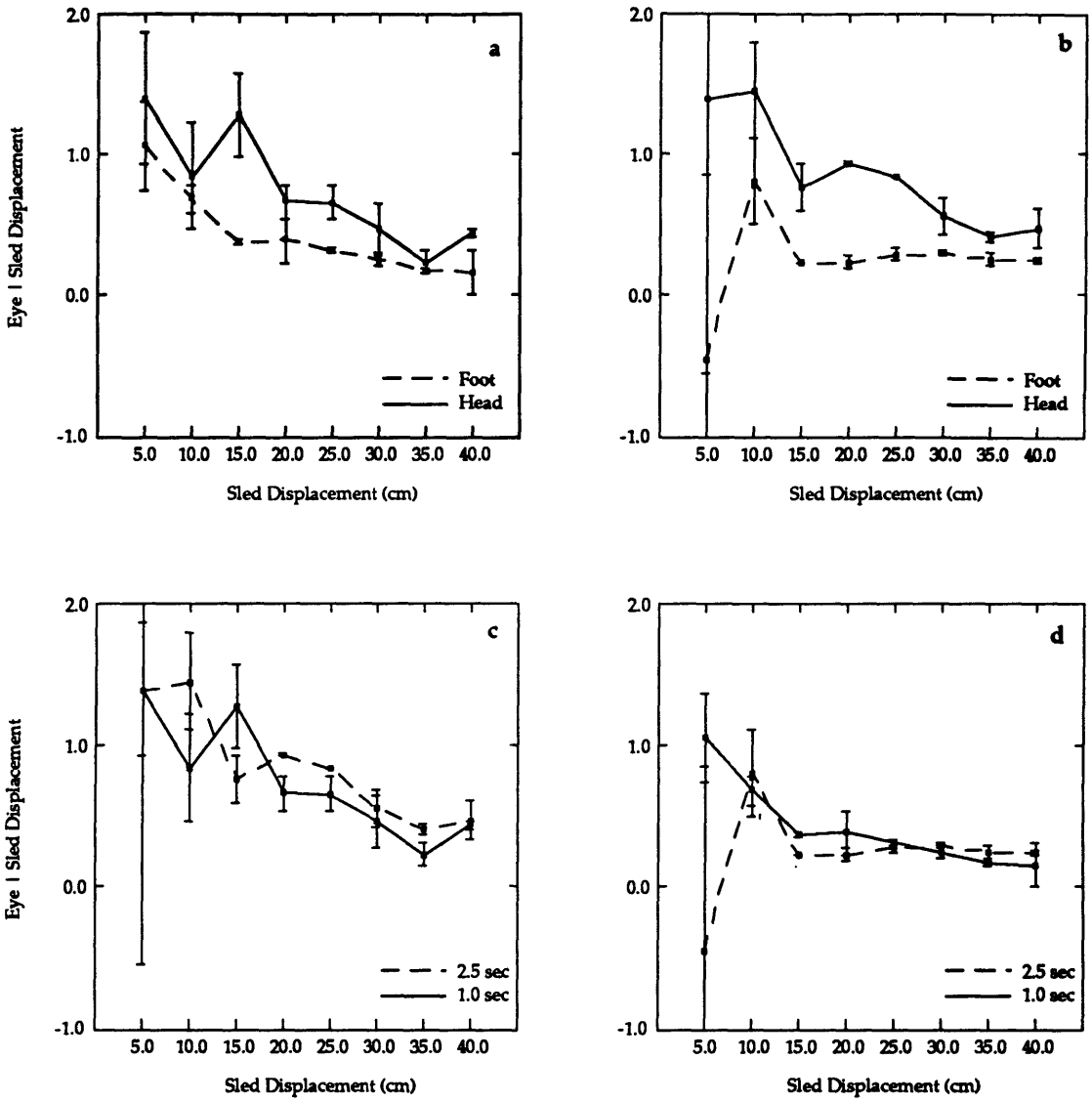

Figure 4.16. Z-axis fixed duration mean normalized eye movement responses versus sled displacement for subject MB. (a) 1.0 sec trials comparing headward and footward, (b) 2.5 sec trials comparing headward and footward, (c) headward trials comparing 1.0 sec and 2.5 sec, and (d) footward trials comparing 1.0 and 2.5 sec. Error bars indicate standard error.

4.16 and statistical analysis of the data was performed to investigate any significant differences between the four test conditions. The difference between each test condition was calculated and then plotted versus sled displacement. (Figure 4.17). Subject MB had consistently larger eye movements during sled displacements toward her head than toward her feet in both the 1.0 and 2.5 second trials. The differences between her responses to the headward and footward trials form a downward trend with sled displacement in both the 1.0 and 2.5 second trials. The downward trend indicates that MB was more biased toward headward displacements at the smaller sled displacements. As the sled displacement increased, the differences between MB's responses to headward and footward trials decreased until almost reaching zero (indicating no difference) during 40 cm displacements. Similar observation of Figure 4.17 (c) and (d) reveals that MB responded with slightly greater eye movements in the 2.5 second headward trials than in the 1.0 second headward trials, but showed no consistent difference dependent upon trial duration in the downward trials.

For statistical purposes a χ^2 test was performed to determine whether the differences shown are significant. If the calculated χ^2 value is significantly different from zero, then one must review the data to determine the direction of the trend (which condition is greater) or if a trend exists. Table 4.13 summarizes the results from the χ^2 test for all subjects. The last column describes the direction of the significant trend, and is left blank for cases where no trend exists.

The calculated χ^2 values confirm that subject MB consistently moved her eyes with larger amplitudes during sled displacements toward her head (i.e., downward eye movements). This trend was statistically significant for both the 1.0 and 2.5 second conditions. In regards to the dependence of the estimation of translation upon trial

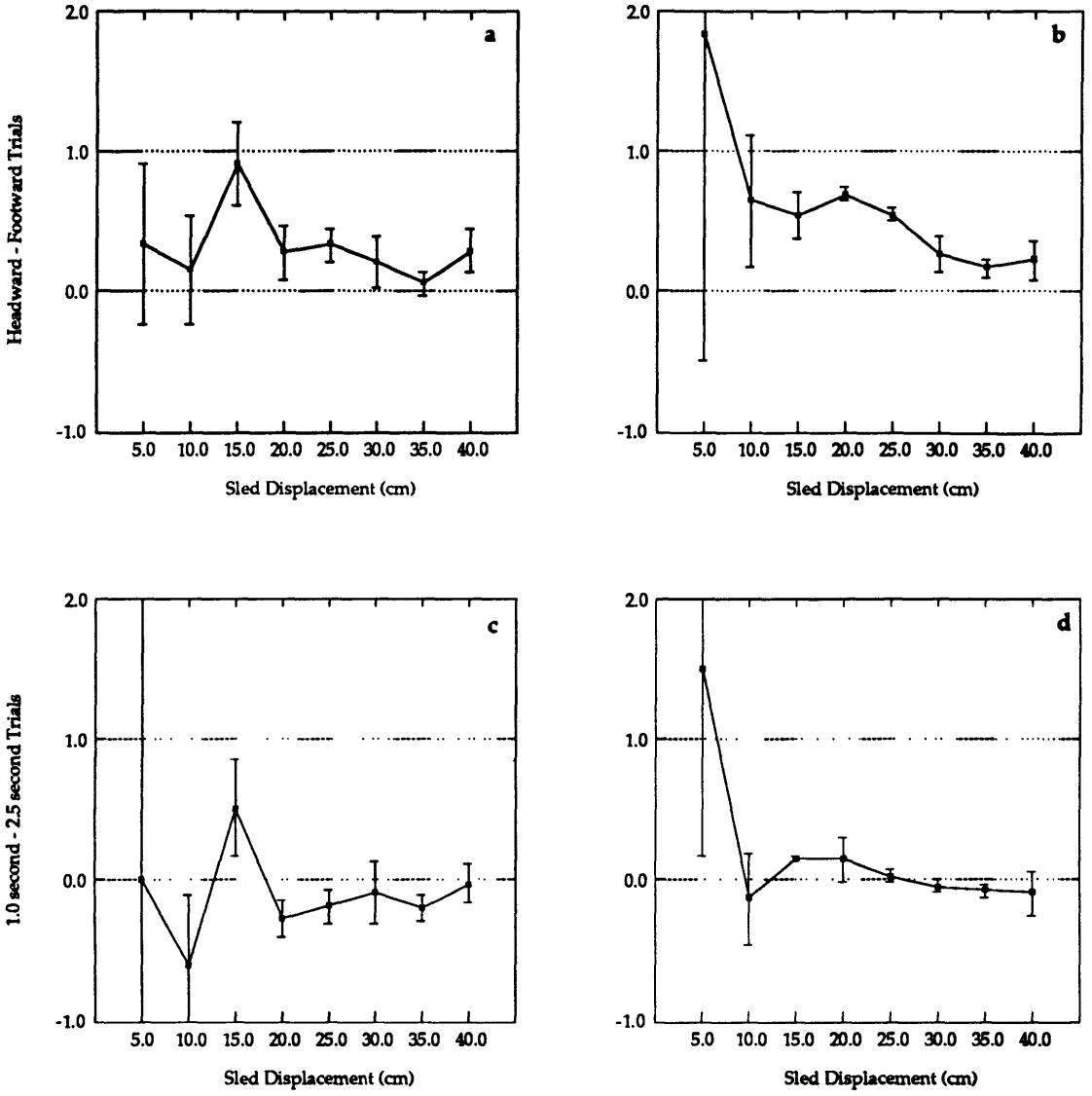

Figure 4.17. Differences in mean normalized eye movement responses versus sled displacement for subject MB. (a) 1.0 sec trials comparing headward and footward, (b) 2.5 sec trials comparing headward and footward, (c) headward trials comparing 1.0 sec and 2.5 sec, and (d) footward trials comparing 1.0 and 2.5 sec. Error bars indicate standard error of the difference.

Table 4.13. Z-axis Fixed Duration summary of χ^2 tests. • = <0.001, √ = <0.005, † = <0.025, Δ = <0.05, blank = no significant trend.

Subj.	Difference Test	N	χ^2	P	Condition
JR	1 s trials: Up - Down	8	291.894	•	Up > Down
	2.5 s trials: Up - Down	8	490.320	•	Up > Down
	Upward trials: 1s - 2.5s	8	9.021		
	Down trials: 1s - 2.5s	8	22.729	√	2.5s > 1.0s
AA	1 s trials: Up - Down	8	56.732	•	Up > Down
	2.5 s trials: Up - Down	8	5.530		
	Upward trials: 1s - 2.5s	8	15.375		
	Down trials: 1s - 2.5s	8	24.837	√	2.5s > 1.0s
GS	1 s trials: Up - Down				
	2.5 s trials: Up - Down				
	Upward trials: 1s - 2.5s				
	Down trials: 1s - 2.5s				
MB	1 s trials: Up - Down	8	25.279	√	Up > Down
	2.5 s trials: Up - Down	8	396.946	•	Up > Down
	Upward trials: 1s - 2.5s	8	15.435		
	Down trials: 1s - 2.5s	8	60.469	•	variable
SS	1 s trials: Up - Down	8	83.517	•	Up > Down
	2.5 s trials: Up - Down	8	1049.698	•	Up > Down
	Upward trials: 1s - 2.5s	8	90.424	•	variable
	Down trials: 1s - 2.5s	8	9.331		
KP	1 s trials: Up - Down	8	55.467	•	Up > Down
	2.5 s trials: Up - Down	8	91.616	•	Up > Down
	Upward trials: 1s - 2.5s	8	6.053		
	Down trials: 1s - 2.5s	8	127.780	•	variable

duration, subject MB responded similarly in both the 1.0 and 2.5 second trials. The χ^2 value calculated for the downward trials was significantly different from zero, but no consistent trend was apparent.

Subjective correct response data could be used to determine if subjects responded correctly more frequently to trials to the left or right or during 1.0 second or 2.5 second trials. Table 4.14 summarizes the percentage of correct responses for each subject at each sled displacement. Subject MB's correct responses were not asymmetric, therefore, the

headward/footward asymmetry shown in the χ^2 table (Table 4.14) was due entirely to differences in the magnitudes of her eye movements, not incorrect responses.

Table 4.14. Percent of correct subjective responses for all subjects during the Z-axis Fixed Duration test.

Subj.	Cond.	5	10	15	20	25	30	35	40	total
JR	Up	75	75	100	100	100	100	50	100	87.500
	Down	100	100	100	100	100	100	100	100	100.00
AA	Up	75	100	100	100	100	100	75	100	93.750
	Down	100	50	100	100	100	100	100	100	93.750
GS	Up	100	100	100	100	100	100	100	100	100.00
	Down	100	100	100	100	100	100	100	100	100.00
MB	Up	75	100	100	100	100	100	75	100	93.750
	Down	75	100	100	100	100	100	100	100	96.875
SS	Up	100	100	100	100	100	100	100	100	100.00
	Down	100	75	75	100	100	100	100	100	93.750
KP	Up	75	100	75	100	75	100	100	100	90.625
	Down	50	100	100	100	100	100	100	100	93.750

Analysis of the subjective estimates of translation can also be used to interpret the quantitative eye movement data shown above. Figure 4.18 shows that subject MB's subjective responses more accurately distinguished between the different sled displacements than her eye movements indicated, evidenced by the slope of the regression line closer to 1.0. However, she greatly overestimated her translation at all sled displacements during both the 1.0 second and 2.5 second trials.

An analysis similar to that performed for the eye movement data was performed on the subjective data to test whether the differences which exist between the four test conditions in the z-axis fixed duration test are statistically significant. To illustrate the process, the mean subjective response gains of the four conditions are given in Figure 4.19. The difference plots, similar those shown for the eye movement analysis, have been excluded. MB's normalized subjective estimates of translation show a downward

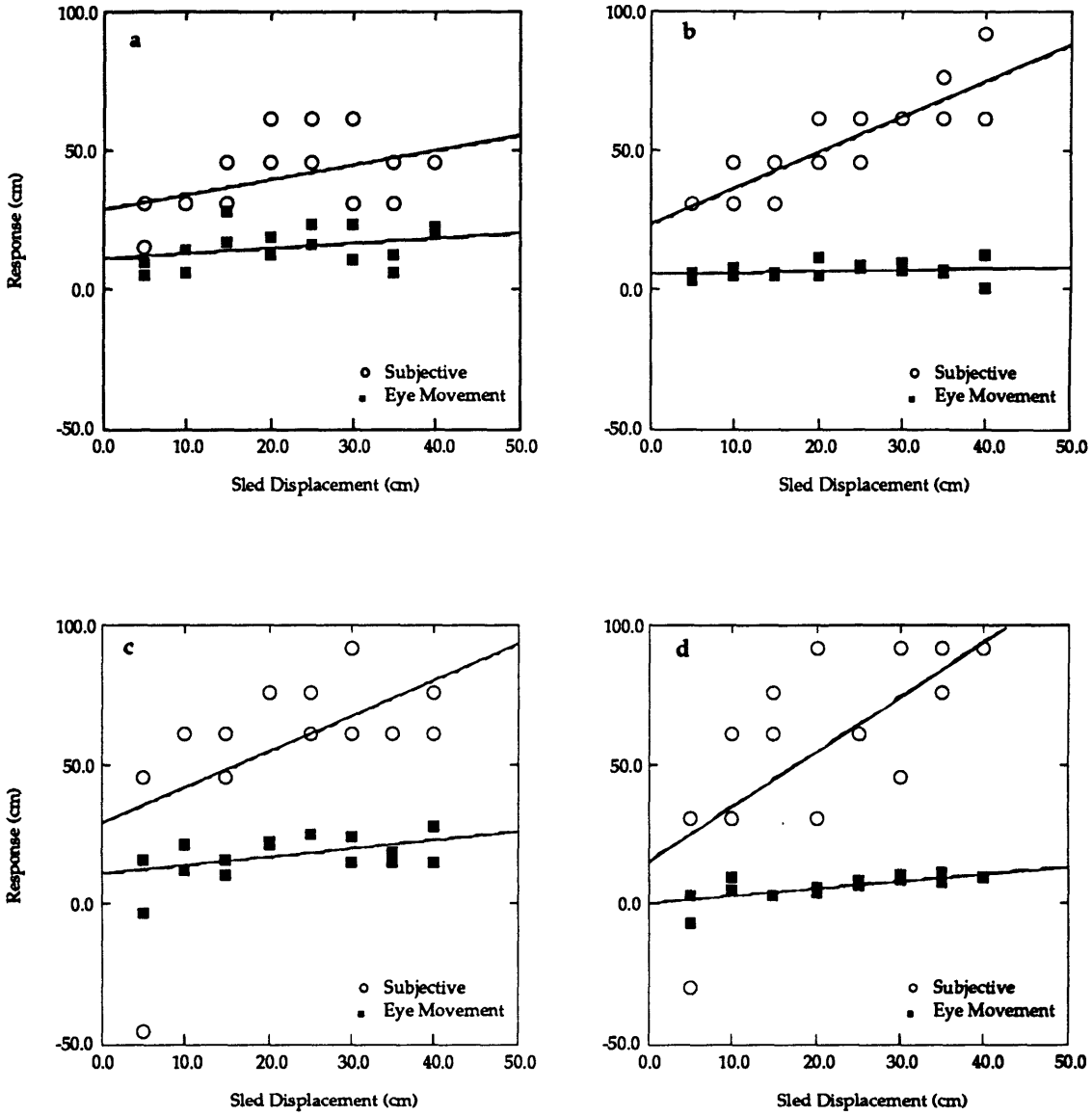

Figure 4.18. Scatter plots comparing subjective response to eye movement data for subject MB. (a) 1.0 second headward trials, (b) 1.0 second footward trials, (c) 2.5 second headward trials, (d) 2.5 second footward trials.

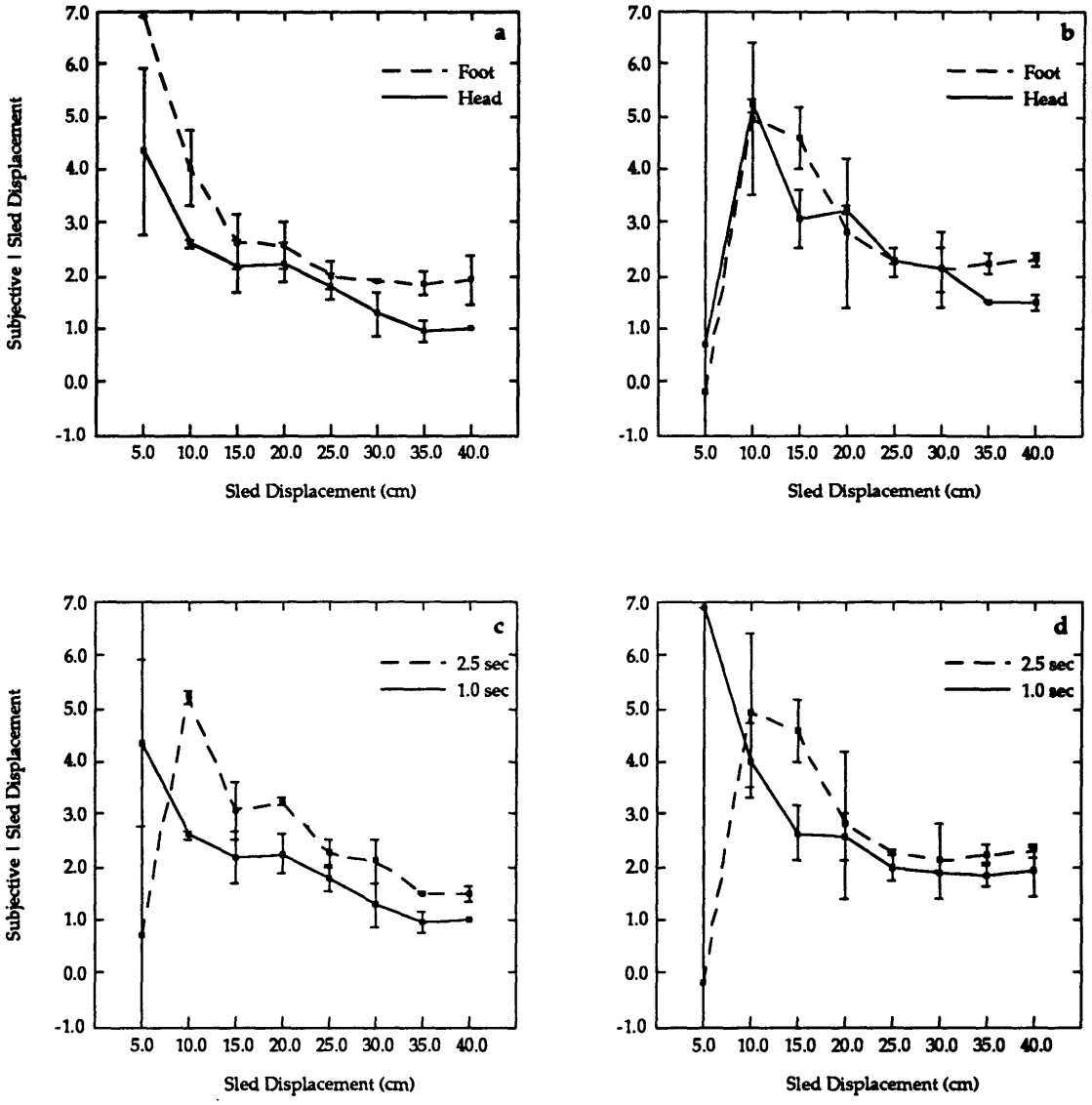

Figure 4.19. Mean normalized subjective responses for subject MB. (a) headward and footward 1.0 second trials, (b) headward and footward 2.5 second trials, (c) 1.0 and 2.5 second headward trials, and (d) 1.0 and 2.5 second footward trials. Error bars indicate the standard error of the difference.

trend as sled displacement increases similar to the trend in the normalized eye movement data. Overall, her subjective estimates are two to five times greater than the actual sled displacement. From the figures, it appears that MB subjectively favored footward trials and trials of longer duration.

A χ^2 test was performed to test whether the differences between the subjective responses are significant. The summary statistics from the χ^2 test are shown in Table 4.15. In the 1.0 second trials, the differences between MB's subjective responses during headward and footward trials were biased toward the footward trials. In the 2.5 second trials her subjective responses were somewhat variable, but were also slightly biased toward the footward displacements. These responses are opposite to her eye movement responses, where she demonstrated a significant bias towards headward translations in both the 1.0 and 2.5 second trials. In the headward cases MB gave a subjective report of moving farther during the 2.5 second trials, but her response during the footward trials varied inconsistently around zero indicating no asymmetry. This agrees with the results from her eye movement responses.

The following is a brief description of the results from the other five subjects. The summary plots and tables similar to those shown for subject MB are included in Appendix D.

Only three of the six subjects (JR, GS, MB) showed some significant difference between the regression coefficients of the headward and footward trials. However, all five of the subjects whose data was analyzable using the χ^2 test (not GS) showed a significant asymmetric trend in their eye movements favoring headward trials. No consistent

Table 4.15. Summary of χ^2 statistical analysis for all subjects for the subjective responses in the Z-axis Fixed Duration test. • = <0.001, √ = <0.005, † = <0.025, Δ = <0.05, blank = not significant.

Subj.	Difference Test	N	χ^2	P	Condition
JR	1 s trials: Up - Down	7	3.617		
	2.5 s trials: Up - Down	8	35.892	•	Down > Up
	Upward trials: 1s - 2.5s	8	8.064		
	Down trials: 1s - 2.5s	7	38.786	•	2.5s > 1.0s
AA	1 s trials: Up - Down	7	8.766		
	2.5 s trials: Up - Down	7	10.450		
	Upward trials: 1s - 2.5s	6	6.070		
	Down trials: 1s - 2.5s	8	34.022	•	2.5s > 1.0s
GS	1 s trials: Up - Down				
	2.5 s trials: Up - Down				
	Upward trials: 1s - 2.5s				
	Down trials: 1s - 2.5s				
MB	1 s trials: Up - Down	8	22.519	√	Down > Up
	2.5 s trials: Up - Down	8	31.075	•	Down > Up
	Upward trials: 1s - 2.5s	8	394.269	•	2.5s > 1.0s
	Down trials: 1s - 2.5s	8	10.405		
SS	1 s trials: Up - Down	7	70.855	•	Up > Down
	2.5 s trials: Up - Down	7	456.474	•	Up > Down
	Upward trials: 1s - 2.5s	7	19.202	Δ	2.5s > 1.0s
	Down trials: 1s - 2.5s	7	15.916	Δ	2.5s > 1.0s
KP	1 s trials: Up - Down	8	10.737		
	2.5 s trials: Up - Down	8	749.360	•	variable
	Upward trials: 1s - 2.5s	8	29.763	•	variable
	Down trials: 1s - 2.5s	8	102.164	•	2.5s > 1.0s

difference existed between their subjective correct responses during headward and footward trials, indicating that the difference was entirely due to the magnitude of their eye movements. This consistent asymmetry in eye movements across subjects supports the similar result in the z-axis fixed displacement test. Subjectively, however, only one of the six subjects (SS) tested gave a consistent subjective response indicating larger motion during headward displacements. Two subjects gave subjective responses consistently biased in the opposite direction of what their eye movements indicated (JR and MB). As in the Z-axis Fixed Displacement experiment, the subjective response data does not consistently support the eye movement data.

No consistent and significant difference was apparent between the regression analysis for the 1.0 and 2.5 second trials across subjects. Many of the regression lines lie directly on top of one another, and it is obvious that the scatter of the raw data points preclude any consistent difference. Using the χ^2 test only two of the six subjects (JR and AA) had any type of consistent trend, both with larger eye movements during the 2.5 second trials than during 1.0 second trials. The other four subjects showed no consistent difference between their eye movement responses to the 1.0 and 2.5 second trials. Based on the subjective responses, however, all five subjects who were analyzed favored the 2.5 second trials.

4.1.2.2.1. Summary of Z-axis Fixed Duration Test

Figure 4.20 clearly displays the difference between the headward and footward trials for all subject. The difference is most noticeable at the lower and middle sled displacements, while as the sled displacement increases the difference gradually decays. However, the asymmetry still exists at the largest displacement. Across subjects, it appears that the difference is due to both overcompensation for the headward trials (gain between 1.0 and 2.0) and undercompensation for the downward trials (gain less than 1.0). The subjective estimates of translation do not support the consistent eye movement asymmetry.

The downward trend overall indicates that on average subjects overcompensated for the small displacements and correctly compensated for the larger displacements. The downward trend is most obvious in the headward trials, but also exists during footward displacements. The downward trend in the normalize eye movements supports the flat regression lines calculated in the regression analysis of the eye movement data.

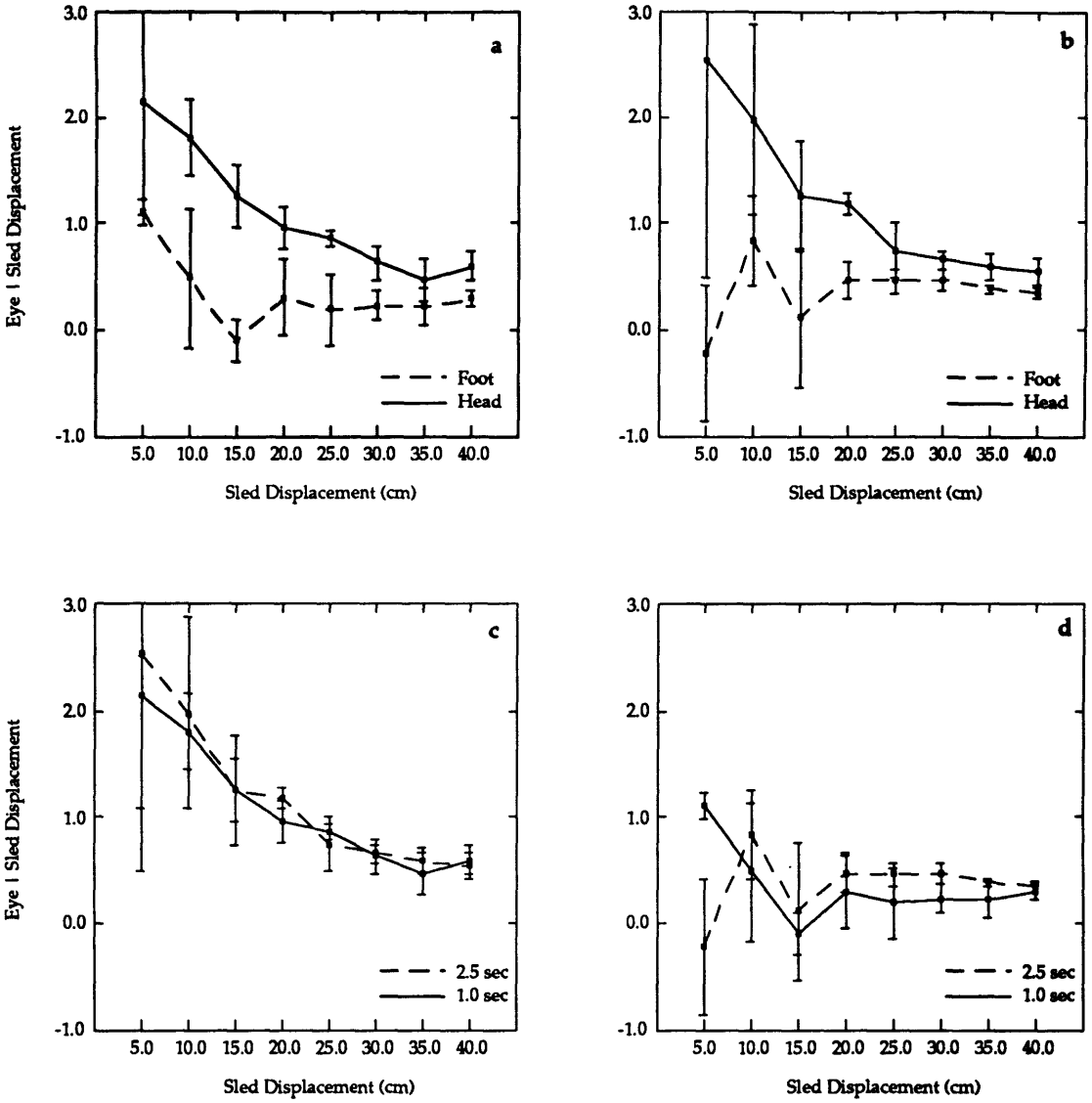

Figure 4.20. Z-axis fixed duration mean normalized eye movement responses versus sled displacement for all subjects. (a) 1.0 sec trials comparing headward and footward, (b) 2.5 sec trials comparing headward and footward, (c) headward trials comparing 1.0 sec and 2.5 sec, and (d) footward trials comparing 1.0 and 2.5 sec. Error bars indicate standard error.

No significant difference exists between the average responses to the 1.0 and 2.5 second trials across subjects in the headward trials. However in the downward trials, the mean eye movement response gains are slightly larger during the 2.5 second trials than the 1.0 second trials across nearly all sled displacements, indicating that the eye movement responses may be dependent upon trial duration in the downward trials. Subjective reports from four of the six subjects support this dependence upon trial duration in the downward trials.

4.2. Linear Adaptation

From previous studies on rotational adaptation, one might expect to see some adaptation after exposure to twenty-five minutes of the linear visual-vestibular adaptation paradigm with the visual field moving twice the distance of the linear displacements. However, very little if any adaptation was observed in any of the three test protocols for any of the subjects. The following section summarizes these results.

4.2.1. Hidden Target Pursuit Experiment

This section presents the results of the magnitudes and directions of the horizontal eye movements during a modified version of the fixed displacement experiment that was performed before and after the linear adaptation paradigm. The ensuing report of the results will follow a similar organization as during the fixed displacement test. Four conditions are compared: two directions (right/left) and pre-/post-adaptation. As the displacement was fixed at 18.20 cm (20 degrees), no comparison is made between sled displacements.

Mean normalized eye movement responses are plotted versus acceleration in Figure 4.21 for subject CL as representative of the sample tested. The eye movement responses were normalized by dividing by the distance the sled traveled during the particular trial which

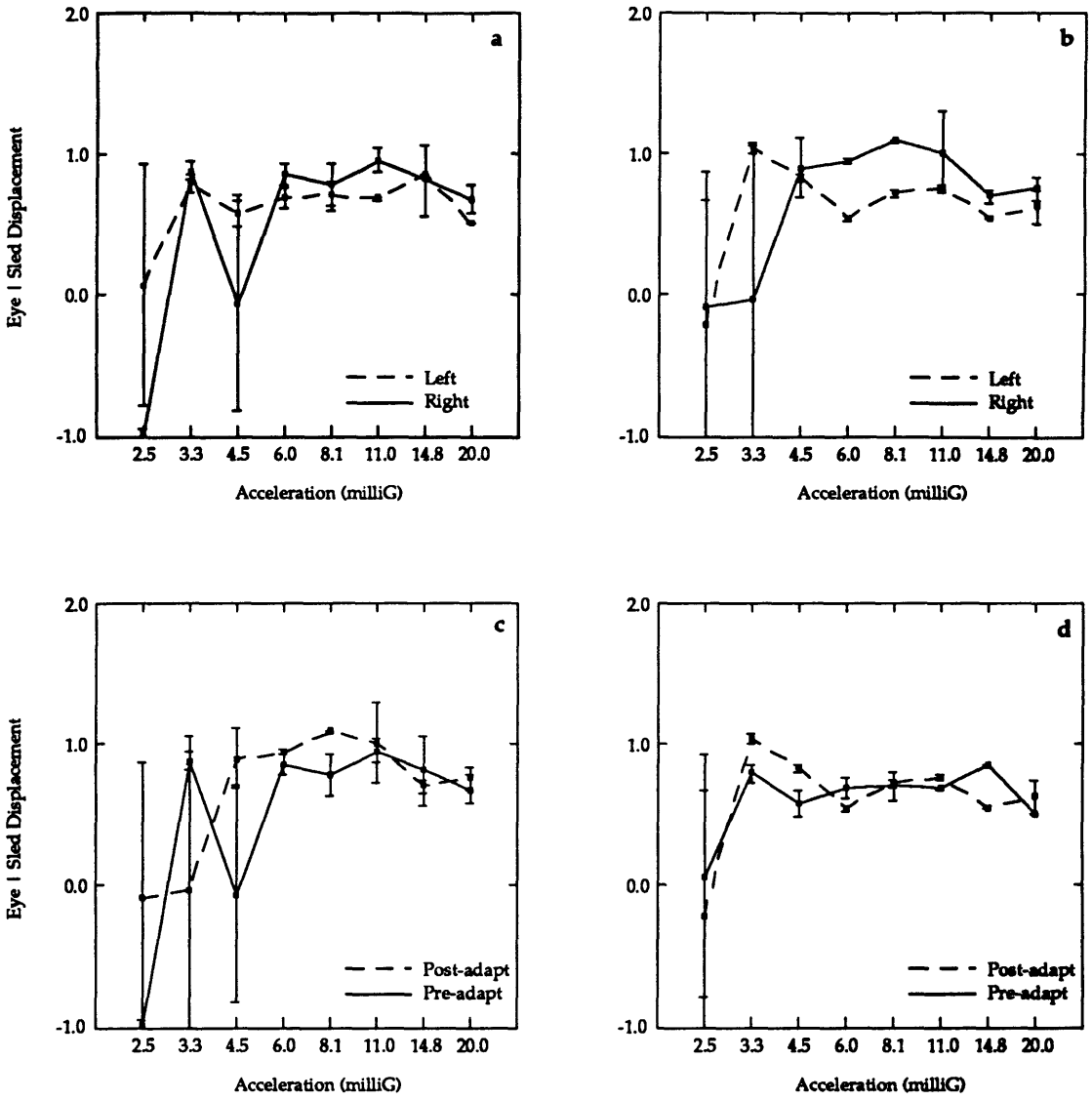

Figure 4.21. Pre-/Post Adaptation Hidden Target Pursuit eye movement data for subject CL. a) rightward and leftward pre-adaptation trials, (b) rightward and leftward post-adaptation trials, (c) pre- and post-adaptation rightward trials, (d) pre- and post-adaptation leftward. Error bars signify standard error.

was calculated from the sled position signal. The four plots in Figure 4.21 compare the mean eye movement response at each acceleration level for the four different trial conditions. The first two plots separate the (a) pre-adaptation trials from the (b) post-adaptation trials and compare the responses to rightward and leftward sled movements. The third and fourth plots separate the data into the (c) rightward and (d) leftward trials and compare the eye movement responses pre-adaptation to those post-adaptation. Similar plots for the other three subjects are included in Appendix E.

Threshold levels for detection of linear acceleration were chosen based on the 'rule' described in the Methods section, namely, *the lowest of two or more consecutive accelerations where the mean eye displacement is significantly different from zero.* Table 4.16 shows the threshold level for perception calculated for each subject pre-adaptation and post-adaptation. One would expect that below a person's threshold the mean response of many trials would average to approximately zero, confirming that the probability of 'guessing' the correct direction is fifty percent. With only two data points at each acceleration level in each condition, an average response of zero is rarely observed, however the variances are usually high.

Table 4.16. Summary of eye movement thresholds for perception pre- and post-adaptation for all subjects. Means and Standard Deviations include trials in both directions at a particular G-level.

Subj.	Pre-Adapt. (milliG)	Post-Adapt. (milliG)
DM	4.5	4.5
CL	6.0	4.5
MB	4.5	6.0
KJ	4.5	< 2.5

An independent t-test was performed on the mean normalized eye movements at each acceleration for each subject to test for a significant difference between the pre- and post-

adaptation conditions. Not one acceleration level for any of the four subjects elicited a significantly different response between the pre- and post-adaptation states. This indicates that either no adaptation occurred or that any adaptation was masked by fatigue. The data looked qualitatively similar to the hidden target pursuit experiments discussed previously in this thesis. Post-adaptation many of the subjects' eye movements were slightly more saccadic than pre-adaptation. This could be attributed to the subjects' high level of fatigue, inhibiting how well they could smoothly track the target, and stimulating the saccadic system to compensate.

The assumption of similarity between directions of sled displacement for this table is based on previous left/right analysis and observation of the plots of the mean responses. Additional analysis of potential right/left asymmetry was performed to confirm this assumption and is discussed in the following paragraphs. A $\chi 2$ test was performed across acceleration levels for each subject to determine if any overall trend existed between any of the four conditions that was not apparent in the figures. To illustrate the process the difference between the pre- and post-adaptation responses and the rightward and leftward responses were calculated and plotted in Figure 4.22 for subject CL.

The difference plots make any significant disparity between the test conditions more visible. For example, in Figure 4.22 (b) it is clear that post-adaptation subject CL responded asymmetrically, favoring sled displacements toward her right at the 6.0 and 8.1 milliG levels. At all other accelerations, however, the difference curve varies insignificantly around zero, indicating no asymmetry. In Figure 4.22 (c) and (d) the mathematical differences between CL's normalized eye movements pre-adaptation and post-adaptation are shown. No consistent trend is apparent in either the rightward or leftward trials for subject CL. Table 4.17 summarizes the results from the χ^2 tests performed across all acceleration levels simultaneously. The p-values associated with the

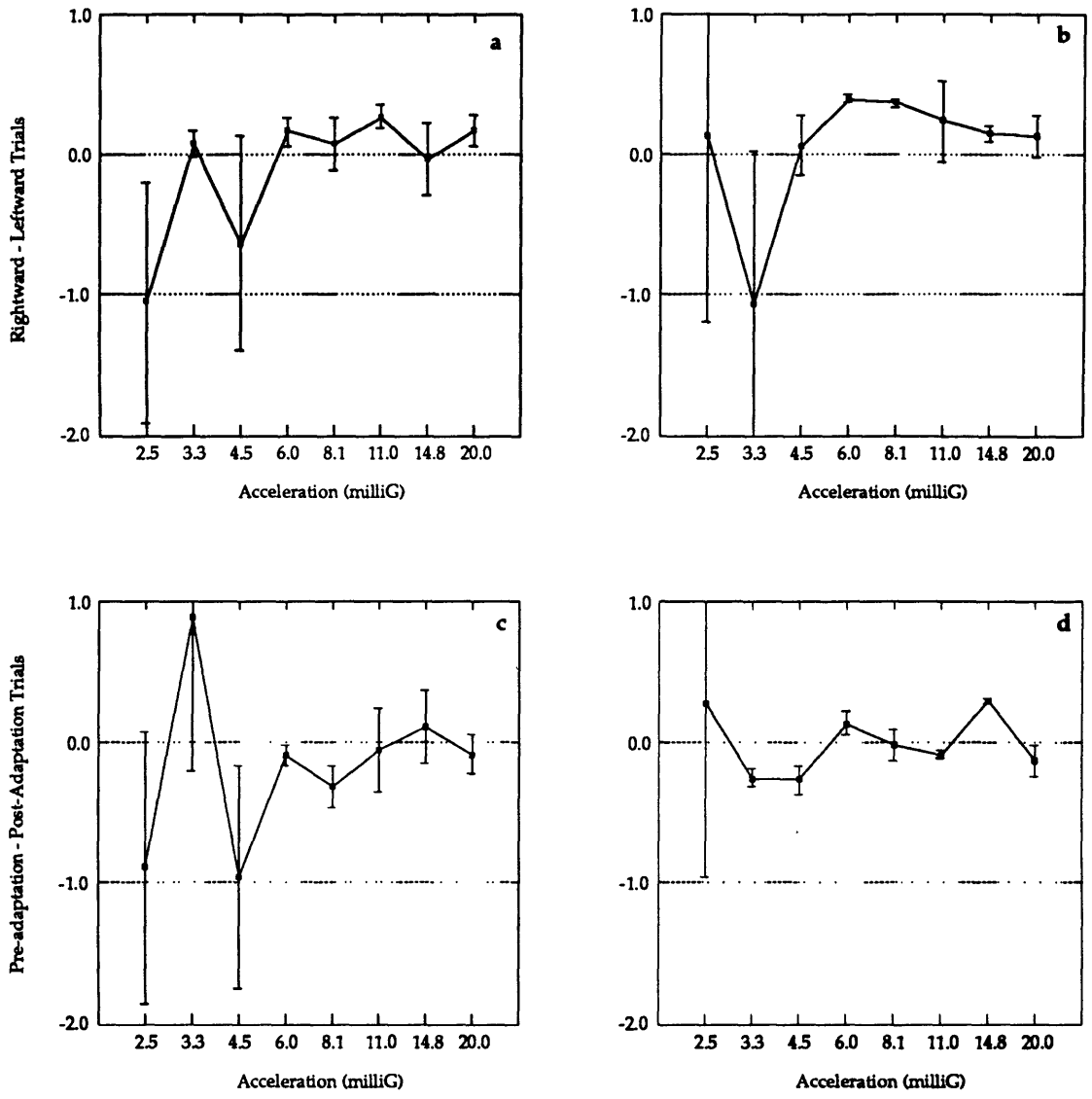

Figure 4.22. Differences in mean normalized eye movement responses versus sled acceleration for subject CL. (a) rightward minus leftward pre-adaptation trials, (b) rightward minus leftward post-adaptation trials, (c) pre-adaptation minus post-adaptation rightward trials, and (d) pre-adaptation minus post-adaptation rightward trials. Error bars indicate standard error of the difference.

Table 4.17. Summary of χ^2 statistical analysis for the eye movement responses of all subjects in the Pre-/Post-adaptation Hidden Target Pursuit experiment. • = <0.001, √ = <0.005, † = <0.025, Δ = <0.05, blank = not significant.

Subj.	Difference Test	N	χ^2	P	Condition
DM	Pre-adapt: Right-Left	8	7.149		
	Post-adapt: Right-Left	8	9.515		
	Right: Pre - Post	8	5.985		
	Left: Pre - Post	8	7.469		
CL	Pre-adapt: Right-Left	8	20.044	†	variable
	Post-adapt: Right-Left	8	376.882	•	Right > Left
	Right: Pre - Post	8	9.193		
	Left: Pre - Post	8	284.469	•	variable
MB	Pre-adapt: Right-Left	8	60.813	•	variable
	Post-adapt: Right-Left	8	8.939		
	Right: Pre - Post	8	10.009		
	Left: Pre - Post	8	108.226	•	Pre > Post
KJ	Pre-adapt: Right-Left	8	45.271	•	Right > Left
	Post-adapt: Right-Left				
	Right: Pre - Post				
	Left: Pre - Post				

χ^2 statistical test are two-tailed. Therefore, if the calculated χ^2 value indicates a significant difference between the two conditions being tested then one must review the data to determine the direction of the trend (which condition is greater) or even if a trend exists.

As confirmed by these statistical tests and examination of the difference plots in Figure 4.22, subject CL displayed no significant asymmetric trend in her eye movement response during the pre-adaptation trials. Post-adaptation, her asymmetric responses at the two accelerations described above were large enough to make the χ^2 significant, but the asymmetry was inconsistent at other G-levels. The lack of a consistent asymmetric trend supports the results from the y-axis fixed displacement and fixed duration Hidden Target Pursuit tests discussed previously. The three experiments together lead to the conclusive result that, although some subjects show asymmetric responses in y-axis

upright accelerations, there is no consistent trend across subjects. With a larger data set, a more detailed investigation could be made of the subjects who did show some sort of right/left asymmetry to determine if the asymmetries were by chance alone.

In regards to differences between pre- and post-adaptation, the χ^2 test statistically proved that no significant difference existed between CL's normalized responses pre- and post-adaptation. During leftward trials, the calculated χ^2 value was statistically significant. However, Figure 4.22 (d) shows no significant trend in the difference across accelerations.

Analysis of the subjective estimates of translation can also be used to more fully understand the quantitative eye movement data. The subjective responses were analyzed to determine if there were any perceptual differences between the four conditions that were not evident in the eye movement data shown above. Figure 4.23 shows the mean responses to the four test conditions for subject CL.

χ^2 tests identical to those performed above were performed on the subjective responses. The results from the χ^2 tests are shown in Table 4.18 for all subjects. Although the differences in CL's responses were variable from one acceleration to another, she showed a slight asymmetry in her subjective responses to accelerations above 8.1 milliG, biased towards sled movements to her right. The χ^2 test also revealed a significant difference between her subjective responses pre-adaptation and post-adaptation. In both directions of sled displacement she responded with larger subjective displacements pre-adaptation. This indicates that the lack of adaptive eye movements was not simply due to fatigue of the eyes. CL was the only subject to produce a significant difference in her subjective responses between pre- and post-adaptation. The differences for the other three subjects were variable from one acceleration to another with no consistent trend.

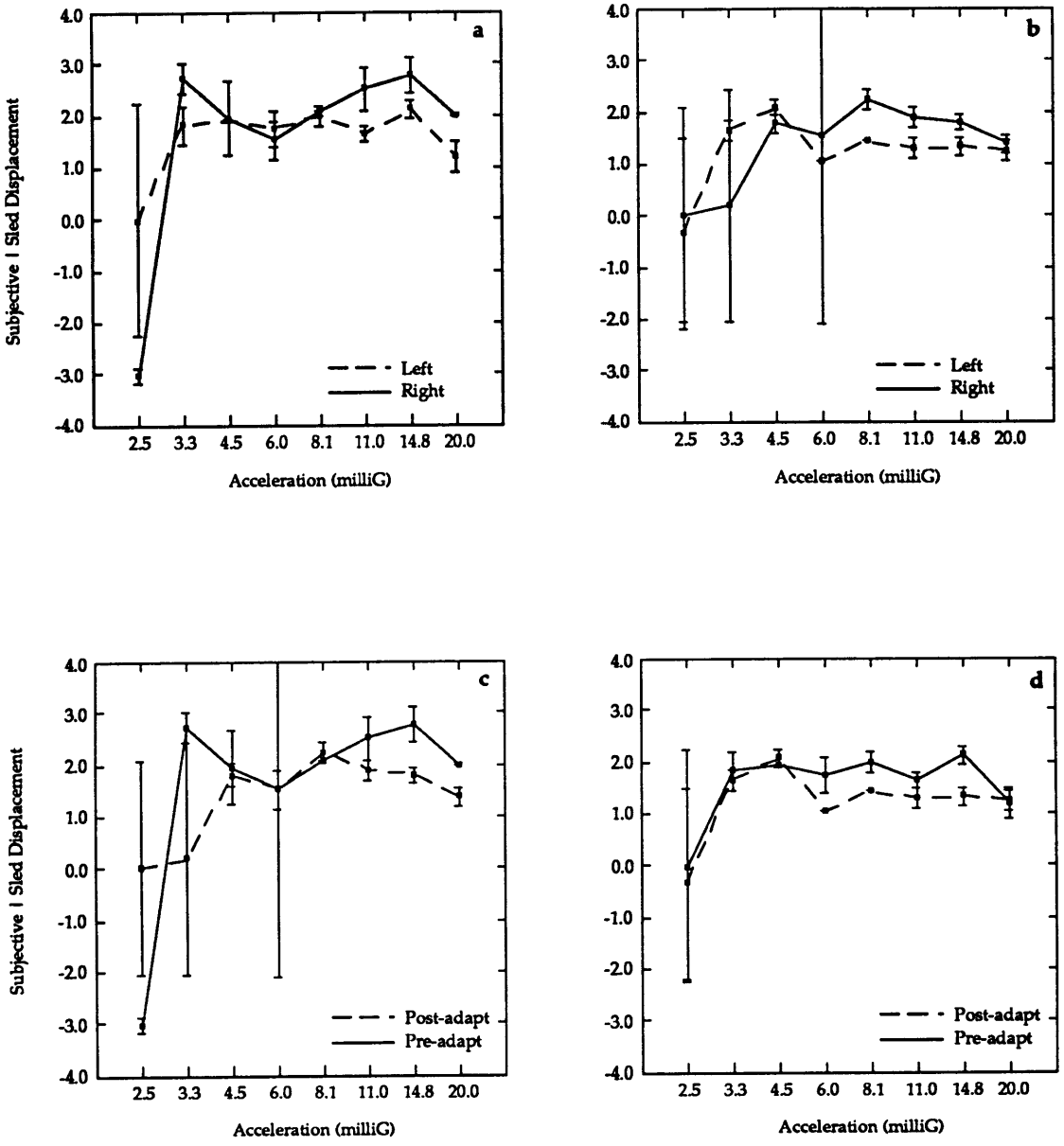

Figure 4.23. Mean normalized subjective responses versus sled acceleration for subject CL. (a) rightward and leftward pre-adaptation trials, (b) rightward and leftward post-adaptation trials, (c) pre-adaptation and post-adaptation rightward trials, and (d) pre-adaptation and post-adaptation rightward trials. Error bars indicate standard error.

Table 4.18. Summary of χ^2 statistical analysis for the subjective responses of all subjects in the Pre-/Post-adaptation Hidden Target Pursuit experiment. • = <0.001, √ = <0.005, † = <0.025, Δ = <0.05, blank = not significant.

Subj.	Difference Test	N	χ^2	P	Condition
DM	Pre-adapt: Right-Left	8	6.896		
	Post-adapt: Right-Left	8	22.738	√	Right > Left
	Right: Pre - Post	8	10.697		
	Left: Pre - Post	8	3.254		
CL	Pre-adapt: Right-Left	7*	20.948	†	variable
	Post-adapt: Right-Left	7*	28.184	•	variable
	Right: Pre - Post	8	26.317	•	Pre > Post
	Left: Pre - Post	8	26.902	•	Pre > Post
MB	Pre-adapt: Right-Left	8	2011.918	•	Right > Left
	Post-adapt: Right-Left	8	71.930	•	variable
	Right: Pre - Post	8	41.058	•	variable
	Left: Pre - Post	8	8.503		
KJ	Pre-adapt: Right-Left	8	16.782	Δ	variable
	Post-adapt: Right-Left				
	Right: Pre - Post				
	Left: Pre - Post				

The following is a brief description of the results from the other three subjects. The summary plots and tables similar to those that were presented for subject CL are included in Appendix E.

Only MB demonstrated a significant difference between pre- and post-adaptation responses. In the rightward trials she had slightly larger eye movements pre-adaptation. This decrease in eye movements post-adaptation is probably due to fatigue, not to adaptation, as the paradigm was designed to increase the gain of the eye movements post-adaptation. DM's responses pre- and post-adaptation were insignificantly different from each other. Unfortunately, three of the four χ^2 tests could not be performed for subject KJ, as the set of repeat trials post-adaptation was lost. However, no significant difference appears to exist between his pre- and post-adaptation responses. Subjectively, CL was the only subject to report any significant difference between pre- and post-adaptation. In

summary, no significant 2x adaptation was evident in any of the subjects tested. If anything, the tendency was for the subjects' eye movements and subjective responses to decrease post-adaptation. As stated before, one explanation for such a trend would be fatigue.

With regards to directional asymmetries, KJ favored trials to the right during the pre-adaptation trials, but not post-adaptation. As stated above, CL also responded with larger eye movements during the rightward trials, but only post-adaptation. DM and MB showed no significant asymmetric trend in their eye movements. Subjectively, however, DM and MB each responded with a bias toward rightward trials in either the pre- or post-adaptation conditions, but not both.

Figure 4.24 compares the normalized eye movement responses during the rightward and leftward and the pre- and post-adaptation trials for all subjects combined. Quantitative conclusions may be inappropriate because of inter-subject variability. However, it provides an overall qualitative understanding of the subjects' responses to changes in acceleration during the different test conditions. Qualitatively the figure demonstrates the lack of difference between the pre- and post-adaptation responses and a small asymmetric trend toward rightward sled movements.

4.2.2. Linear VOR experiment

Similar to the Hidden Target Pursuit experiment, very little adaptation, if any at all, was evident in the VOR gain of the horizontal eye movements. Table 4.19 summarizes the amplitude and standard deviation of the slow phase velocity (SPV) pre- and post-adaptation for the three different trials. The p-values provided for the DC Values and the First Harmonic indicate whether a significant response exists in these conditions. The first harmonic of subject CL's slow phase velocity in each condition was significant,

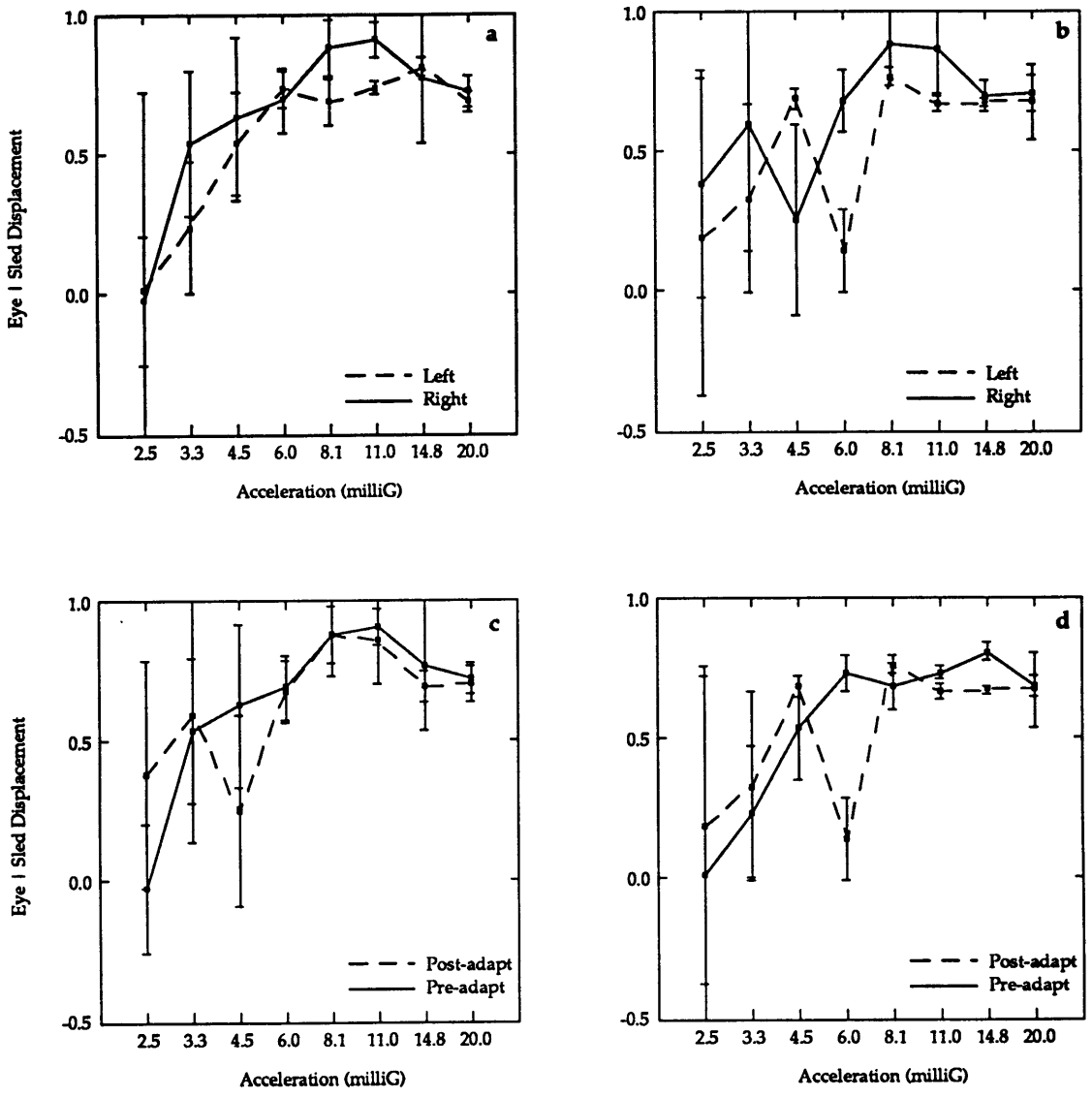

Figure 4.24. Pre-/Post Adaptation Hidden Target Pursuit eye movement data for all subjects. (a) rightward and leftward pre-adaptation trials, (b) rightward and leftward post-adaptation trials, (c) pre- and post-adaptation rightward trials, and (d) pre- and post-adaptation leftward trials. Error bars indicate standard error.

Table 4.19. Summary of Horizontal Linear VOR data for all subject.

			DC Values			First Harmonic				
Subj	Condition		Ampl	StDev	Pr.	Ampl.	StDev	Phase	StDev	Pr.
CL	Pre-Adapt	Dark	-.292	.561		1.294	.549	-157.6	31.258	.001
		OK alone	.220	1.581		45.051	4.463	-4.8	1.466	.001
		OK+Sled	-1.125	1.323	.050	57.269	1.905	-166.4	1.433	.001
	Post-Adapt	Dark	-.614	.414	.010	2.026	.547	134.0	16.877	.001
		OK alone	-1.479	1.775	.050	39.631	5.654	-3.7	2.617	.001
		OK+Sled	-1.336	.698	.001	60.952	2.102	166.2	.990	.001
KJ	Pre-Adapt	Dark	-2.897	.864	.001	8.766	.792	128.68	7.046	.001
		OK alone	.429	.769		58.953	1.906	-3.39	1.860	.001
		OK+Sled	-.420	.657		64.253	1.275	164.50	1.337	.001
	Post-Adapt	Dark	-.816	1.583		8.327	1.762	132.08	6.881	.001
		OK alone	.332	.781		57.623	.779	-2.60	1.063	.001
		OK+Sled	-.246	.780		62.786	1.612	164.24	1.079	.001
MB	Pre-Adapt	Dark	-.668	.569	.050	3.570	.840	158.6	15.879	.001
		OK alone	-3.982	1.831	.001	39.591	9.291	-2.2	3.288	.001
		OK alone	-4.443	3.288	.010	40.591	7.089	-2.0	3.750	.001
		OK+Sled	.611	.668	.050	62.800	2.202	-105.7	.763	.001
	Post-Adapt	Dark	.009	.573		5.951	1.202	-145.8	8.495	.001
		OK alone	-.463	2.473		40.197	4.444	-.5	2.444	.001
		OK+Sled	-.779	2.815		56.882	3.281	161.8	2.094	.001
DM	Pre-Adapt	Dark	-1.137	.544	.001	3.780	1.015	-164.1	11.205	.001
		OK alone	.759	1.063	.100	57.646	2.297	-3.7	.768	.001
		OK+Sled	-.349	.776		64.060	.820	-164.9	.440	.001
	Post-Adapt	Dark	.306	.619		2.798	.795	-136.8	12.982	.001
		OK alone	.106	1.017		54.777	1.684	-1.9	1.359	.001
		OK alone	.239	.645		56.908	2.204	-2.4	.592	.001
		OK+Sled	-.157	.599		62.244	.893	-15.4	.941	.001

indicating that either or both the vestibular or optokinetic stimuli elicited a significant response at the amplitudes given in the table. Her responses at the second at harmonic were only significant during the dark and OK+Sled trials pre-adaptation.

The gain of subject CL's response increased slightly post-adaptation in the dark trial, decreased slightly in the OK alone trial and increased slightly in the OK+Sled. However, none of these differences were statistically significant. Figure 4.25 shows the confidence areas around the resultant mean of subject CL's responses during each condition. As stated in the Methods, the ellipse is used to define the 95 percent confidence area around the mean. A confidence area is necessary (as opposed to a confidence interval for a univariate case) because the responses consist of two components, the sine and cosine, which define the relationship of the magnitude and phase. If a significant difference were to exist, the ellipses would not overlap. Without any further analysis, it is obvious that no significant difference exists between pre- and post-adaptation for any of the conditions.

Like CL, the other three subjects tested (DM, KJ, and MB) had a significant SPV at the first harmonic. The amplitudes of their responses in the dark condition ranged from 1.294°/s (CL) to 8.766 °/s (KJ) pre-adaptation, and did not change significantly following adaptation. Subject KJ and DM's SPVs were close to the visual stimulus velocity during both the OK trial and larger than the stimulus velocity in the OK+Sled condition both pre- and post-adaptation. Subject DM's SPV decreased slightly in all three trials after the adaptation session, probably indicating an effect due to fatigue, while subject KJ's SPV remained unchanged in the dark trial and decreased slightly in both the OK and the OK+Sled trials. MB's SPV in the light were slightly lower than DM or KJ. Her responses increased slightly in the dark, remained about the same in the OK trial, and decreased in the OK+Sled trial. As stated above, none of the differences between pre- and post-adaptation just described were statistically significant.

4.2.3. Angular VOR experiment

Since no change was observed during the linear VOR trials, a change post-adaptation in the angular VOR experiments was not expected, and no significant adaptation was

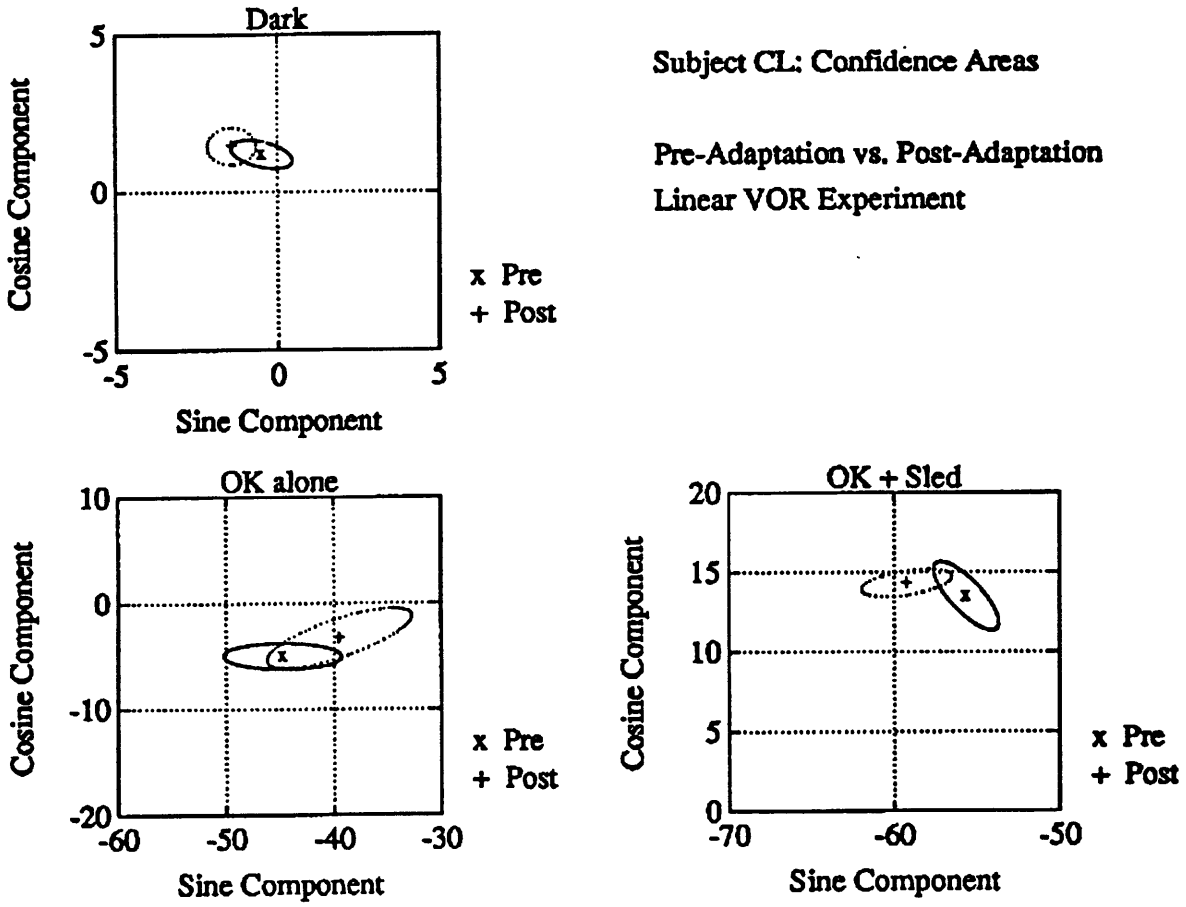

Figure 4.25. Plot of confidence areas for linear VOR comparison of pre-/post-adaptation for subject CL. (a) dark run, (b) optokinetic stimulus alone, and (c) optokinetic + sled. Ellipses represent confidence interval about the mean amplitude.

observed. Table 4.20 summarizes the amplitude and standard deviation of the subjects' horizontal slow phase velocity (SPV) pre- and post-adaptation for the angular VOR trials.

At the first harmonic, CL's slow phase velocity was highly significant during all trials. The rotating chair velocity was 60°/s, and her slow phase eye movements were between 25 and 45 °/s. The table makes obvious the downward trend of the amplitude of her eye movement response with time (i.e., from pre-adapt to post-adapt). The decrease in

Table 4.20. Summary of angular VOR adaptation data for all subjects.

			DC Values			First Harmonic				
Subj	Condition		Ampl	StDev	Pr.	Ampl.	StDev	Phase	StDev	Pr.
CL	Pre-Adapt	Dark #1	-3.156	4.131	0.05	45.242	7.786	-160.7	17.55	0.00
		Dark #2	-1.610	4.950		42.505	5.932	-168.4	109.71	0.00
	Post-Adapt	Dark #1	-2.269	3.902	0.10	25.358	12.815	-158.3	105.11	0.00
		Dark #2	-1.807	8.074		31.575	8.233	-152.4	104.60	0.00
KJ	Pre-Adapt	Dark #1	-1.397	9.721		71.946	29.748	-176.5	164.8	.001
		Dark #2	1.500	6.784		60.478	11.602	-174.3	147.2	.001
	Post-Adapt	Dark #1	-6.074	8.987	.100	53.632	15.045	-169.7	109.1	.001
		Dark #2	.155	8.375		54.718	8.695	-170.8	108.9	.001
MB	Pre-Adapt	Dark #1	2.633	4.803		36.147	7.992	-172.0	4.894	.001
		Dark #2	7.152	4.811	.001	35.067	4.826	-169.3	4.898	.001
	Post-Adapt	Dark #1	-2.009	7.949		31.810	6.977	-166.2	5.240	.001
		Dark #2	-7.159	5.631	.010	34.486	11.283	-165.7	15.294	.001
DM	Pre-Adapt	Dark #1	.487	1.950		34.567	7.179	-176.1	148.5	.001
		Dark #2	-.186	2.123		36.749	3.852	-175.2	2.8	.001
		Dark #3	1.751	1.666	.050	36.565	1.868	-174.1	124.8	.001
	Post-Adapt	Dark #1	1.034	1.297	.050	43.825	2.930	-172.3	3.0	.001
		Dark #2	-2.750	3.842	.050	36.110	7.085	-171.6	4.4	.001

amplitude is probably due to the high level of fatigue generated during the course of the experiment.

Although significant care was taken to remove any chance of 'normal' visual-vestibular interaction between the experiments following the adaptation paradigm, the angular VOR experiment was the last set of trials performed post-adaptation. There is some reason to believe that, even if there had been some adaptation, the subject might have returned to a normally adapted state by the time of the final testing on the rotating chair. On average, the post-adaptation rotating chair trials were 40 minutes after the end of the 30 minute adaptation paradigm.

Inspection of the first harmonic only indicates that the amplitude of subject CL's slow phase velocity decreased post-adaptation (average: pre = 43.9 °/s, post = 28.5 °/s). However, the decrease post-adaptation was not statistically significant. Figure 4.26 shows the confidence areas around the resultant mean of subject CL's responses. All four of the ellipse confidence areas overlap to some degree. The first pre-adaptation and the second post-adaptation trials were very close to statistical significance, indicating an effect opposite in direction to the adaptation effect we were looking for.

As expected, the SPV of all four subjects in this experiment were much larger than in the linear VOR experiment. Although KJ's SPV in the linear VOR experiment was high (8.76 °/s) compared to the other subjects, he also had a very large SPV in the angular VOR experiment (average 66.2 °/s pre-adaptation). Subject KJ's response decreased post-adaptation (average = 54.2 °/s). The amplitude of DM's slow phase velocity increased slightly, but not significantly, from pre- to post-adaptation (pre = 35.9 °/s, post = 39.5 °/s), while subject MB's SPV decreased from pre- to post-adaptation (pre = 35.6 °/s, post = 33.1 °/s). As stated above, none of the differences just described were statistically significant.

4.2.4. Adaptation Paradigm

Since no significant adaptation was evident in any of the three pre-/post-adaptation experiments, it is important to examine the adaptation paradigm for potential problems.

From Snyder and King (1988) we know that adaptation works best at the frequency of the stimulus and degrades the farther the test frequency is from that adaptation frequency. One would expect that a pseudo-random stimulus used for adaptation would either adapt a broad band of frequencies or not adapt any frequency very well. In this experiment, the

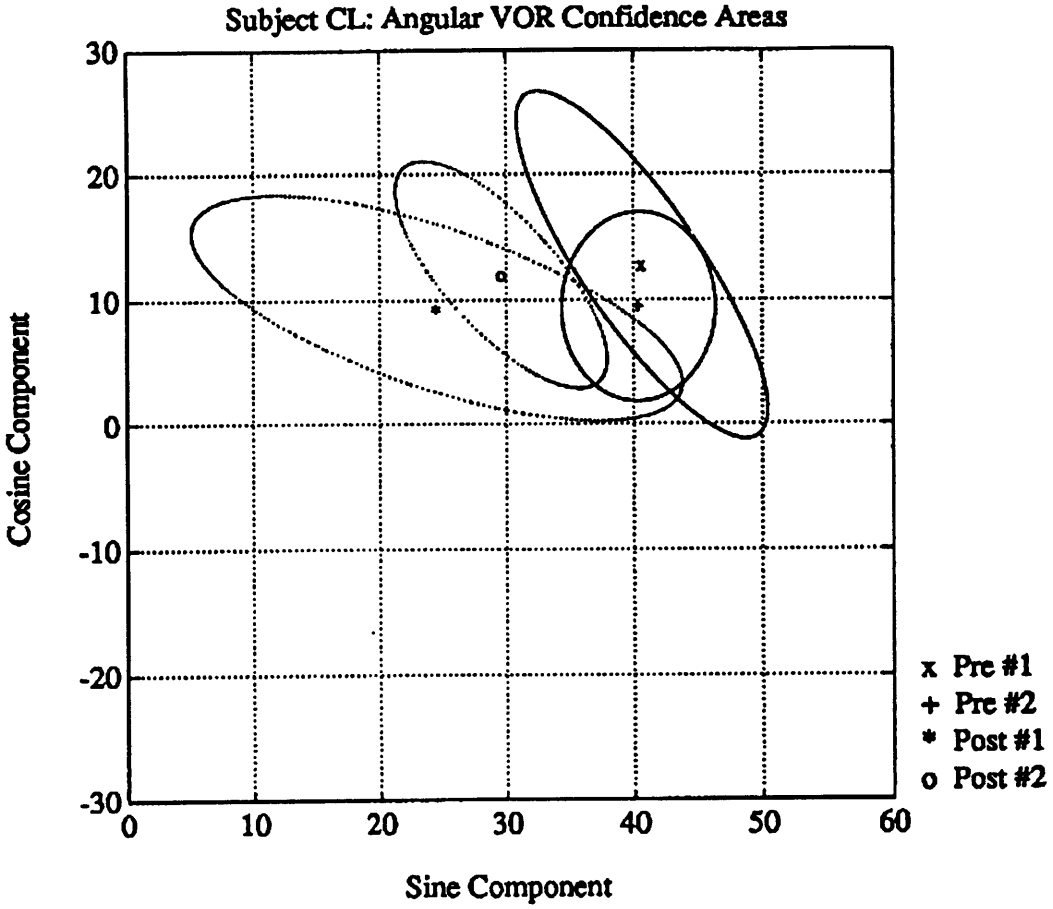

Figure 4.26. Plot of confidence areas for angular VOR comparison of pre-/post-adaptation for subject CL. Ellipses represent confidence interval about the mean amplitude.

stimulus for the adaptation was actively input by the subject using a joystick. Therefore, there was no single adaptation frequency, as if a passive sinusoidal stimulus was used. Although all of the test frequencies were included in the primary range of the adaptation stimulus input by the subjects (0.01 - 0.3 Hz), an adaptive response may have been observed if only a single stimulus frequency been used.

Figure 4.27 shows the power spectral density function calculated for four segments of subject CL's adaptation session. The segment shown in the top right hand corner was not a full five minute session because she exceeded the safety limits of the track during her

session. As stated in the Methods, in such a case a new five minute session is started until at least five full, five minute sessions are completed. Example plots of the power spectral density functions for the other three subjects are included in Appendix E.

It is evident from the figure below that subject CL reduced the range of her input frequencies as time went on. In the first two plots her primary frequencies ranged from 0.01 to 0.3. In the third and fourth adaptation segments shown, her joystick input was almost entirely less than 0.2 Hz. The stimulus frequencies for the VOR trials on the sled were 0.25 Hz. Therefore, if adaptation is frequency specific, it is possible that CL was not adapted at the appropriate frequencies.

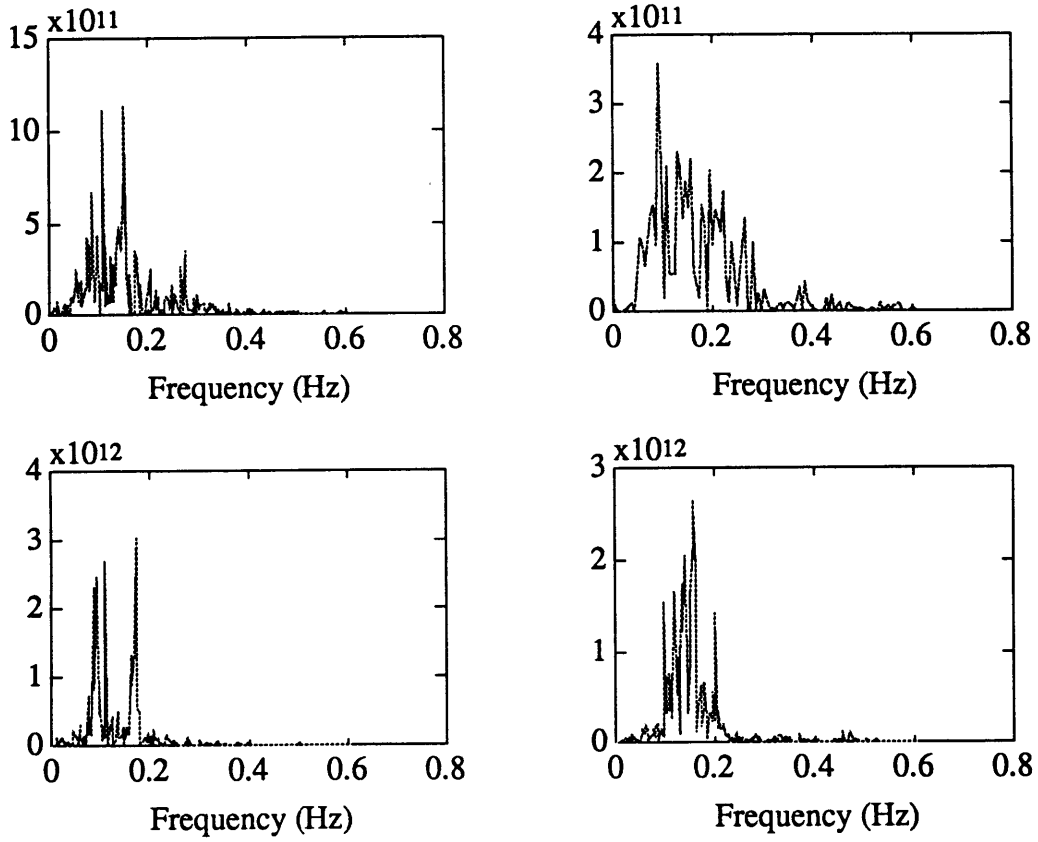

Figure 4.27. Power spectral density functions for four segments of subject CL's adaptation paradigm.

5. DISCUSSION

The experiments described in this thesis were performed to develop a test to help quantify human perception of linear translation using voluntary saccadic eye movements. By instructing subjects to visually track an imagined target fixed in space while they were linearly accelerated using a "damped position step" displacement, insight into the subjects' perception of translation was gained. The current study had three primary objectives: (1) Replicate and further explore the y-axis eye movement experiments performed by Israel and Berthoz (1989) by developing a new test that quantifies subject's perception of translation. (2) Once defined, extend the experiments to z-axis accelerations which until now have not been quantitatively investigated using this paradigm. (3) Experiment with a visual linear adaptation paradigm to extend the well-defined angular adaptation paradigms to a new, less defined modality, while utilizing the Hidden Target Pursuit experiment to help quantify potential changes following adaptation.

To meet these goals, two different hidden target pursuit experiments, the fixed displacement test and the fixed duration test, were performed with the linear motion along the subjects' y- and z-axes. In the fixed displacement test, subjects were exposed to eight or ten different sled accelerations while the sled displacement was held constant at two amplitudes (8.82 cm and 18.20 cm corresponding to the 10 and 20 degree trials) in both directions. In the fixed duration test, eight sled displacements were tested while the duration of the trials were held constant at either 1.0 second or 2.5 seconds. The magnitude and direction of the eye movements during translation were used to obtain thresholds of perception of linear acceleration that a human can detect on earth, to test the accuracy that humans can estimate their displacement, to determine the dependence of displacement estimation on trial duration, and to investigate directional asymmetries in human perception.

Eventually, the Hidden Target Pursuit experiment developed for this thesis will be used to measure differences in eye movement responses following adaptation to spaceflight. No preflight/postflight tests have attempted to quantify the human's perception of linear translation as these experiments do. A one-G adaptation experiment using conflicting visual and vestibular stimuli was performed to ascertain if adaptation might be quantifiable using eye movements. The adaptation paradigm used, however, had never before been attempted. Several previous experiments have altered the angular VOR pathways, but until now no one had reported attempts to alter the linear VOR pathways by using linear acceleration and linear visual stimulation as adaptation stimulation.

Three general engineering tasks were completed in preparation for the hidden target pursuit experiments just described. (1) Design and implementation of the software code to enable the sled to move in a "damped position step" motion (code included in Appendix F). (2) Design and implementation of an integrated sled helmet, communication, and noise cancellation system. The primary design criteria were to rigidly fix the subject's head to the sled, provide open communication between the subject and the experimenter, eliminate or mask all acoustic cues from the sled motion, and maintain subject comfort for a minimum of thirty minutes. (3) Design of an automated Target Pursuit Shade controlled by the sled computer to block the visual target from the subject's view.

The following sections discuss the results and conclusions from the experiments described, compare them with previous experiments, and discuss ideas for future research.

5.1. Hidden Target Pursuit

Eye movement thresholds varied from one subject to another, however, they averaged approximately 0.003 G in the y-axis and 0.006 G in the z-axis. This is in agreement with previous studies that showed perceptual thresholds for direction of linear motion are slightly higher in the z-axis (0.154 m/s^2 = 0.016 G) than in the y-axis (0.057 m/s^2 = 0.005 G) using a single cycle of sine acceleration as the stimulus. (Benson, 1986).

5.1.1. Y-axis Experiments

Although several subjects had slightly asymmetric eye movement responses at some accelerations during the fixed displacement test, no consistent pattern existed across subjects. (3 = rightward > leftward, 4 = symmetric, 1 = leftward> rightward). No consistent right/left asymmetry existed in subjects' eye movements or in their subjective responses in either of the y-axis experiments. A significant difference existed, however, between the normalized eye movement responses to the two different amplitudes of sled displacement (8.82 cm and 18.20 cm corresponding to the 10 and 20 degree trials). On average, the majority of the subjects overcompensated for the 10 degree trials, resulting in a gain of greater than 1.0, and approximately correctly compensated for the 20 degree trials. In all eight subjects a significant difference existed between the normalized eye movement responses to the two displacements. The average gain of the eye movements during the 10 degree trials was approximately 2.0, while that of the 20 degree trials was approximately 1.0 indicating that the subjects did not accurately discriminate between the two sled displacements.

This inability is also evident in the large amount of scatter in the fixed duration experiment. For most of the subjects, the scatter was as large as ±15 cm at any one sled displacement while the stimulus itself ranged only from 5 cm to 40 cm. The slopes of the regression lines fit to the data ranged between 0.231 and 0.584. If the subjects were to

perfectly compensate for the sled displacement, on average the regression lines would have a slope of 1.0. Since subjects were not able to accurately discriminate between the different sled displacements, responding to each similarly, they produced a flatter response overall than expected. Responses to the 2.5 second trials were larger than responses to the 1.0 second trials in four of the five subjects tested in either the leftward or rightward trials, but not both, as shown by the χ^2 test. This indicates that the subjects' responses may be dependent upon the duration (or frequency) of the stimulus. This was consistent with the subjective responses given by three of the four subjects following each trial.

The fixed duration test is similar to the hidden target pursuit experiment performed by Israel and Berthoz (1989) where the duration of the trials was fixed at 2.5 seconds. They did not compare different trial durations, as they were primarily interested in whether subjects could accurately track a hidden target and what types of eye movements were used, smooth pursuit or saccades. Their results should be similar to the 2.5 second trials in the current study, however the two data sets are significantly different from one another. Most significantly, their subjects were able to compensate for the sled displacement much more accurately. Figure 5.1 shows a summary plot of the regression lines for each of the subjects in their study. The slopes of the regression lines are very close to 1.0, meaning their subjects were able to accurately compensate different sled displacements.

The large differences between the two data sets are surprising since the design of the experiments was very similar. One obvious difference between the two experiments is in the feedback given to the subjects after each trial. In Israel and Berthoz's experiment the subject was shown a small white target while the sled was at rest, the room lights were turned off and a curtain was lowered between the subject and the target, the sled would

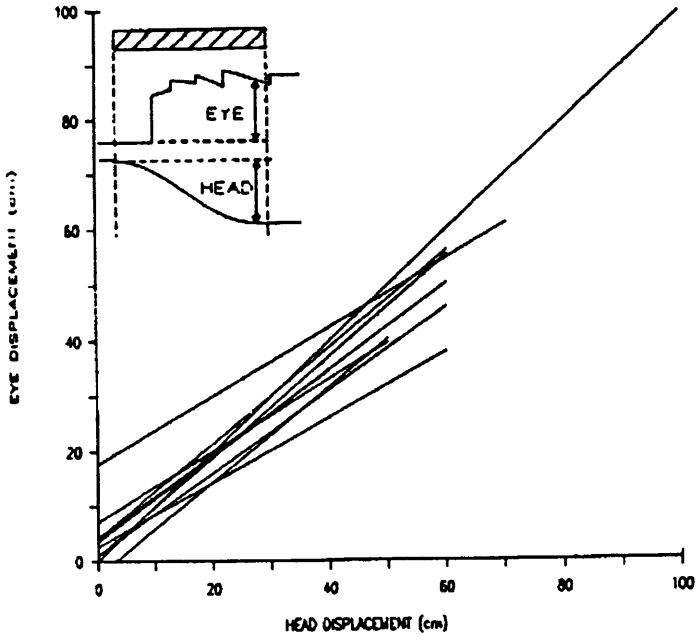

Figure 5.1. Summary plot of regression lines for all subjects from Israel and Berthoz (1989)

move, 2-3 seconds after the sled stopped the room lights were turned on and curtain was raised so the subject could see the target, and the sled would move back to the center. The last two steps of their protocol are reversed in the current study. Showing the subject the target before positioning the sled back in the center allowed the experimenters to measure the subject's corrective saccade to the target, which is a more accurate method of measuring eye movements during EOG recordings. However, letting the subject see the target after each trial gives performance feedback as to her, thereby closing the loop of the "control system". One could imagine that the subject was calibrating her perceptions of target translation by seeing how well she was tracking the hidden target. In the current experiment, the system remained open loop as the subject was not shown the target position until the sled had returned to center.

A second difference between the two experiments involves the lighting in the sled. Israel and Berthoz turned on the room lights before and after each trial allowing the subject to view the white target, while during the sled motion the subject was in complete darkness. In the current experiment, the room lights were extinguished throughout the test session to eliminate external visual cues, and two fluorescent lights inside the sled were continuously shining toward the subject to maintain a constant light level. Therefore, although all external visual motion cues were eliminated, the subject was able to see the inside of the black cloth covering the sled. The visual targets used for tracking in the two experiments were also different: a red LED located 50 cm (y-axis) or 52 cm (z-axis) in front of the subject was used in the current experiments, and a "small white object" located 63 cm away from the subject was used in the previous study. Likewise, the experiments were performed on two different linear accelerators that most likely have different characteristics of movement (vibration, noise, friction) that could cause differences in perception and in eye movement responses.

5.1.2. Z-axis Experiments

Similar to the y-axis experiments, a significant difference existed between the normalized responses to the 10 and 20 degree trials in the z-axis. The eye movement gains during the 10 degree trials were in many cases twice as large as the gains during the 20 degree trials. This implies that the subjects were not accurately discriminating between the two sled displacements. As in the y-axis, this finding is consistent with the fixed duration experiment. The regression coefficients for the six subjects ranged between -0.331 to 0.739. (For perfect compensation the slopes of the lines should have been 1.0.) No significant difference was found between the 1.0 second and 2.5 second cases, meaning the subjects' responses were not dependent on the duration of the trial in either sled orientation.

While in the y-axis no consistent directional asymmetry was apparent, the same experiments in the z-axis elicited a bias towards headward translation across nearly all subjects. The difference was primarily evident in the magnitude of the subjects' eye movements, downward eye movements being larger than upward. The asymmetric eye movement trend was most noticeable at the lowest accelerations. At the largest accelerations, where the subjects were probably more confident of their displacement, the difference between the upward and downward responses was smaller, but in most cases, still existent. Several subjects also answered correctly more frequently when the sled was moving toward their heads. Subjective estimates of translation, however, did not consistently support the directional asymmetry. The majority of the subjective responses were symmetrical, and in some cases an asymmetry was found in the opposite direction (Downward trials > Upward trials).

The consistency in the eye movement asymmetry across all subjects is undeniable. The mechanism that causes this asymmetry in the z-axis (supine) experiments is not so clear. The most obvious possibility to investigate is the effect of gravity. As bipeds evolving in the one-G earth environment, humans spend the majority of their awake hours with gravity acting as a shearing force on the saccular otoliths. One might hypothesize a correction bias in the neural processes between the sacculus and the central nervous system. Figure 5.2 gives a graphical depiction of the expected bias due to gravity. Although the bias would occur in the neural pathways, for simplicity, the expected bias is depicted as affecting the saccular end organ. In the upright position, the sacculus experiences an effective upward acceleration due to the downward force of gravity. With the subject stationary, the saccular otoliths would need to develop a neural bias acting like a downward acceleration (upward force) to counteract the force of gravity so that the subject does not perceive that she is accelerating upward while upright. If the sacculus were not biased due to the upward acceleration due to gravity, then a larger footward

(downward) acceleration would be necessary to produce the same response to an headward (upward) acceleration. However, no directional asymmetry exists during z-axis (vertical) accelerations when the head is upright (Young, et al., 1978). When the subject is supine gravity no longer produces a shearing force on the saccular otoliths. However, based on the above assumption, the saccular otoliths might still have a bias acting like a footward acceleration. Therefore, a larger stimulus would be needed during headward accelerations to produce the same sensation as during footward accelerations. In the current experiment, headward accelerations produced larger eye movements than downward accelerations, i.e., an asymmetry opposite to the proposed gravity explanation. Therefore, the hypothesis of a gravity compensation bias does not explain the asymmetry found in the data.

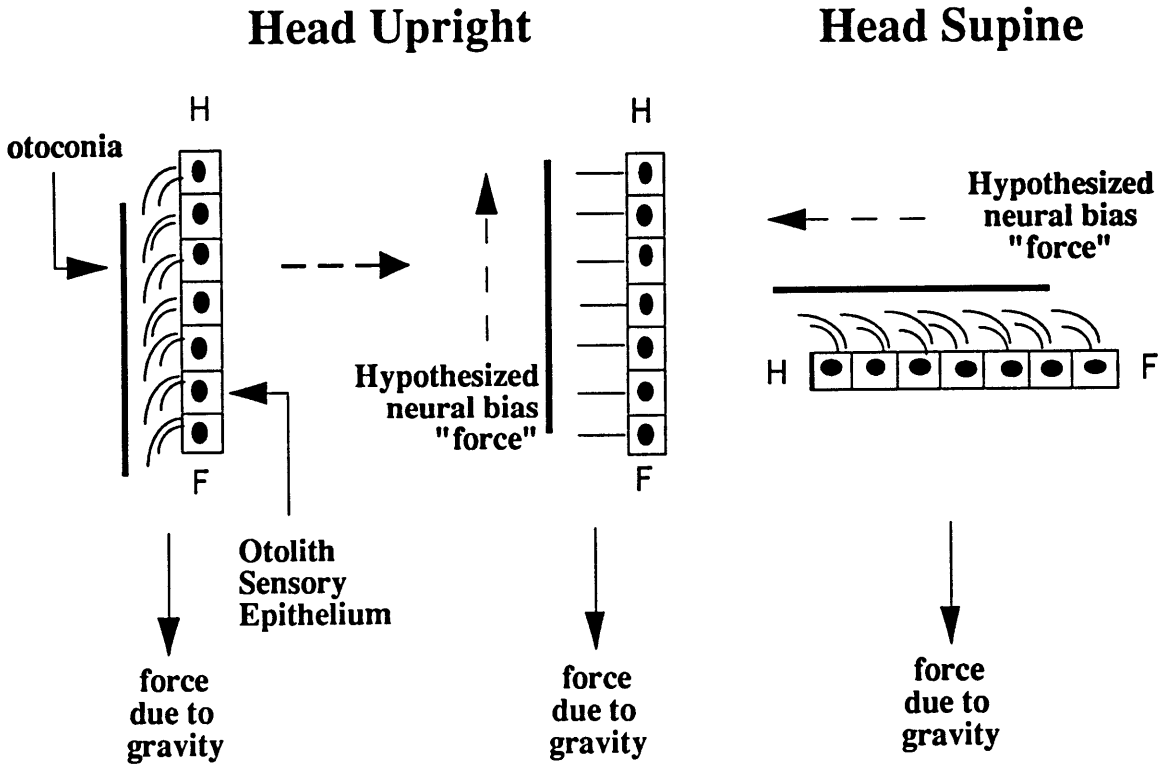

Figure 5.2. Graphical depiction of the expected bias in the saccular otoliths due to gravity.

In previous studies, z-axis directional asymmetries have been identified in vertical optokinetic nystagmus (OKN), optokinetic afternystagmus (OKAN), and angular VOR (Baloh, et al., 1983; Matsuo and Cohen, 1984; Böhmer and Baloh, 1991). In these experiments, upward slow phase velocities, produced by an optokinetic stimulus moving downward, were greater than downward slow phase velocities. This asymmetry favors the direction opposite of that found in the current experiments. As the OKN, OKAN, and angular VOR are reflexive eye movements evoked by the moving stimulus, and the observed asymmetry is in the opposite direction, the possibility that the asymmetry found in the current experiments is due to the same mechanism is extremely unlikely.

Another possible explanation for the asymmetric responses includes the effects of the asymmetries in the visual system. Due to facial bone and muscle structure, large eye movements are more limited upward than downward. This supports the direction of the asymmetry observed in the data, so it could feasibly explain the difference. However, the asymmetry in the eye movement data was frequently most apparent at the smaller sled displacements during the fixed duration experiment, i.e., the difference between the eye movement gains during headward and footward trials was larger at small displacements and decayed to approximately zero at the larger displacements. In the fixed displacement experiment, the asymmetry was equally apparent in both the 10 and 20 degree cases, if not more so in the 10 degree cases. Based on the anatomy and physiology of the eyes and the structures surrounding them, no limitations should be observed for small eye movements and the limitations should increase for larger eye movements. Therefore, this explanation is not consistent with the data.

A final potential explanation of the asymmetry in the eye movement data is that the sled stimulus was asymmetric. Careful analysis of the sled position signal elicited a slight

positional asymmetry, with slightly (less than 10%) larger sled movements toward the subjects' head than toward the feet , i.e., in the same direction as the asymmetry found in the eye movement responses. This difference in position was accounted for in the z-axis experiments by normalizing each eye displacement by the actual sled displacement for each particular trial. As the figures in the text and in the appendices show, the asymmetry was still clearly evident (Figures 4.11 and 4.16 and Appendices C and D). One could suggest that the accelerations in the two directions must be different to yield different displacements. However, the data indicates that subjects are insensitive to small changes in acceleration, as shown by the relatively constant gain of the eye movements across acceleration in all of the fixed displacement experiments. In addition, the exact same sled profiles (trials) were run during both the z- and the y-axis experiments. One would expect, especially since subjects are more sensitive to accelerations in the y-axis (e.g., lower threshold), that if any motion asymmetry was significant, the responses should have been asymmetric in the y-axis experiments as well as in the z-axis. Such a consistent asymmetry was not observed in the y-axis experiments.

The preceding discussion provides several potential explanations for the z-axis asymmetry. However, each interpretation is refutable with the counter arguments presented. Subsequent experiments should be performed to further investigate this asymmetry to isolate the mechanism(s) involved.

5.2. Linear Adaptation

As was shown in the Results chapter (Chapter 4), no significant differences emerged between the pre- and post-adaptation experiments. Fatigue may have masked some of the adaptation, but one might expect to at least see some differences immediately following the adaptation paradigm. More likely, other factors inhibited the adaptation process from occurring. This experiment was the first linear adaptation scheme performed to alter the

response of the neural pathways to the brain, and the lack of a significant result does not show that linear adaptation is not possible. The adaptation paradigm employed may not have been appropriate to produce any changes. Many questions emerge from this experiment that need to be further investigated by subsequent experiments, including: Is twenty-five minutes a long enough time to induce linear adaptation? Is active input by the subject the appropriate means of attaining adaptation? Or would passive sinusoidal (single frequency) or pseudo-random oscillations be more appropriate?

The frequencies at which the subjects adapted themselves may not be adaptable. Possibly, since the amplitude of linear VOR horizontal eye movements is small compared to angular VOR responses, the neural pathways may simply be more complicated and require a longer adaptation period to exhibit any changes. Finally, although there is significant physiological and anatomical data showing that some of the neural pathways from the vestibular system are modifiable, no one has established that the pathways leading specifically from the otoliths to the vestibular nucleus adapt.

5.3. Recommendation for Further Study

The results gathered from the experiments in this thesis suggest several ideas that necessitate further experimentation. Most importantly, a larger data set is needed to confirm the results and allow for a deeper understanding of the mechanisms at work. With so many variables under investigation, (i.e., trial duration, sled acceleration, sled displacement, and direction of sled displacement) it is difficult to get a significant number of repeat trials for each condition. Therefore, replication of the current studies would be useful to confirm the conclusions drawn.

Additional analysis of the eye movement data gathered in these experiment may also be useful in understanding the mechanisms causing the different responses to the various

trial conditions. For example, further analysis should be performed on the differences between the eye movement responses to headward and footward displacements. As stated in the Results and in the previous discussion, the difference between these two conditions decreases as sled displacement increases, i.e., the asymmetry is more significant at smaller sled displacements. A more quantitative analysis of this difference should be performed to better define that asymmetry.

In addition, different linear adaptation paradigms should be experimented with to elicit a neural adaptation in the linear VOR pathways to the brain. Adaptation using passive linear oscillations, either sinusoidal or pseudo-random stimulation, should be used to gain more control over the stimulation frequencies. However, steps must be taken to keep the subject alert if an active paradigm is not used. In addition, since significant adaptation has been observed in angular VOR following adaptation paradigms using rotational visual and vestibular stimulation, it would be interesting to test whether the neural adaptation of the angular VOR pathways would manifest itself in the linear pre-/post-adaptation tests performed in this thesis (Hidden Target Pursuit and linear VOR).

Lastly, these results indicate that the voluntary saccadic eye movements evoked by the hidden target pursuit task can be used to quantify sensations of translation. Extension of the hidden target pursuit experiment to quantify changes due to adaptation to micro-gravity may provide further understanding of the effects of spaceflight on signal processing, as well as the role of gravity in perception of body movement.

Currently, the Hidden Target Pursuit test is manifested as a preflight/postflight test on the SpaceLab Life Sciences-2 (SLS-2) Shuttle mission to complement the existing battery of biomedical experiments designed to quantify changes in humans following adaptation to microgravity. The experiment will be similar to the fixed displacement test described

above, with the displacement fixed at 12.06 cm, which would evoke 15 degree eye movements during perfect compensation. Because of limited experimental time, and the need for repeat trials, three accelerations (0.010, 0.015, and 0.020 G) will be tested in each direction and will be repeated four times for a total of twenty-four trials. The experiment will be performed in both the y- and z-axes.

REFERENCES

Arrott, A.P., Young, L.R., MIT/Canadian Vestibular Experiments on the Spacelab-1 Mission: 6. Vestibular Reactions To Lateral Acceleration Following Ten Days Of Weightlessness. Experimental Brain Research. 64: 347-357, 1986.

Baker, J., Harrison, R.E.W., Isu, N., Wickland, C.R., Petterson, B.W., Dynamics of Adaptive Change in Vestibulo-Ocular Reflex Direction. II. Sagittal Plane Rotations. Brain Research, 371, pp. 166-170, 1986

Balkwill, M. D., Changes in Human Horizontal Angular VOR After the Spacelab SLS-1 Mission. SM Thesis, Massachusetts Institute of Technology, Cambridge, MA, Feb. 1992.

Baloh, R. W., Richman, L., Yee, R. D., Honrubia, V., The Dynamics of Vertical Eye Movements in Normal Human Subjects. Aviation, Space and Environmental Medicine, January 1983.

Baloh, R.W., Beykirch, K., Honrubia, V., Yee, R.D. Eye Movements Induced by Linear Acceleration on a Parallel Swing. Journal of Neurophysiology. 60: 2000-2013, 1988

Benson, A.J., The Senses. Chapter 16: The Vestibular Sensory System. Ed. by Barlow, H.B. and Mollon, J.D., Cambridge University Press, 1982

Benson, A.J., Thresholds of Perception of Whole Body Linear Oscillation: Modification by Spaceflight. Proceedings of Second European Symposium on Life Sciences Research in Space. Porz Wahn, Germany 4-6 June 1984 (ESA SP-212 - August 1984).

Benson, A.J., Spencer, M.B., Stott, J.R.R., Thresholds for the Detection of the Direction of Whole-Body, Linear Movement in the Horizontal Plane. Aviation, Space, and Environmental Medicine, pp. 1088-1096, November, 1986.

Bloomberg, Melvill Jones, Segal, McFarlane, Soul. Vestibular-Contingent Voluntary Saccades Based on Cognitive Estimates of Remembered Vestibular Information. Advances in Oto-Rhino-Laryng. 41: 71-75

Böhmer, A. Baloh, R. W., Vertical Optokinetic Nystagmus and Optokinetic Afternystagmus in Humans. Journal of Vestibular Research, Vol. 1, pp. 309-315, 1990/91,

Boff, K.R., Lincoln, J.E., Engineering Data Compendium: Human Perception and Performance. AAMRL, Wright-Patterson AFT, OH, pp. 770-781, 1988.

Buizza, A., Leger, A., Berthoz, Schmid, R. Otolithic-acoustic Interaction in the Control of Eye Movement. Experimental Brain Research. 36: 509-522, 1979

Buizza, A., Schmid, R., Droulez, J. Influence of Linear Acceleration on Oculomotor Control. Progress in Oculomotor Research. 1981

Clement, G., Reschke, M., Chapter 6. Response of the Neurovestibular System: Introduction to Space Life Science. edited by Churchill, S., unpublished version, pp. 105-133, Jan. 1992.

Cohen, B., Kozlovskaya, I., Raphan, T., Solomon, D., Helwig, D., Cohen, N., Sirota, M., Yakushin, S., Vestibuloocular Reflex of Rhesus Monkeys After Spaceflight. The American Physiological Society, pp. 121S-131S, 1992

Correia, M.J., Perachio, A.A., Dickman, J.D., Kozlovskaya, I.B., Sirota, M.G., Yakushin, S.B., Beloozerova, I.N., Changes In Monkey Horizontal Semicircular Canal Afferent Responses Following Space Flight. In Press, Supp. to the J. Appl. Physiol., Aug. 1992

Demer, J.L., Porter, F.I., Goldberg, J., Jenkins, H.A., Schmidt, K., Adaptation to Telescopic Spectacles: Vestibulo-ocular Reflex Plasticity. Investigative Ophthalmology & Visual Science, 30, pp. 159-170, January 1989

Fernandez, C., Goldberg, J., Physiology of Peripheral Neurons Innervating Otolith Organs of the Squirrel Monkey. I. Response to Static Tilts and to Long-Duration Centrifugal Force. Journal of Neurophysiology, Vol. 39, No. 5, pp. 970-984, September 1976

Fernandez, C. Goldberg, J., Physiology of Peripheral Neurons Innervating Otolith Organs of the Squirrel Monkey. II. Directional Selectivity and Force-Response Relations. Journal of Neurophysiology, Vol. 39, No. 5, pp. 985-995, September 1976

Fernandez, C. Goldberg, J., Physiology of Peripheral Neurons Innervating Otolith Organs of the Squirrel Monkey. III. Response Dynamics. Journal of Neurophysiology, Vol. 39, No. 5, pp. 996-1008, September 1976

Fernandez, C. Goldberg, J., Abend, W., Response to Static Tilts of Peripheral Neurons Innervating Otolith Organs of the Squirrel Monkey. Journal of Neurophysiology, Vol. 35, pp. 978-996, 1972

Gonshor, A. Melvill Jones, G., Short Term Adaptive Changes In the Human Vestibulo-Ocular Reflex Arc. Journal of Physiology, 256, pp. 361-379, 1976

Gonshor, A. Melvill Jones, G., Extreme Vestibulo-Ocular Adaptation Induced By Prolonged Optical Reversal of Vision. Journal of Physiology, 256, pp. 381-414, 1976

Guedry Jr., F. E. Chapter 1. Pyschophysics of Vestibular Sensation. Handbook of Sensory Physiology, Vol. VI/2, pp. 67-104, edited by H. H. Kornhuber, Springer-Verlag, 1974.

Gundry, A. J. Thresholds of Perception for Periodic Linear Motion. Aviation, Space, and Environmental Medicine, May, 1978.

Harrison, R.E.W., Baker, J.F., Isu, N., Wickland, C.R., Petterson, B.W., Dynamics of Adaptive Change in Vestibulo-Ocular Reflex Direction. I. Rotations in the Horizontal Plane. Brain Research, 371, pp. 162-165, 1986

Henn, V., Cohen, B., Young, L.R., Visual-Vestibular Interaction in Motion Perception and the Generation of Nystagmus. Neurosciences Research Program Bulletin. Vol. 18, No. 4, September, 1980

Israël, I., Berthoz, A. Contribution of the Otoliths to the Calculation of Linear Displacement. Journal of Neurophysiology. 62: 247-263, 1989

Kozlovskaya, I.B., Babaev, B.M., Barmin, V.A., Beloozerova, I.I., Kreidich, Y.V., Sirota, M.G., The Effect of Weightlessness on Motor and Vestibulo-Motor Reactions. The Physiologist, Vol. 27, No. 6, Suppl., 1984

Lisberger, S.G., The Neural Basis for Learning of Simple Motor Skills. Science, Vol. 242, pp. 728-735, 1988

Mah, R. W. , Young, L. R., Steele, C. R., Schubert, E. D., Threshold Perception of Whole-body Motion to Linear Sinusoidal Stimulation. AIAA Flight Simulation Technologies Conference and Exhibit, August 14-16, 1989, Boston, MA.

Massoumnia, M., Detection of Fast Phase of Nystagmus Using Digital Filtering. SM Thesis, Massachusetts Institute of Technology, Cambridge, MA, 1983

Matsuo, V., Cohen, B., Vertical Optokinetic Nystagmus and Vestibular Nystagmus in the Monkey: Up-down Asymmetry and Effects of Gravity. Experimental Brain Research 53: 197-216, 1984.

Melvill Jones, G., Young, L. R., Subjective Detection of Vertical Acceleration: A Velocity-Dependent Response? Acta Otolaryngol 85:45-53, 1978.

Mendoza, J.C., Investigation of Optokinetic Nystagmus and the Linear Vestibular-ocular Reflex. SM Thesis, Massachusetts Institute of Technology, Cambridge, MA, June 1993

Merfeld, D.M., Spatial Orientation in the Squirrel Monkey: An Experimental and Theoretical Investigation. PhD Thesis, Massachusetts Institute of Technology, Cambridge, MA, 1990.

Miles, F.A., Eighmy, B.B., Long-Term Adaptive Changes in Primate Vestibuloocular Reflex. I. Behavioral Observations. Journal of Neurophysiology, Vol. 43, No. 5, May 1990

Oman, C.M. Space Motion Sickness and Vestibular Experiments in Spacelab. Society of Automotive Engineers, Inc. 1982

Oman, C.M., Balkwill, M.D., Horizontal Angular VOR, Nystagmus Dumping and Sensation Duration in Spacelab SLS-1 Crewmembers. XVII Barany Society Meeting. Space and the Vestibular System Symposium. Prague, Czechoslovakia, June 4, 1992.

Oman, C.M., Young, L.R., Watt, D.G.D., Money, K.E., Lichtenberg, B.K., Kenyon, R.V., Arrott, A.P., MIT/Canadian Spacelab Experiments On Vestibular Adaptation and Space Motion Sickness. Basic and Applied Aspects of Vestibular Function. pp. 183-192, 1988

Shelhamer, M.J. Linear Acceleration and Horizontal Eye Movements in Man. Massachusetts Institute of Technology. 1990

Shelhamer, M., Robinson, D.A., Tan, H.S., Context-Specific Adaptation of the Gain of the Vestibulo-Ocular Reflex in Humans. Journal of Vestibular Research, Vol. 2, pp. 89-96, 1992

Snyder, L.H., King, M., Vertical Vestibuloocular Reflex in Cat: Asymmetry and Adaptation. Journal of Neurophysiology, Vol. 59, No. 2, February 1988

Welch, R.B., Perceptual Modification: Adapting to Altered Sensory Environments. Academic Press, Inc. 1978

Wilson, V.J., Melvill Jones, G., Mammalian Vestibular Physiology. Plenum Press, New York, 1979

Young, L. R., Role of the Vestibular System in Posture and Movement. Medical Physiology, Vol. I, pp. 704-721, 1974.

Young, L. R., Human Orientation in Space. AIAA-82-0422. AIAA 20th Aerospace Sciences Meeting, Orlando, FL, Jan. 11-14, 1982.

Young, L. R., Chapter 22: Perception of the Body in Space: Mechanisms. Handbook of Physiology - The Nervous System III. pp. 1023-1066, 1983

Young, L. R., Meiry, J. L., A Revised Dynamic Otolith Model. Aerospace Medicine, Vol. 39, No. 6, June, 1968.

Young, L. R., Meiry, J. L., Li, Y.T., Control Engineering Approaches to Human Dynamic Space Orientation. Reprinted from Second Symposium on The Role of the Vestibular Organs in Space Exploration, National Aeronautics and Space Administration, Ames Research Center, Moffett Field, CA, Jan. 25-27, 1966, NASA SP-115.

Young, L.R., Oman, C.M., Watt, D.G.D., Money, K.E., Lichtenberg, B.K., Kenyon, R.V., Arrott, A.P., MIT/Canadian Vestibular Experiments on the Spacelab-1 Mission: 1. Sensory adaptation to weightlessness and readaptation to one-g: an overview. Experimental Brain Research. 64: 291-298, 1986

Young, L. R., Sheena, D., Methods & Designs. Survey of Eye Movement Recording Methods. Behavior Research Methods & Instrumentation, Vol. 7(5), 397-429, 1975.

Zambarbieri, D., Schmid, R., Prablanc, C., Magenes, G. Characteristics of Eye Movements Evoked by the Presentation of Acoustic Targets. Progress in Oculomotor Research. 1981

APPENDIX A: Y-AXIS FIXED DISPLACEMENT RESULTS

This appendix contains the data plots from the Y-axis fixed displacement test. An identical figure was provided in Chapter 4 (Results) for the representative subject BP (Figure 4.2). In this appendix, one figure (A.1.) is shown for each of the eight subjects summarizing the mean normalized eye movements (Eye/Commanded Sled Displacement) in the four different trial conditions. (a) 10 degree leftward and rightward trials, (b) 20 degree leftward to rightward trials, (c) rightward 10 and 20 degree trials, (d) leftward 10 and 20 degree trials. Error bars signify standard error.

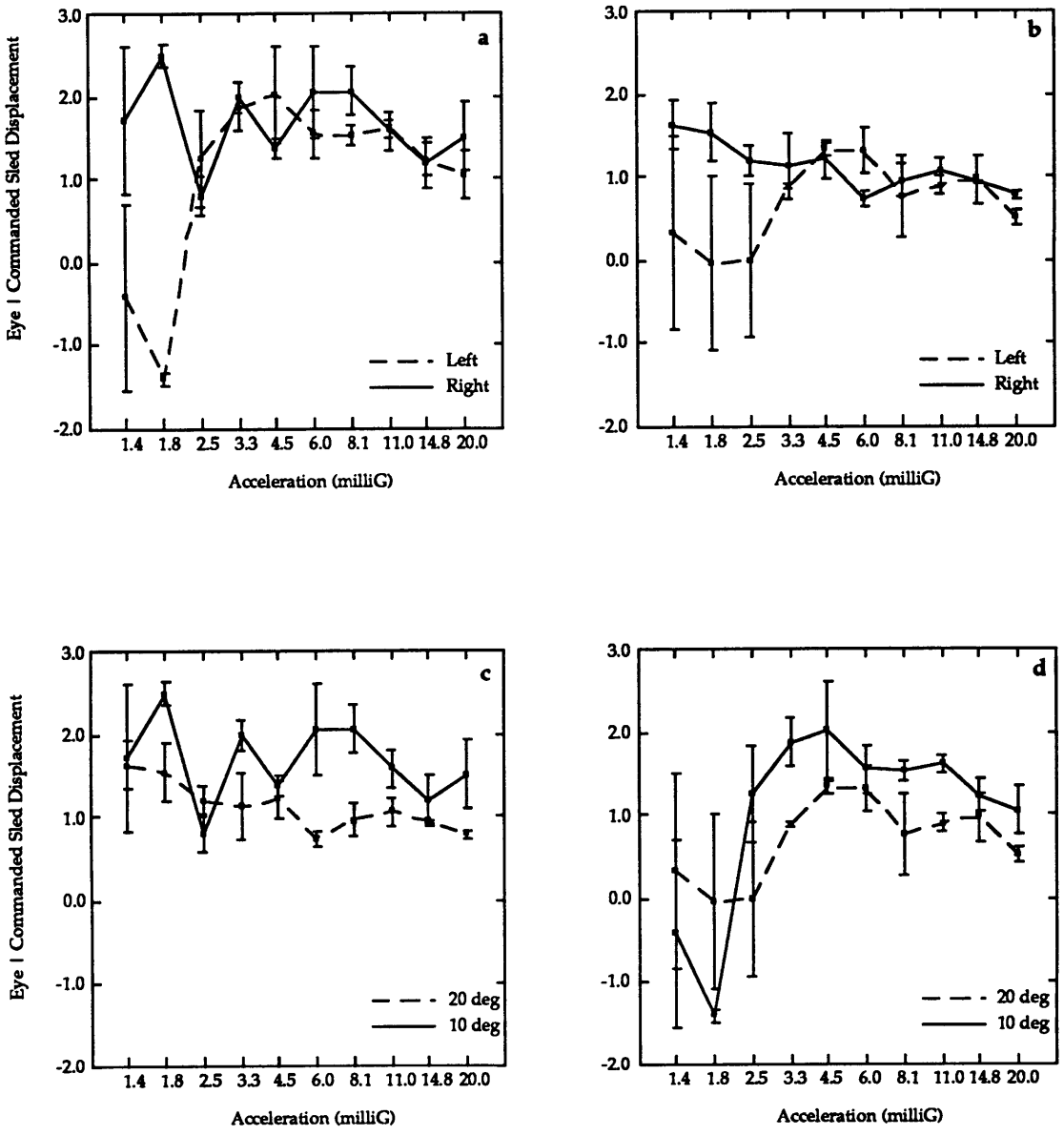

Figure A.1. Y-Axis Fixed Displacement eye movement data for subject KP. a) 10 degree leftward and rightward trials, (b) 20 degree leftward to rightward trials, (c) rightward 10 and 20 degree trials, (d) leftward 10 and 20 degree trials. Error bars signify standard error.

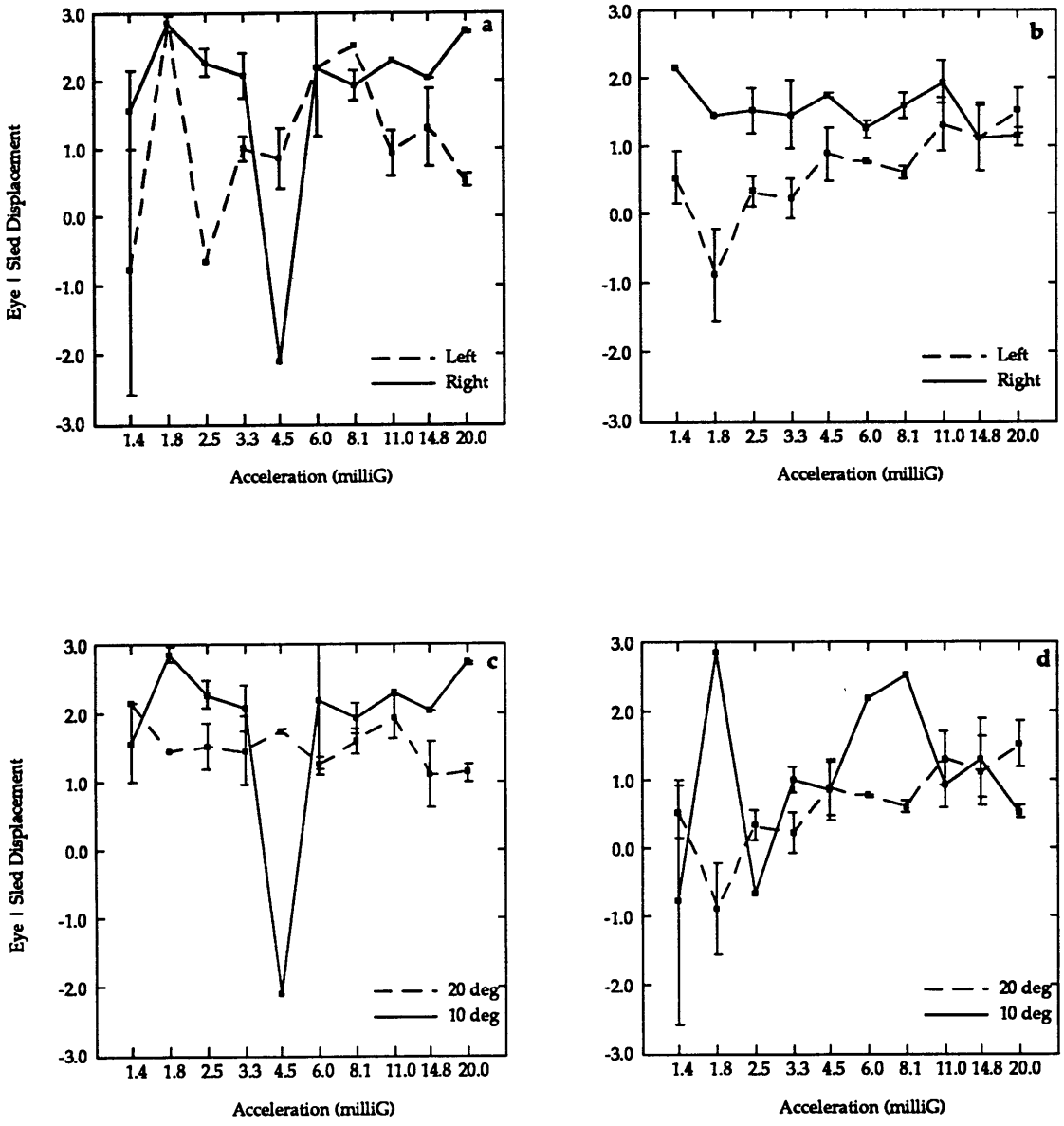

Figure A.1. Y-Axis Fixed Displacement eye movement data for subject JM. a) 10 degree leftward and rightward trials, (b) 20 degree leftward to rightward trials, (c) rightward 10 and 20 degree trials, (d) leftward 10 and 20 degree trials. Error bars signify standard error.

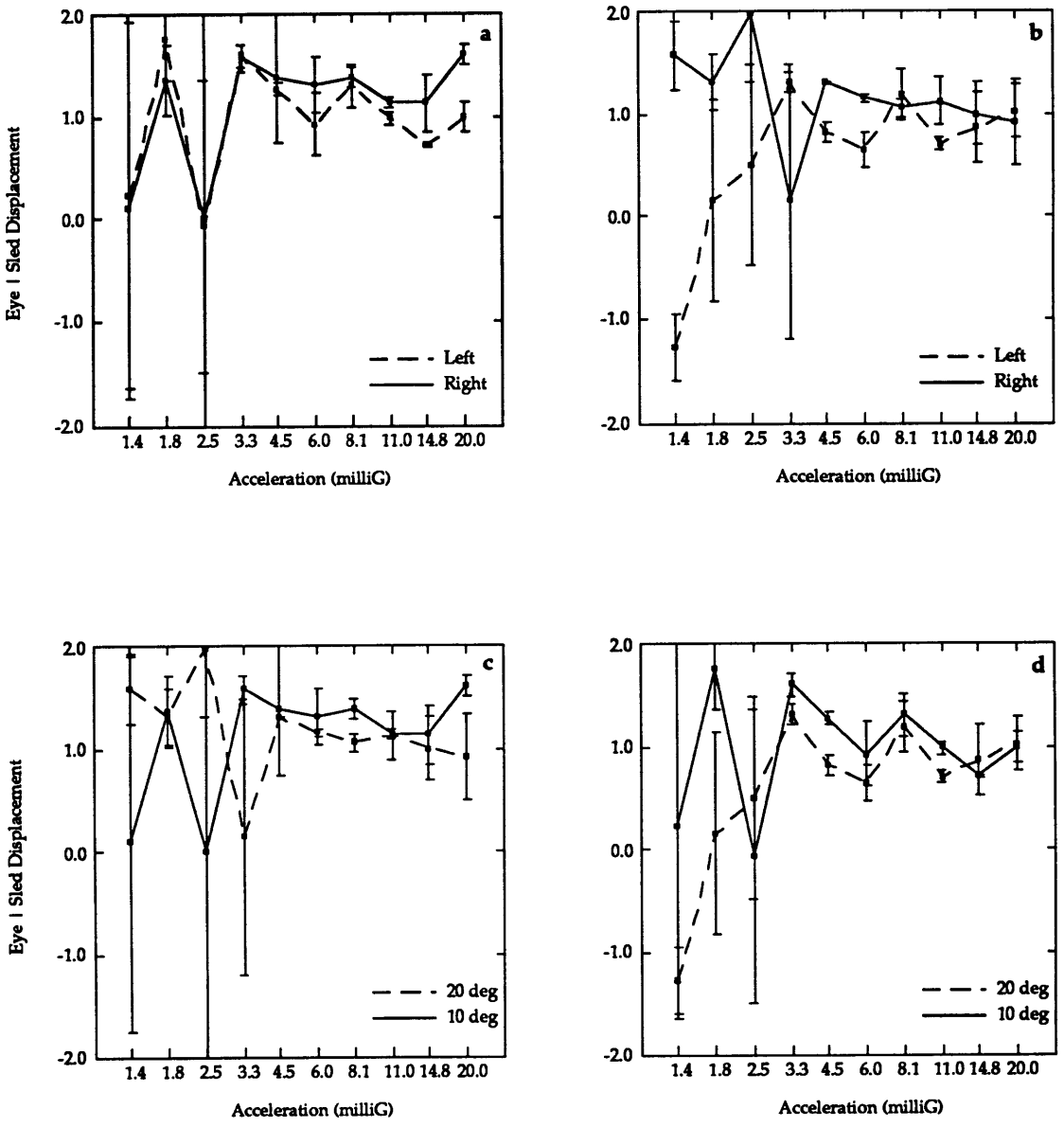

Figure A.1. Y-Axis Fixed Displacement eye movement data for subject KP. a) 10 degree leftward and rightward trials, (b) 20 degree leftward to rightward trials, (c) rightward 10 and 20 degree trials, (d) leftward 10 and 20 degree trials. Error bars signify standard error.

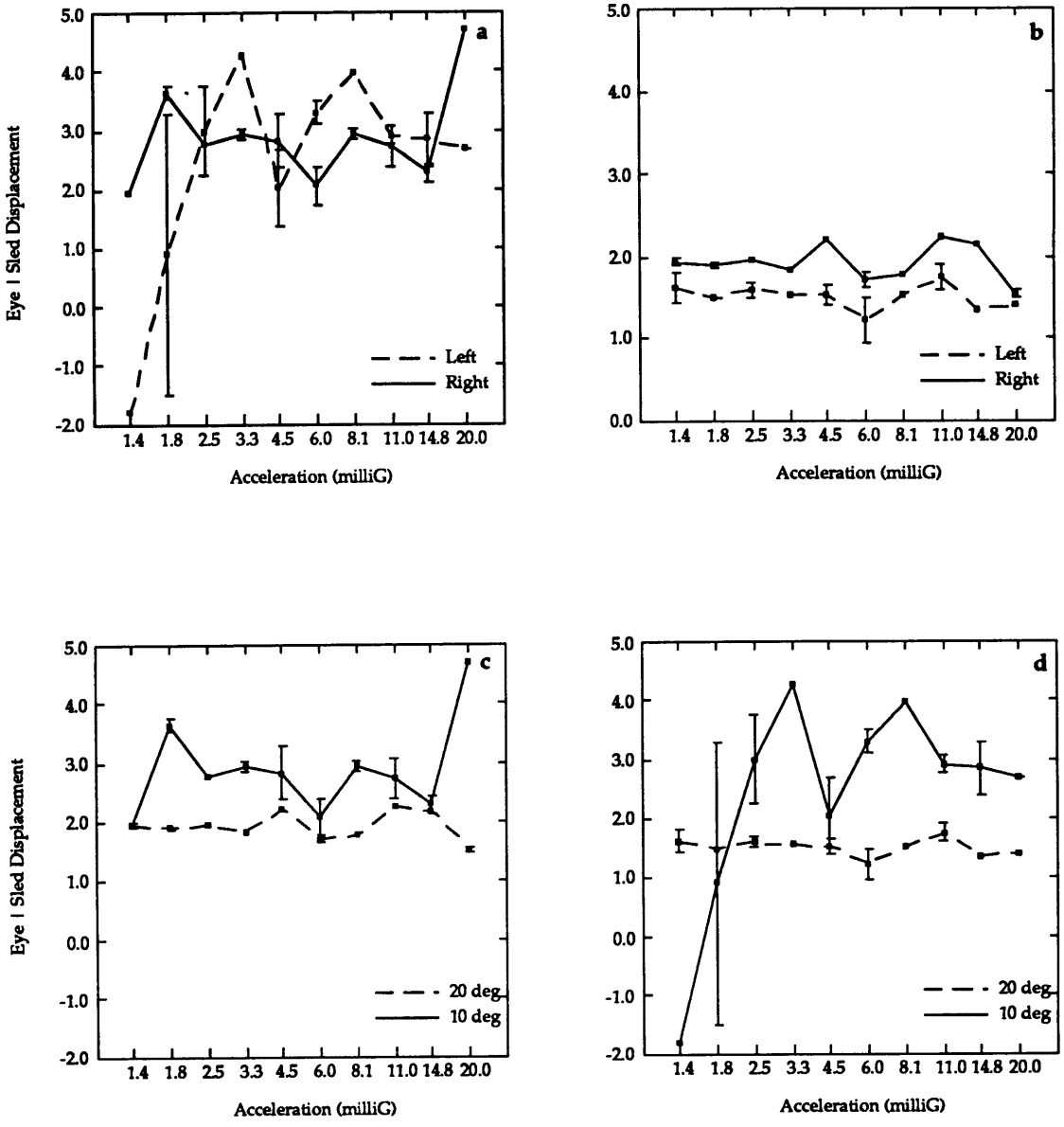

Figure A.1. Y-Axis Fixed Displacement eye movement data for subject LF. a) 10 degree leftward and rightward trials, (b) 20 degree leftward to rightward trials, (c) rightward 10 and 20 degree trials, (d) leftward 10 and 20 degree trials. Error bars signify standard error.

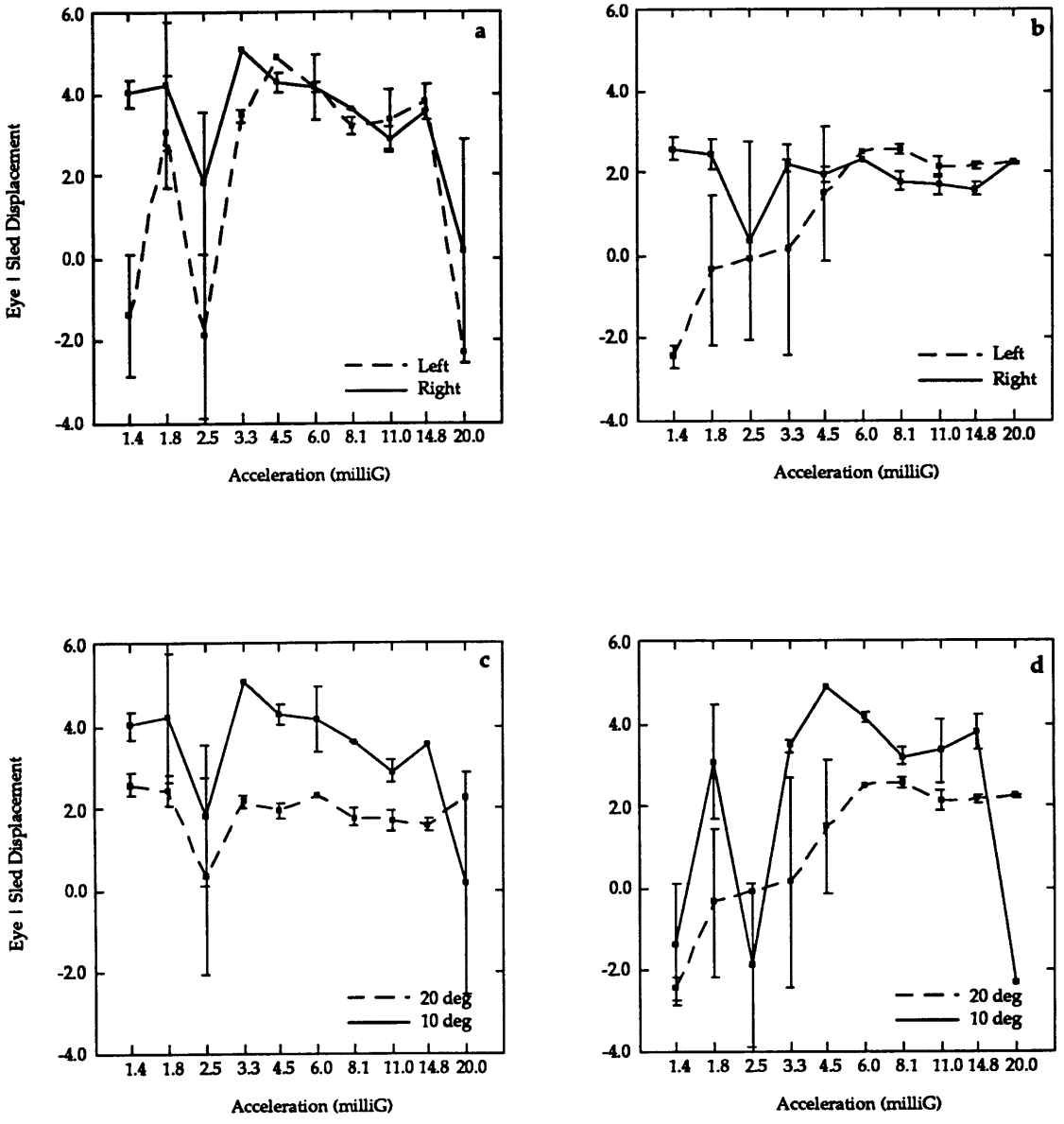

Figure A.1. Y-Axis Fixed Displacement eye movement data for subject LH. a) 10 degree leftward and rightward trials, (b) 20 degree leftward to rightward trials, (c) rightward 10 and 20 degree trials, (d) leftward 10 and 20 degree trials. Error bars signify standard error.

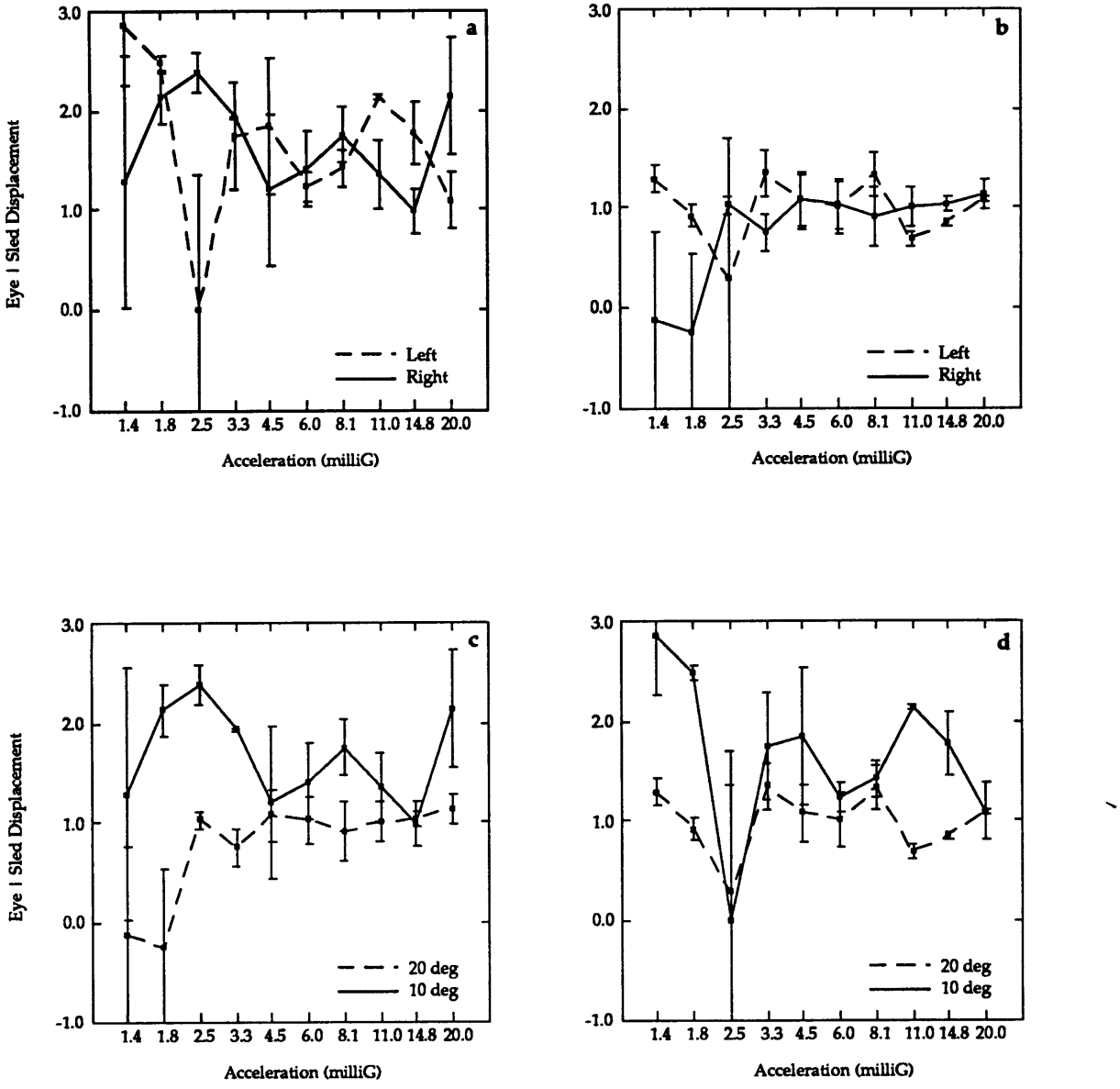

Figure A.1. Y-Axis Fixed Displacement eye movement data for subject SS. a) 10 degree leftward and rightward trials, (b) 20 degree leftward to rightward trials, (c) rightward 10 and 20 degree trials, (d) leftward 10 and 20 degree trials. Error bars signify standard error.

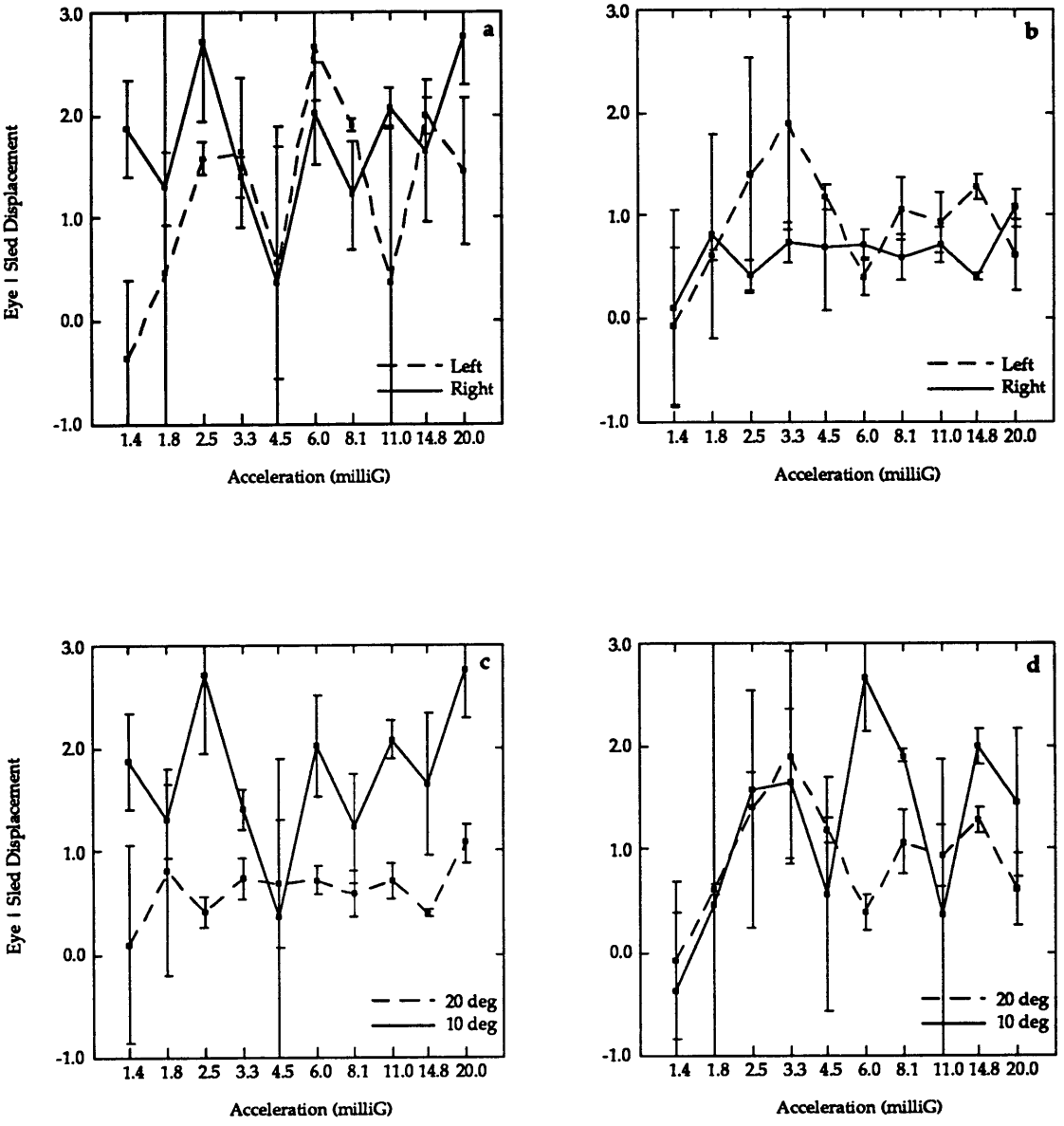

Figure A.1. Y-Axis Fixed Displacement eye movement data for subject TL. a) 10 degree leftward and rightward trials, (b) 20 degree leftward to rightward trials, (c) rightward 10 and 20 degree trials, (d) leftward 10 and 20 degree trials. Error bars signify standard error.

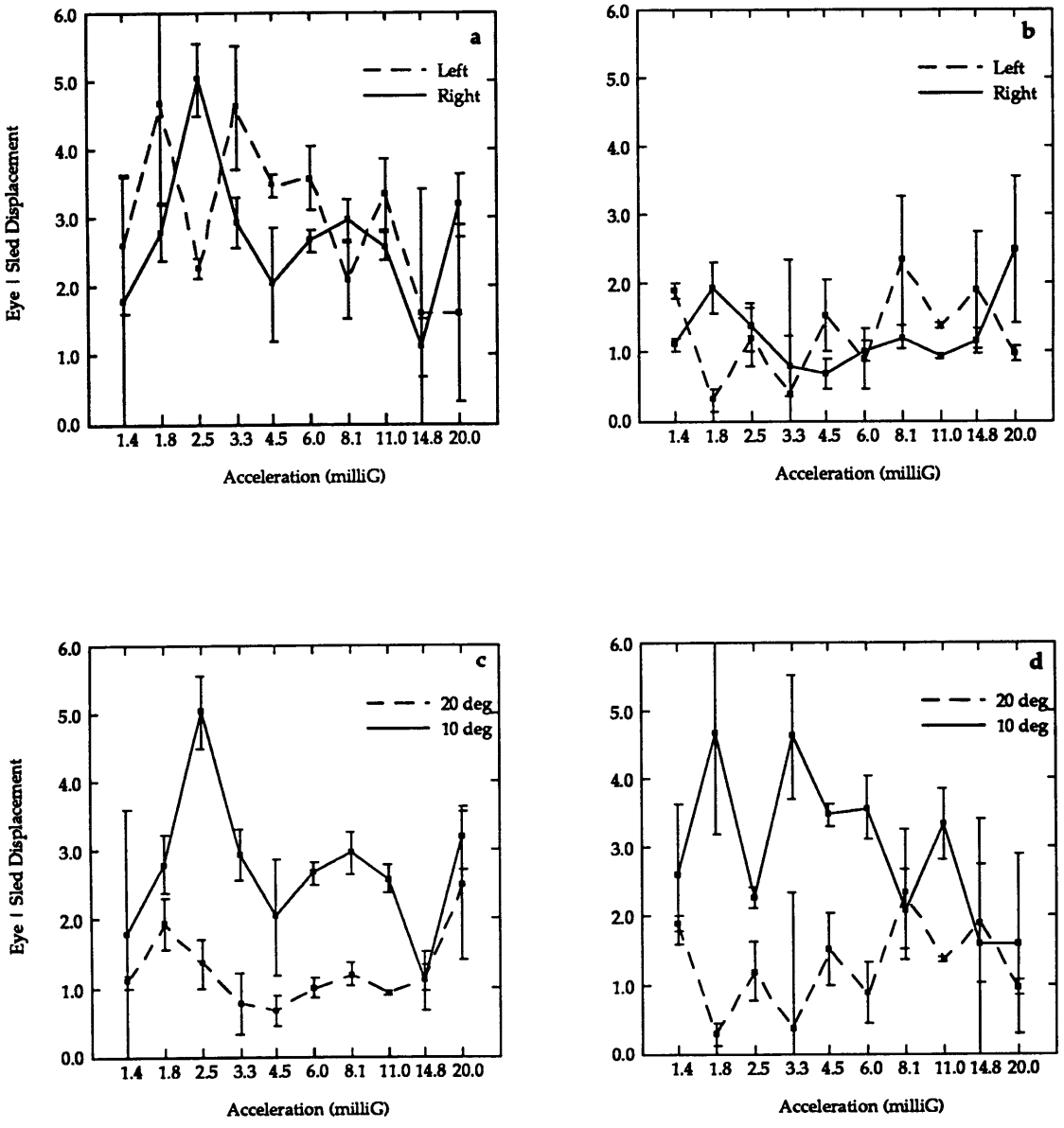

Figure A.1. Y-Axis Fixed Displacement eye movement data for subject WT. a) 10 degree leftward and rightward trials, (b) 20 degree leftward to rightward trials, (c) rightward 10 and 20 degree trials, (d) leftward 10 and 20 degree trials. Error bars signify standard error.

APPENDIX B: Y-AXIS FIXED DURATION RESULTS

This appendix contains the data plots from the Y-axis fixed duration test. These plots were provided in Chapter 4 (Results) for the representative subject MB (Figures 4.5, 4.6, and 4.9). In this appendix, three figures (containing four plots each) are shown for each of the five subjects: (B.1.) Scatter plots of raw eye movement data versus commanded sled displacement, (B.2.) Mean normalized eye movements (Eye/Commanded Sled Displacement), and (B.3.) Mean normalized subjective estimate of translation (Subjective/Commanded Sled Displacement. In each figure, the four different trial conditions are compared. (a) 1.0 second leftward and rightward trials, (b) 2.5 second leftward to rightward trials, (c) rightward 1.0 and 2.5 second trials, (d) leftward 1.0 and 2.5 second trials. Error bars signify standard error.

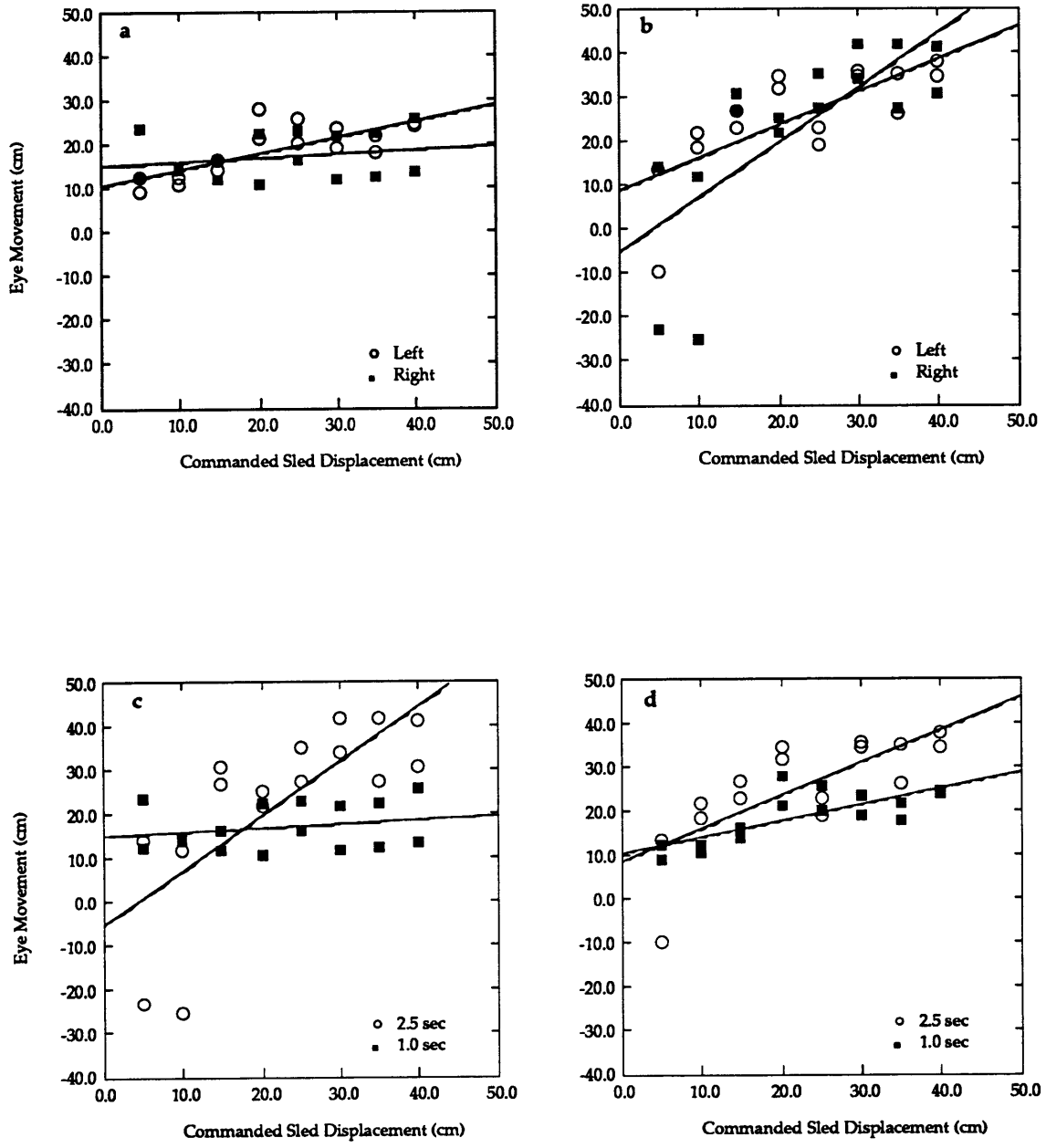

Figure B.1. Y-Axis Fixed Duration eye movement data comparing 1.0 sec trials and 2.5 sec trials for subject CL. (a) 1.0 second trials comparing leftward and rightward trials, (b) 2.5 second trials comparing leftward to rightward trials, (c) rightward trials comparing 1.0 and 2.5 second trials, (d) leftward trials comparing 1.0 and 2.5 second trials. Error bars signify standard error.

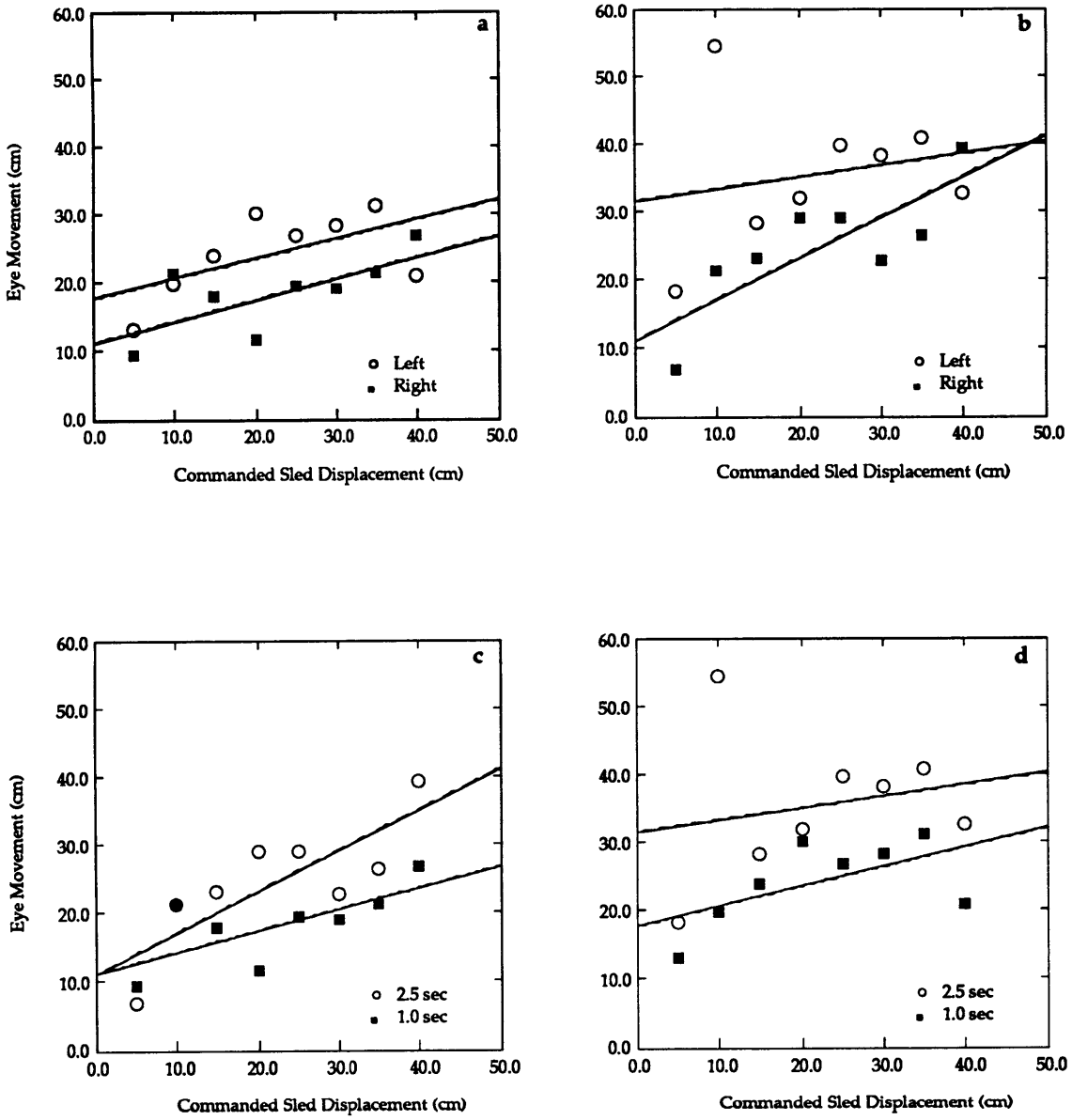

Figure B.1. Y-Axis Fixed Duration eye movement data comparing 1.0 sec trials and 2.5 sec trials for subject GS. (a) 1.0 second trials comparing leftward and rightward trials, (b) 2.5 second trials comparing leftward to rightward trials, (c) rightward trials comparing 1.0 and 2.5 second trials, (d) leftward trials comparing 1.0 and 2.5 second trials. Error bars signify standard error.

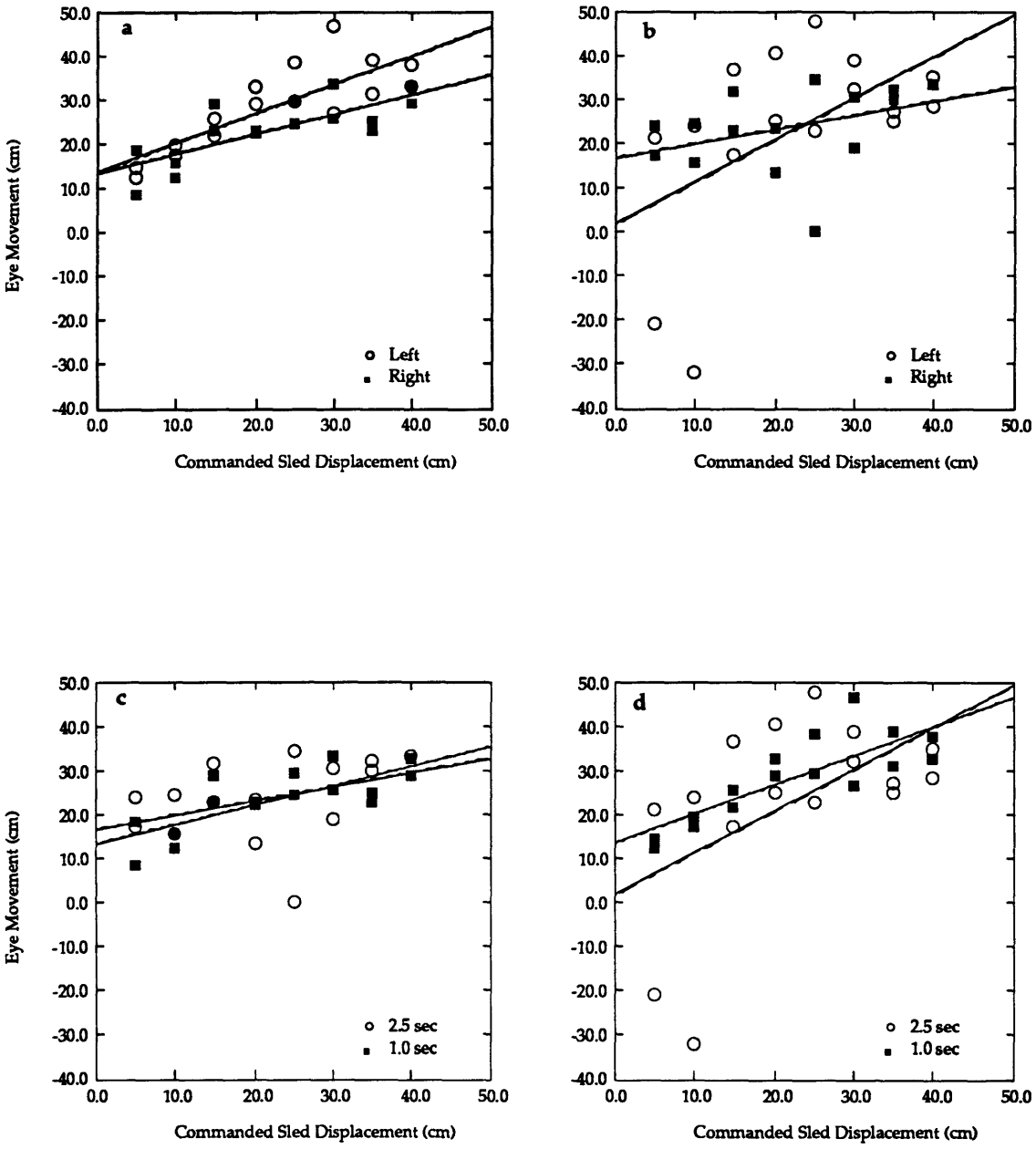

Figure B.1. Y-Axis Fixed Duration eye movement data comparing 1.0 sec trials and 2.5 sec trials for subject JM. (a) 1.0 second trials comparing leftward and rightward trials, (b) 2.5 second trials comparing leftward to rightward trials, (c) rightward trials comparing 1.0 and 2.5 second trials, (d) leftward trials comparing 1.0 and 2.5 second trials. Error bars signify standard error.

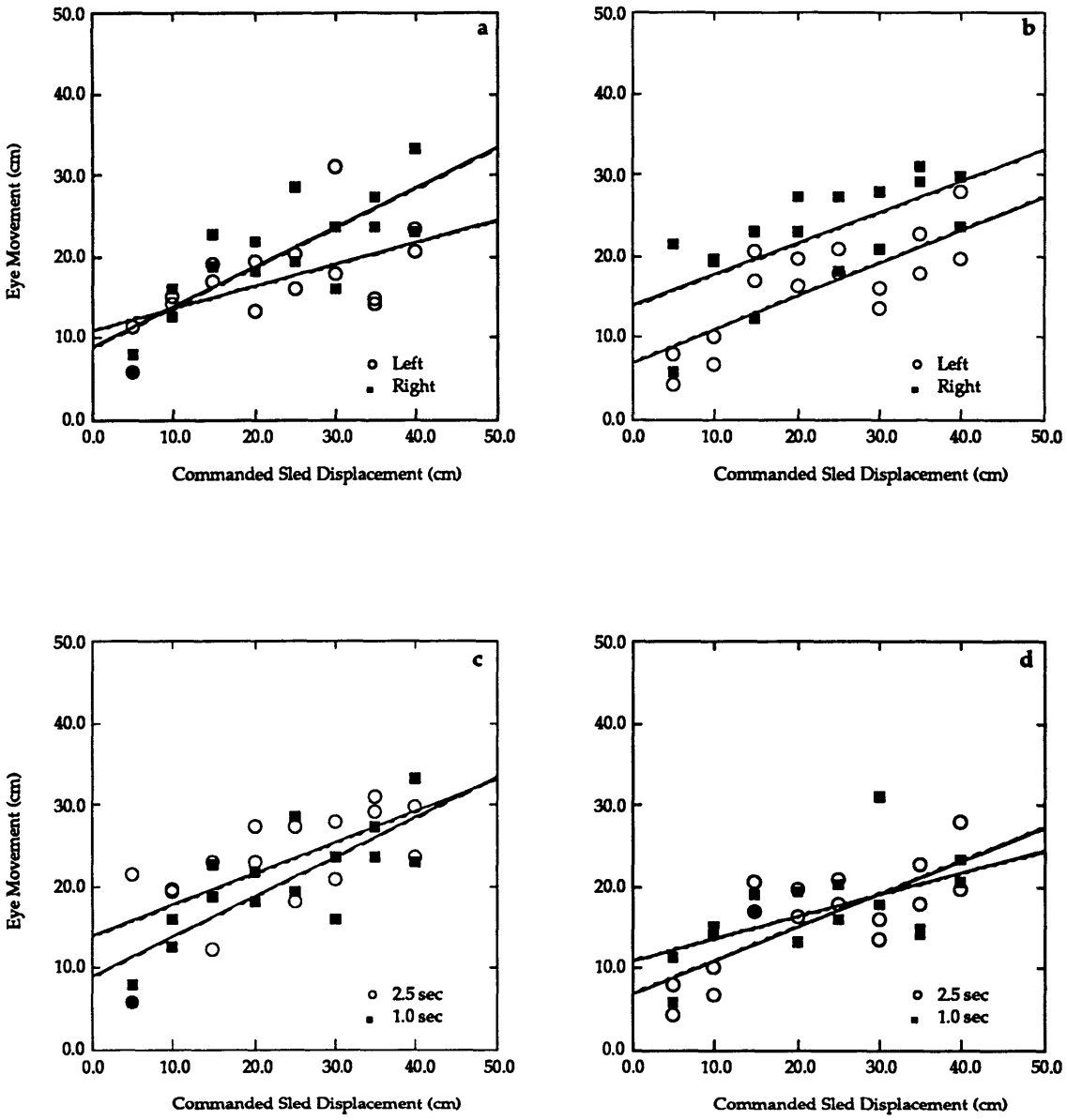

Figure B.1. Y-Axis Fixed Duration eye movement data comparing 1.0 sec trials and 2.5 sec trials for subject MB. (a) 1.0 second trials comparing leftward and rightward trials, (b) 2.5 second trials comparing leftward to rightward trials, (c) rightward trials comparing 1.0 and 2.5 second trials, (d) leftward trials comparing 1.0 and 2.5 second trials. Error bars signify standard error.

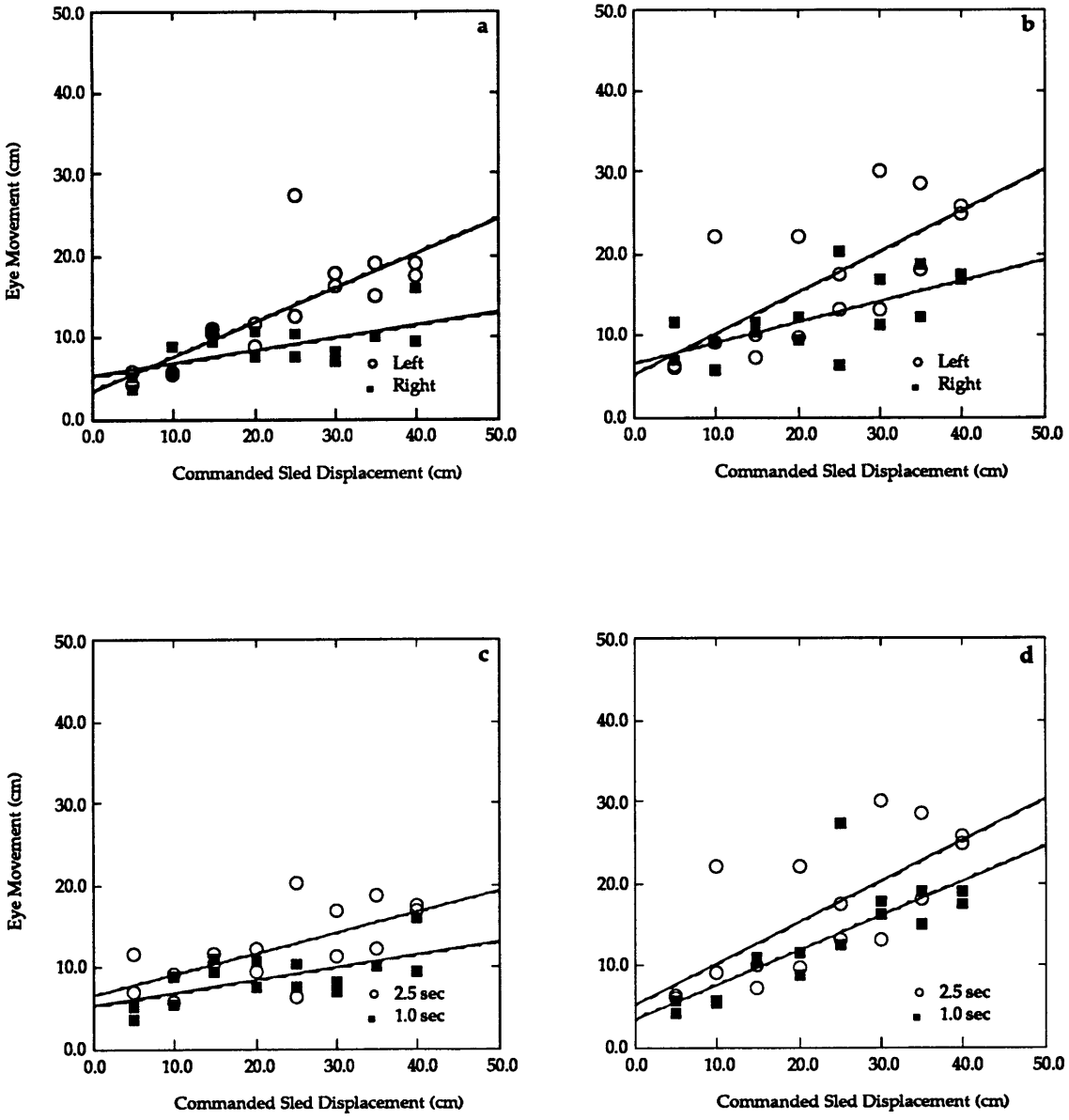

Figure B.1. Y-Axis Fixed Duration eye movement data comparing 1.0 sec trials and 2.5 sec trials for subject TC. (a) 1.0 second trials comparing leftward and rightward trials, (b) 2.5 second trials comparing leftward to rightward trials, (c) rightward trials comparing 1.0 and 2.5 second trials, (d) leftward trials comparing 1.0 and 2.5 second trials. Error bars signify standard error.

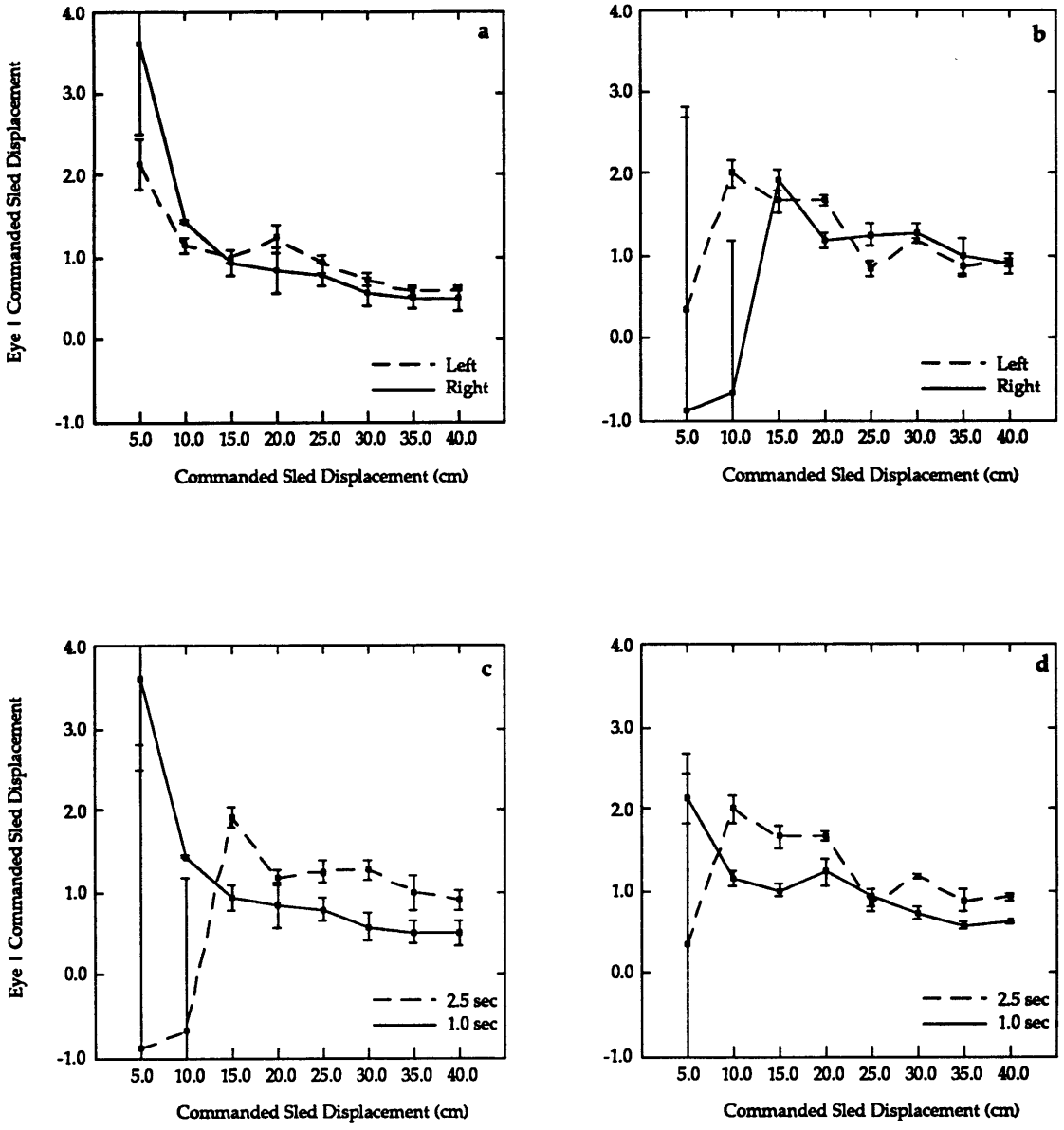

Figure A.2.2.. Y-Axis Fixed Duration mean normalized eye movements for subject CL. (a) 1.0 second trials comparing leftward and rightward trials, (b) 2.5 second trials comparing leftward to rightward trials, (c) rightward trials comparing 1.0 and 2.5 second trials, (d) leftward trials comparing 1.0 and 2.5 second trials. Error bars signify standard error.

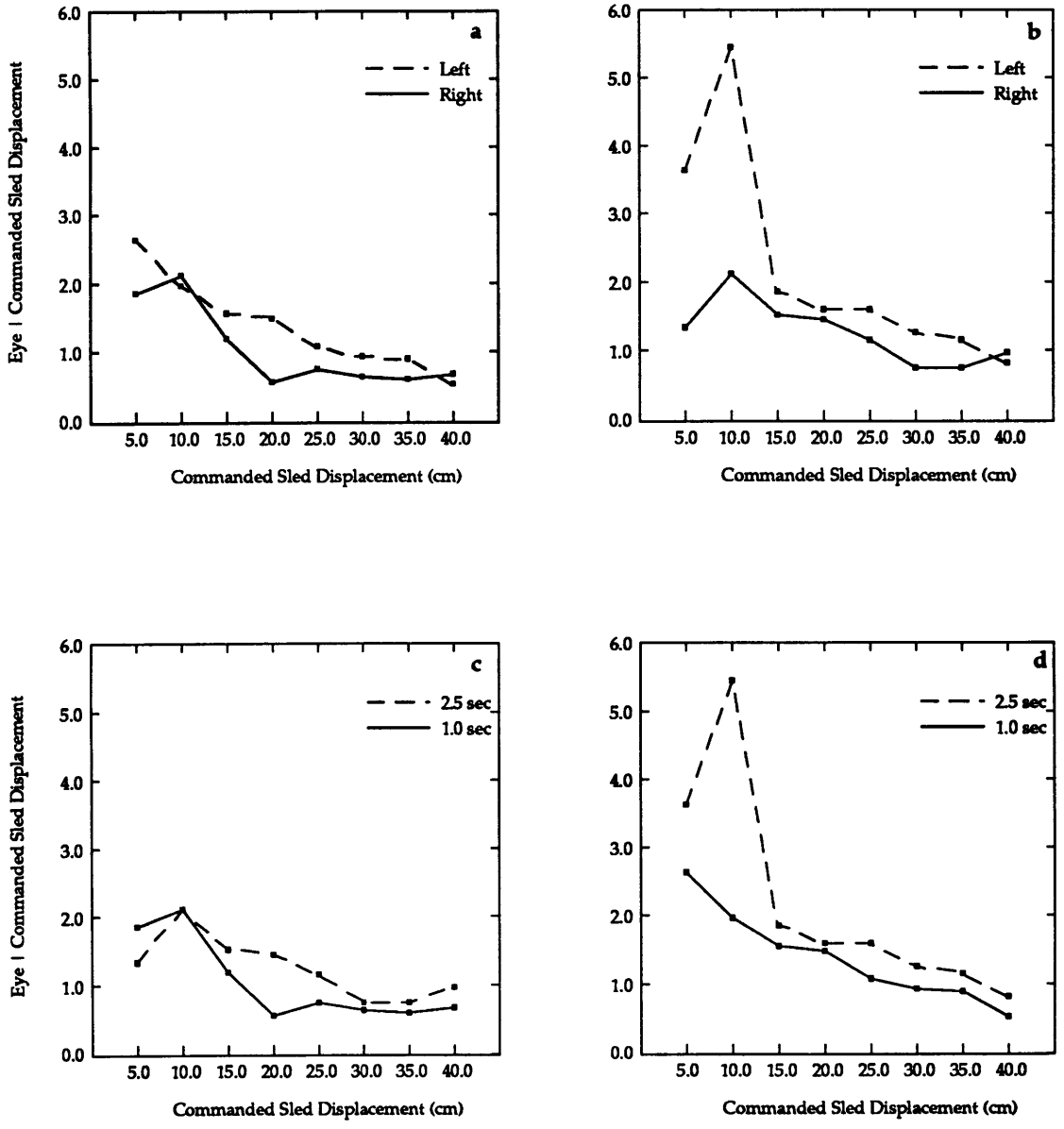

Figure A.2.2.. Y-Axis Fixed Duration mean normalized eye movements for subject GS. (a) 1.0 second trials comparing leftward and rightward trials, (b) 2.5 second trials comparing leftward to rightward trials, (c) rightward trials comparing 1.0 and 2.5 second trials, (d) leftward trials comparing 1.0 and 2.5 second trials. Error bars signify standard error.

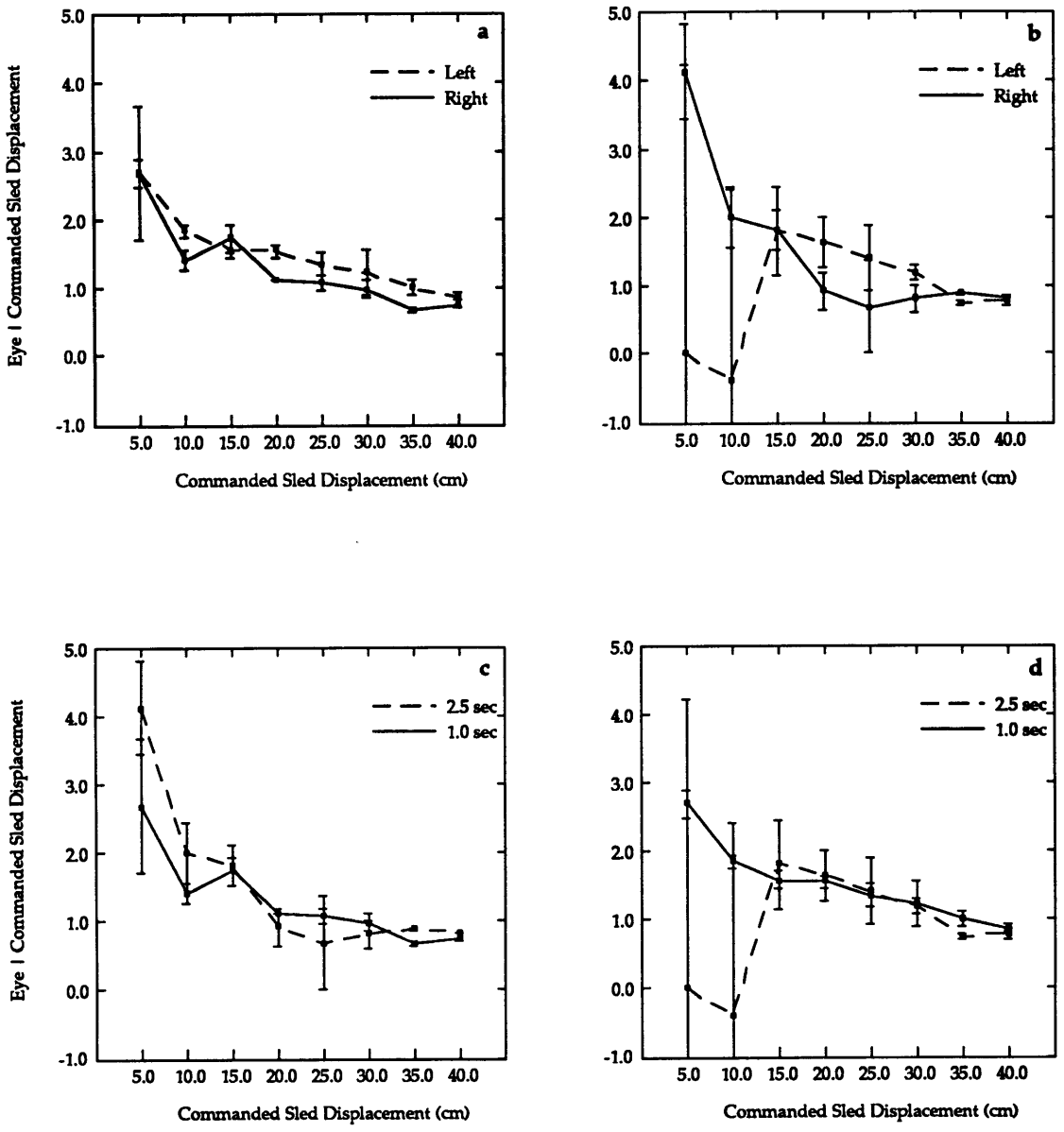

Figure A.2.2.. Y-Axis Fixed Duration mean normalized eye movements for subject JM. (a) 1.0 second trials comparing leftward and rightward trials, (b) 2.5 second trials comparing leftward to rightward trials, (c) rightward trials comparing 1.0 and 2.5 second trials, (d) leftward trials comparing 1.0 and 2.5 second trials. Error bars signify standard error.

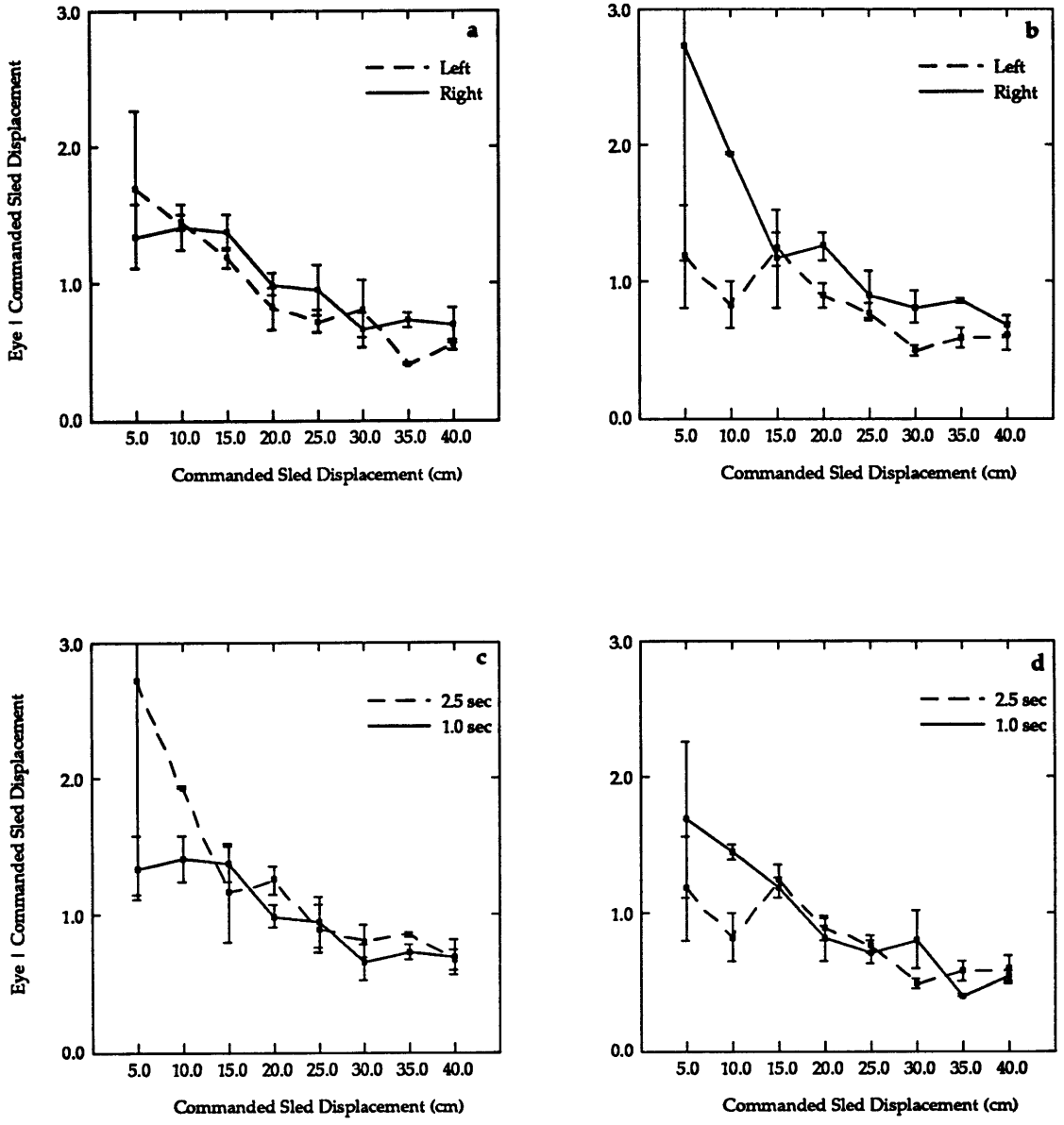

Figure A.2.2.. Y-Axis Fixed Duration mean normalized eye movements for subject MB. (a) 1.0 second trials comparing leftward and rightward trials, (b) 2.5 second trials comparing leftward to rightward trials, (c) rightward trials comparing 1.0 and 2.5 second trials, (d) leftward trials comparing 1.0 and 2.5 second trials. Error bars signify standard error.

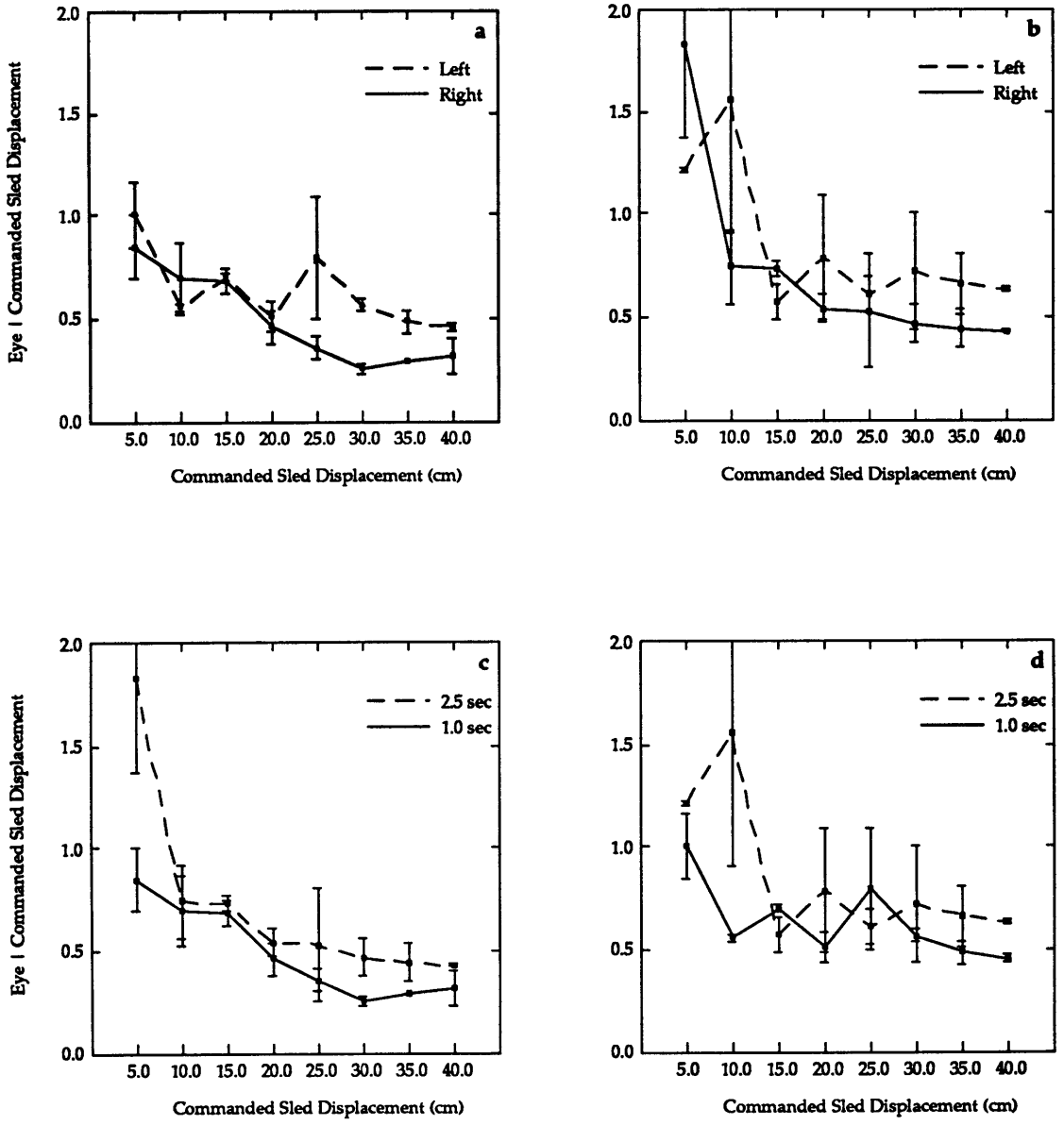

Figure A.2.2.. Y-Axis Fixed Duration mean normalized eye movements for subject TC. (a) 1.0 second trials comparing leftward and rightward trials, (b) 2.5 second trials comparing leftward to rightward trials, (c) rightward trials comparing 1.0 and 2.5 second trials, (d) leftward trials comparing 1.0 and 2.5 second trials. Error bars signify standard error.

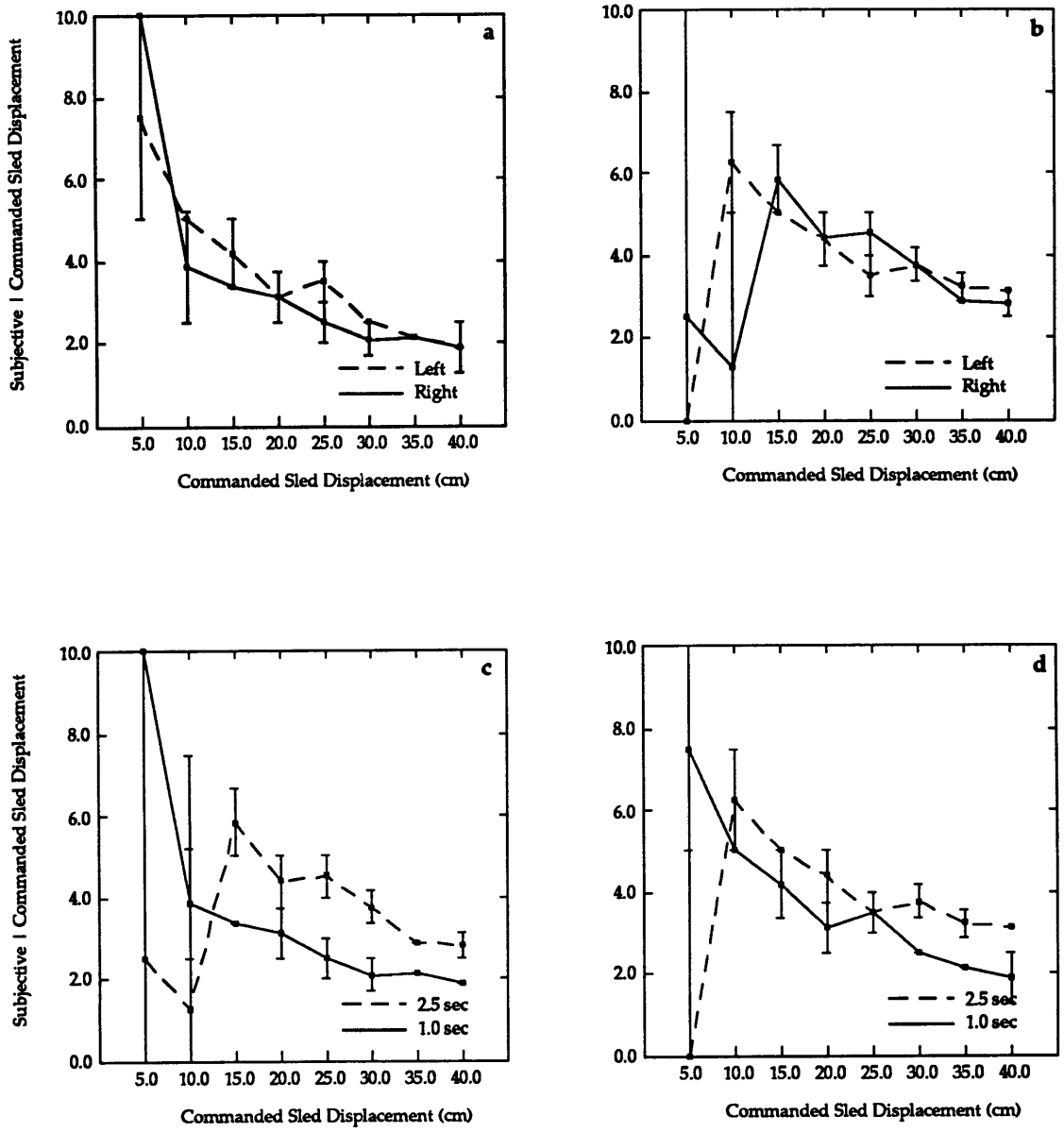

Figure B.3. Mean normalized subjective responses for subject CL. (a) difference between rightward and leftward 1.0 second trials, (b) difference between rightward and leftward 2.5 second trials, (c) difference between 1.0 and 2.5 second rightward trials, and (d) difference between 1.0 and 2.5 second leftward trials. Error bars indicate the standard error of the difference.

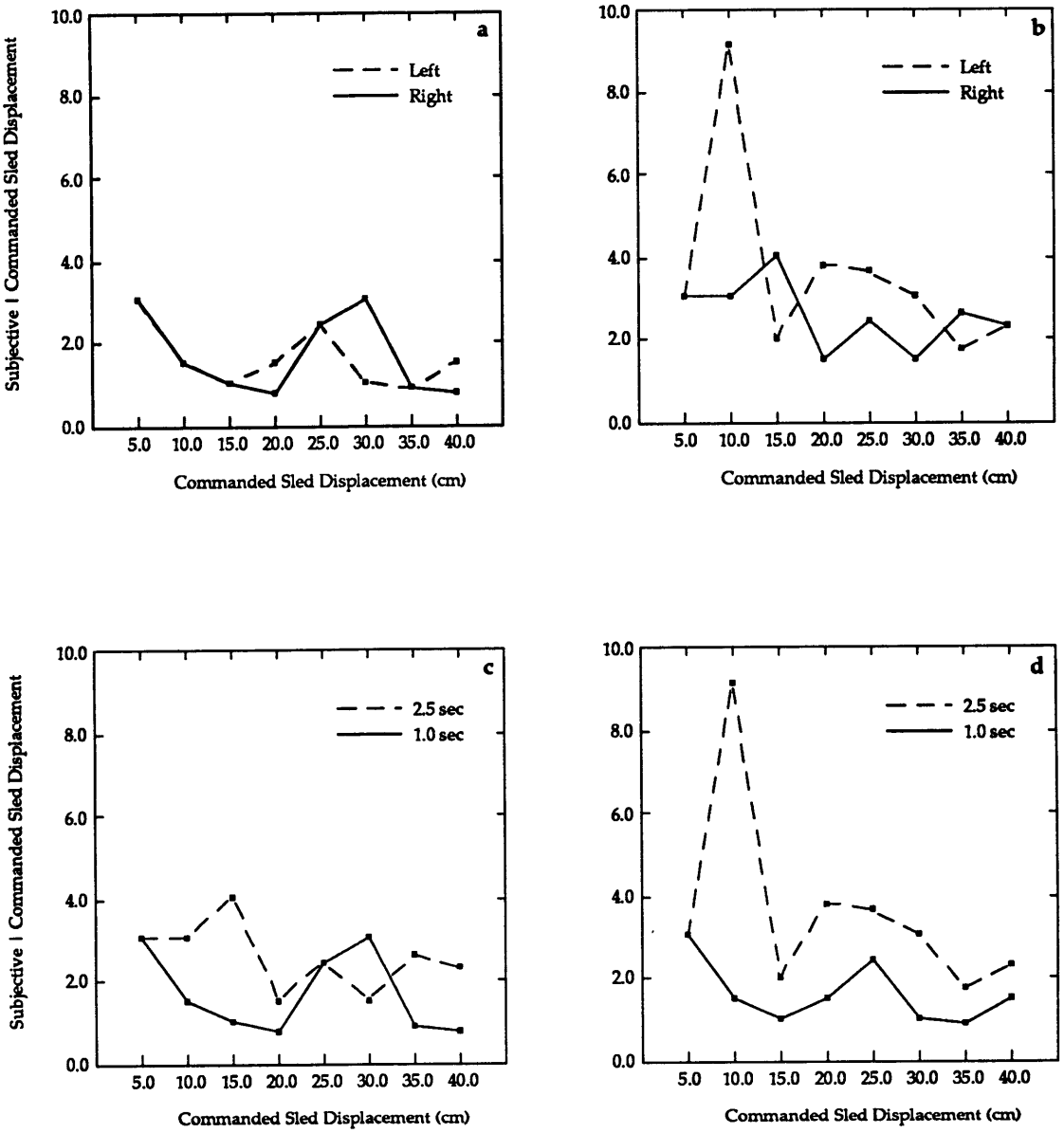

Figure B.3. Mean normalized subjective responses for subject GS. (a) difference between rightward and leftward 1.0 second trials, (b) difference between rightward and leftward 2.5 second trials, (c) difference between 1.0 and 2.5 second rightward trials, and (d) difference between 1.0 and 2.5 second leftward trials. Error bars indicate the standard error of the difference.

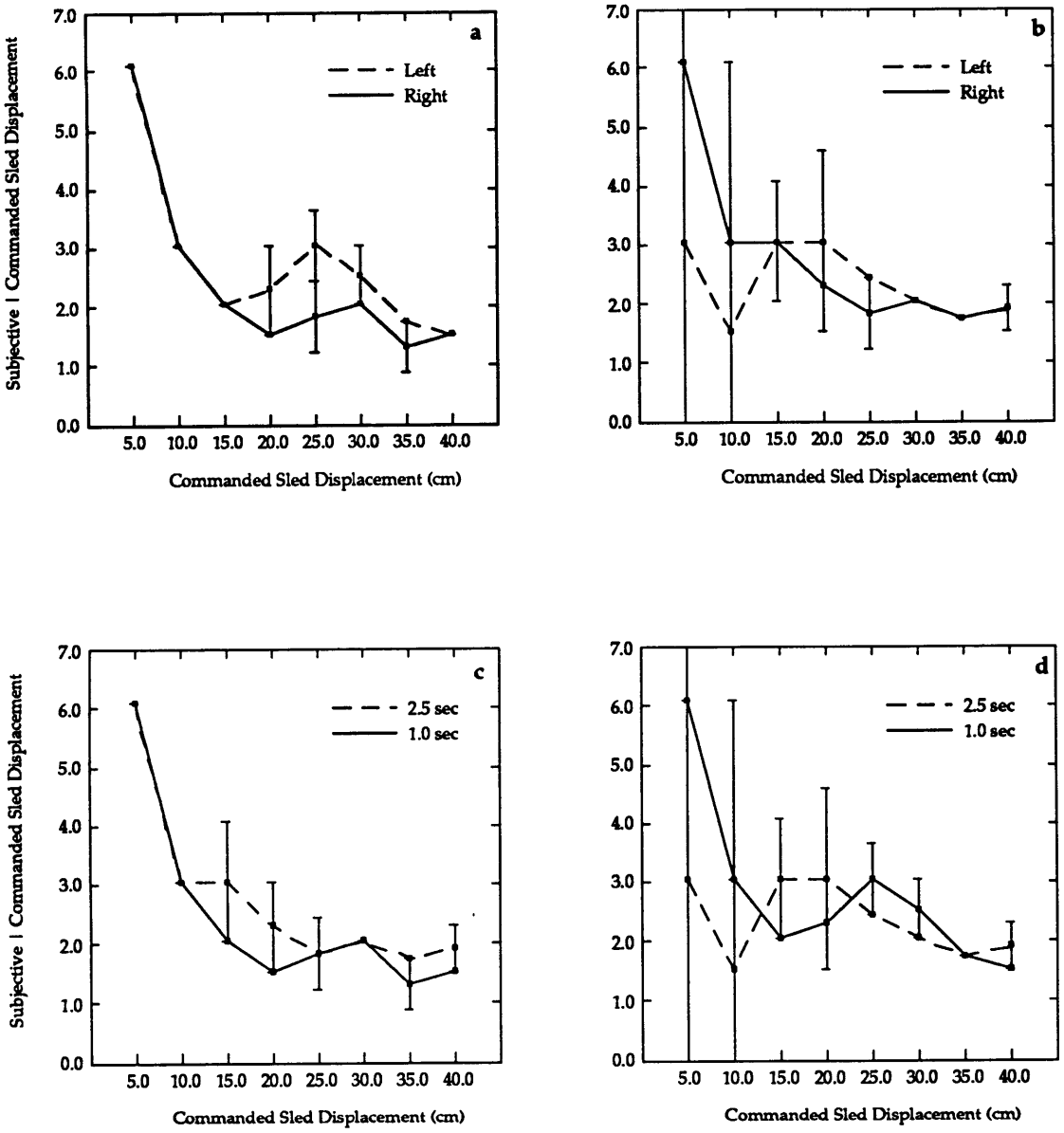

Figure B.3. Mean normalized subjective responses for subject JM. (a) difference between rightward and leftward 1.0 second trials, (b) difference between rightward and leftward 2.5 second trials, (c) difference between 1.0 and 2.5 second rightward trials, and (d) difference between 1.0 and 2.5 second leftward trials. Error bars indicate the standard error of the difference.

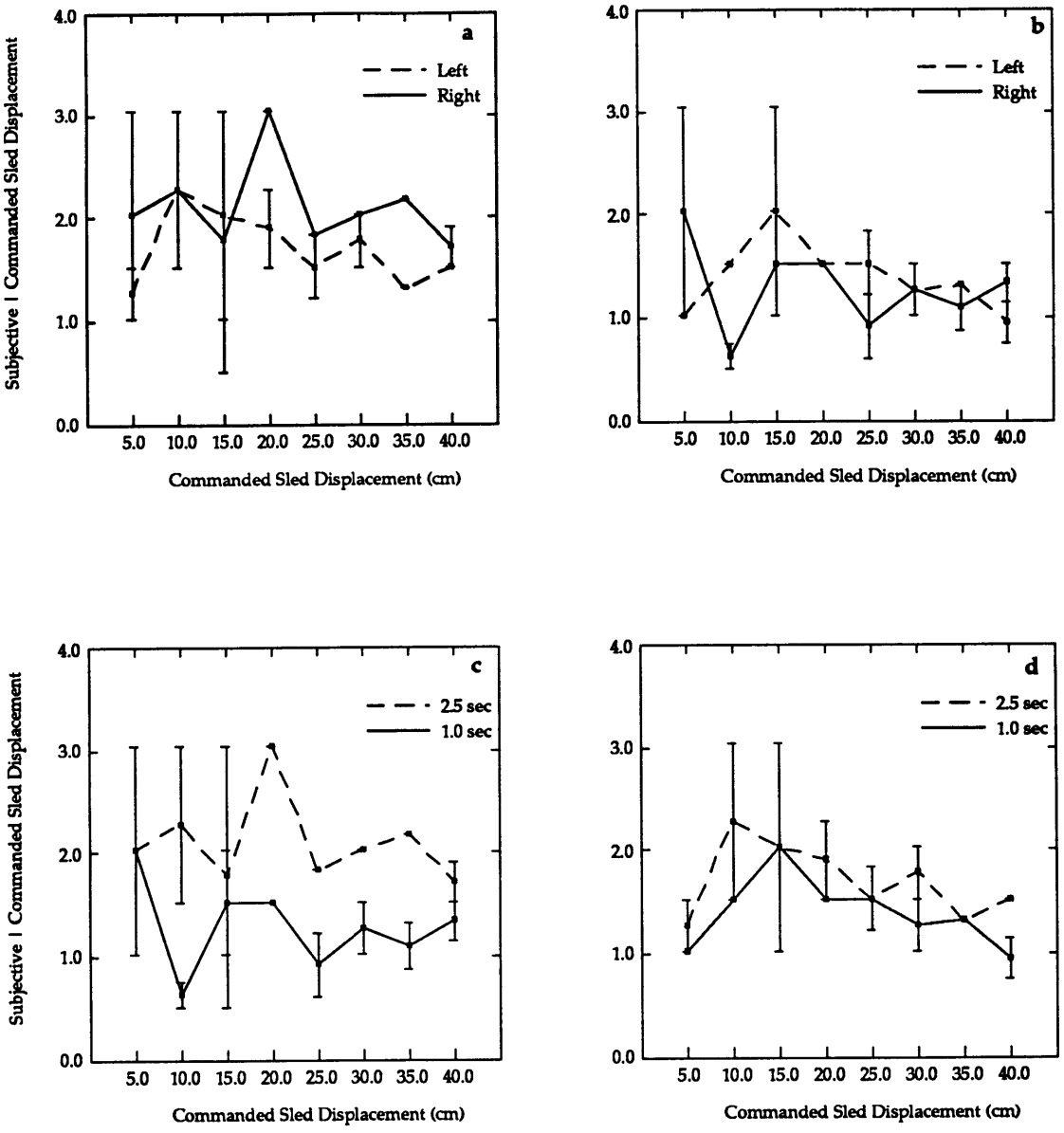

Figure B.3. Mean normalized subjective responses for subject MB. (a) difference between rightward and leftward 1.0 second trials, (b) difference between rightward and leftward 2.5 second trials, (c) difference between 1.0 and 2.5 second rightward trials, and (d) difference between 1.0 and 2.5 second leftward trials. Error bars indicate the standard error of the difference.

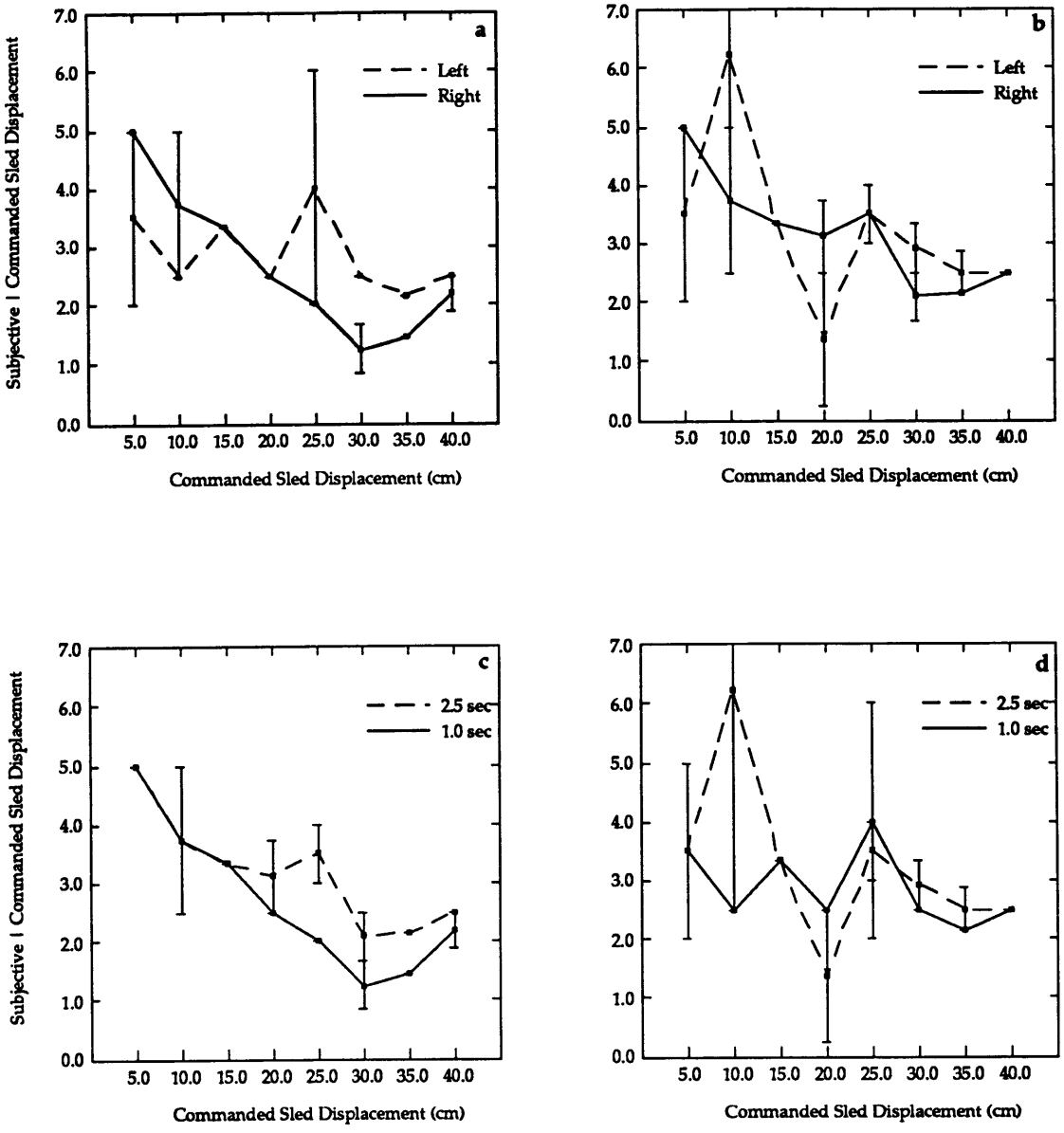

Figure B.3. Mean normalized subjective responses for subject TC. (a) difference between rightward and leftward 1.0 second trials, (b) difference between rightward and leftward 2.5 second trials, (c) difference between 1.0 and 2.5 second rightward trials, and (d) difference between 1.0 and 2.5 second leftward trials. Error bars indicate the standard error of the difference.

APPENDIX C: Z-AXIS FIXED DISPLACEMENT RESULTS

This appendix contains the data plots from the Z-axis fixed displacement test. Identical figures were provided in Chapter 4 (Results) for the representative subject KJ (Figures 4.11 and 4.13). In this appendix, two figures (containing four plots each) are shown for each of the six subjects summarizing the (C.1.) mean normalized eye movements (Eye/Sled Displacement) and the (C.2.) mean normalized subjective responses (Subjective/Sled Displacement) in the four different trial conditions. (a) 10 degree headward and footward trials, (b) 20 degree headward and footward trials, (c) headward 10 and 20 degree trials, (d) footward 10 and 20 degree trials. Error bars signify standard error.

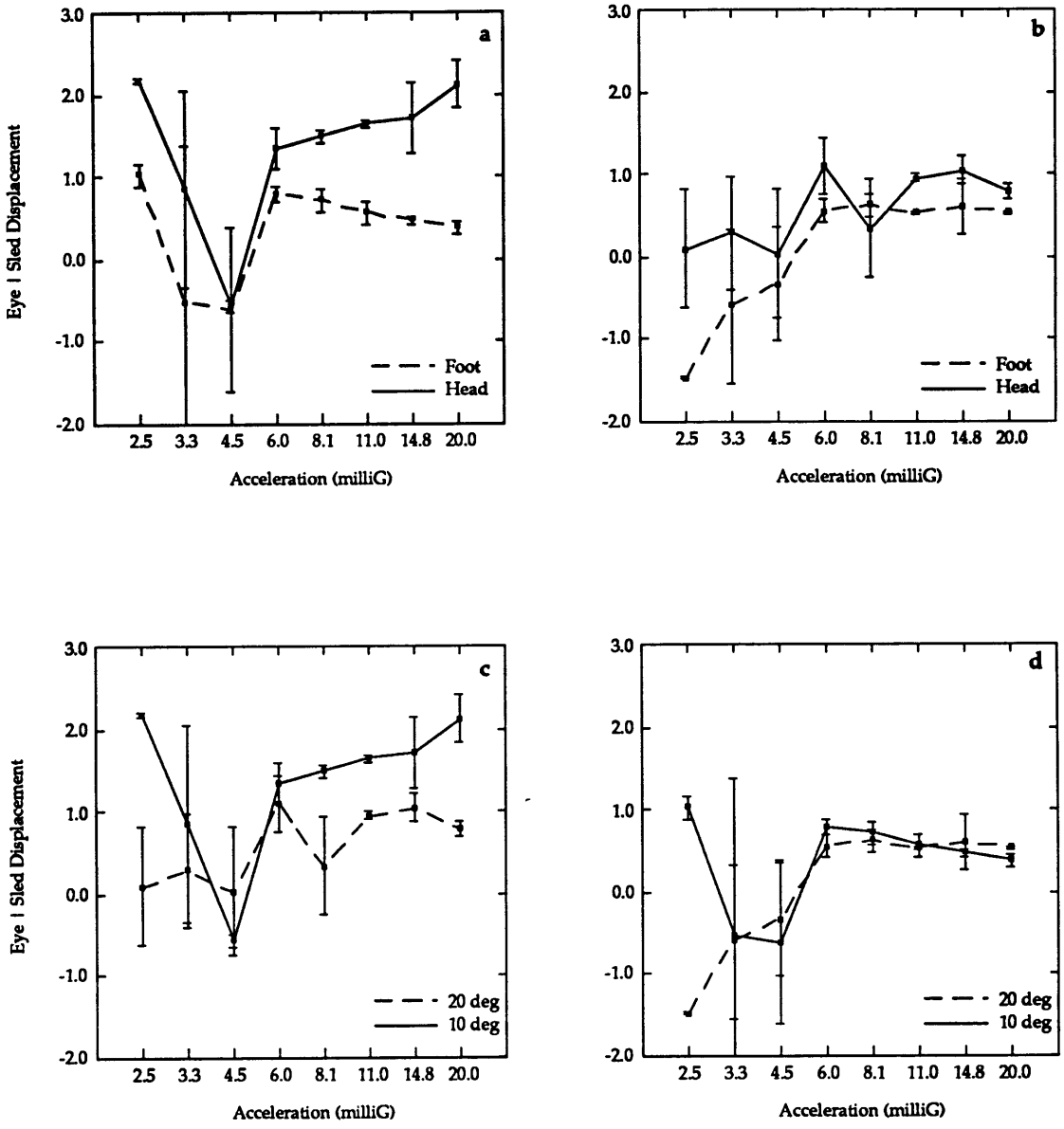

Figure C.1. Z-Axis Fixed Displacement normalized eye movement data for subject CL. (a) headward and footward 10 degree trials, (b) headward and footward 20 degree trials, (c) 10 and 20 degree headward trials, (d) 10 and 20 degree footward trials. Error bars signify standard error.

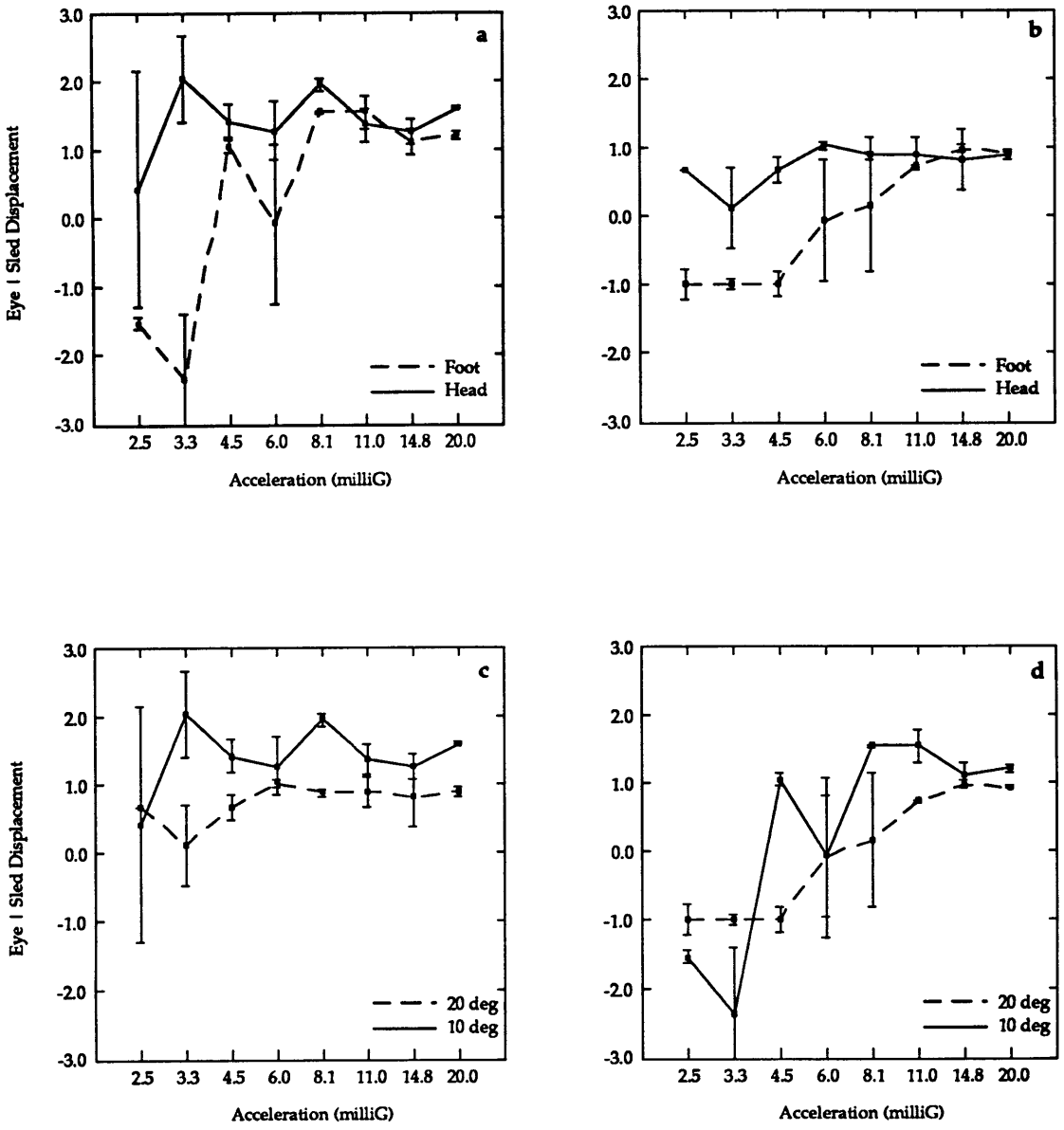

Figure C.1. Z-Axis Fixed Displacement normalized eye movement data for subject JM. (a) headward and footward 10 degree trials, (b) headward and footward 20 degree trials, (c) 10 and 20 degree headward trials, (d) 10 and 20 degree footward trials. Error bars signify standard error.

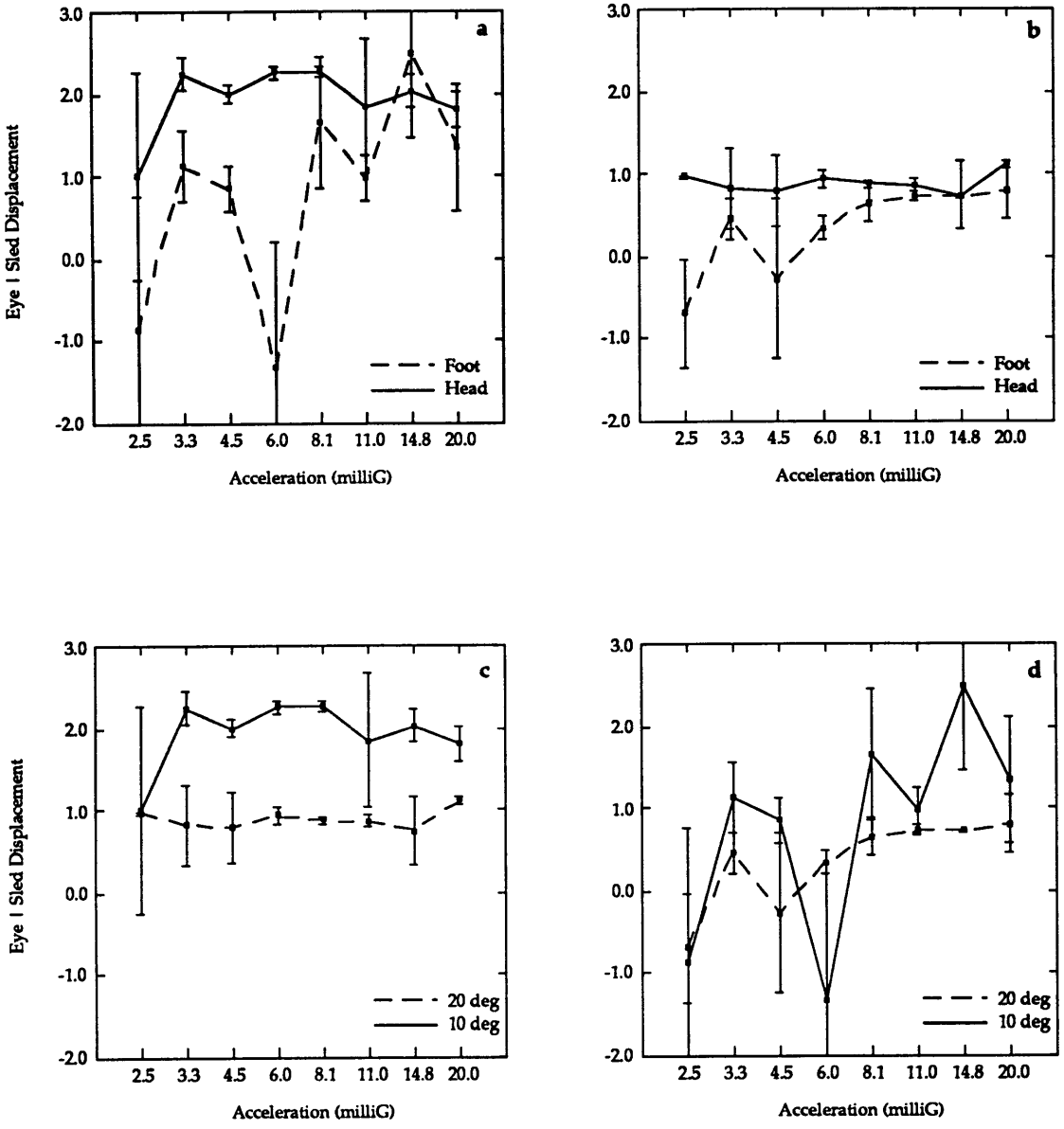

Figure 4.11. Z-Axis Fixed Displacement normalized eye movement data for subject KJ. (a) headward and footward 10 degree trials, (b) headward and footward 20 degree trials, (c) 10 and 20 degree headward trials, (d) 10 and 20 degree footward trials. Error bars signify standard error.

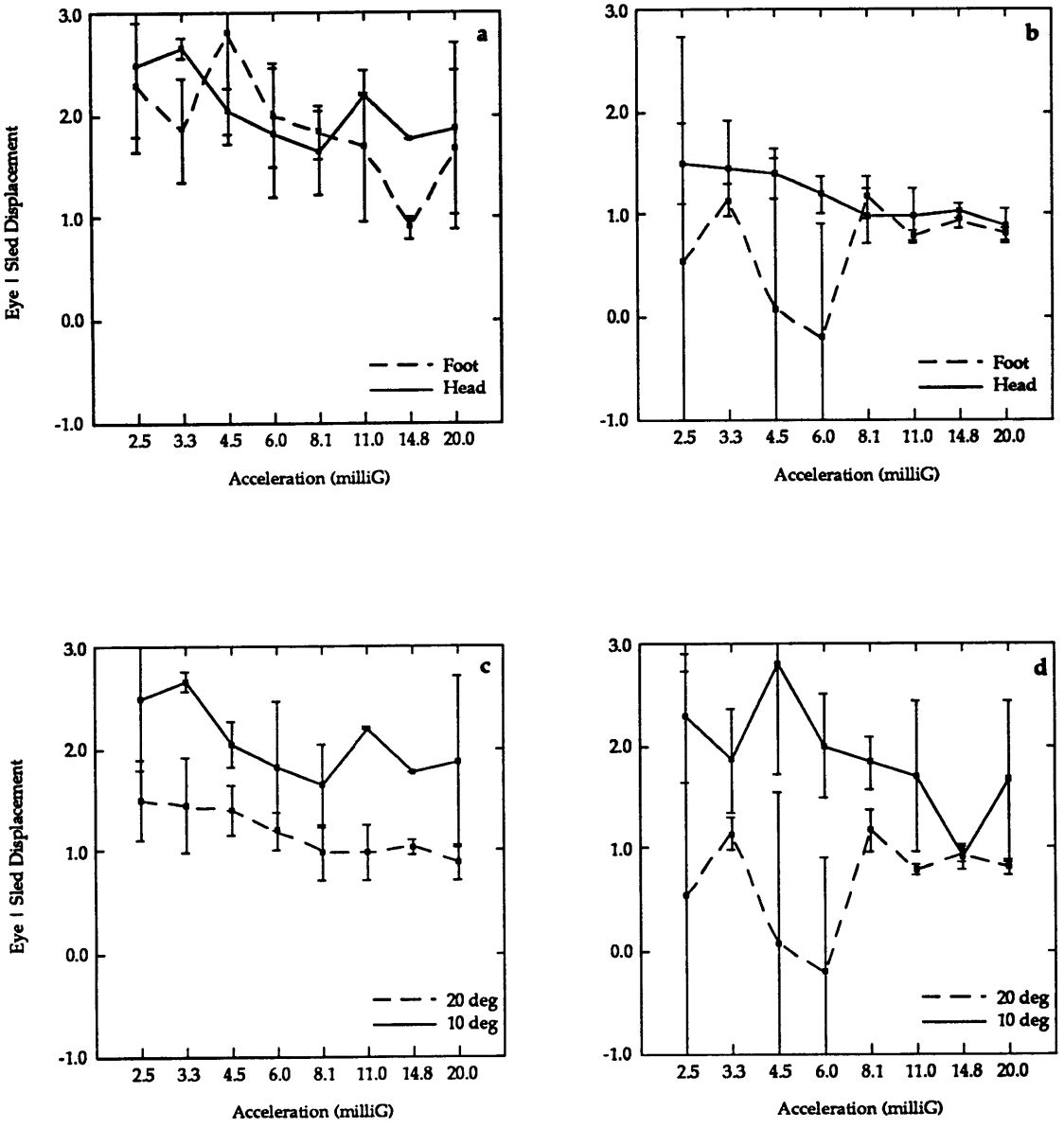

Figure C.1. Z-Axis Fixed Displacement normalized eye movement data for subject KP. (a) headward and footward 10 degree trials, (b) headward and footward 20 degree trials, (c) 10 and 20 degree headward trials, (d) 10 and 20 degree footward trials. Error bars signify standard error.

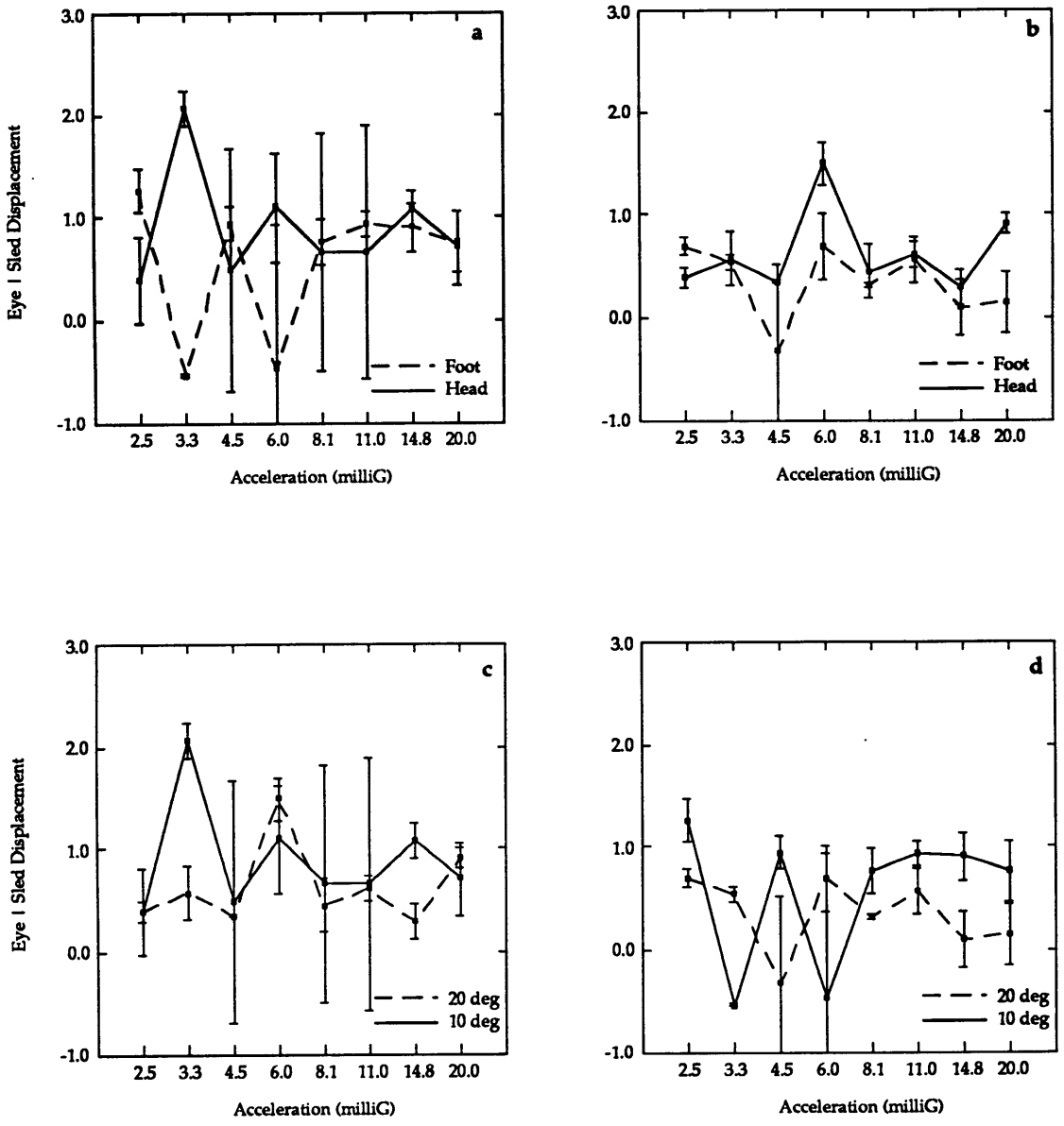

Figure C.1. Z-Axis Fixed Displacement normalized eye movement data for subject RZ. (a) headward and footward 10 degree trials, (b) headward and footward 20 degree trials, (c) 10 and 20 degree headward trials, (d) 10 and 20 degree footward trials. Error bars signify standard error.

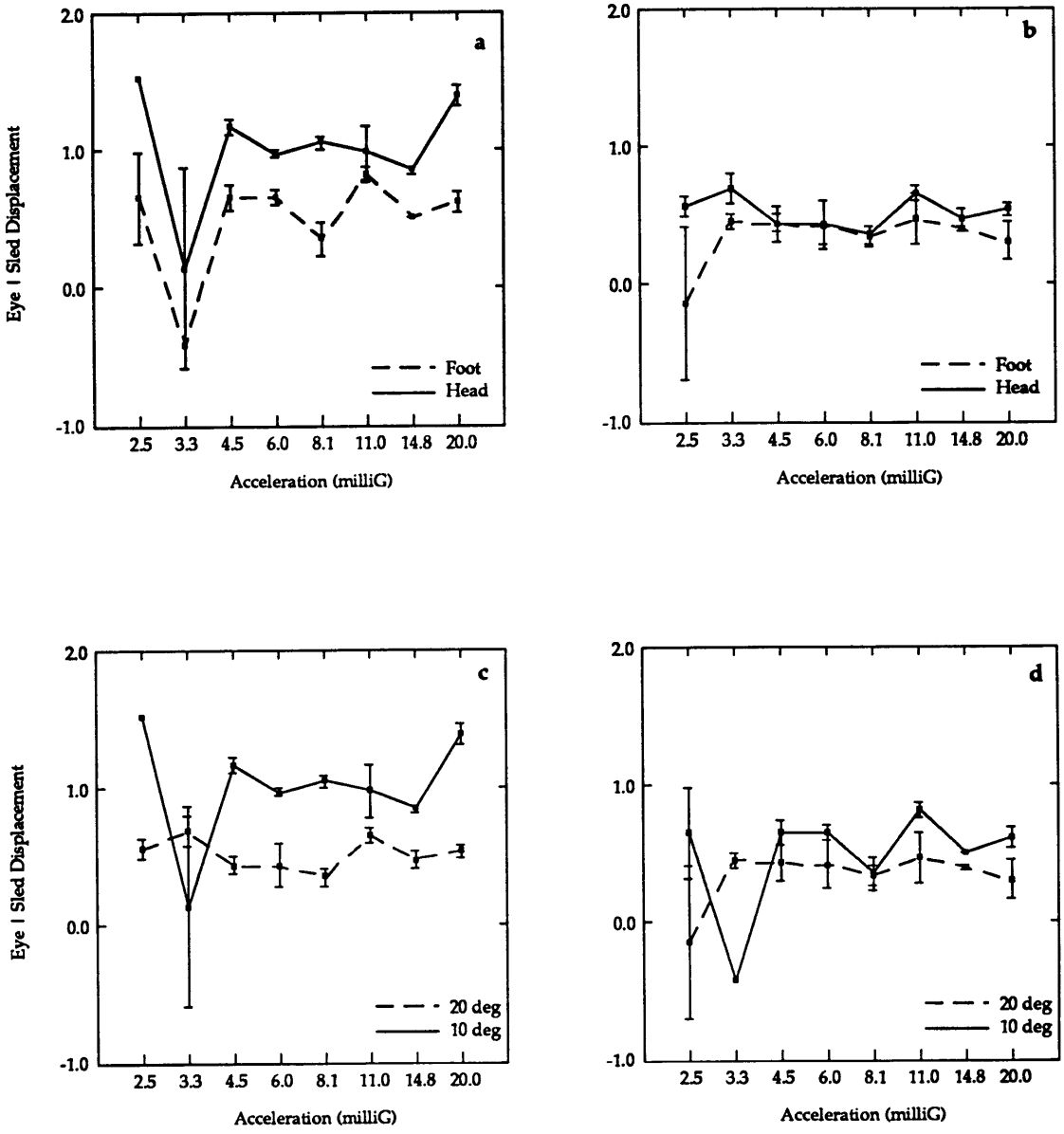

Figure C.1. Z-Axis Fixed Displacement normalized eye movement data for subject TC. (a) headward and footward 10 degree trials, (b) headward and footward 20 degree trials, (c) 10 and 20 degree headward trials, (d) 10 and 20 degree footward trials. Error bars signify standard error.

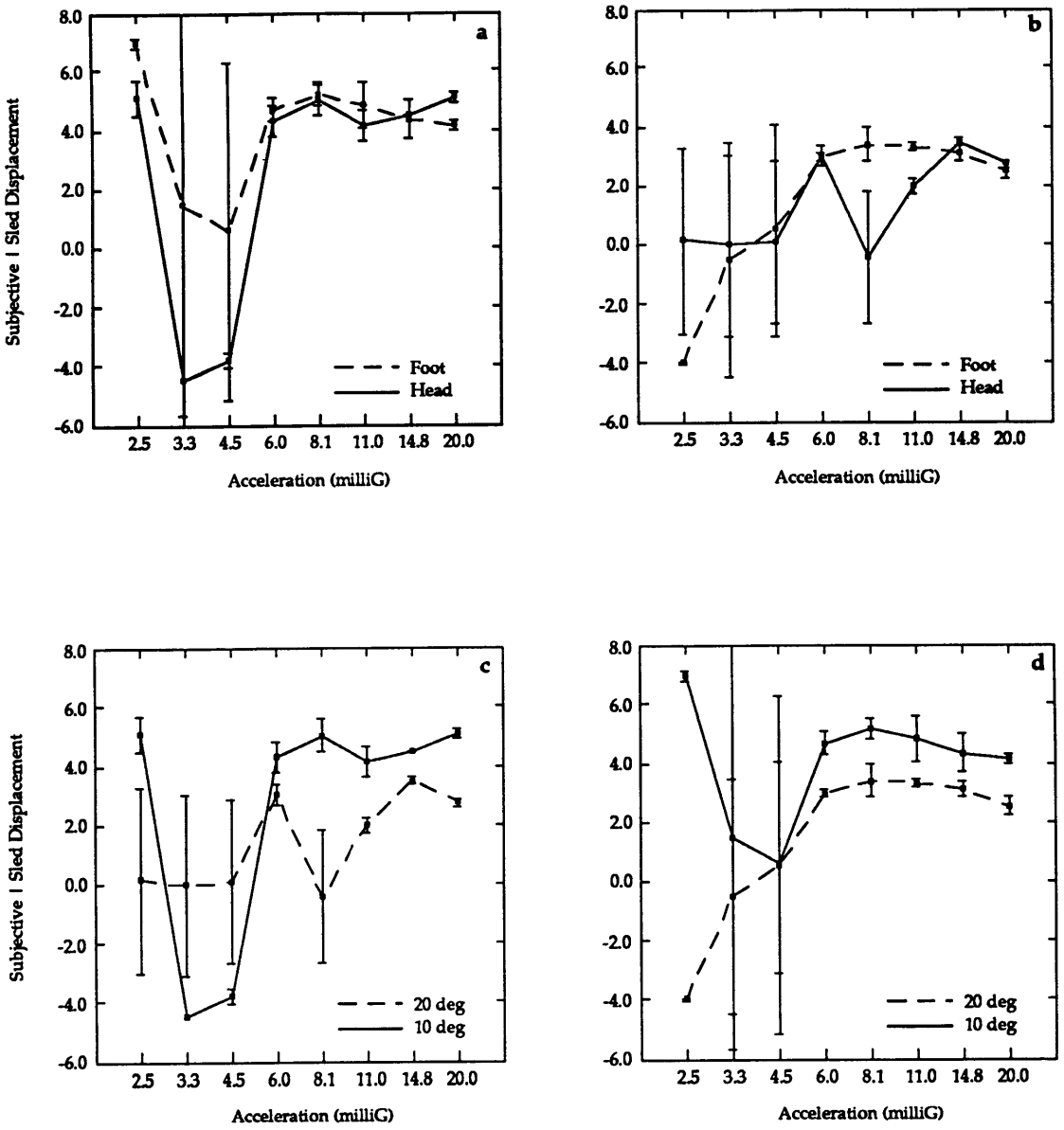

Figure C.2. Mean normalized subjective responses for subject CL. (a) headward and footward 10 degree trials, (b) headward and footward 20 degree trials, (c) 10 and 20 degree headward trials, and (d) 10 and 20 degree footward trials. Error bars indicate the standard error of the mean difference.

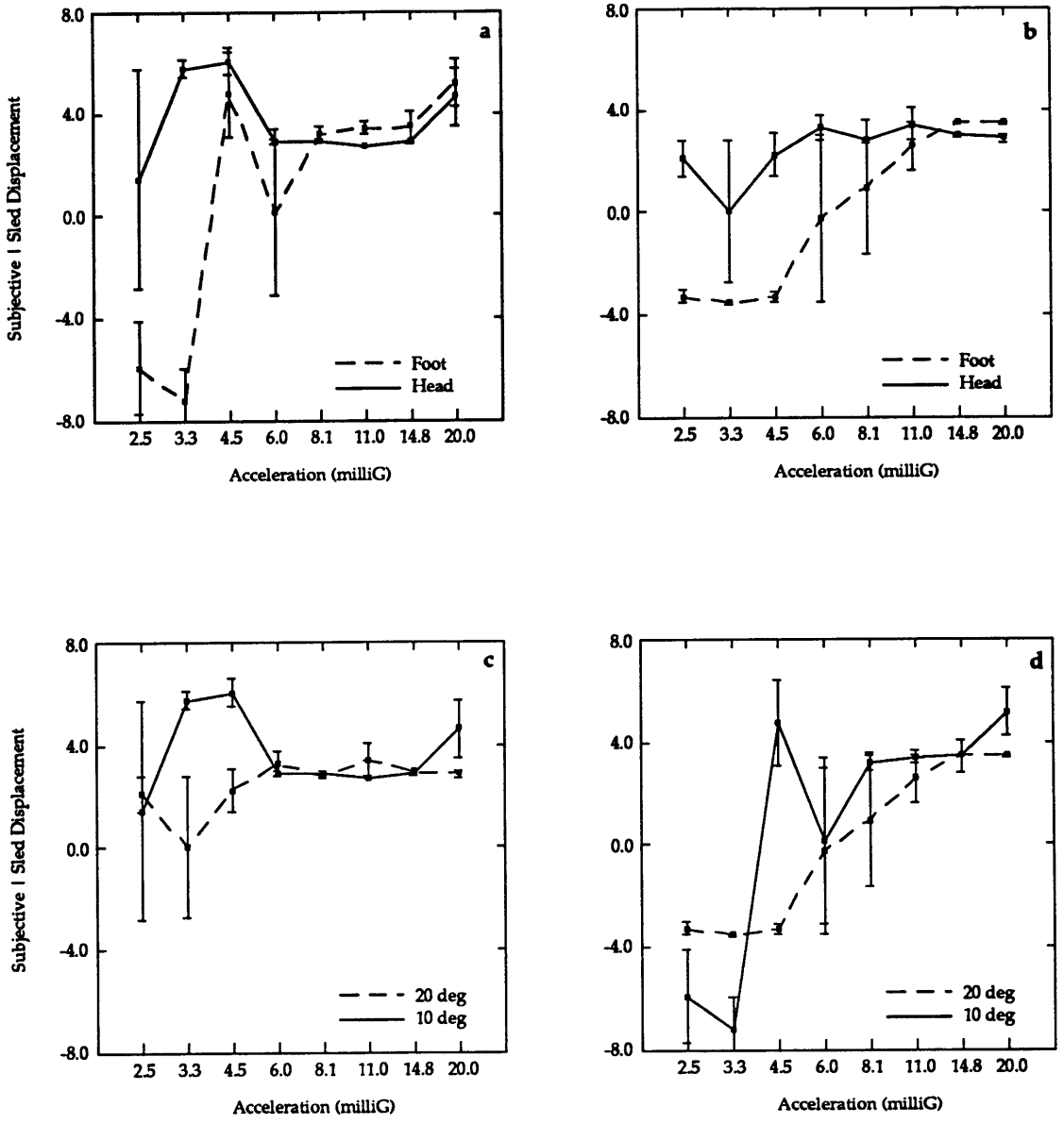

Figure C.2. Mean normalized subjective responses for subject JM. (a) headward and footward 10 degree trials, (b) headward and footward 20 degree trials, (c) 10 and 20 degree headward trials, and (d) 10 and 20 degree footward trials. Error bars indicate the standard error of the mean difference.

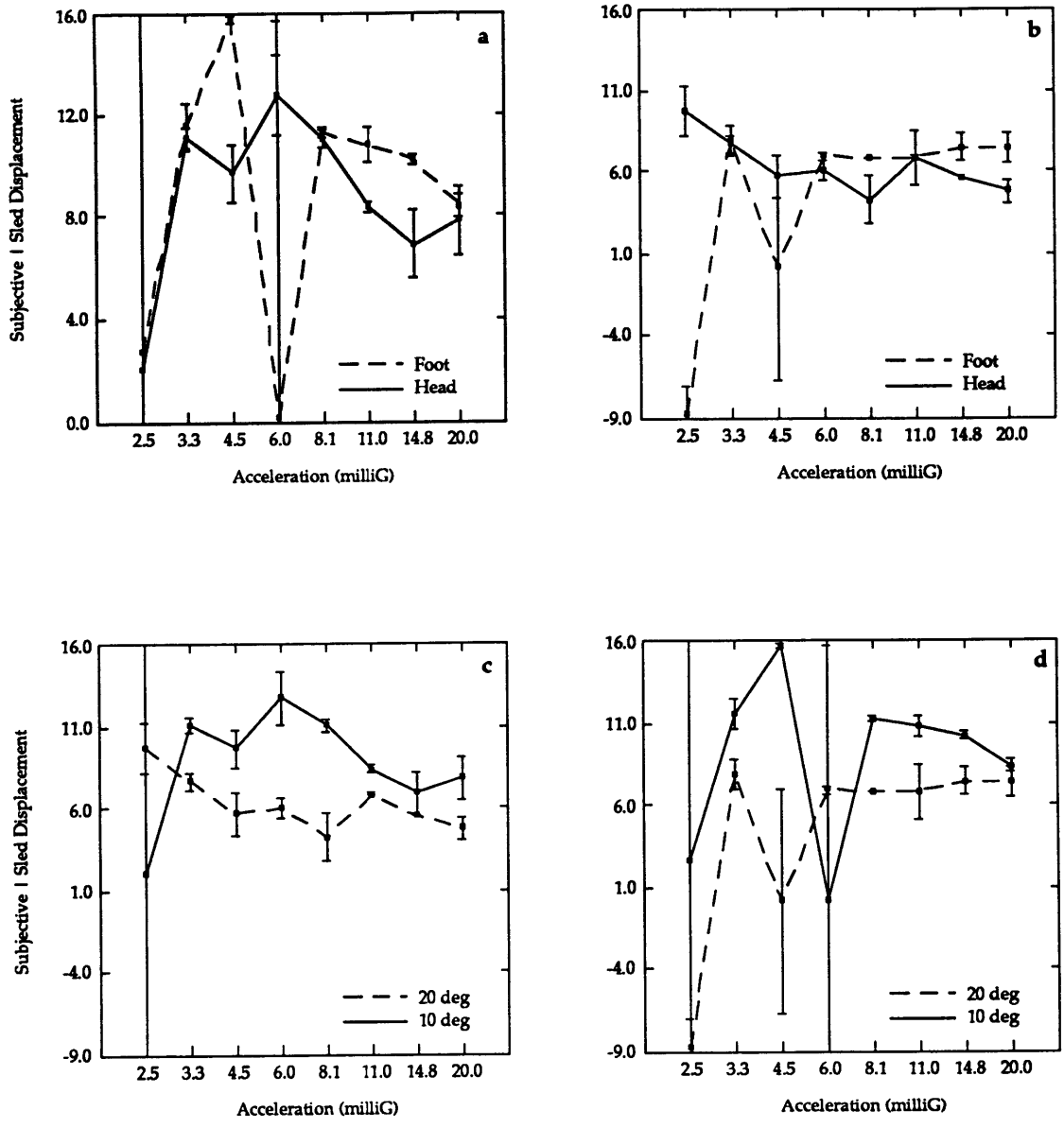

Figure C.2. Mean normalized subjective responses for subject KJ. (a) headward and footward 10 degree trials, (b) headward and footward 20 degree trials, (c) 10 and 20 degree headward trials, and (d) 10 and 20 degree footward trials. Error bars indicate the standard error of the mean difference.

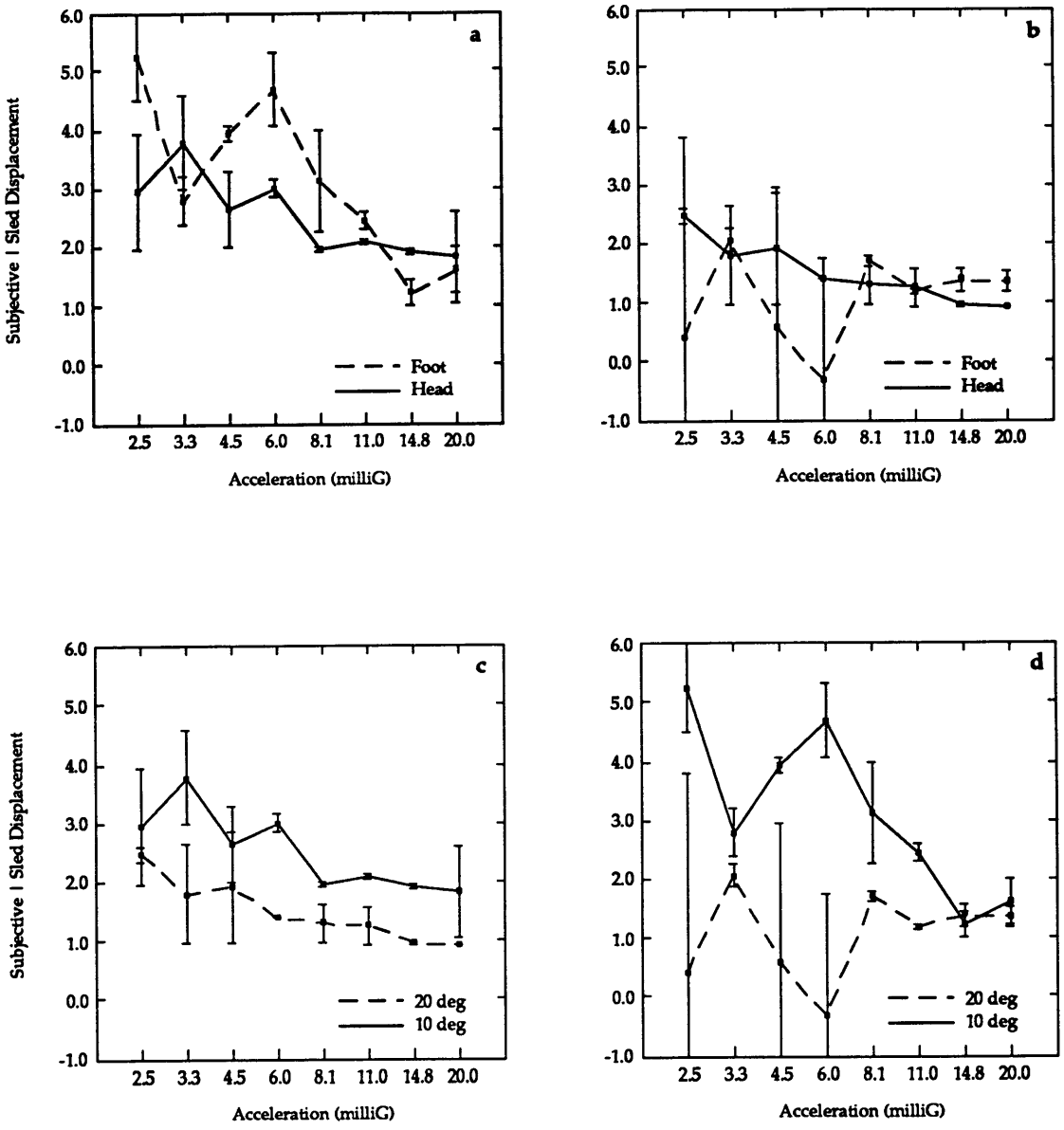

Figure C.2. Mean normalized subjective responses for subject KP. (a) headward and footward 10 degree trials, (b) headward and footward 20 degree trials, (c) 10 and 20 degree headward trials, and (d) 10 and 20 degree footward trials. Error bars indicate the standard error of the mean difference.

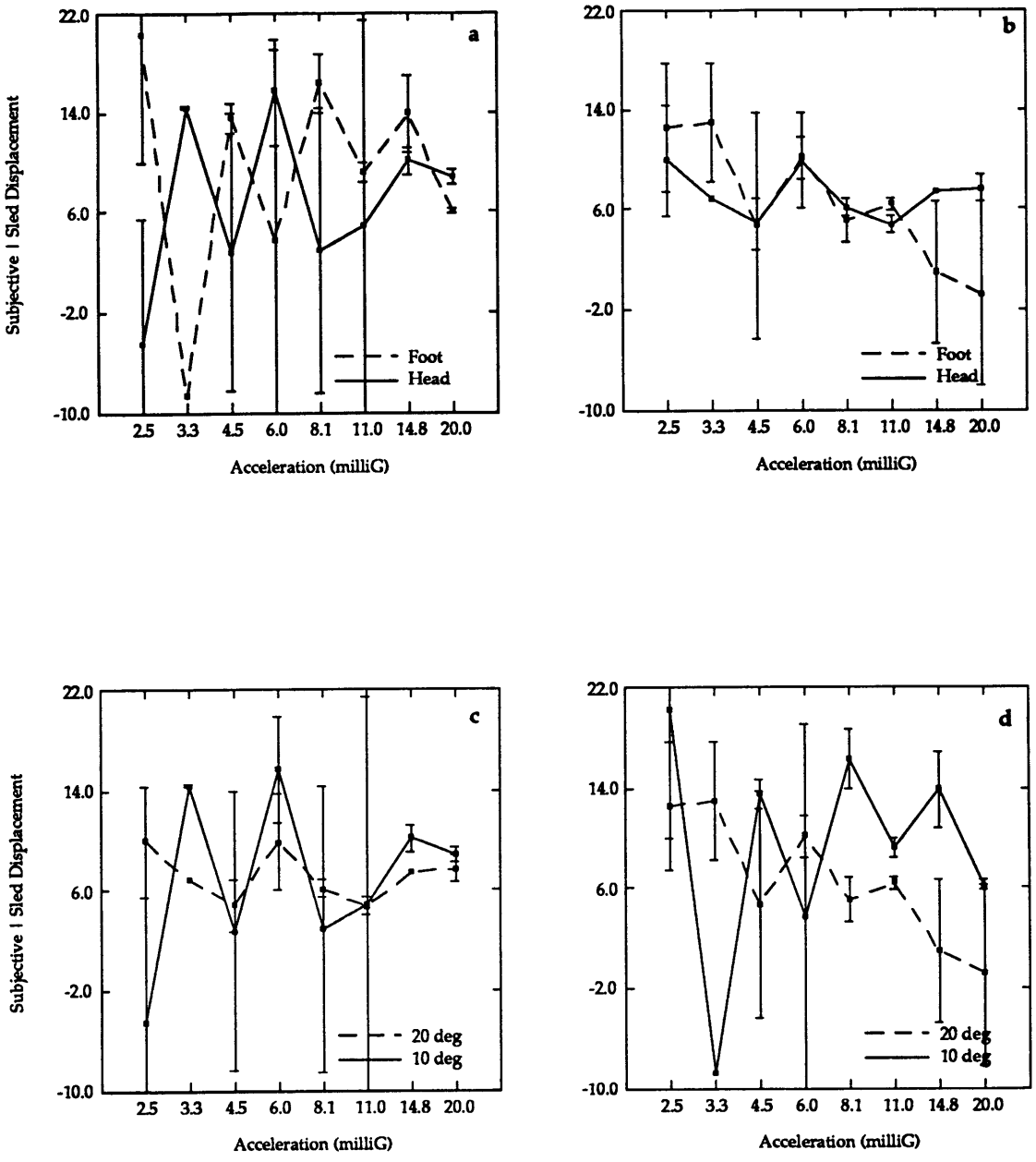

Figure C.2. Mean normalized subjective responses for subject RZ. (a) headward and footward 10 degree trials, (b) headward and footward 20 degree trials, (c) 10 and 20 degree headward trials, and (d) 10 and 20 degree footward trials. Error bars indicate the standard error of the mean difference.

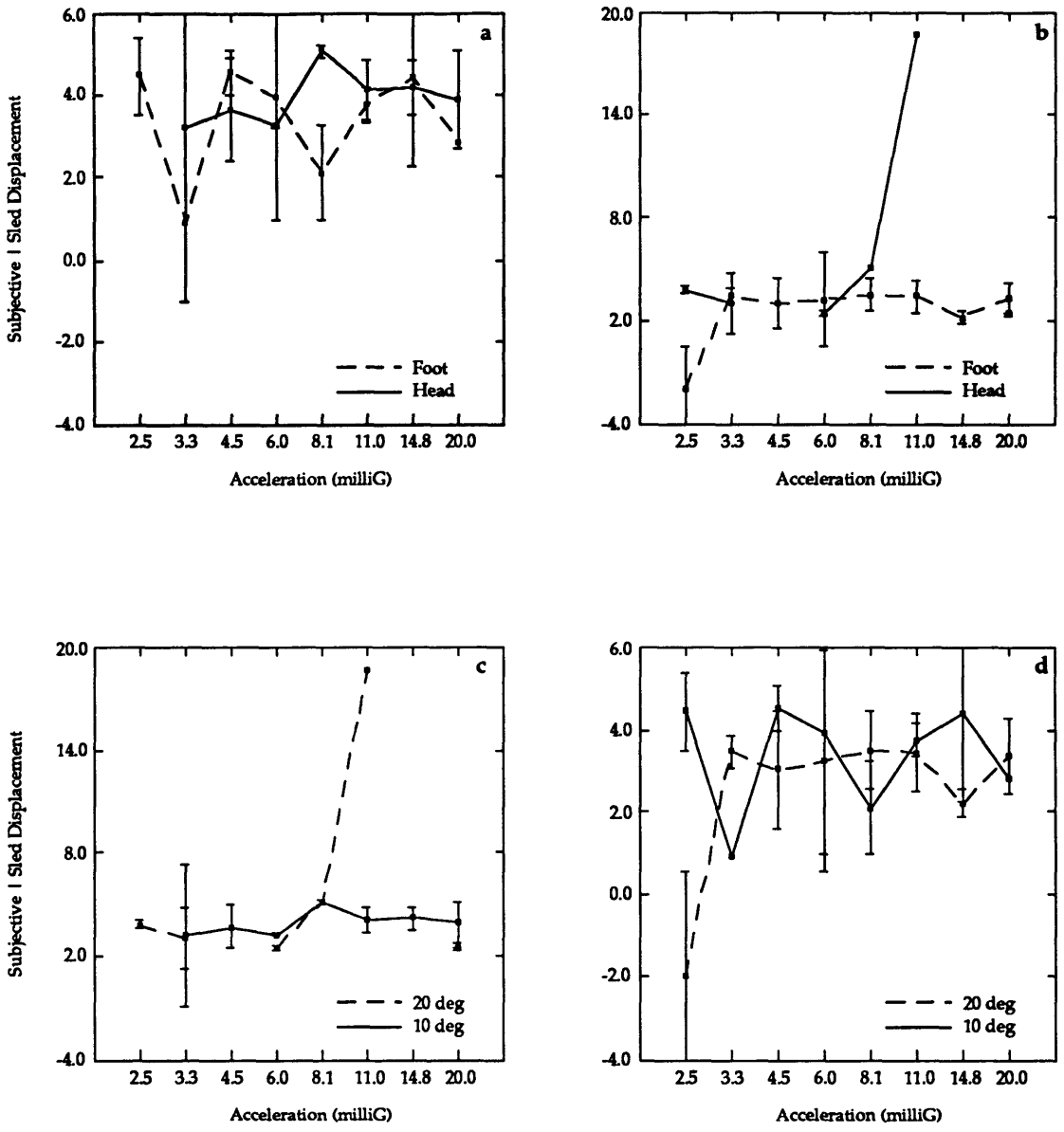

Figure C.2. Mean normalized subjective responses for subject TC. (a) headward and footward 10 degree trials, (b) headward and footward 20 degree trials, (c) 10 and 20 degree headward trials, and (d) 10 and 20 degree footward trials. Error bars indicate the standard error of the mean difference.

APPENDIX D: Z-AXIS FIXED DURATION RESULTS

This appendix contains the data plots from the Z-axis fixed duration test. These plots were provided in Chapter 4 (Results) for the representative subject MB (Figures 4.15, 4.16, and 4.18). In this appendix, three figures (containing four plots each) are shown for each of the six subjects: (D.1.) Scatter plots of raw eye movement data versus commanded sled displacement, (D.2.) Mean normalized eye movements (Eye/Sled Displacement), and (D.3.) Mean normalized subjective estimate of translation (Subjective/Sled Displacement. In each figure, the four different trial conditions are compared. (a) 1.0 second headward and footward trials, (b) 2.5 second headward to footward trials, (c) headward 1.0 and 2.5 second trials, (d) footward 1.0 and 2.5 second trials. Error bars signify standard error.

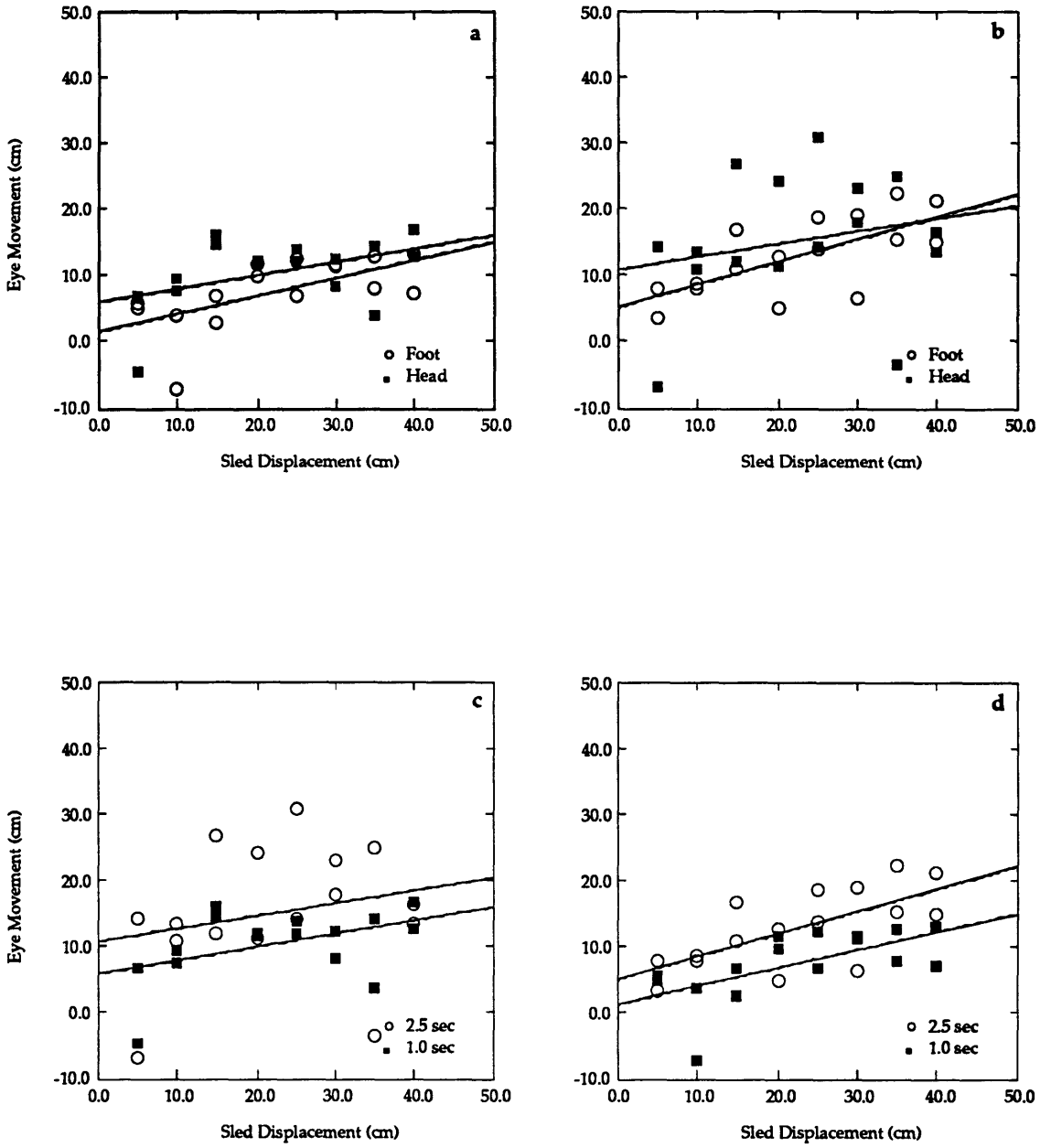

Figure D.1. Scatter plot of the Z-Axis Fixed Duration eye movement data comparing 1.0 and 2.5 second trials for subject AA. (a) 1.0 second trials comparing headward and footward trials, (b) 2.5 second trials comparing headward and footward trials, (c) headward trials comparing 1.0 and 2.5 second trials, (d) footward trials comparing 1.0 and 2.5 second trials. Error bars signify standard error.

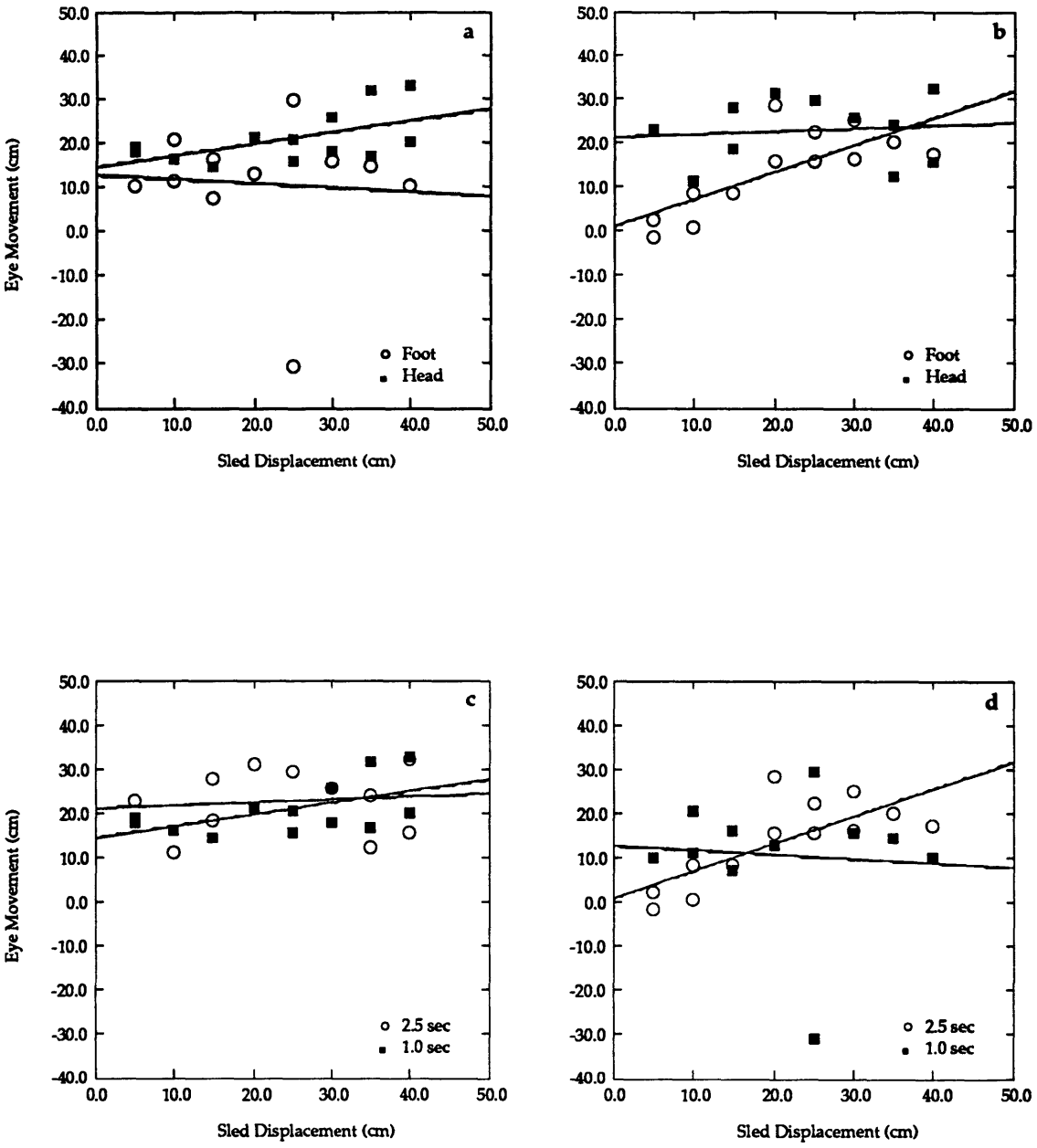

Figure D.1. Scatter plot of the Z-Axis Fixed Duration eye movement data comparing 1.0 and 2.5 second trials for subject GS. (a) 1.0 second trials comparing headward and footward trials, (b) 2.5 second trials comparing headward and footward trials, (c) headward trials comparing 1.0 and 2.5 second trials, (d) footward trials comparing 1.0 and 2.5 second trials. Error bars signify standard error.

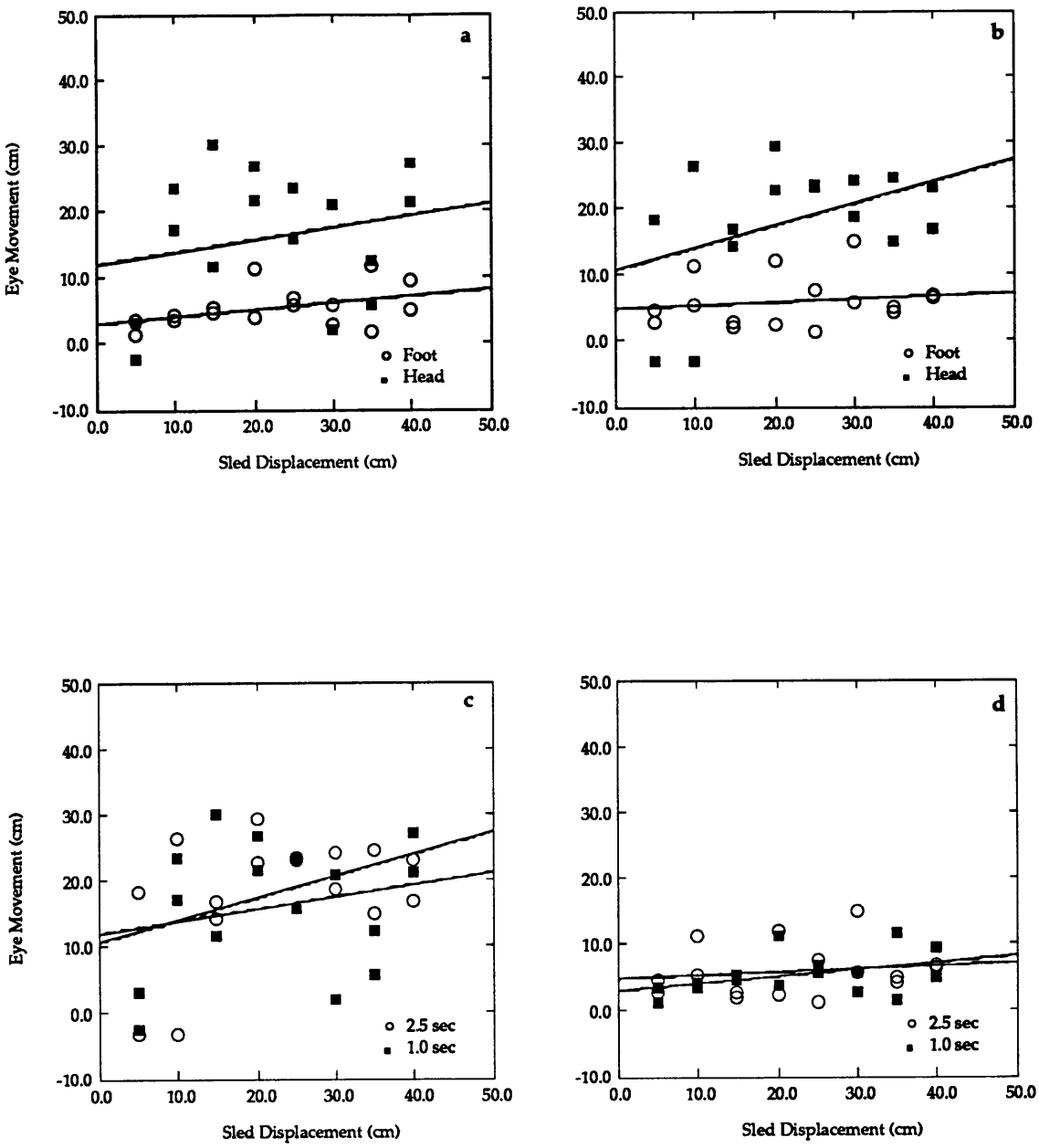

Figure D.1. Scatter plot of the Z-Axis Fixed Duration eye movement data comparing 1.0 and 2.5 second trials for subject JR. (a) 1.0 second trials comparing headward and footward trials, (b) 2.5 second trials comparing headward and footward trials, (c) headward trials comparing 1.0 and 2.5 second trials, (d) footward trials comparing 1.0 and 2.5 second trials. Error bars signify standard error.

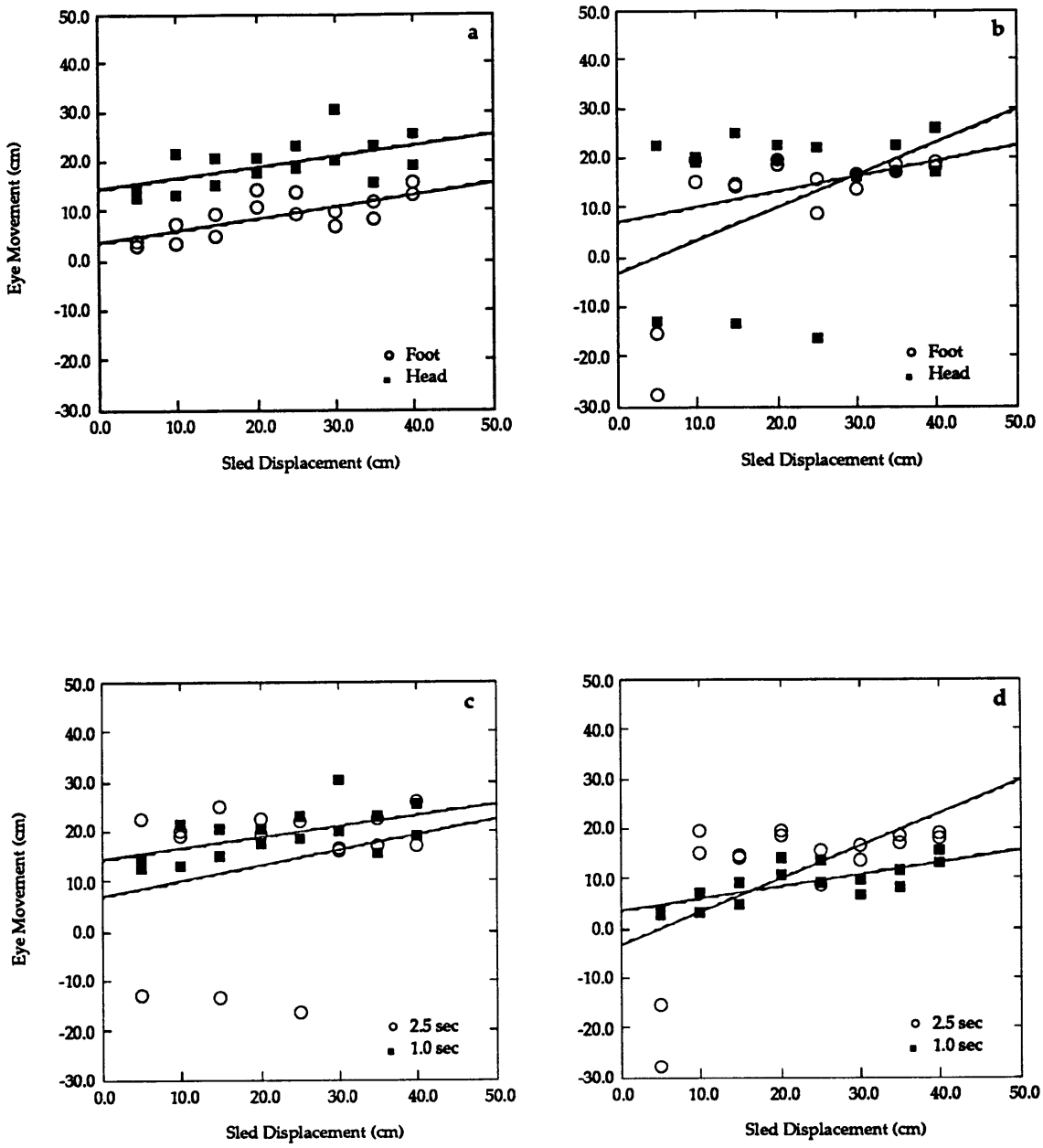

Figure D.1. Scatter plot of the Z-Axis Fixed Duration eye movement data comparing 1.0 and 2.5 second trials for subject KP. (a) 1.0 second trials comparing headward and footward trials, (b) 2.5 second trials comparing headward and footward trials, (c) headward trials comparing 1.0 and 2.5 second trials, (d) footward trials comparing 1.0 and 2.5 second trials. Error bars signify standard error.

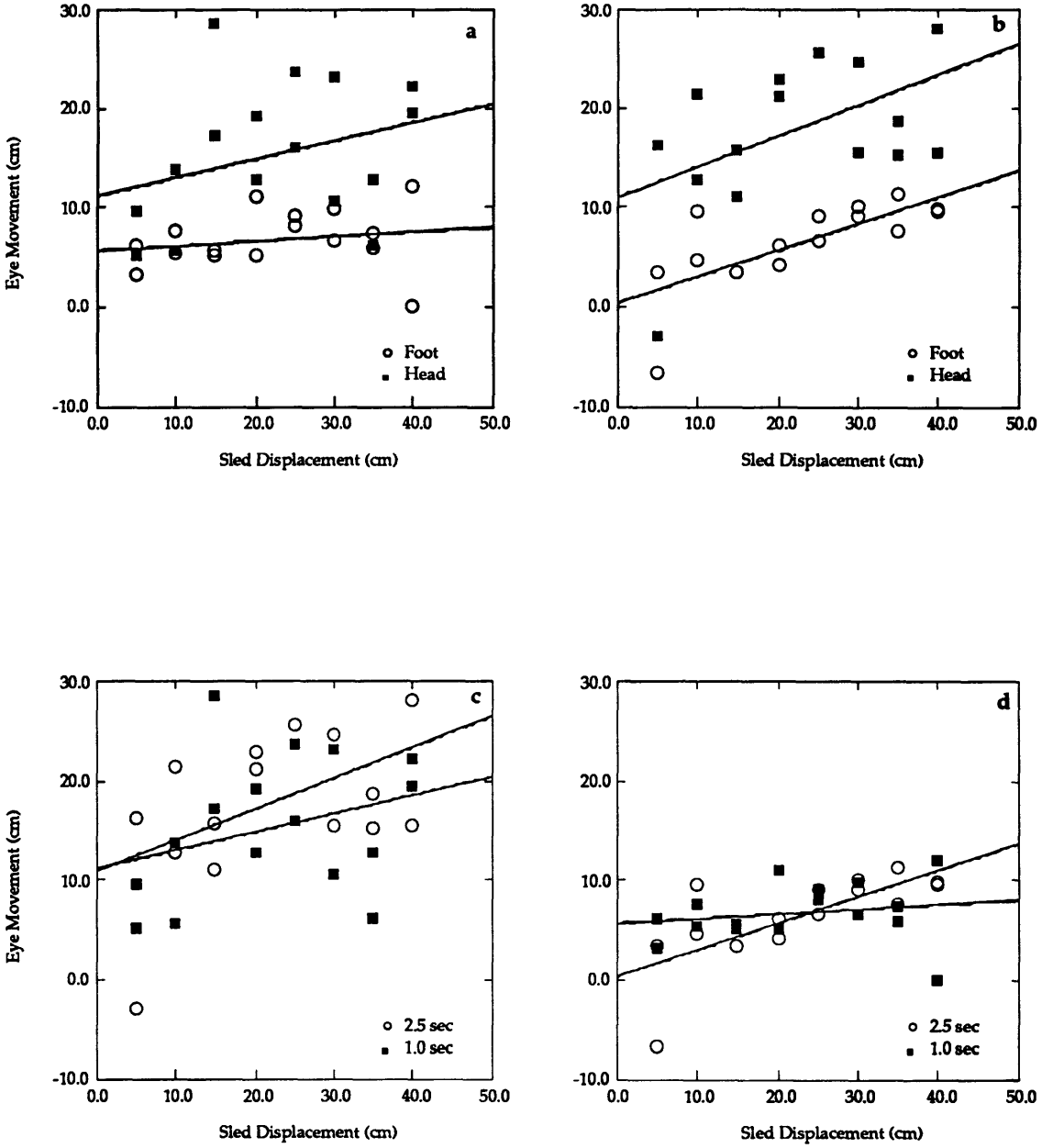

Figure D.1. Scatter plot of the Z-Axis Fixed Duration eye movement data comparing 1.0 and 2.5 second trials for subject MB. (a) 1.0 second trials comparing headward and footward trials, (b) 2.5 second trials comparing headward and footward trials, (c) headward trials comparing 1.0 and 2.5 second trials, (d) footward trials comparing 1.0 and 2.5 second trials. Error bars signify standard error.

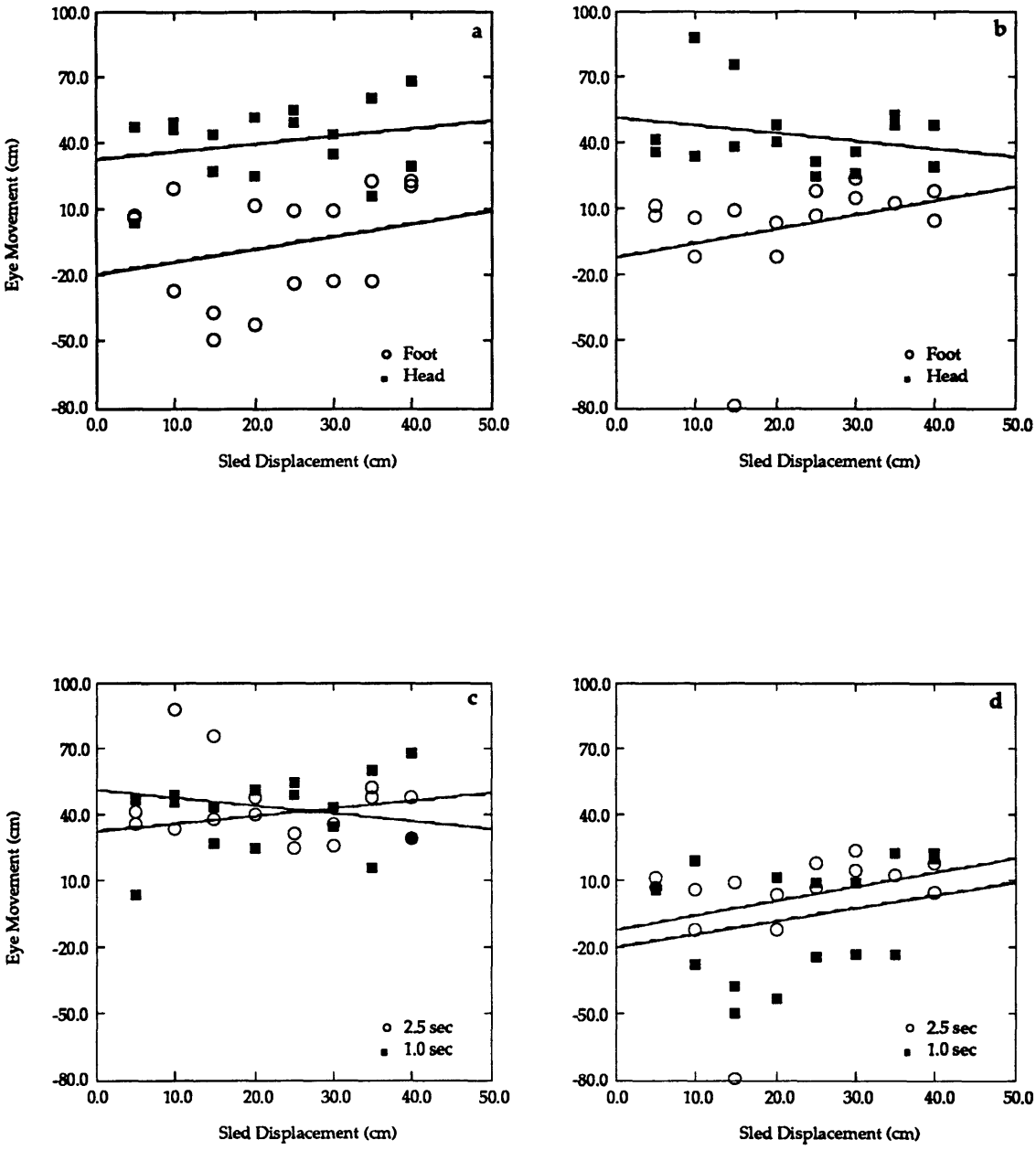

Figure D.1. Scatter plot of the Z-Axis Fixed Duration eye movement data comparing 1.0 and 2.5 second trials for subject SS. (a) 1.0 second trials comparing headward and footward trials, (b) 2.5 second trials comparing headward and footward trials, (c) headward trials comparing 1.0 and 2.5 second trials, (d) footward trials comparing 1.0 and 2.5 second trials. Error bars signify standard error.

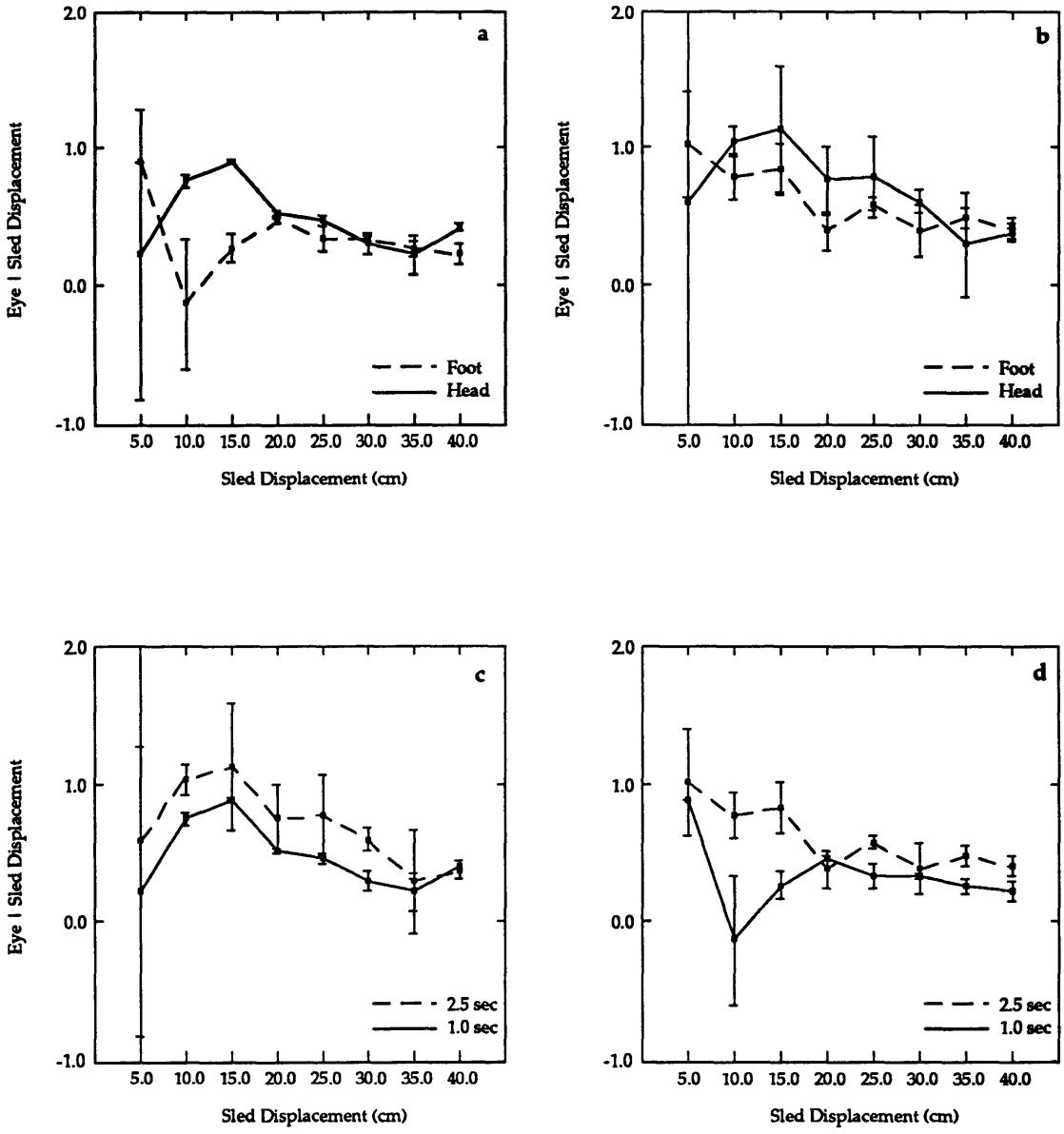

Figure D.2. Z-axis fixed duration mean normalized eye movement responses versus sled displacement for subject AA. (a) 1.0 sec trials comparing headward and footward, (b) 2.5 sec trials comparing headward and footward, (c) headward trials comparing 1.0 sec and 2.5 sec, and (d) footward trials comparing 1.0 and 2.5 sec. Error bars indicate standard error.

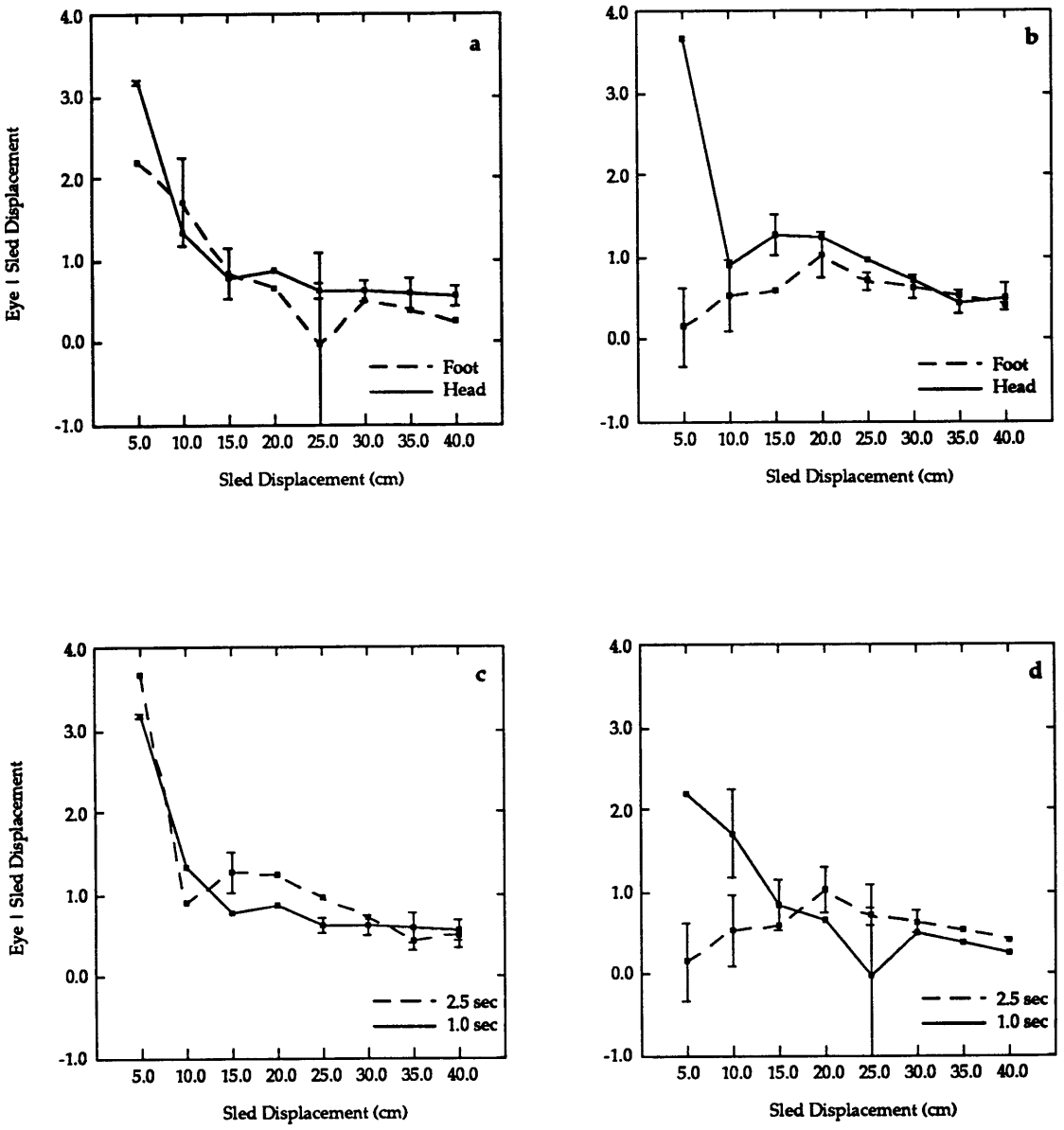

Figure D.2. Z-axis fixed duration mean normalized eye movement responses versus sled displacement for subject GS. (a) 1.0 sec trials comparing headward and footward, (b) 2.5 sec trials comparing headward and footward, (c) headward trials comparing 1.0 sec and 2.5 sec, and (d) footward trials comparing 1.0 and 2.5 sec. Error bars indicate standard error.

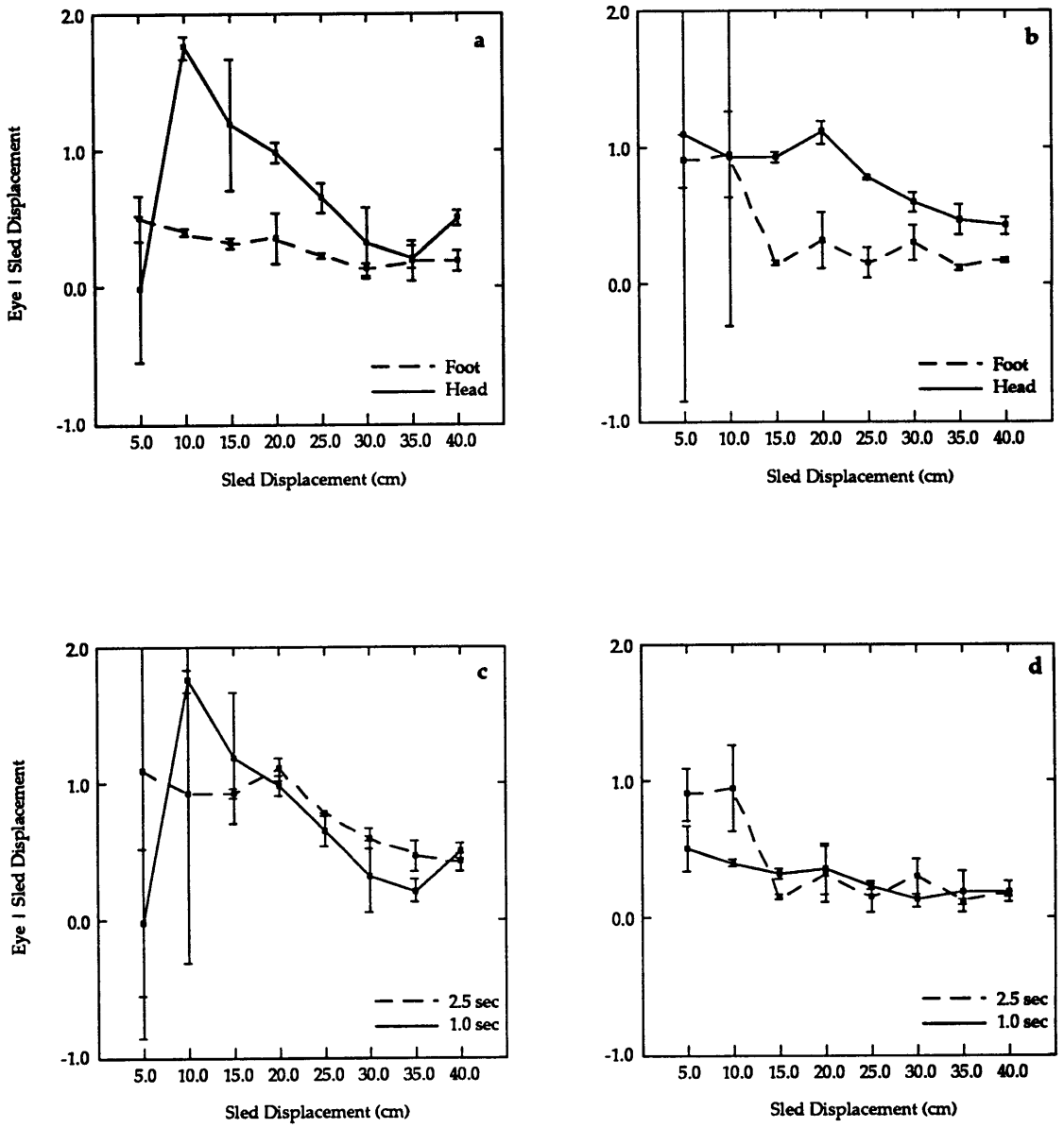

Figure D.2. Z-axis fixed duration mean normalized eye movement responses versus sled displacement for subject JR. (a) 1.0 sec trials comparing headward and footward, (b) 2.5 sec trials comparing headward and footward, (c) headward trials comparing 1.0 sec and 2.5 sec, and (d) footward trials comparing 1.0 and 2.5 sec. Error bars indicate standard error.

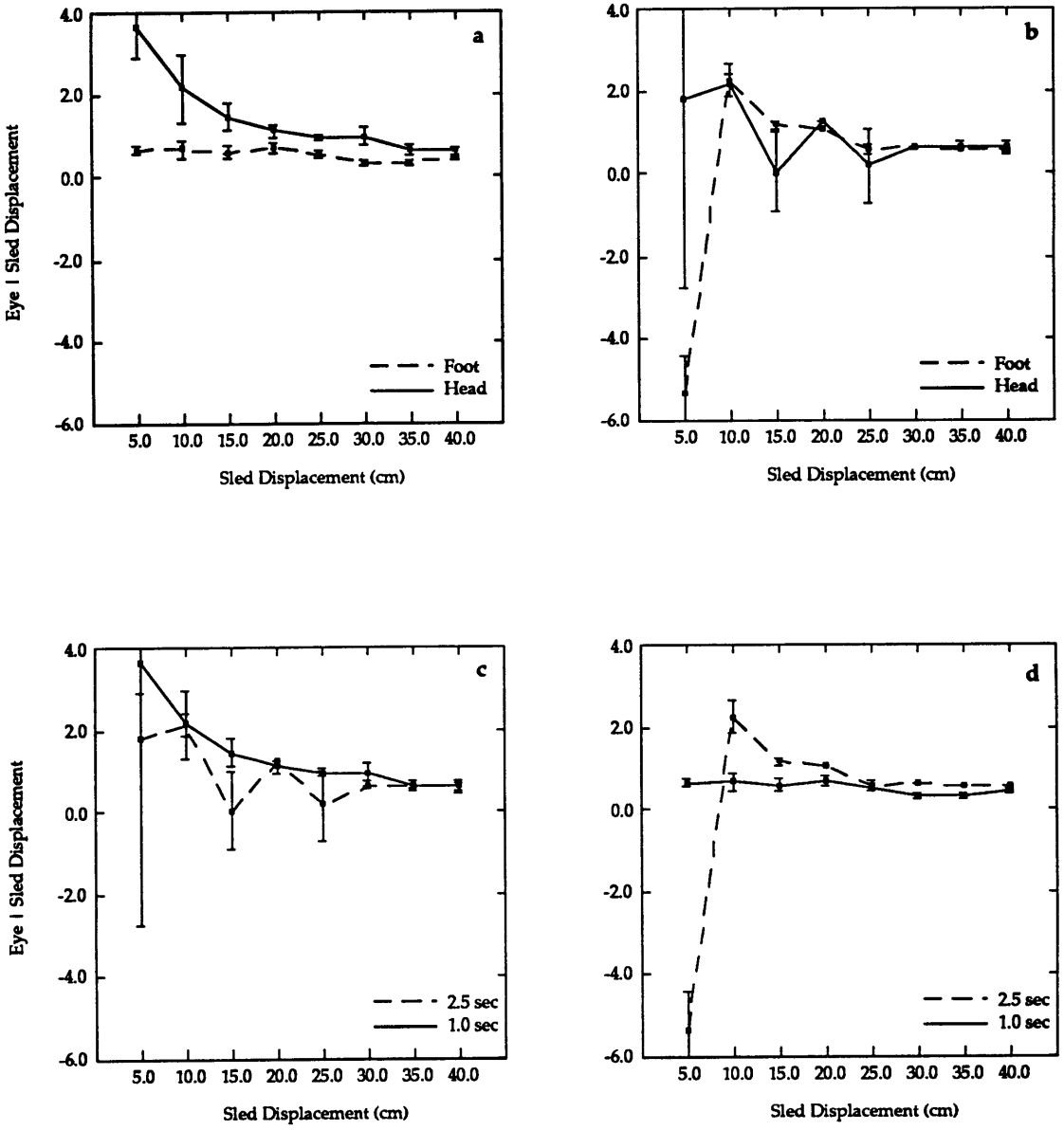

Figure D.2. Z-axis fixed duration mean normalized eye movement responses versus sled displacement for subject KP. (a) 1.0 sec trials comparing headward and footward, (b) 2.5 sec trials comparing headward and footward, (c) headward trials comparing 1.0 sec and 2.5 sec, and (d) footward trials comparing 1.0 and 2.5 sec. Error bars indicate standard error.

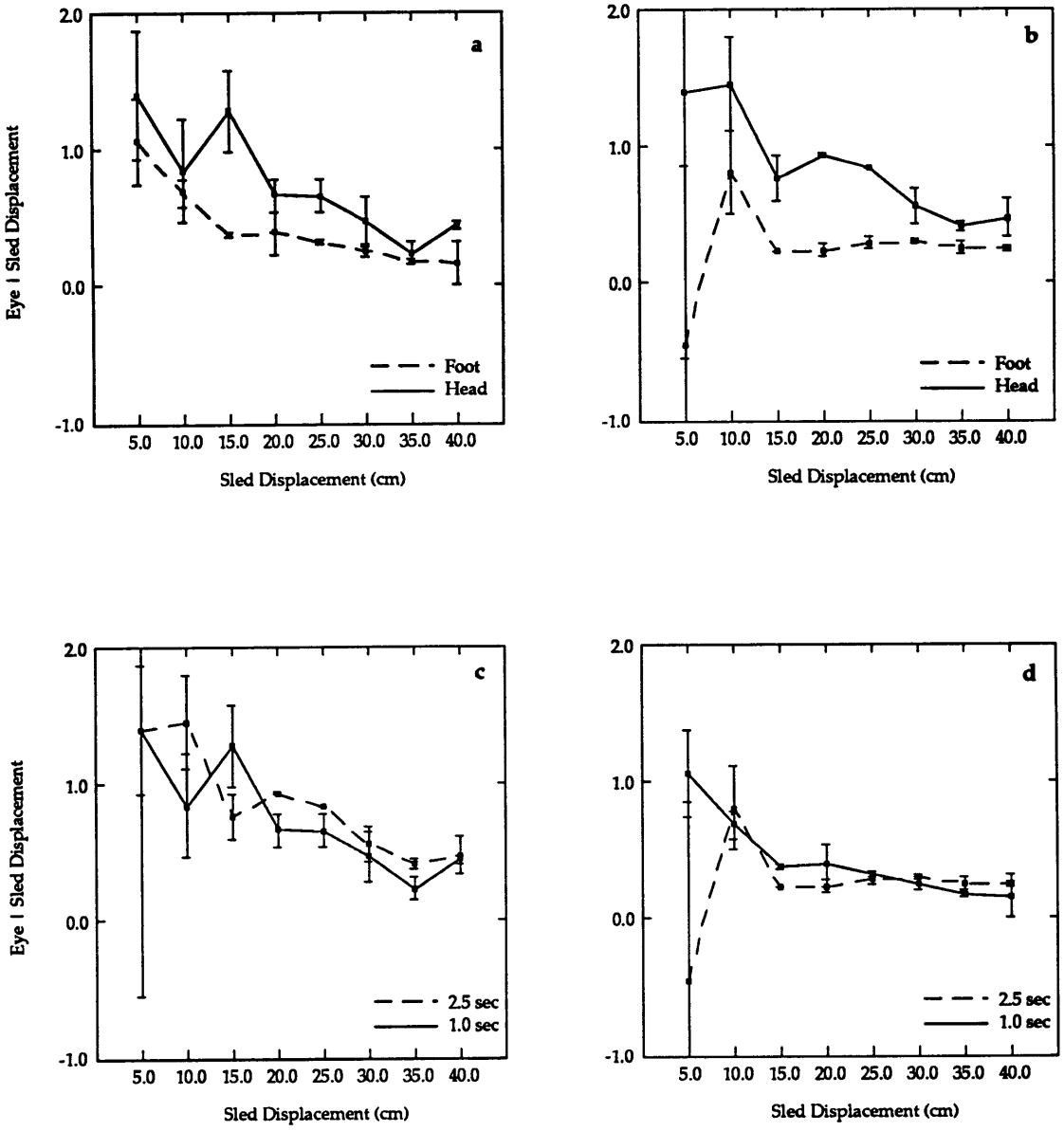

Figure D.2. Z-axis fixed duration mean normalized eye movement responses versus sled displacement for subject MB. (a) 1.0 sec trials comparing headward and footward, (b) 2.5 sec trials comparing headward and footward, (c) headward trials comparing 1.0 sec and 2.5 sec, and (d) footward trials comparing 1.0 and 2.5 sec. Error bars indicate standard error.

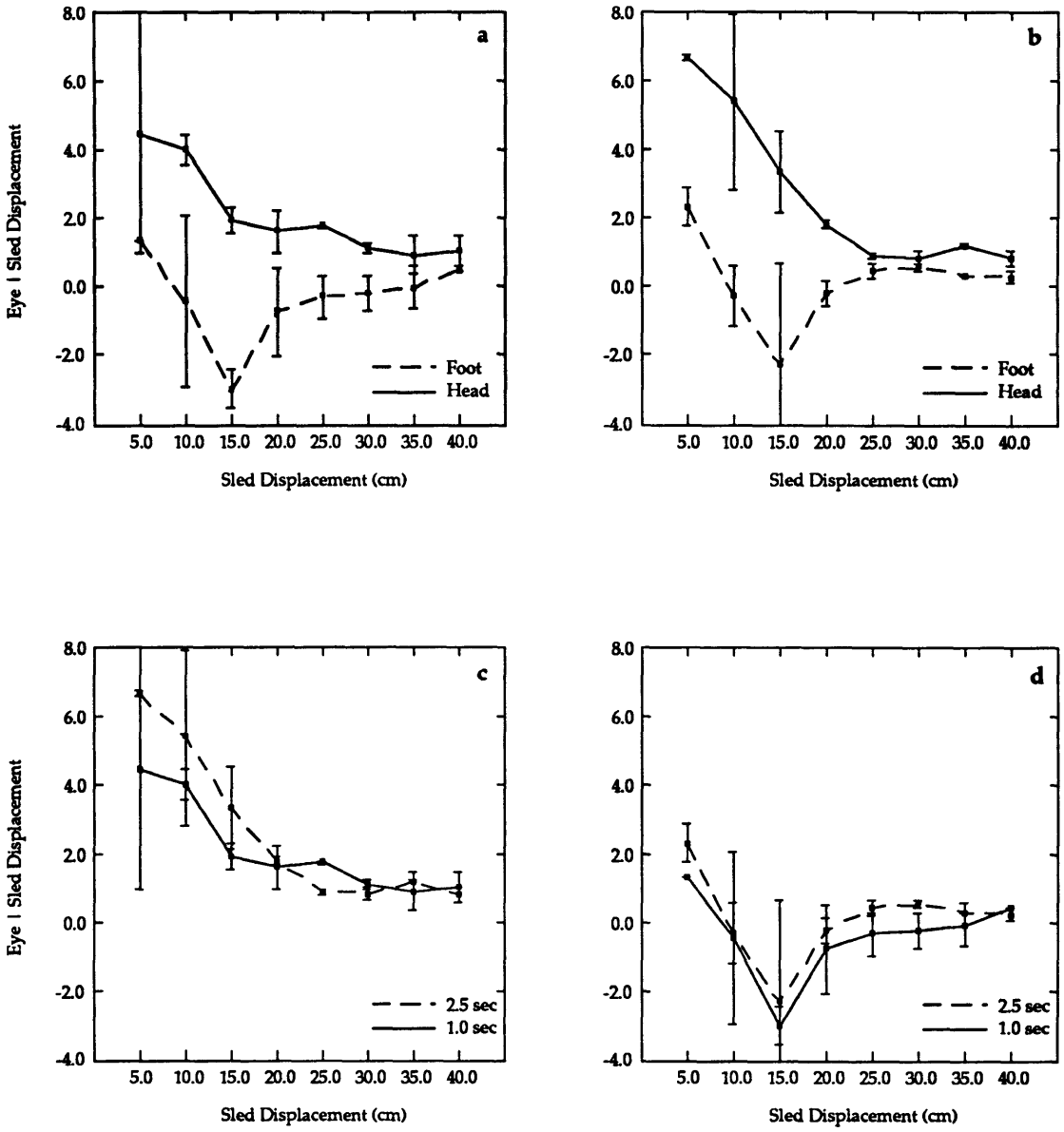

Figure D.2. Z-axis fixed duration mean normalized eye movement responses versus sled displacement for subject SS. (a) 1.0 sec trials comparing headward and footward, (b) 2.5 sec trials comparing headward and footward, (c) headward trials comparing 1.0 sec and 2.5 sec, and (d) footward trials comparing 1.0 and 2.5 sec. Error bars indicate standard error.

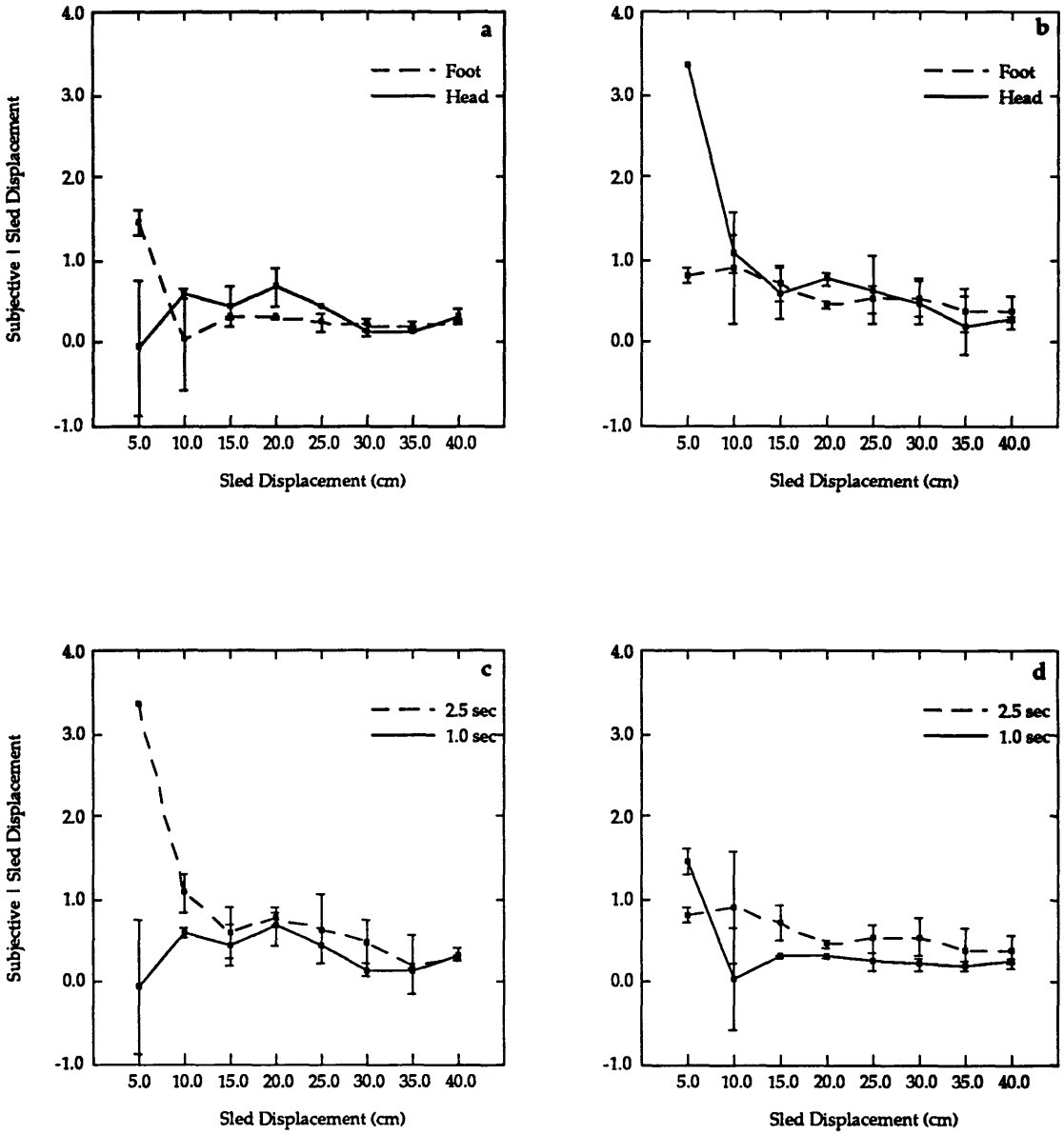

Figure D.3. Mean normalized subjective responses for subject AA. (a) headward and footward 1.0 second trials, (b) headward and footward 2.5 second trials, (c) 1.0 and 2.5 second headward trials, and (d) 1.0 and 2.5 second footward trials. Error bars indicate the standard error of the difference.

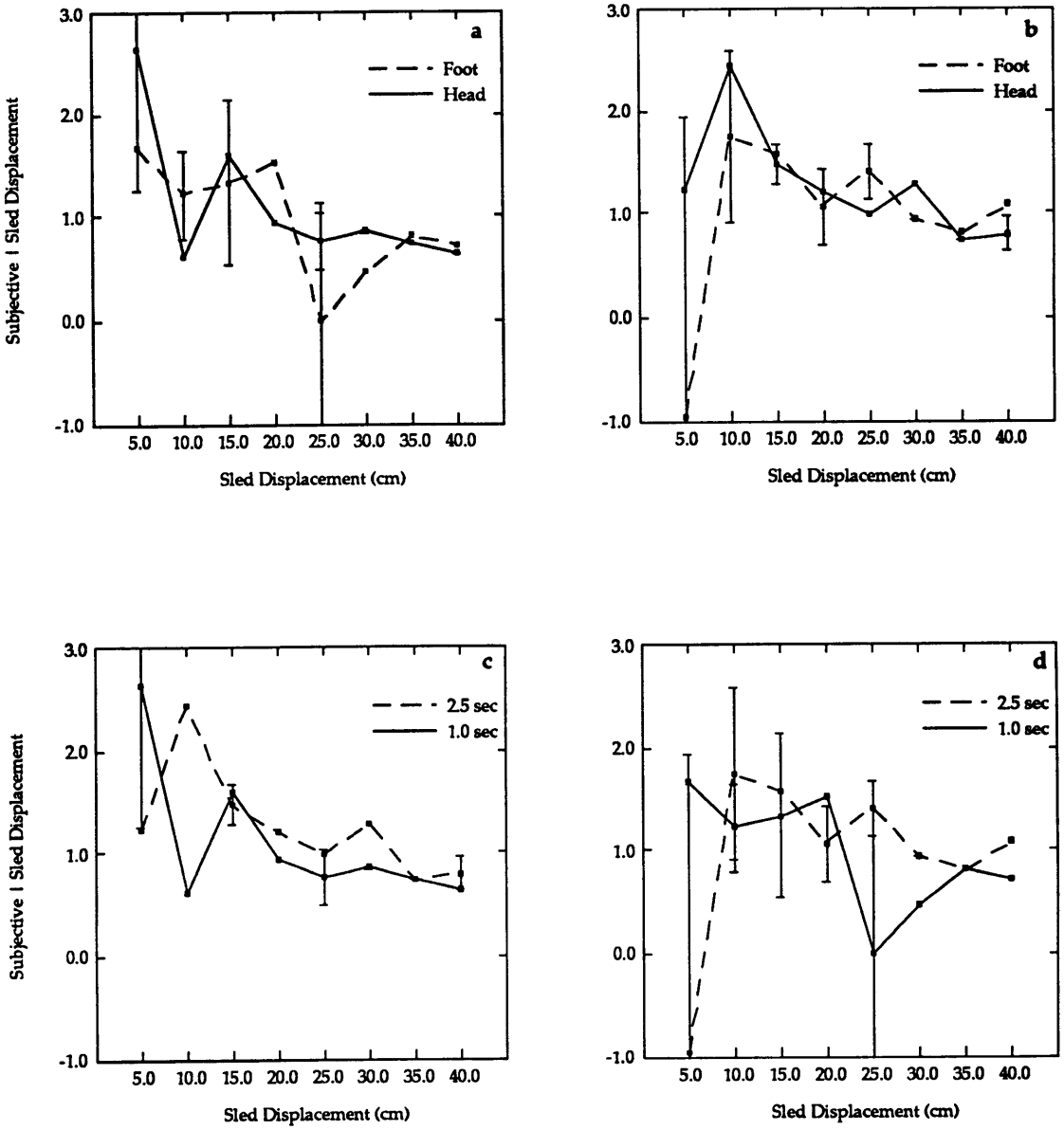

Figure D.3. Mean normalized subjective responses for subject GS. (a) headward and footward 1.0 second trials, (b) headward and footward 2.5 second trials, (c) 1.0 and 2.5 second headward trials, and (d) 1.0 and 2.5 second footward trials. Error bars indicate the standard error of the difference.

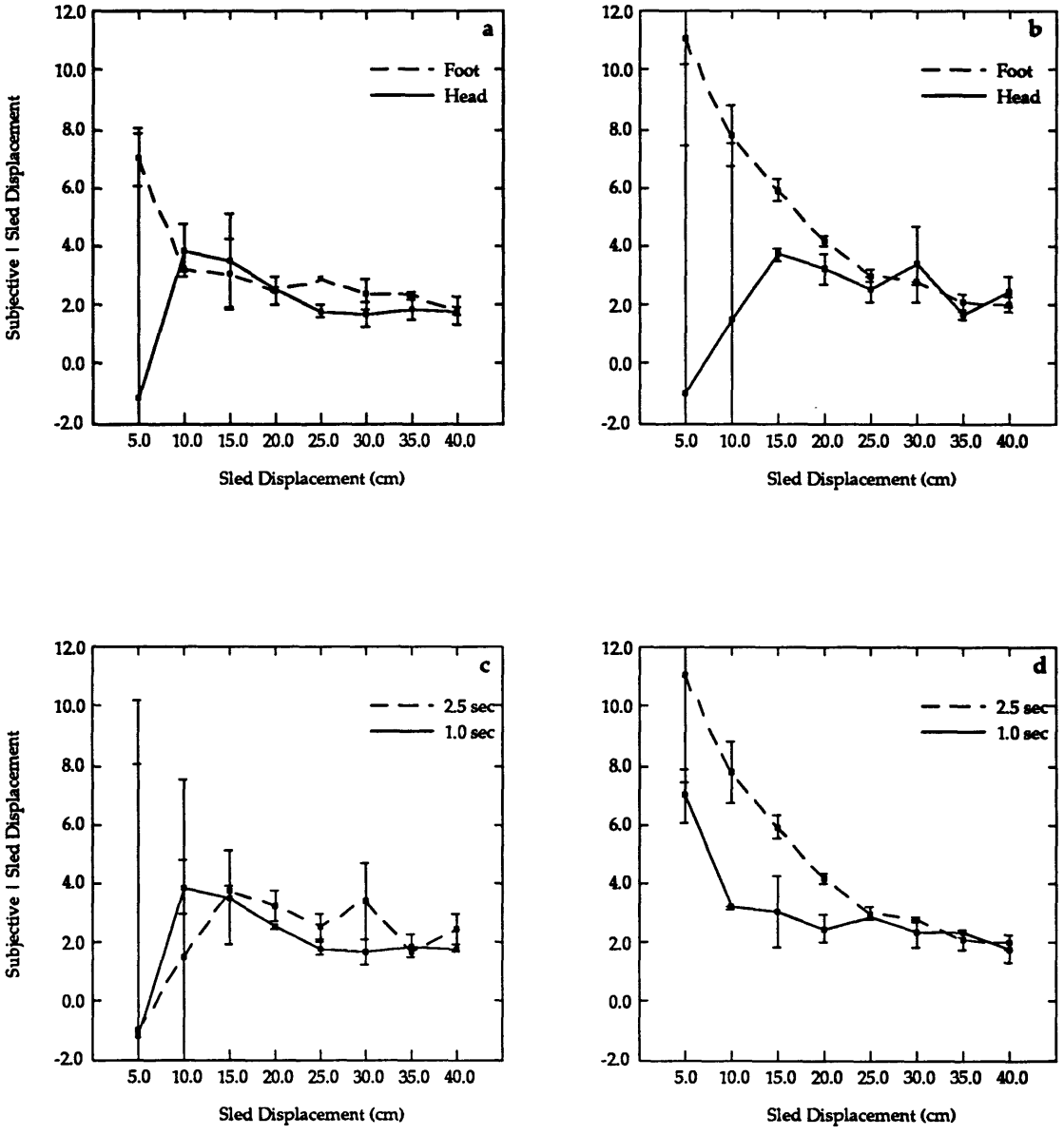

Figure D.3. Mean normalized subjective responses for subject JR. (a) headward and footward 1.0 second trials, (b) headward and footward 2.5 second trials, (c) 1.0 and 2.5 second headward trials, and (d) 1.0 and 2.5 second footward trials. Error bars indicate the standard error of the difference.

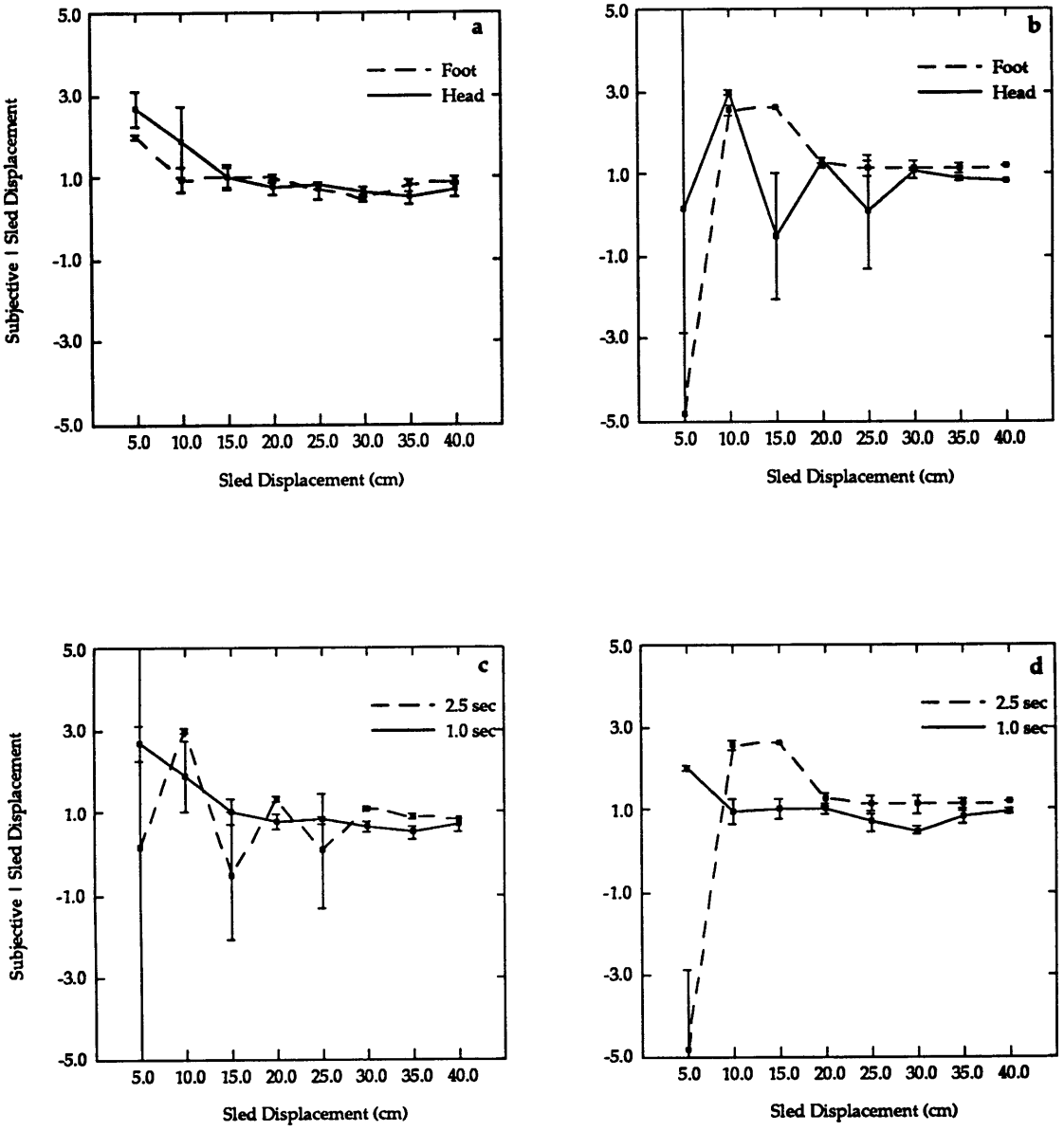

Figure D.3. Mean normalized subjective responses for subject KP. (a) headward and footward 1.0 second trials, (b) headward and footward 2.5 second trials, (c) 1.0 and 2.5 second headward trials, and (d) 1.0 and 2.5 second footward trials. Error bars indicate the standard error of the difference.

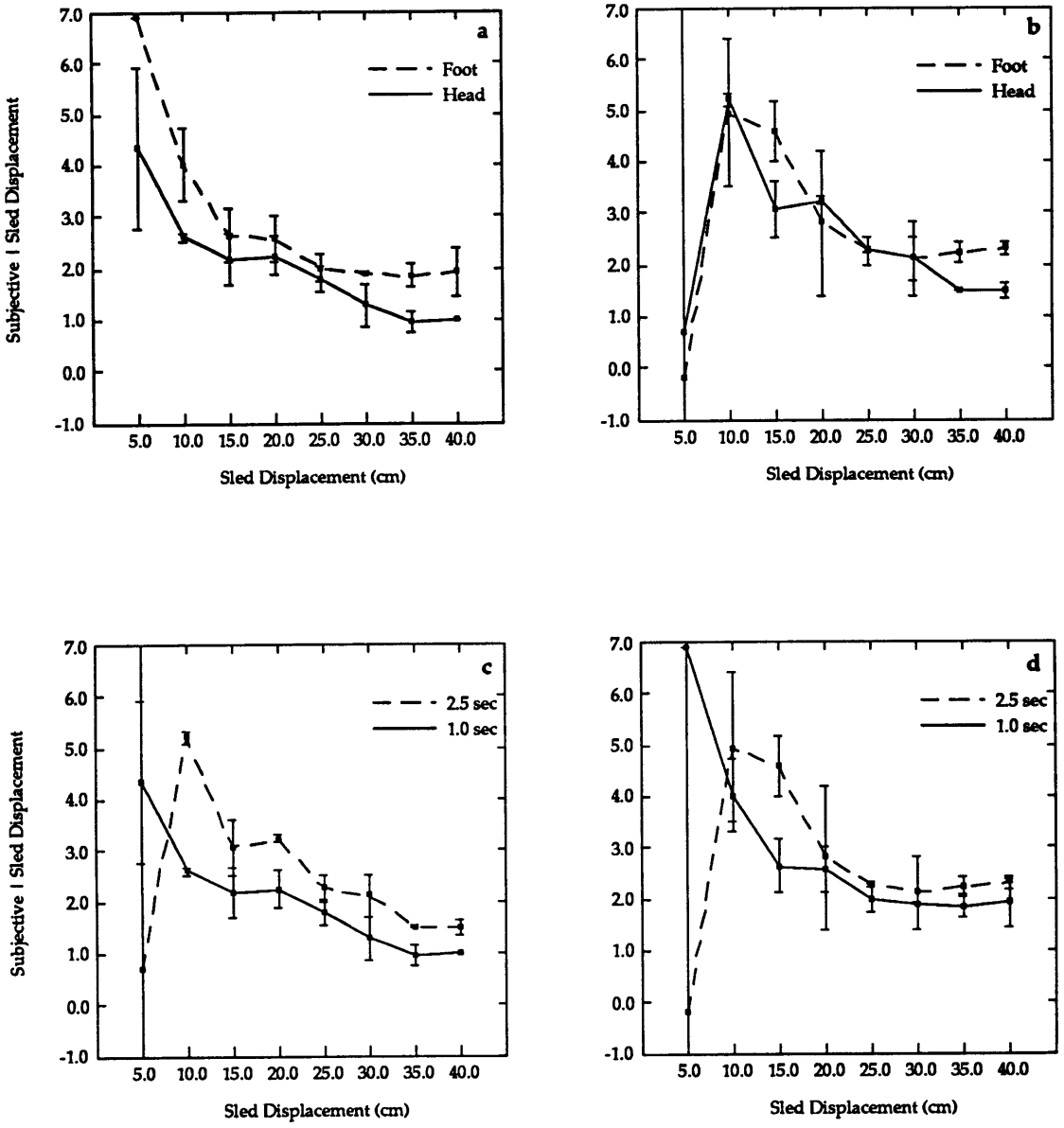

Figure D.3. Mean normalized subjective responses for subject MB. (a) headward and footward 1.0 second trials, (b) headward and footward 2.5 second trials, (c) 1.0 and 2.5 second headward trials, and (d) 1.0 and 2.5 second footward trials. Error bars indicate the standard error of the difference.

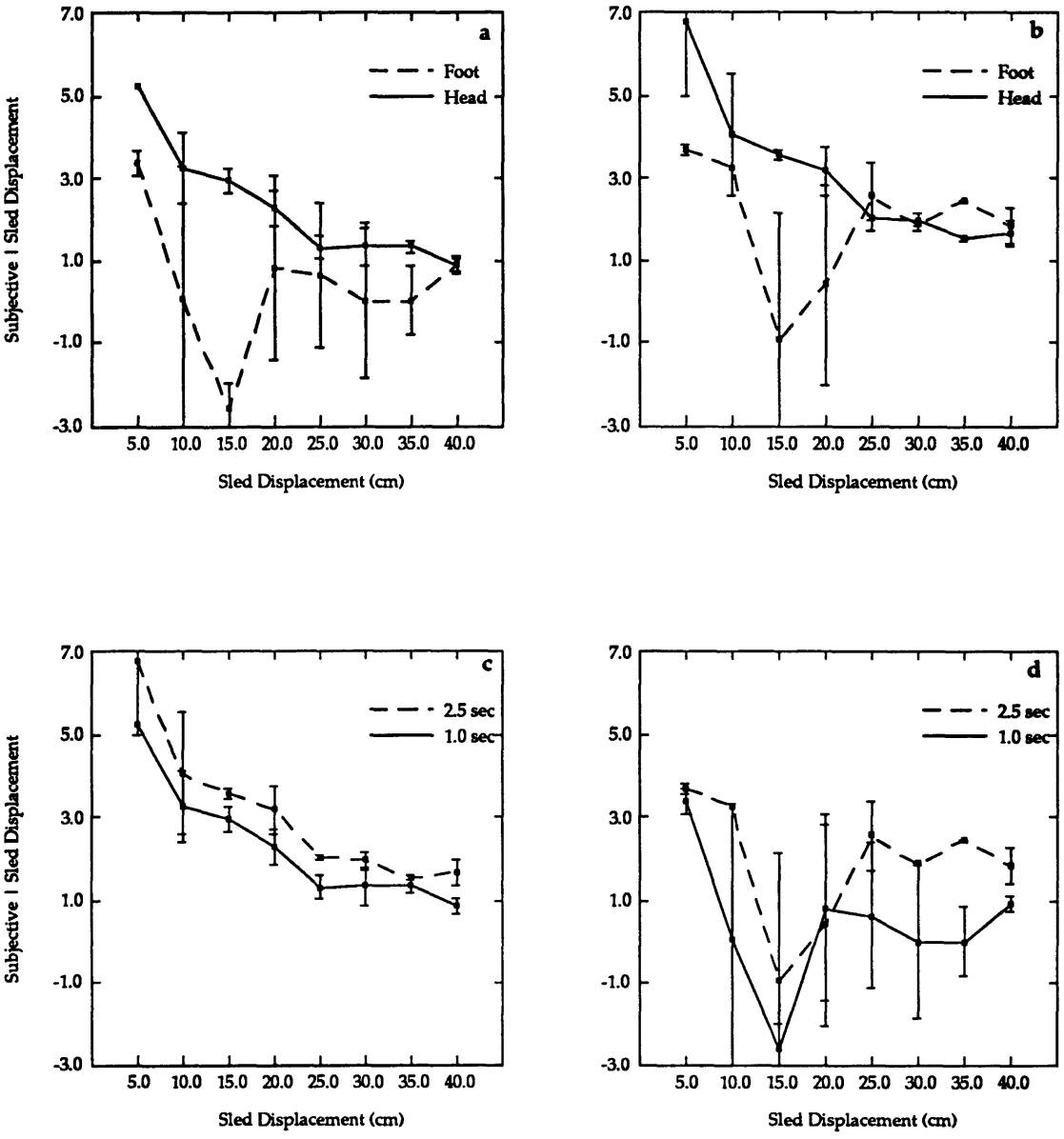

Figure D.3. Mean normalized subjective responses for subject SS. (a) headward and footward 1.0 second trials, (b) headward and footward 2.5 second trials, (c) 1.0 and 2.5 second headward trials, and (d) 1.0 and 2.5 second footward trials. Error bars indicate the standard error of the difference.

APPENDIX E: LINEAR ADAPTATION RESULTS

This appendix contains the data plots from the linear adaptation test performed in the y-axis. Identical figures were provided in Chapter 4 (Results) for the representative subject CL (Figures 4.21, 4.23, 4.25, 4.26, 4.27).

E.1. and E.2. For the hidden target pursuit experiment, two figures (containing four plots each) are shown for each of the four subjects summarizing the mean normalized eye movements (Eye/Sled Displacement) and the mean normalized subjective responses (Subjective/Sled Displacement) in the four different trial conditions. (a) Pre-adaptation rightward and leftward trials, (b) Post-adaptation rightward and leftward trials, (c) rightward pre- and post-adaptation trials, (d) leftward pre- and post-adaptation trials. Error bars signify standard error.

E.3. For the linear VOR experiment, one figure is shown for each of the four subjects showing the confidence areas for comparison of the pre-/post-adaptation trials in each of three test conditions: dark, OK alone, and OK+Sled.

E.4. For the angular VOR experiment, one figure is shown for each of the four subjects showing the confidence areas for comparison of the pre-/post-adaptation responses.

E.5. For the adaptation paradigm, one plot is shown for each of the four subjects showing the power spectral density functions of the subjects' joystick input.

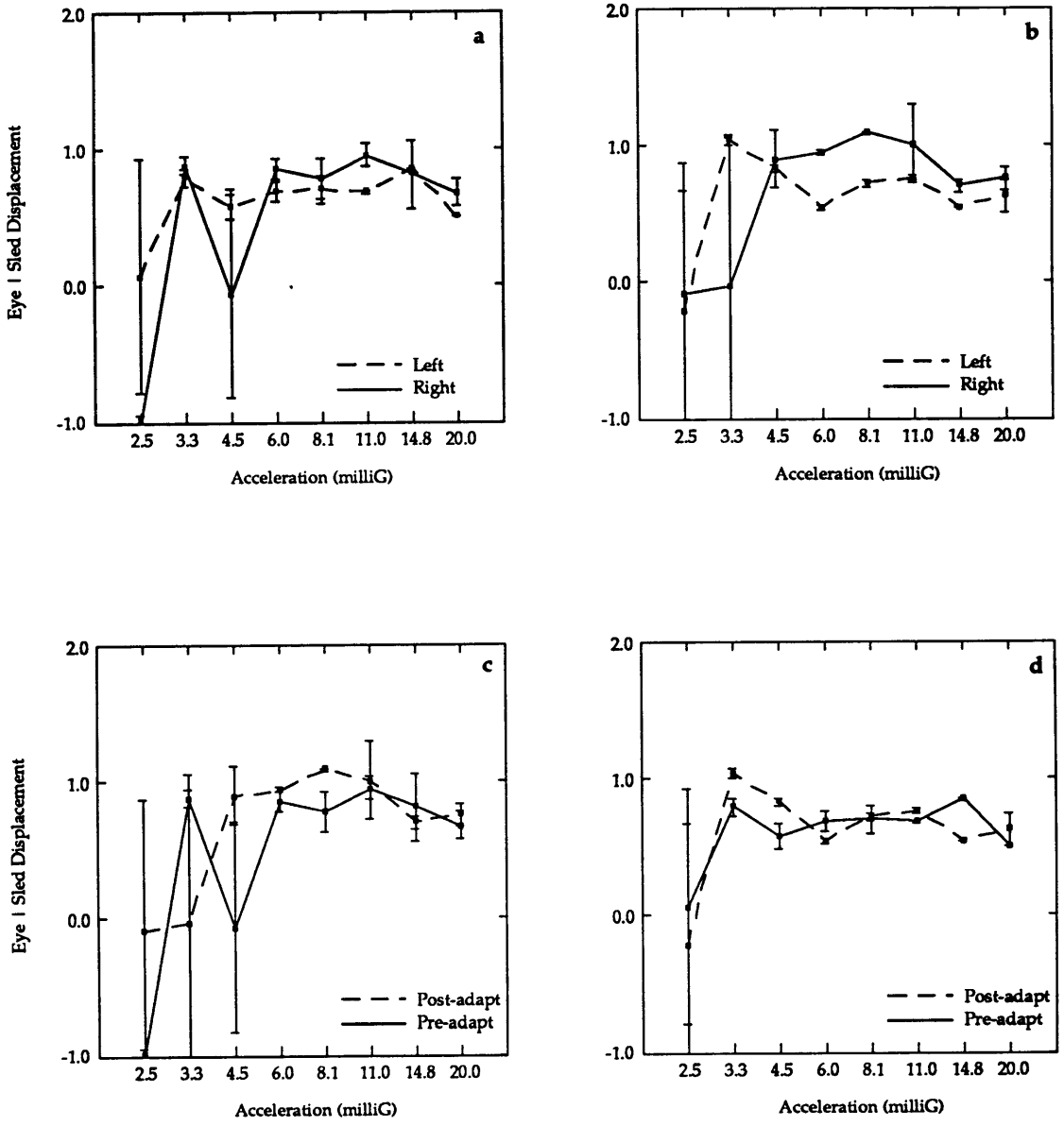

Figure E.1. Pre-/Post Adaptation Hidden Target Pursuit eye movement data for subject CL. a) rightward and leftward pre-adaptation trials, (b) rightward and leftward post-adaptation trials, (c) pre- and post-adaptation rightward trials, (d) pre- and post-adaptation leftward. Error bars signify standard error.

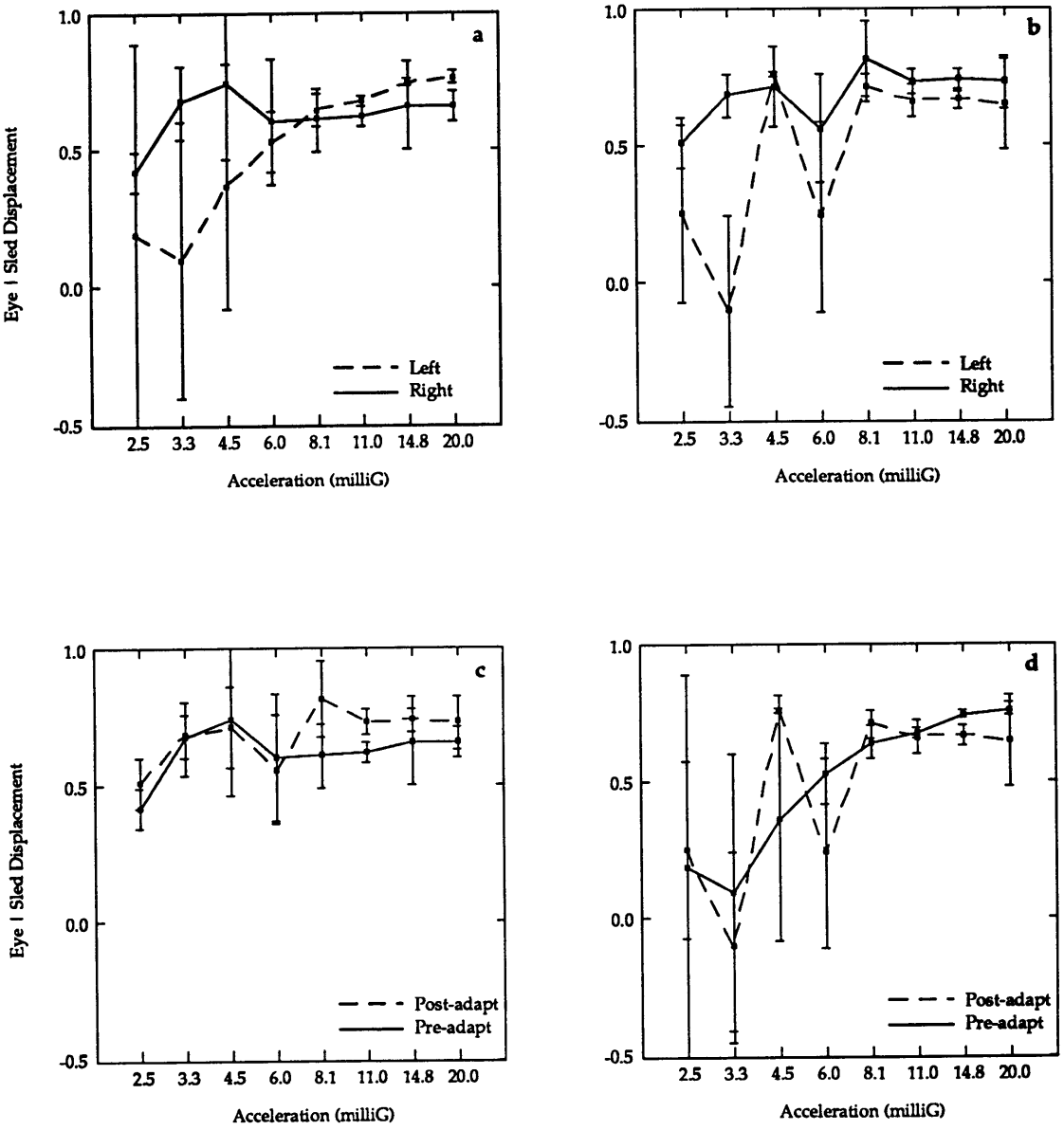

Figure E.1. Pre-/Post Adaptation Hidden Target Pursuit eye movement data for subject DM. a) rightward and leftward pre-adaptation trials, (b) rightward and leftward post-adaptation trials, (c) pre- and post-adaptation rightward trials, (d) pre- and post-adaptation leftward. Error bars signify standard error.

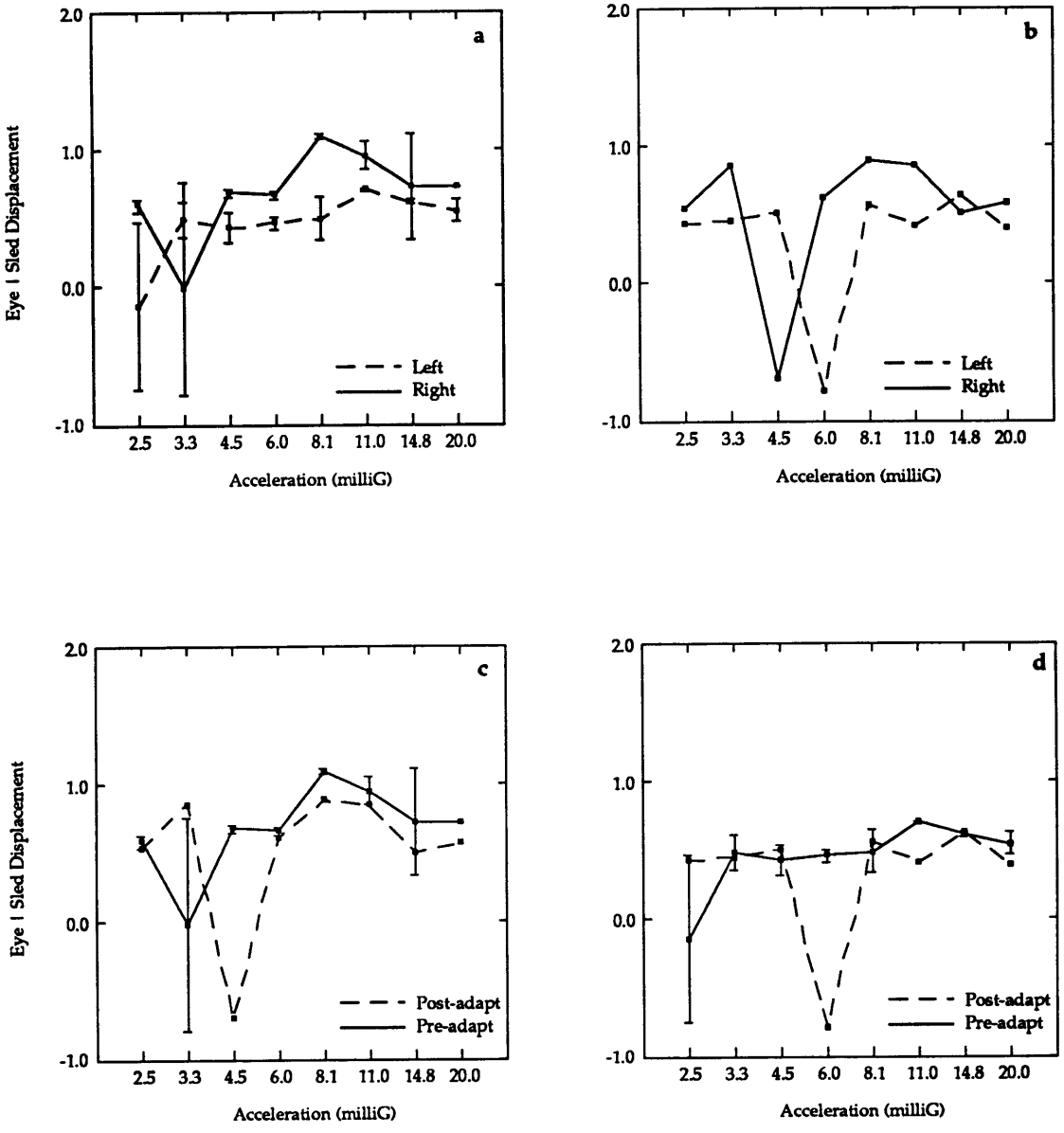

Figure E.1. Pre-/Post Adaptation Hidden Target Pursuit eye movement data for subject KJ. a) rightward and leftward pre-adaptation trials, (b) rightward and leftward post-adaptation trials, (c) pre- and post-adaptation rightward trials, (d) pre- and post-adaptation leftward. Error bars signify standard error.

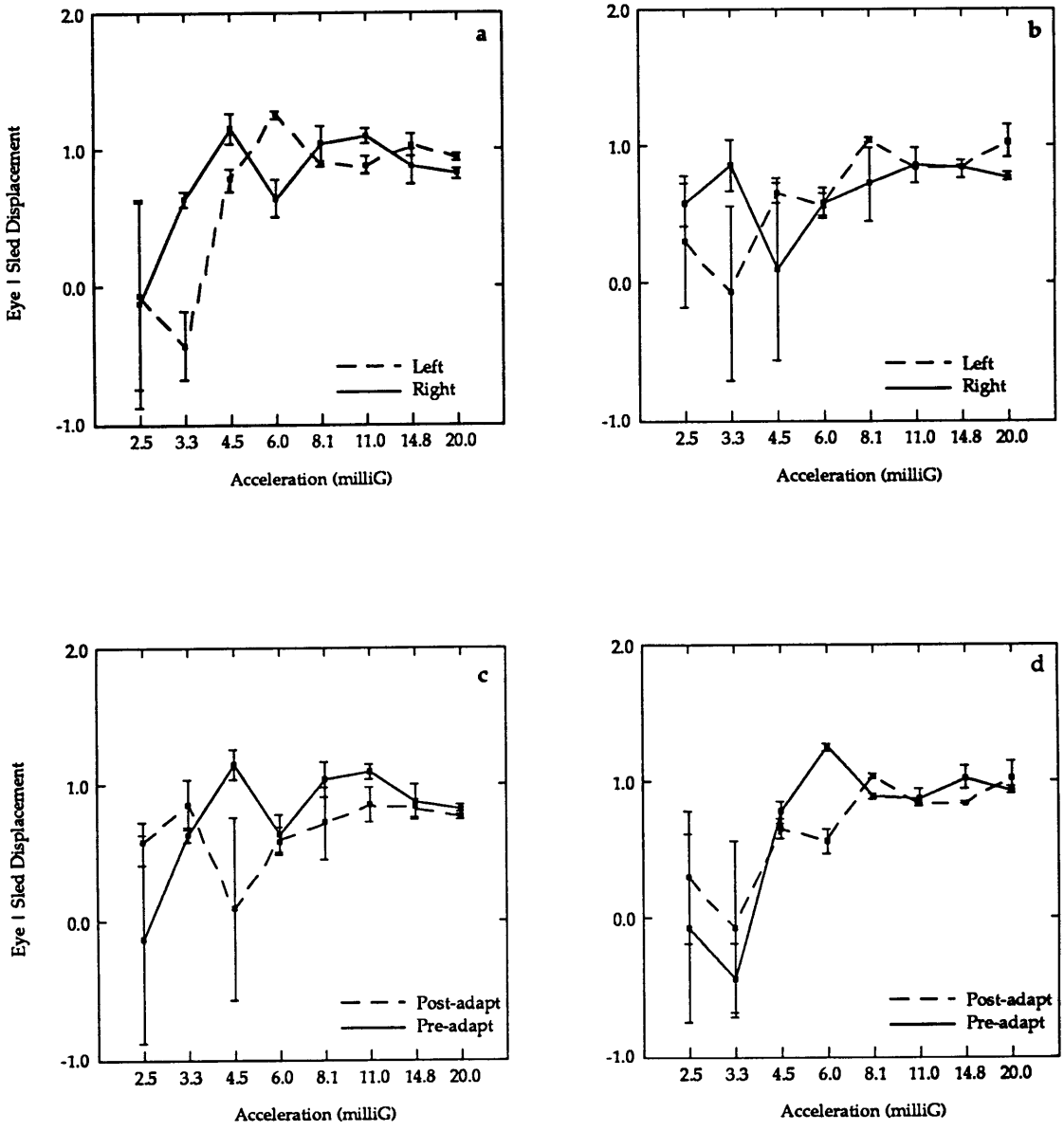

Figure E.1. Pre-/Post Adaptation Hidden Target Pursuit eye movement data for subject MB. a) rightward and leftward pre-adaptation trials, (b) rightward and leftward post-adaptation trials, (c) pre- and post-adaptation rightward trials, (d) pre- and post-adaptation leftward. Error bars signify standard error.

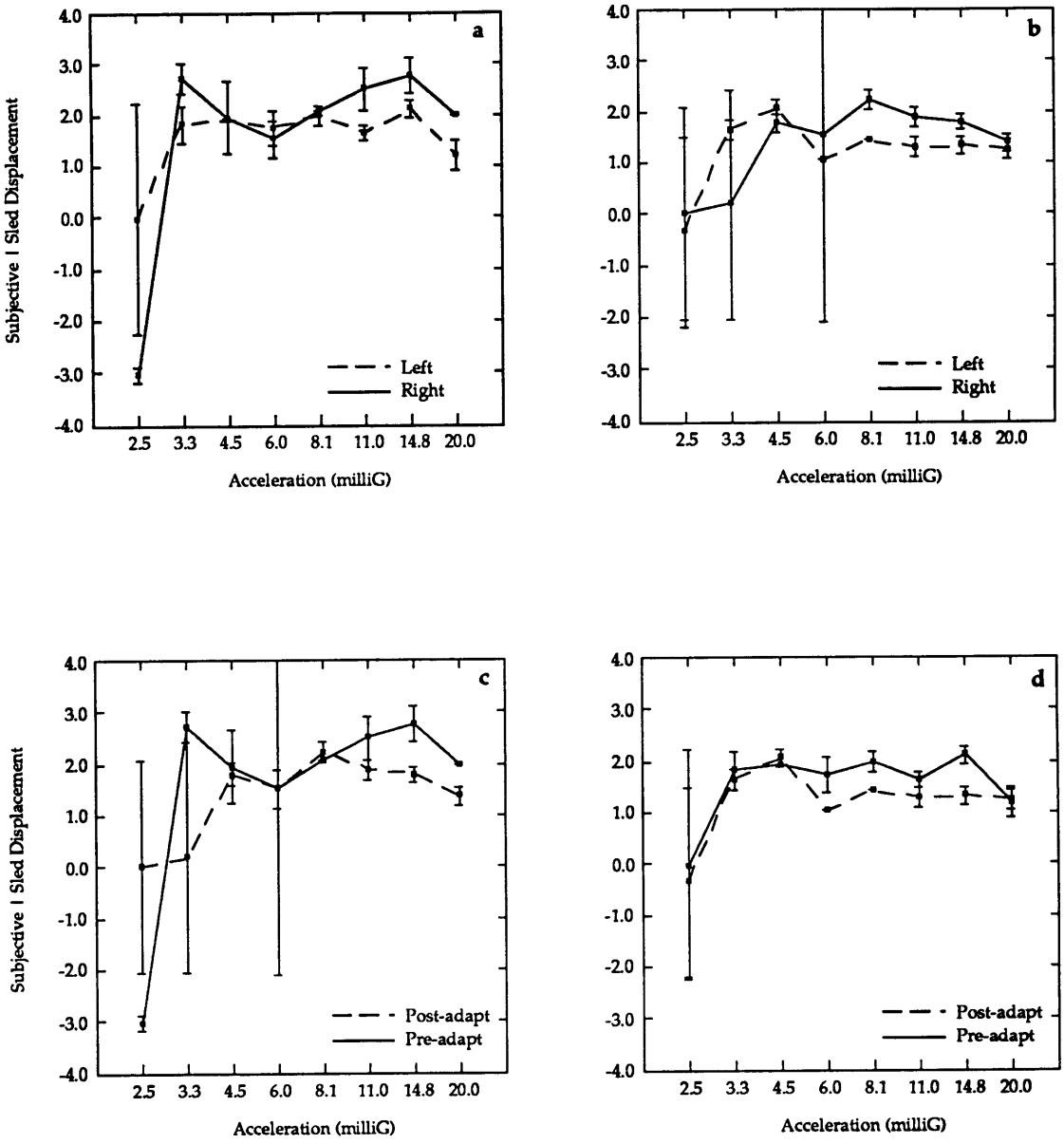

Figure E.2. Mean normalized subjective responses versus sled acceleration for subject CL. (a) rightward and leftward pre-adaptation trials, (b) rightward and leftward post-adaptation trials, (c) pre-adaptation and post-adaptation rightward trials, and (d) pre-adaptation and post-adaptation rightward trials. Error bars indicate standard error.

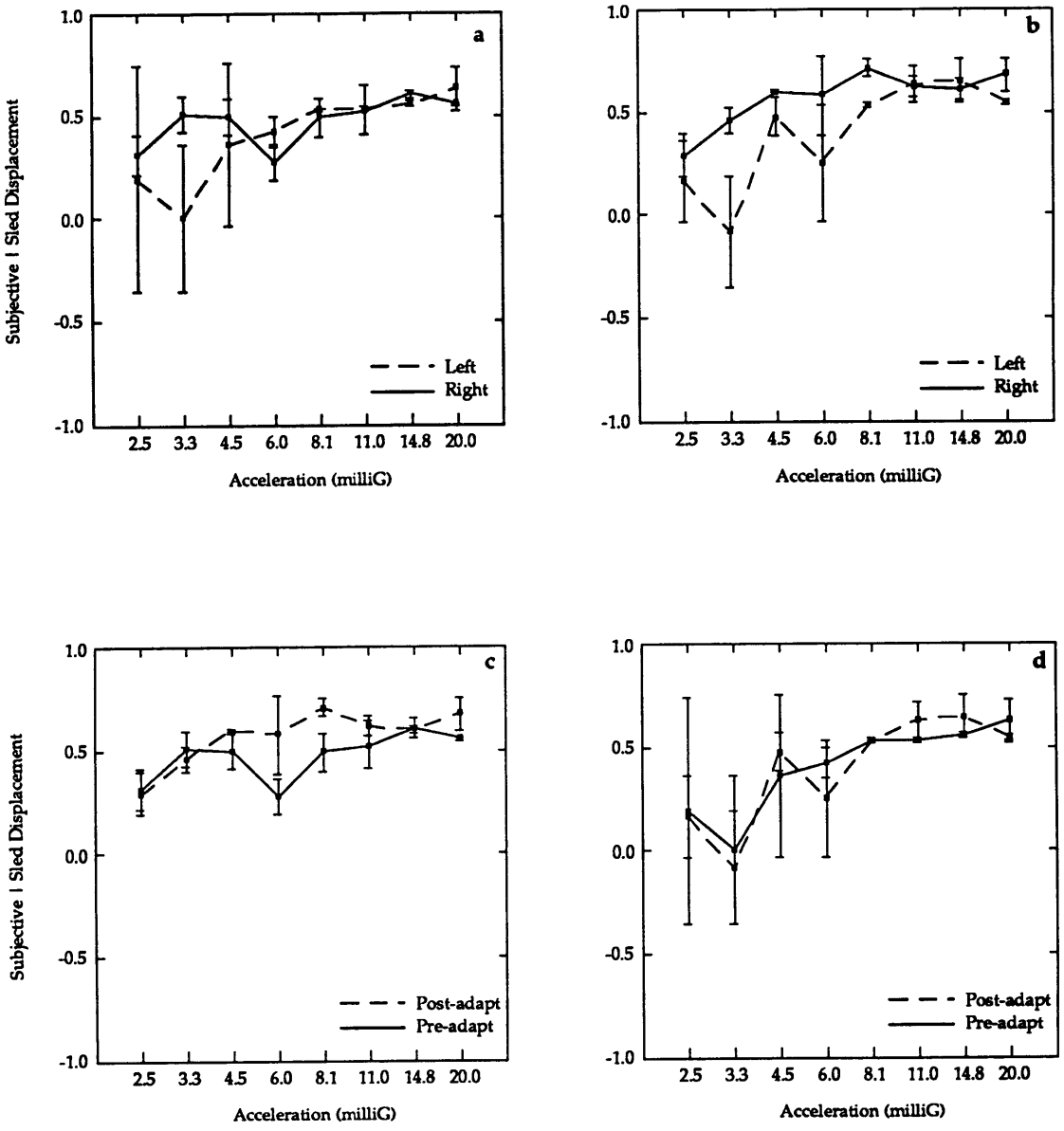

Figure E.2. Mean normalized subjective responses versus sled acceleration for subject DM. (a) rightward and leftward pre-adaptation trials, (b) rightward and leftward post-adaptation trials, (c) pre-adaptation and post-adaptation rightward trials, and (d) pre-adaptation and post-adaptation rightward trials. Error bars indicate standard error.

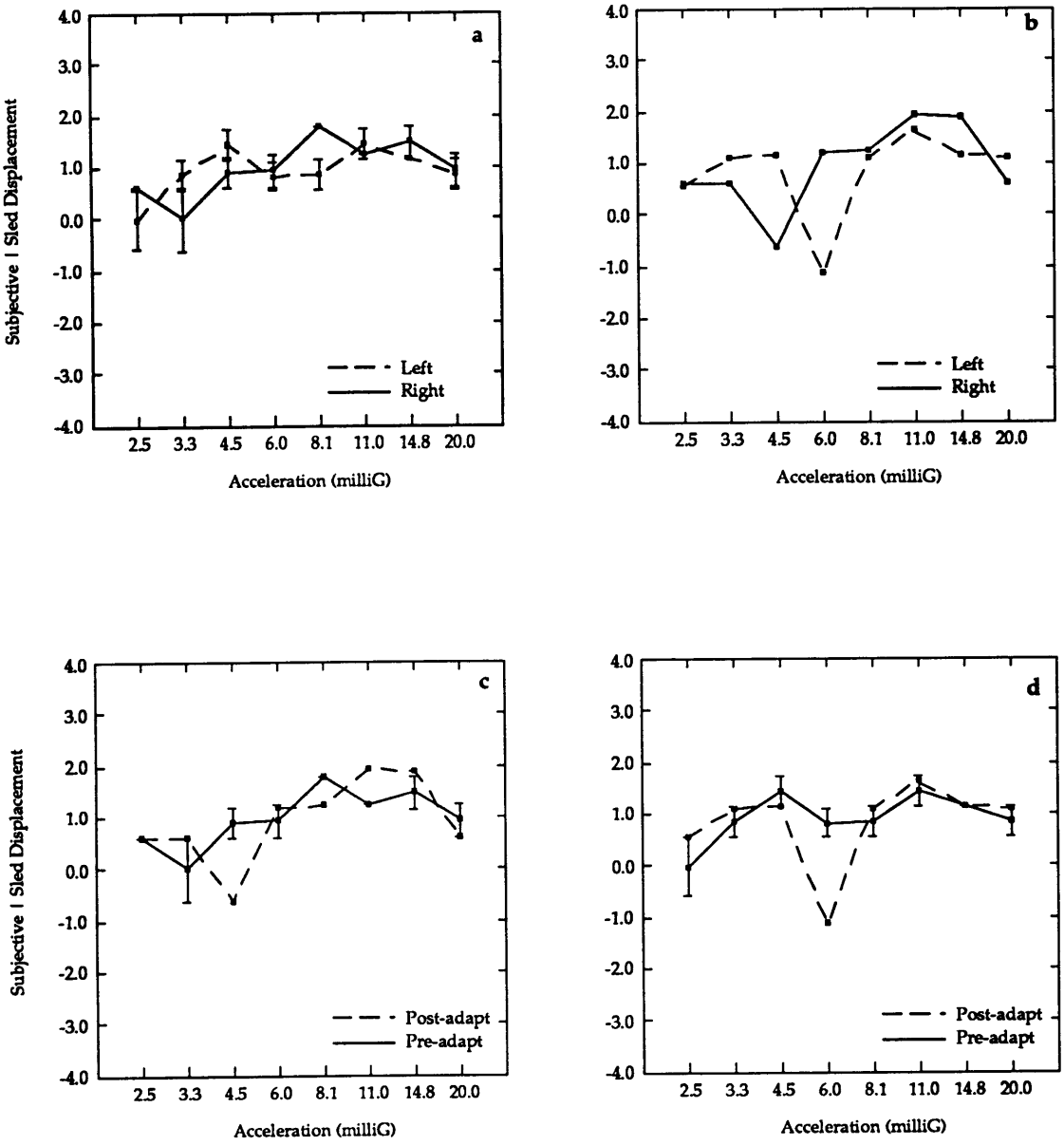

Figure E.2. Mean normalized subjective responses versus sled acceleration for subject KJ. (a) rightward and leftward pre-adaptation trials, (b) rightward and leftward post-adaptation trials, (c) pre-adaptation and post-adaptation rightward trials, and (d) pre-adaptation and post-adaptation rightward trials. Error bars indicate standard error.

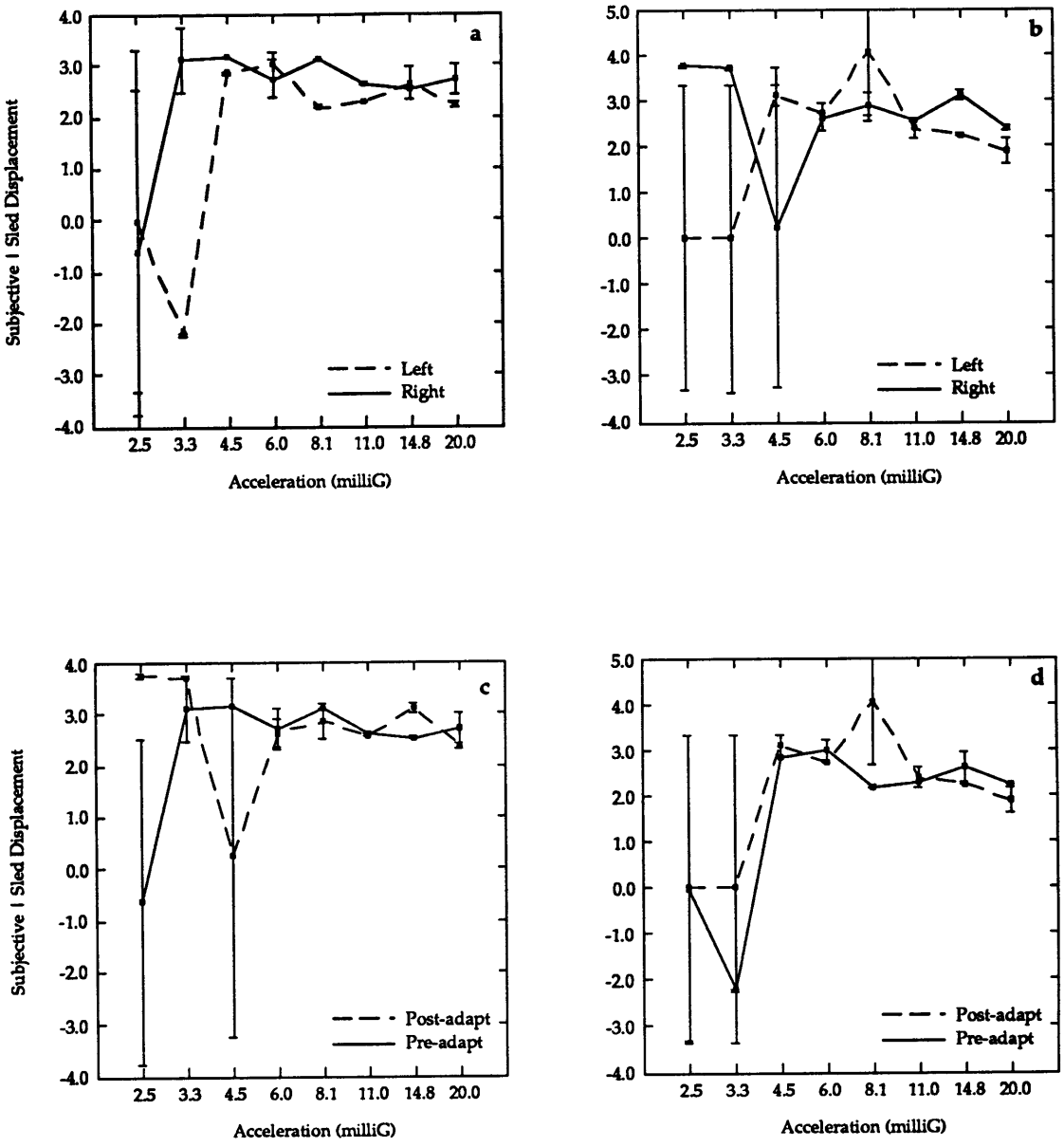

Figure E.2. Mean normalized subjective responses versus sled acceleration for subject MB. (a) rightward and leftward pre-adaptation trials, (b) rightward and leftward post-adaptation trials, (c) pre-adaptation and post-adaptation rightward trials, and (d) pre-adaptation and post-adaptation rightward trials. Error bars indicate standard error.

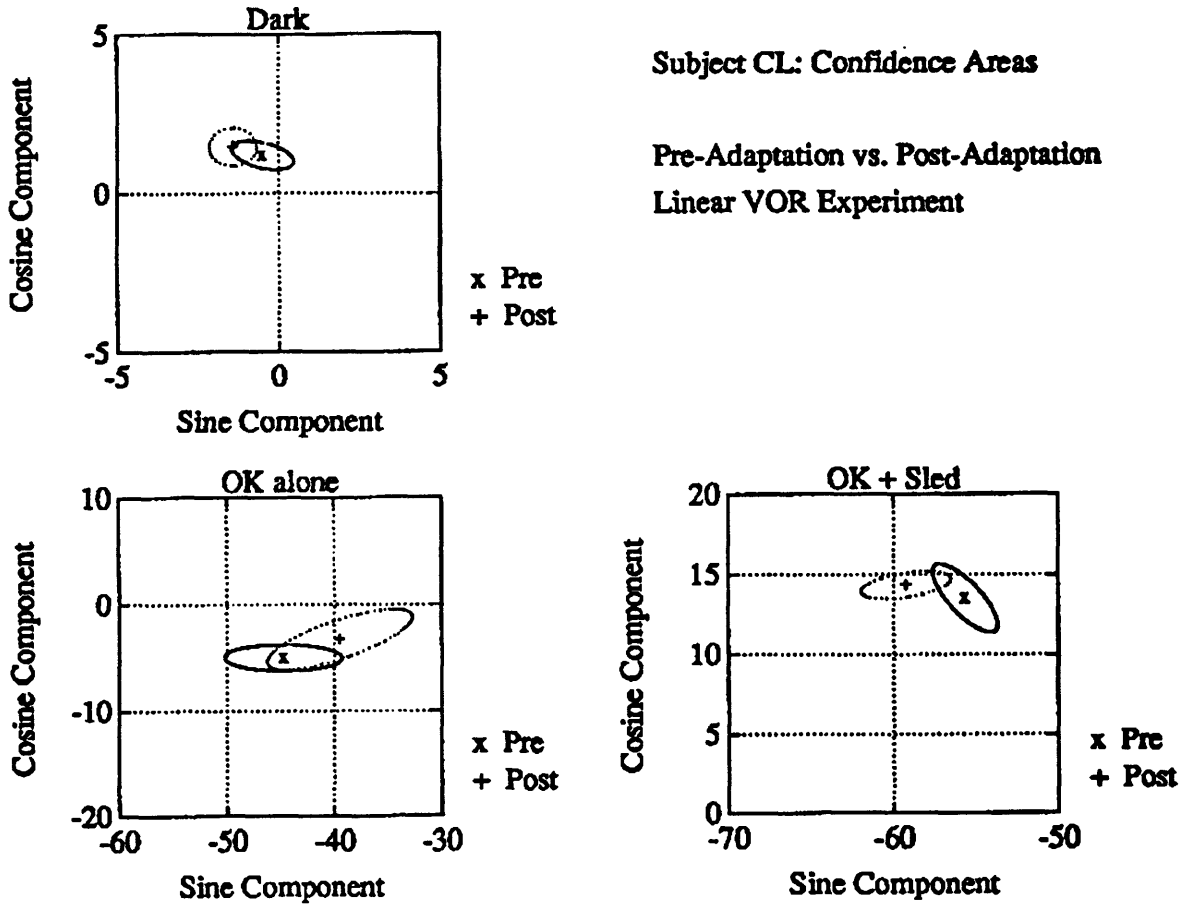

Figure E.3. Plot of confidence areas for linear VOR comparison of pre-/post-adaptation for subject CL. (a) dark run, (b) optokinetic stimulus alone, and (c) optokinetic + sled. Ellipses represent confidence interval about the mean amplitude.

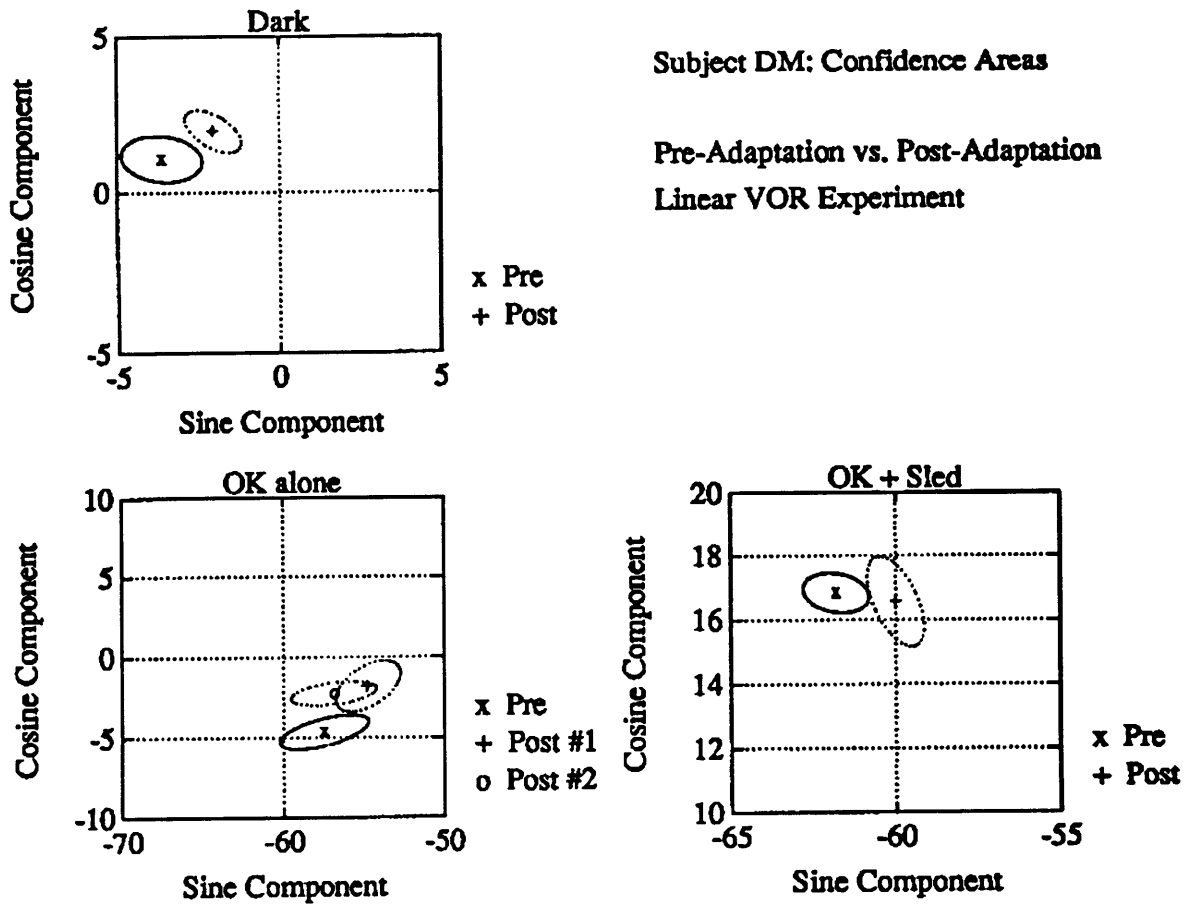

Figure E.3. Plot of confidence areas for linear VOR comparison of pre-/post-adaptation for subject DM. (a) dark run, (b) optokinetic stimulus alone, and (c) optokinetic + sled. Ellipses represent confidence interval about the mean amplitude.

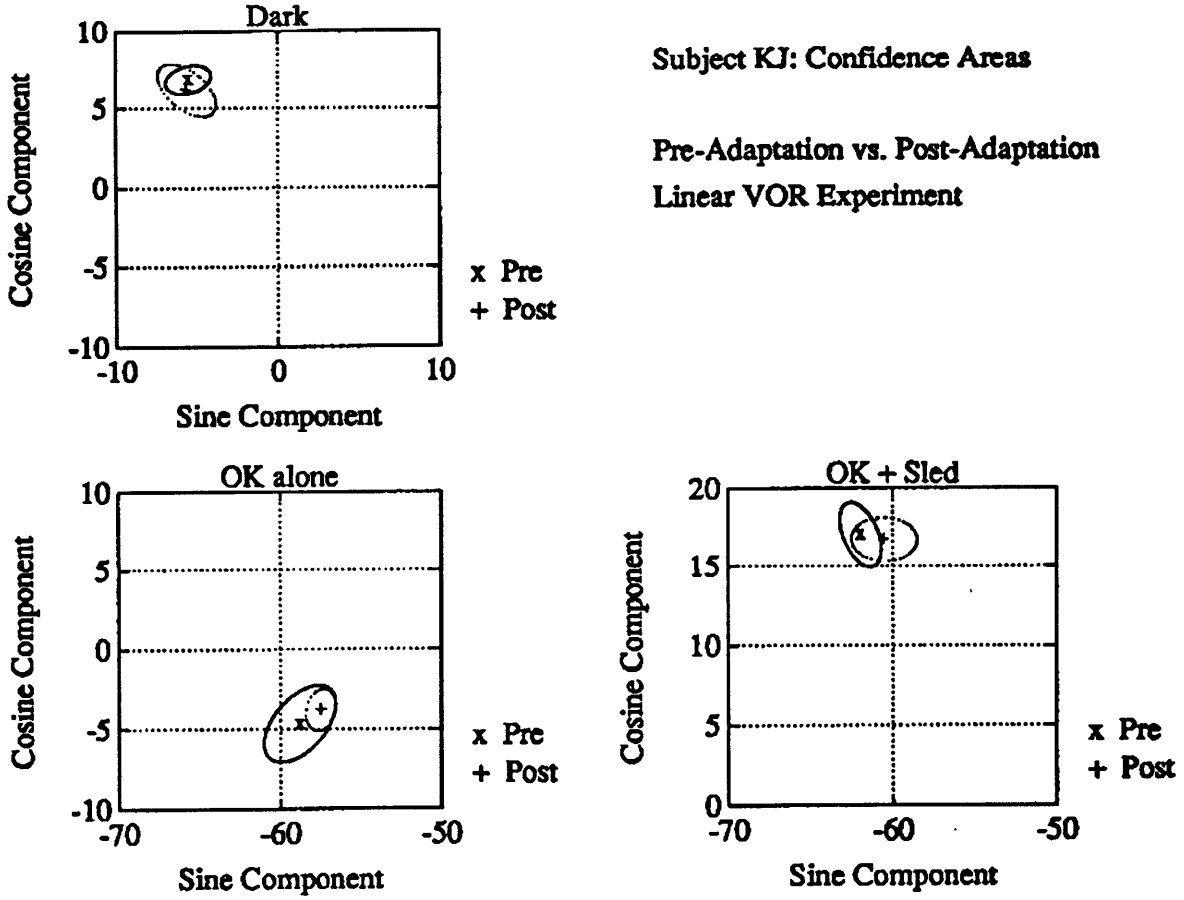

Figure E.3. Plot of confidence areas for linear VOR comparison of pre-/post-adaptation for subject KJ. (a) dark run, (b) optokinetic stimulus alone, and (c) optokinetic + sled. Ellipses represent confidence interval about the mean amplitude.

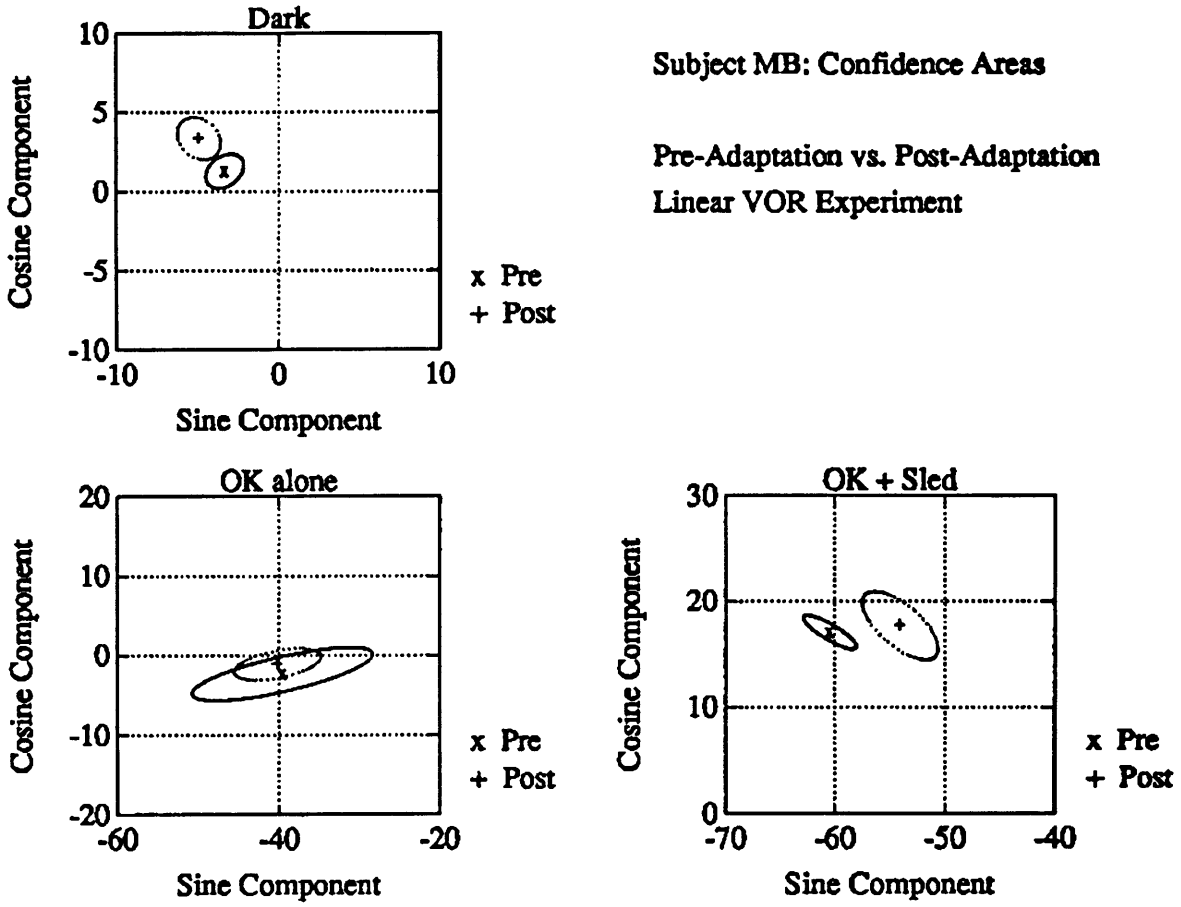

Figure E.3. Plot of confidence areas for linear VOR comparison of pre-/post-adaptation for subject MB. (a) dark run, (b) optokinetic stimulus alone, and (c) optokinetic + sled. Ellipses represent confidence interval about the mean amplitude.

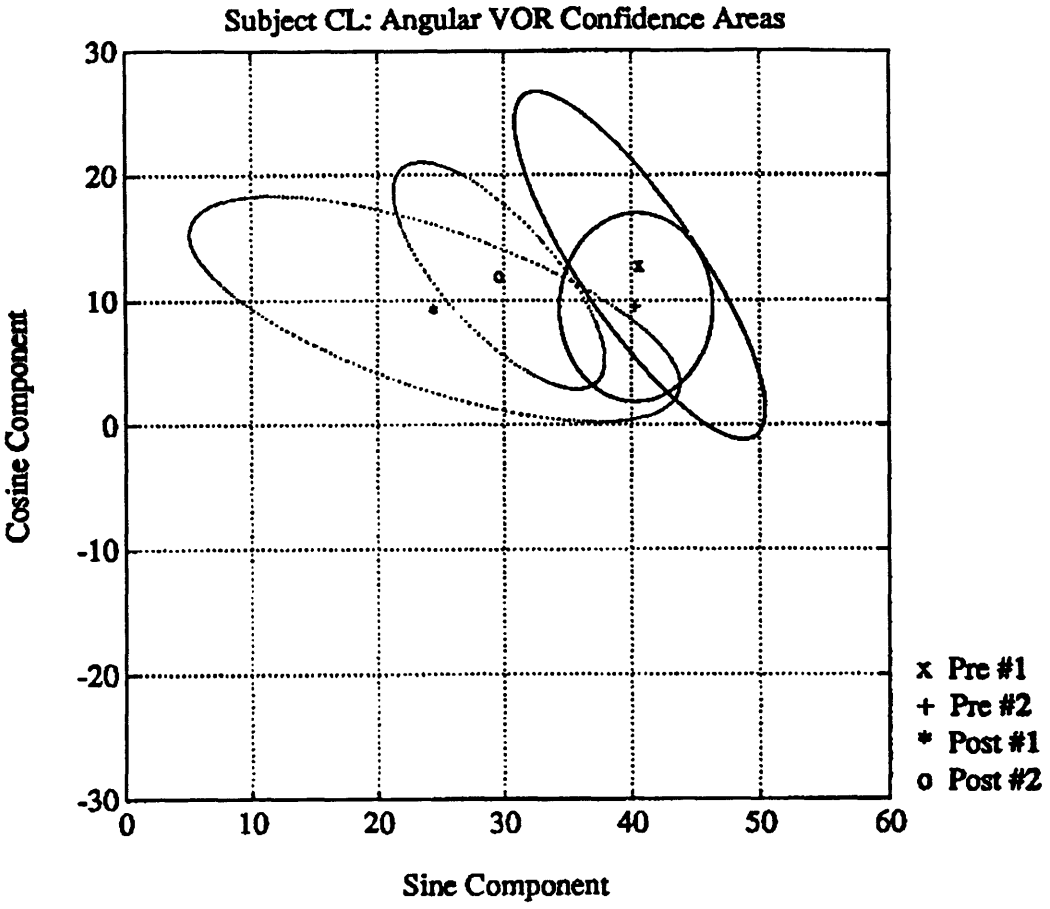

Figure E.4. Plot of confidence areas for angular VOR comparison of pre-/post-adaptation for subject CL. Ellipses represent confidence interval about the mean amplitude.

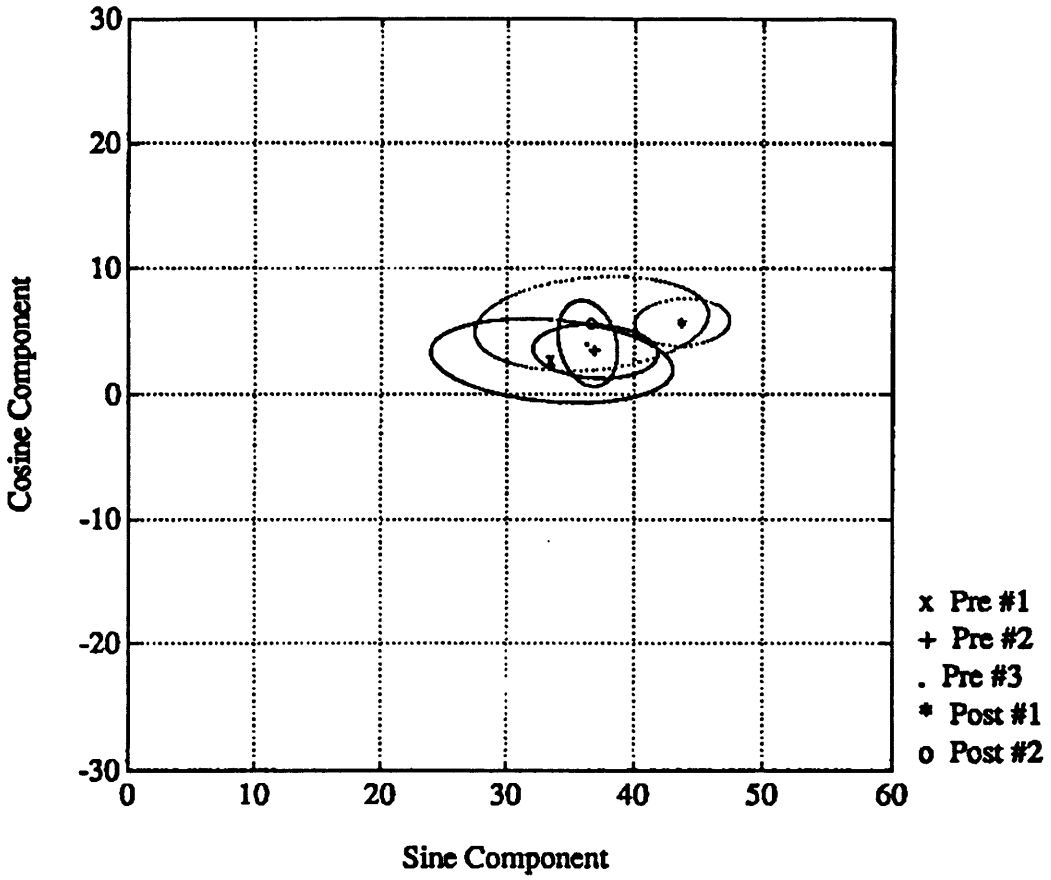

Figure E.4. Plot of confidence areas for angular VOR comparison of pre-/post-adaptation for subject DM. Ellipses represent confidence interval about the mean amplitude.

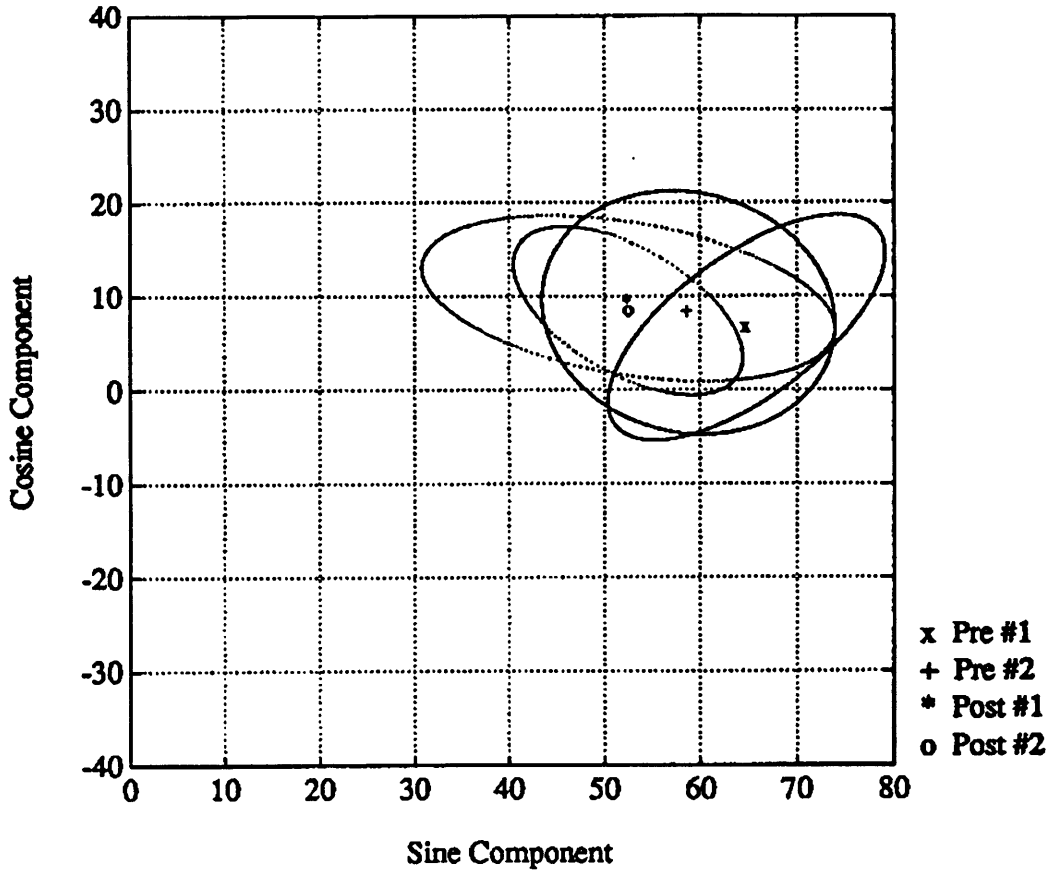

Figure E.4. Plot of confidence areas for angular VOR comparison of pre-/post-adaptation for subject KJ. Ellipses represent confidence interval about the mean amplitude.

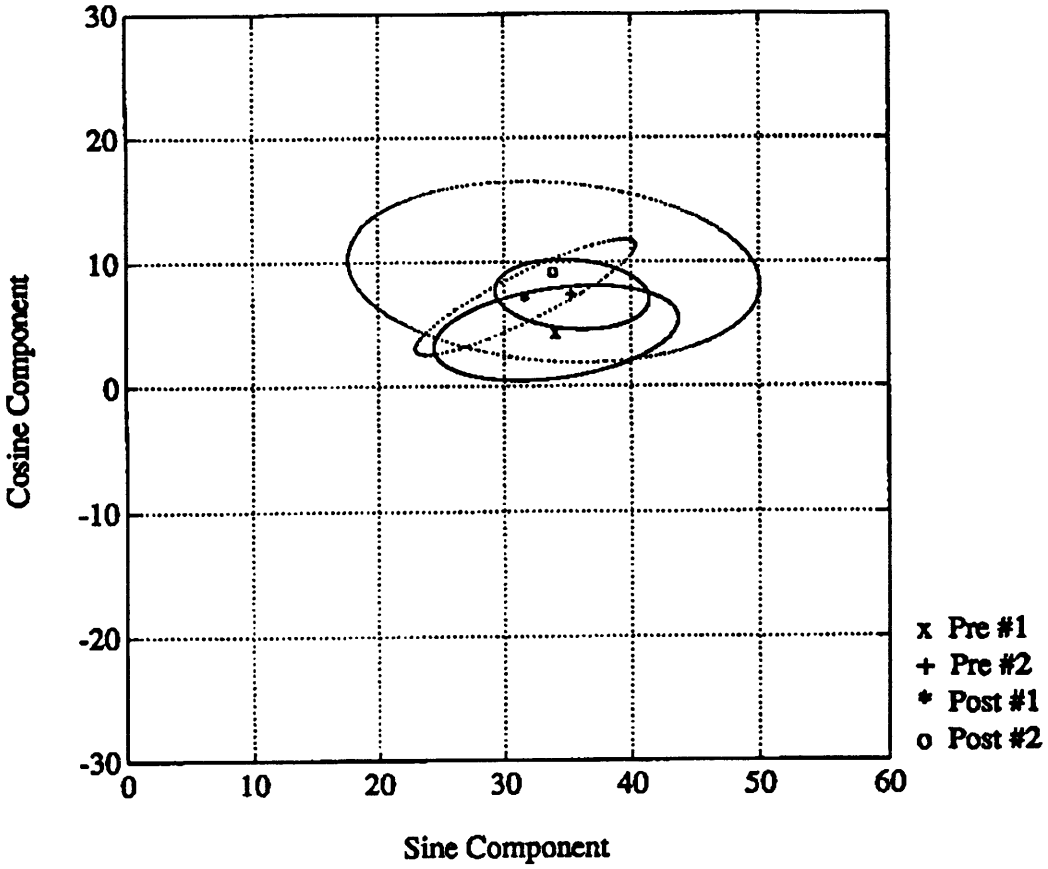

Figure E.4. Plot of confidence areas for angular VOR comparison of pre-/post-adaptation for subject MB. Ellipses represent confidence interval about the mean amplitude.

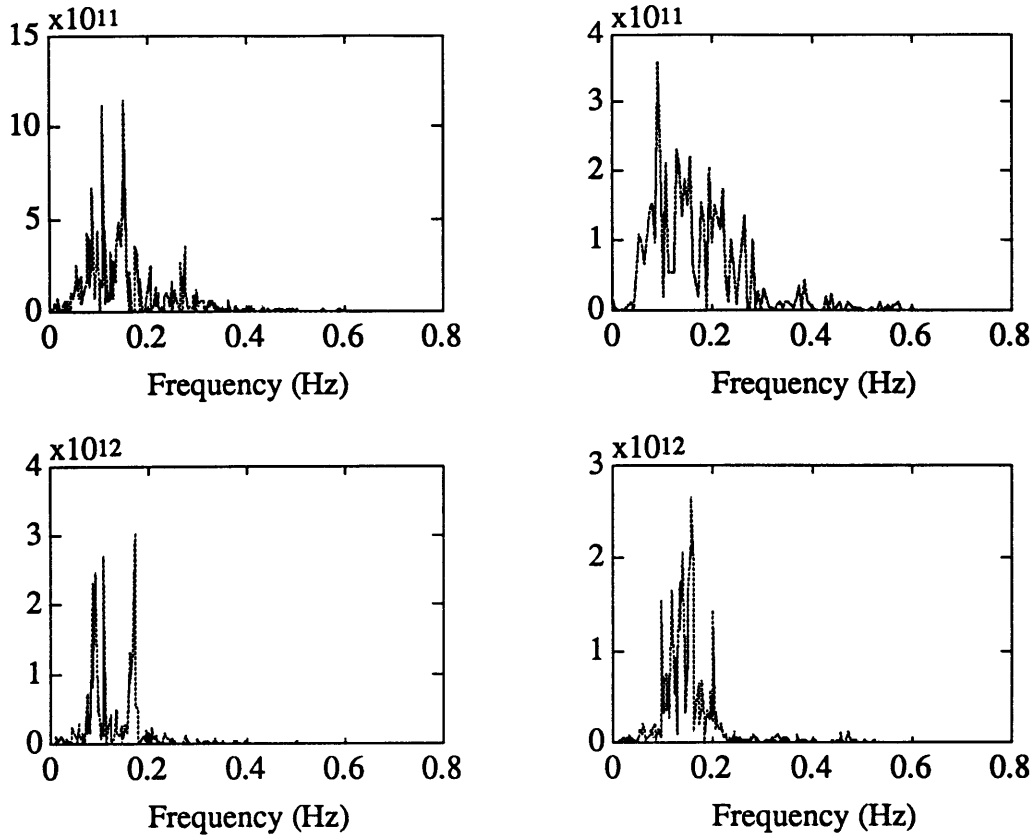

Figure E.5. Power spectral density functions for four segments of subject CL's adaptation paradigm.

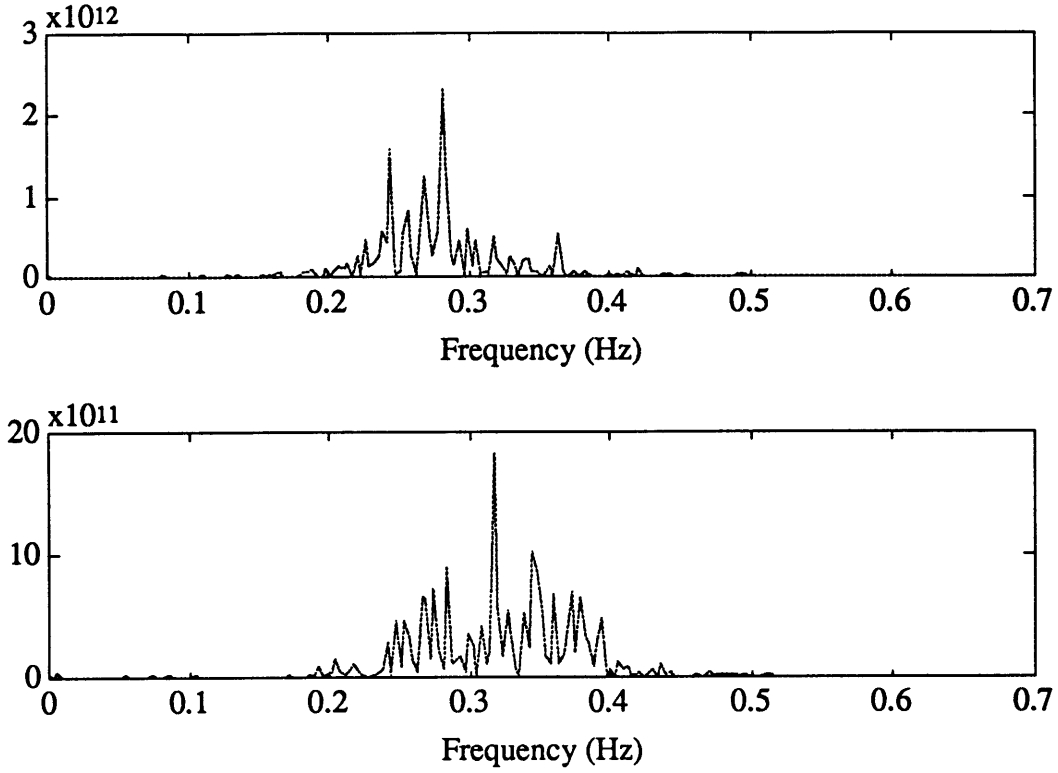

Figure E.5. Power spectral density functions for two segments of subject DM's adaptation paradigm.

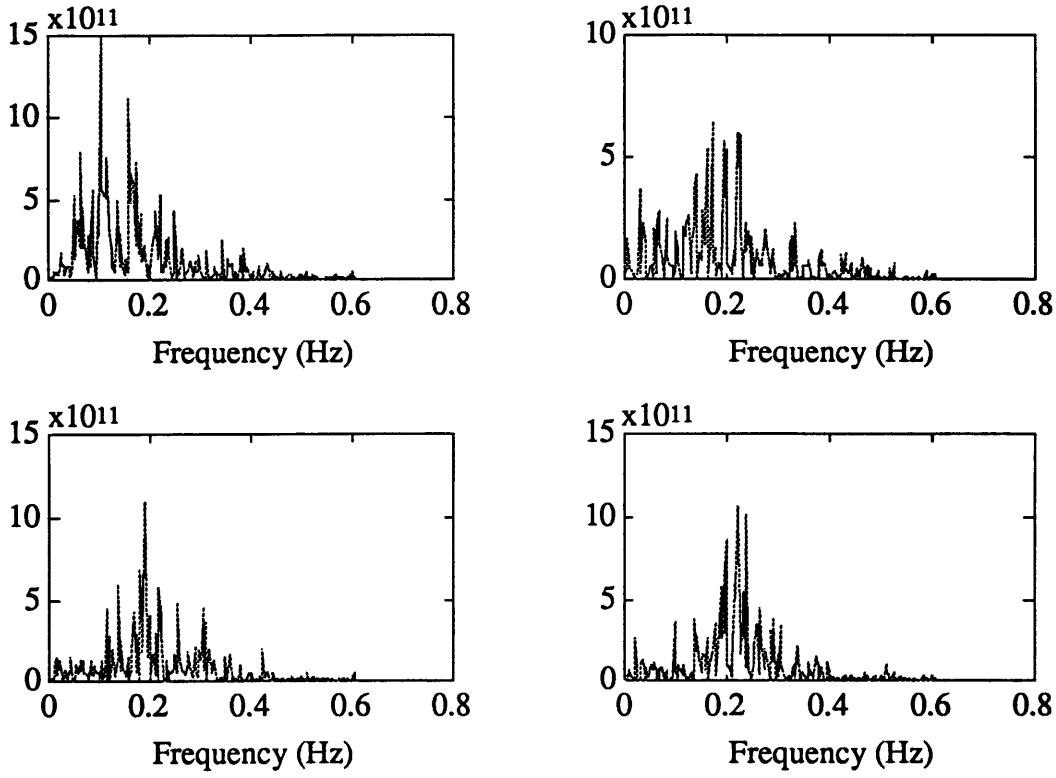

Figure E.5. Power spectral density functions for four segments of subject KJ's adaptation paradigm.

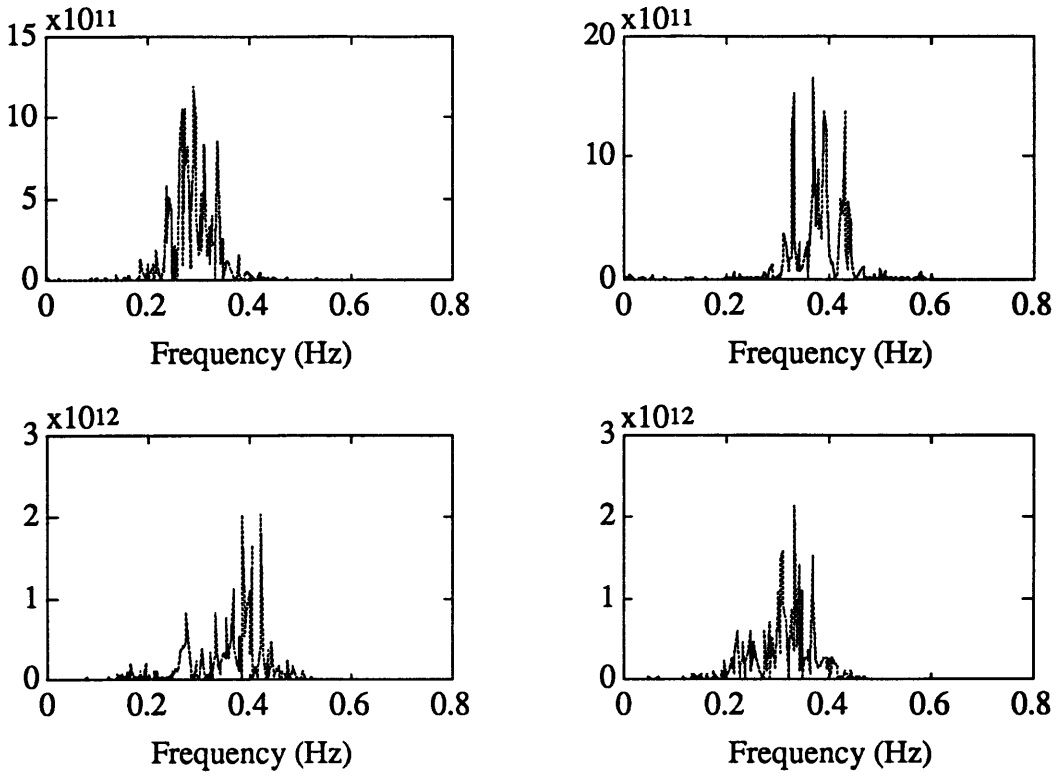

Figure E.5. Power spectral density functions for four segments of subject KJ's adaptation paradigm.

APPENDIX F: DATA ANALYSIS SCRIPTS

This appendix contains the MatLab scripts used for the analysis of the Hidden Target Pursuit data. The following gives a brief description of the function of each program.

Calibrate: Allows the user to obtain a calibration factor in degrees/unit. It assumes a three point calibration in each direction, although the zero is optional. For each axis (horizontal and vertical) the user must specify the angular deviations and select the "flat" regions of the trace which correspond to fixations on the calibration targets.

Calibrate_sled: A modified version of *Calibrate* that allows for the user to obtain a calibration factor in centimeters/unit for the sled position signal.

three_point: Inputs the angular deviations from the user, and calls *pick_regions* so that the fixation regions can be selected. For each deviation, the average value over all of the regions is calculated. The calibration factor for each axis is calculated as the angular difference between the positive and negative deviations (in degrees), divided by the difference between the mean positive and negative deviations (in A/D units). The calculated mean values are displayed to the user graphically, as dotted lines for inspection.

pick_regions: This is the main algorithm for the manual picking of calibration regions and fixation regions during hidden target pursuit. A region is selected by picking its beginning and end with the mouse. A selected region is highlighted by picking within that region. A highlighted region is un-highlighted by picking again within that region. A selected region is de-selected by highlighting it, and then pressing the delete key. The user has complete control over pan and zoom features, as well as selection and de-selection of regions. The plotting makes use of different colors and line types, as available.

Target_Pursuit: This is the main program for the eye movement and sled position analysis. Based on the same concept as *Calibrate*, the user chooses points on the plot where the sled is at rest and the subject is fixating on the visual target. A second point is then chosen after the sled has stopped and the subject is fixating on the imagined target. The magnitude of the eye movement in centimeters and the magnitude of the sled displacement in centimeters is then calculated using the calibration factors found in *Calibrate* and *Calibrate_sled.*

two_point: A modified version of three_point that is used for calculation of the amplitudes of the eye movements and sled displacements during the Hidden Target Pursuit experiment. Calls *pick_regions* so that the fixation regions can be selected.

file_specs: Allows the user to specify the data_path and stat_path for the script to read data from and save calculated results to. The # sign is a place-holder for a run code to distinguish between different files; whereas, the remainder of the filename is constant for all run codes.

file_name: Returns the input file name, given the file spec and run code.

Adaptation: Calculates the power spectral density function of the sled signal during the adaptation paradigm and plots it versus frequency.

```
%*****************************************************************
% calibrate
%
% This script allows the user to obtain a calibration factor
% in degrees/unit. It assumes a three point calibration in
% each direction, although the zero is optional. For each axis,
% the user must specify the angular deviations and select the
% "flat" regions of the trace which correspond to fixations on
% the targets.
%
% written by D. Balkwill 11/27/90
% modified by K. Polutchko 6/92
% *****************************************************************

file_specs
colour = 'y';
code = input('Enter Run Code: ','s');
data_file = file_name(Data_File, code);
eval(['load ',data_path,data_file]);

sample = 200;
pos = ADCData(:,2);
pos2 = ADCData(:,3);
clear ADCData
t = (([1:length(pos)] - 1)/sample)';

  fprintf('\nCalibration #1...\n');
  [scale1,noise1,offset1] = three_point(t,pos,colour);
  fprintf('\nAxis#1 scale factor = %6.4f deg/unit\n',scale1);

  fprintf('\nCalibration #2...\n');
  [scale2,noise2,offset2] = three_point(t,pos2,colour);
  fprintf('\nAxis#2 scale factor = %6.4f deg/unit\n',scale2);

eval(['save ',stat_path,code,'.cal scale1 offset1 scale2 offset2']);

clear nysa_path code A B sample dim t pos pos2 cal_file
clear scale1 noise1 offset1 scale2 noise2 offset2
clear data_path stat_path data_file
```

```
% ****************************************************************
% calibrate_sled
%
% This script allows the user to obtain a calibration factor
% in centimeters/unit. It assumes a three point calibration in
% each direction, although the zero is optional. For each axis,
% the user must specify the linear deviations and select the
% "flat" regions of the trace which correspond to when the sled
% is still.
%
% written by D. Balkwill 11/27/90
% modified by K. Polutchko 6/92
% ****************************************************************

file_specs
colour = 'y';
code = input('Enter Run Code: ','s');
data_file = file_name(Data_File, code);
eval(['load ',data_path,data_file]);

sample = 200;
pos = ADCData(:,1);
%pos2 = ADCData(:,3);
clear ADCData
t = (([1:length(pos)] - 1)/sample)';

  fprintf('\nCalibration #1...\n');
  [scale1,noise1,offset1] = three_point_sled(t,pos,colour);
  fprintf('\nAxis#1 scale factor = %6.4f deg/unit\n',scale1);

  fprintf('\nCalibration #2...\n');
  [scale2,noise2,offset2] = three_point_sled(t,pos,colour);
  fprintf('\nAxis#2 scale factor = %6.4f deg/unit\n',scale2);

eval(['save ',stat_path,code,'.sled scale1 scale2']);

clear nysa_path code A B sample dim t pos pos2 cal_file
clear scale1 noise1 offset1 scale2 noise2 offset2
clear data_path stat_path data_file
```

```
function [scale,noise,offset] = three_point(t,pos,colour)

%*****************************************************************
% This script inputs the angular deviations from the user, and
% calls the 'pick_regions' script so that the fixation regions
% can be selected. For each deviation, the average value over
% all of the regions is calculated. The calibration factor for
% each axis is calculated as the angular difference between the
% positive and negative deviations (in degrees), divided by the
% difference between mean positive and negative deviations (in
% arbitrary units). The calculated mean values are displayed
% to the user graphically as dotted lines, for inspection.
%
% If a zero fixation point is specified, it is used to
% determine the offset value.
%
% The noise is estimated by taking the root-mean-square value of
% the fluctuations about all selected regions.
%
% D. Balkwill 11/27/90
%*****************************************************************

pos_deg = input('Specify eye movement in degrees, positive trace deflection: ');
if isempty(pos_deg)
  disp('  Default calibration target assumed to be 10 degrees.');
  pos_deg = 10;
end
neg_deg = input('Eye displacement for negative trace deflection: ');
if isempty(neg_deg)
  disp('  Default calibration assumed -10 degrees.');
  neg_deg = -10;
end
if (pos_deg == neg_deg)
  disp('Calibration range cannot be zero, Symmetrical calibration assumed.');
  neg_deg = -1 * pos_deg;
end

% select positive trace deflection regions
disp('');
disp('Use mouse to select flat-top regions of positive trace deflection.');
pos_regions = pick_regions(t,pos,colour);
[m,n] = size(pos_regions);
if (m == 0)
  error('No positive trace deflection flat-top regions, Cannot calibrate.');
end
for i=1:m
   xpos = [xpos ; pos(pos_regions(i,1):pos_regions(i,2))];
end
mpos = mean(xpos);
hold on
if (colour == 'y')
   plot([t(1),t(length(t))],[mpos,mpos],'r:');
else
   plot([t(1),t(length(t))],[mpos,mpos],':');
```

```
end
hold off

% select negative trace deflection regions
disp('Now select flat-top regions of negative trace deflection.');
neg_regions = pick_regions(t,pos,colour);
[m,n] = size(neg_regions);
if (m == 0)
  error('Cannot calibrate, no negative trace deflections selected.');
end
for i=1:m
   xneg = [xneg ; pos(neg_regions(i,1):neg_regions(i,2))];
end
mneg = mean(xneg);
hold on
if (colour == 'y')
   plot([t(1),t(length(t))],[mneg,mneg],'r:');
else
   plot([t(1),t(length(t))],[mneg,mneg],':');
end
hold off

% calculate scale factor in deg/unit
scale = (pos_deg - neg_deg) ./ (mpos - mneg);

% select optional zero trace deflection regions
y=input('Is there a zero degree calibration target? (y,n) [default = n]  ','s');
if isempty(y)
  y='n';
end
xzero = [];
if y=='y' | y=='Y'
   disp('Select regions in which subject fixated on zero reference.');
   zero_regions = pick_regions(t,pos,colour);
   [m,n] = size(zero_regions);
   if (m == 0)
      offset = 0;
   else
      for i=1:m
         xzero = [xzero ; pos(zero_regions(i,1):zero_regions(i,2))];
      end
      offset = mean(xzero);
      hold on
      if (colour == 'y')
         plot([t(1),t(length(t))],[offset,offset],'r:');
      else
         plot([t(1),t(length(t))],[offset,offset],':');
      end
      hold off
   end
else
   offset = 0;
end
```

```
% display positive and negative mean values
hold on
if (colour == 'y')
   plot([t(1),t(length(t))],[mneg,mneg],'r:');
   plot([t(1),t(length(t))],[mpos,mpos],'r:');
else
   plot([t(1),t(length(t))],[mneg,mneg],':');
   plot([t(1),t(length(t))],[mpos,mpos],':');
end
hold off

% estimate noise, in rms degrees
xpos = xpos - mean(xpos);
xneg = xneg - mean(xneg);
if (isempty(xzero) == 0)
   xzero = xzero - mean(xzero);
end
x = [xpos ; xneg ; xzero ];
noise = scale * sqrt(mean(x.*x))

clear pos_regions neg_regions zero_regions xpos xneg xzero x
clear i m n y neg_deg pos_deg
return;
```

```
function regions = pick_regions(t,pos,colour)

%*************************************************************************
% This is the main algorithm for the manual picking of
% calibration regions
%    t     = time coordinate, equally spaced at sampling period
%    pos   = eye position vector
%    colour = flag for colour monitor
%
% A region is selected by picking its beginning and end with
% the mouse. A selected region is highlighted by picking within
% that region. A highlighted region is un-highlighted by
% picking again withing that region. A selected region is
% de-selected by highlighting it, and then pressing the delete
% key.
%
% The user has complete control over pan and zoom features, as
% well as selection and de-selection of regions. The plotting
% makes use of different colours and line types, as available.
%
% D. Balkwill  11/27/90
%*************************************************************************

l = length(pos);
sample = round(1/(t(2) - t(1)));   % assumes t is periodic

key = 0;
FINISHED = 27;    % escape
PAN_LEFT = 28;    % left arrow
PAN_RIGHT = 29;   % right arrow
SCROLL_LEFT = 11;  % page down
SCROLL_RIGHT = 12; % page up
DELETE_1 = 8;     % backspace
DELETE_2 = 127;   % delete
ZOOM_IN = 30;     % up arrow
ZOOM_OUT = 31;    % down arrow
FAST_ZOOM_IN = 46;  % decimal
FAST_ZOOM_OUT = 48;  % zero
COMPLETE_PLOT_1 = 97; % 'a' key
COMPLETE_PLOT_2 = 65; % 'A' key
% note: 1, 2, and 3 are reserved for mouse button(s)

num_pick = 0;   % number of points picked
num_regions = 0; % number of regions picked
num_highs = 0;   % number of regions highlighted
os = 1;         % offset of start of current trace, in samples
w = l - 1;      % width of trace, in samples
redraw = 1;     % flag for plotting
mf = 1;         % magnification factor

while (key ~= FINISHED)

   if (redraw == 1)
```

```
    df = floor(w/2000);
    if (df < 1)
       df = 1;
    end
    tr = t(os:df:os+w);
    pr = pos(os:df:os+w);

% leave some blank space above and below trace for aesthetics
    mx = max(pr);
    if (mx < 0)
       mx = mx * 0.9;
    else
       mx = mx * 1.1;
    end
    mn = min(pr);
    if (mn < 0)
       mn = mn * 1.1;
    else
       mn = mn * 0.9;
    end

    hold off
    axis([tr(1) tr(length(tr)) mn mx]);
    if (colour == 'y')

       % plot eye position signal in black, solid
       plot(tr,pr,'w')

       % plot picked regions in blue, dash-dotted
       hold on
       for i=1:num_regions
          t3 = (regions(i,1) - 1)/sample;
          plot([t3,t3],[mn,mx],'b-.')
          t4 = (regions(i,2) - 1)/sample;
          plot([t4,t4],[mn,mx],'b-.')
          plot([t3,t4],[mn,mx],'b-.')
       end
       % plot currently picked point in blue, dotted
       if (num_pick == 1)
          plot([t1,t1],[mn,mx],'b:')
       end

       % plot highlighted regions in green, solid
       for i=1:num_highs
          t3 = (highs(i,1) - 1)/sample;
          plot([t3,t3],[mn,mx],'g')
          t4 = (highs(i,2) - 1)/sample;
          plot([t4,t4],[mn,mx],'g')
          plot([t3,t4],[mn,mx],'g')
       end

    else

       % plot eye position signal in solid
```

```
      plot(tr,pr,'-')

      % plot picked regions in dash-dotted
      hold on
      for i=1:num_regions
         t3 = (regions(i,1) - 1)/sample;
         plot([t3,t3],[mn,mx],'-.')
         t4 = (regions(i,2) - 1)/sample;
         plot([t4,t4],[mn,mx],'-.')
         plot([t3,t4],[mn,mx],'-.')
      end
      % plot currently picked point in dotted
      if (num_pick == 1)
         plot([t1,t1],[mn,mx],':')
      end

      % plot highlighted regions in dashed
      for i=1:num_highs
         t3 = (highs(i,1) - 1)/sample;
         plot([t3,t3],[mn,mx],'--')
         t4 = (highs(i,2) - 1)/sample;
         plot([t4,t4],[mn,mx],'--')
         plot([t3,t4],[mn,mx],'--')
      end
   end

   text(.7,.93,['magnification = ',int2str(round(mf)),' X'],'sc')
   redraw = 0;

end

[x,y,key] = ginput(1);

if (key==ZOOM_IN)      % increase magnification factor

   old=mf;
   mf=min(old*2,max(old,floor(l/100)));
   if mf==old     % maximum magnification of 100X
      redraw=0;
   else
      redraw=1;
      w=floor(l/mf);
   end

elseif (key == FAST_ZOOM_IN)    % fast two-point zoom

   % first point of region to zoom into
   [t3,y,key] = ginput(1);
   if ((key ~= DELETE_1) & (key ~= DELETE_2))

      % bounds check on first point of region
      if (t3 < tr(1))
         t3 = tr(1);
      elseif (t3 > tr(length(tr)))
```

```
    t3 = tr(length(tr));
  end
  x3 = 1 + round(t3 * sample);
  t3 = (x3 - 1)/sample;

  % display first point
  hold on
  if (colour == 'y')
    plot([t3,t3],[mn,mx],'r:');
  else
    plot([t3,t3],[mn,mx],':');
  end
  hold off
  redraw = 1;

  % second point of region to zoom into
  [t4,y,key] = ginput(1);

  % allow user to abort zoom via delete key
  if ((key ~= DELETE_1) & (key ~= DELETE_2))

    % bounds check on second point of region
    if (t4 < tr(1))
      t4 = tr(1);
    elseif (t4 > tr(length(tr)))
      t4 = tr(length(tr));
    end
    x4 = 1 + round(t4 * sample);
    t4 = (x4 - 1)/sample;

    % display second point
    hold on
    if (colour == 'y')
      plot([t4,t4],[mn,mx],'r:');
    else
      plot([t4,t4],[mn,mx],':');
    end
    hold off

    % swap order of points if needed
    if (x4 < x3)
      old = x4;
      x4 = x3;
      x3 = old;
    end

    % calculate new magnification parameters
    if (x3 ~= x4)
      os = x3;
      w = x4 - x3;
      mf = l/w;
    end
  end
end
```

```
  elseif (key==ZOOM_OUT)  % decrease magnification

    if (mf == 1)  % already completely zoomed out
      redraw = 0;
    else
      redraw=1;
      old=mf;
      mf=max(floor(old/2),1);
      w=floor(l/mf);
      if (w >= l)
        w = l - 1;
      end
      if ((os+w)>l)
        os=floor(max(1,l-w));
      end
    end

  elseif ((key == COMPLETE_PLOT_1) | (key == COMPLETE_PLOT_2) | (key ==
FAST_ZOOM_OUT))  % display entire plot

    os = 1;
    mf = 1;
    w = l - 1;
    redraw = 1;

  elseif (key==PAN_RIGHT)  % increase offset by quarter-screen

    old=os;
    os=floor(max(1,min(l-w,os+0.25*w)));
    if old==os      % already panned to end
      redraw=0;
    else
      redraw=1;
    end

  elseif (key==PAN_LEFT)  % decrease offset by quarter-screen

    old=os;
    os=floor(max(1,os-0.25*w));
    if os==old      % already panned to beginning
      redraw=0;
    else
      redraw=1;
    end

  elseif (key==SCROLL_RIGHT)  % jump display one screenful right

    old=os;
    os=floor(max(1,min(os+w,l-w)));
    if os==old      % already panned to end
      redraw=0;
    else
      redraw=1;
```

```
   end

elseif (key==SCROLL_LEFT)  % jump display one screenful left

   old=os;
   os=floor(max(1,os-w));
   if old==os      % already panned to beginning
      redraw=0;
   else
      redraw=1;
   end

elseif ((key==DELETE_1) | (key==DELETE_2))

   if (num_pick > 0)  % wipe out currently picked point
      num_pick = 0;
      redraw = 1;
   elseif (num_highs > 0)  % wipe out highlit regions
      for i=1:num_highs
         index = InList(highs(i,1),regions);
         regions = DeleteRow(index,regions);
      end
      num_regions = num_regions - num_highs;
      num_highs = 0;
      clear highs
      redraw = 1;
   end

elseif (key==1) | (key==2) | (key==3)   % up to three-button mouse input

   if (num_pick == 0)  % this is the first picked point

      % bounds check on picked point
      if (x < tr(1))
         x = tr(1);
      elseif (x > tr(length(tr)))
         x = tr(length(tr));
      end

      % convert time value to sample number
      x1 = 1 + round(x * sample);

      % see if point is in a selected region
      index1 = InList(x1,regions);
      if (index1 > 0)
         index2 = InList(x1,highs);
         if (index2 > 0)  % de-highlight region
            num_highs = num_highs - 1;
            highs = DeleteRow(index2,highs);
            redraw = 1;
         else  % highlight region for future deletion
            x1 = regions(index1,1);
            x2 = regions(index1,2);
            t1 = (x1 - 1)/sample;
```

```
        t2 = (x2 - 1)/sample;
        num_highs = num_highs + 1;
        highs(num_highs,:) = [x1 x2];
        if (colour == 'y')
          hold on
          plot([t1,t1],[mn,mx],'g');
          plot([t2,t2],[mn,mx],'g');
          plot([t1,t2],[mn,mx],'g');
        else
          hold on
          plot([t1,t1],[mn,mx],'-');
          plot([t2,t2],[mn,mx],'-');
          plot([t1,t2],[mn,mx],'-');
        end
      end
    else  % point is not already in a selected region
      % display as first point of region being selected
      t1 = (x1 - 1)/sample;
      num_pick = 1;
      hold on
      if (colour == 'y')
        plot([t1,t1],[mn,mx],'b:');
      else
        plot([t1,t1],[mn,mx],':');
      end
      hold off
    end
  elseif (num_pick == 1)  % second picked point

    % bounds check on picked point
    if (x < tr(1))
      x = tr(1);
    elseif (x > tr(length(tr)))
      x = tr(length(tr));
    end

    % convert time value to sample number
    x2 = 1 + round(x * sample);
    t2 = (x2 - 1)/sample;

    if (x2 == x1)  % cannot have interval of zero width
      num_pick = 0;
      redraw = 1;
    else
      hold on
      if (colour == 'y')
        plot([t2,t2],[mn,mx],'b:');
      else
        plot([t2,t2],[mn,mx],':');
      end
      if (x2 < x1)   % order picked points
        old = x1;
        x1 = x2;
        x2 = old;
```

```
            old = t1;
            t1 = t2;
            t2 = old;
          end
          num_pick = 0;
          if (colour == 'y')
            plot([t1,t2],[mn,mx],'b:');
          else
            plot([t2,t2],[mn,mx],':');
          end

          % add picked region to list
          num_regions = num_regions + 1;
          regions(num_regions,:) = [x1 x2];
          hold off
        end
      end
    end
end

clear i index index1 index2 t1 t2 x1 x2 x y mn mx mnv sample
clear highs num_highs num_regions old num_pick
clear key redraw os w mf l df pr tr
return;
```

```
%*************************************************************************
% target_pursuit
%
% This script allows the user to obtain the amplitude and direction
% of the horizontal & vertical eye movements, and the sled position
% signal.
%
% K. Polutchko 6/92
%
%*************************************************************************

file_specs
hmag_matrix = [];
hdir_matrix = [];
vmag_matrix = [];
vdir_matrix = [];
sled_matrix = [];
hmag_matrix(1,:) = 0;
hdir_matrix(1,:) = '0';
vmag_matrix(1,:) = 0;
vdir_matrix(1,:) = '0';
sled_matrix(1,:) = 0;


colour = 'y';
code = input('Enter Run Code: ','s');
%file_number = input('Enter the file number (1-2): ');
start_number = input('Enter the trial # at which you wish to start: ');
%if(file_number == 1)
   g_level = [9; 5; 7; 8; 10; 9; 4; 7; 3; 4; 8; 5; 6; 10; 3; 6];
   sled_profile = [-20; +20; -20; -20; +20; +20; -20; +20; -20; +20; 20; -20; +20; -20;
+20; -20];
%end

num_trials = 16;
cal_sled = input('Specify the sled calibration factor (deg/unit): ');
cal_h = input('Specify the horizontal calibration factor (deg/unit): ');
cal_v = input('Specify the vertical calibration factor (deg/unit): ');
data_file = file_name(Data_File, code);
eval(['load ',data_path,data_file]);

sled_pos=ADCData(:,1);
pos = ADCData(:,3);      %h_coil
pos2 = ADCData(:,2);     %v_coil
clear ADCData

sled_pos = sled_pos*cal_sled;
pos2=pos2*cal_v;
pos=pos*cal_h;
sample = 200;
t = (([1:length(pos)] - 1)/sample)';

for i=start_number:num_trials
  fprintf('\nAnalyzing trial number %2.0f \n',i);
```

```
  [mag_deg1,direction1,mag_deg2,direction2,mag_sled] =
two_point(t,pos,pos2,sled_pos,colour,sled_profile(i,:));

fprintf('\nMagnitude of eye movement for trial#%2.0f (HCOIL) = %6.4f deg. %The
direction of the eye movement was: ',i,mag_deg1);
fprintf(direction1);

fprintf('\nMagnitude of eye movement for trial#%2.0f (VCOIL) = %6.4f deg. %The
direction of the eye movement was: ',i,mag_deg2);
fprintf(direction2);

fprintf('\nMagnitude of eye movement for trial#%2.0f (SLED) = %6.4f cm. ',i,mag_sled);

  hmag_matrix(i,:) = mag_deg1;
  hdir_matrix(i,:) = direction1;
  vmag_matrix(i,:) = mag_deg2;
  vdir_matrix(i,:) = direction2;
  sled_matrix(i,:) = mag_sled;
end

eval(['save ',stat_path,code,'.stats g_level sled_profile hmag_matrix hdir_matrix
vmag_matrix vdir_matrix']);

eval(['save ',stat_path,code,'.sled sled_matrix']);

vmag_matrix
vdir_matrix
hmag_matrix
hdir_matrix
sled_matrix

clear_specs
clear code A B sample t pos pos2 pos3 sled_pos sled_file heog_file veog_file i j
clear mag_deg1 mag_deg2 mag_deg3 direction1 direction2 direction3 file_number
clear hmag_matrix hdir_matrix vmag_matrix vdir_matrix sled_profile duration
clear num_trials colour data_path stat_path another start_number
clear cal_heog heog_matrix hedir_matrix

fprintf('Thank you for coming in today! ');
```

```
function [mag_deg1,direction1,mag_deg2,direction2,mag_sled] =
two_point(t,pos,pos2,sled_pos,colour,sled_profile)

%*********************************************************************
%two_point
%
%This script inputs the angular deviations from the user, and
% calls the 'pick_regions2' script so that the fixation regions
% can be selected.  For each deviation, the average value over
% all of the regions is calculated. The calculated mean values
%are displayed to the user graphically as dotted lines, for inspection.
%*********************************************************************

% select flat region during target fixation
disp('');
disp('Use mouse to select flat region during target fixation.');
fix_regions = pick_regions2(t,pos,sled_pos,colour);
[m,n] = size(fix_regions);
if (m == 0)
  error('No flat region found.');
end
for i=1:m
   xfix = [xfix ; pos(fix_regions(i,1):fix_regions(i,2))];
   xfix2 = [xfix2 ; pos2(fix_regions(i,1):fix_regions(i,2))];
   xfix3 = [xfix3 ; sled_pos(fix_regions(i,1):fix_regions(i,2))];
end
mfix = mean(xfix)
mfix2 = mean(xfix2);
mfix3 = mean(xfix3);
%hold on
%if (colour == 'y')
%   subplot(211)
%   plot([t(1),t(length(t))],[mfix,mfix],'r:');
%   subplot(212)
%   plot([t(1),t(length(t))],[mfix,mfix],'r:');
%else
%   subplot(211)
%   plot([t(1),t(length(t))],[mfix,mfix],':');
%   subplot(212)
%   plot([t(1),t(length(t))],[mfix,mfix],':');
%end
%hold off

% select flat region after sled motion has stopped
disp('Now select flat region after sled motion has stopped.');
post_regions = pick_regions2(t,pos,sled_pos,colour);
[m,n] = size(post_regions);
if (m == 0)
  error('No flat region.');
end
for i=1:m
   xpost = [xpost ; pos(post_regions(i,1):post_regions(i,2))];
   xpost2 = [xpost2 ; pos2(post_regions(i,1):post_regions(i,2))];
```

```
   xpost3 = [xpost3 ; sled_pos(post_regions(i,1):post_regions(i,2))];
end
mpost = mean(xpost)
mpost2 = mean(xpost2);
mpost3 = mean(xpost3);
hold on
%if (colour == 'y')
%   subplot(211)
%   plot([t(1),t(length(t))],[mpost,mpost],'r:');
%   subplot(212)
%   plot([t(1),t(length(t))],[mpost,mpost],'r:');
%else
%   subplot(211)
%   plot([t(1),t(length(t))],[mpost,mpost],':');
%   subplot(212)
%   plot([t(1),t(length(t))],[mpost,mpost],':');
%end
%hold off

% calculate magnitude of eye movement
mag_deg1 = mpost - mfix;
mag_deg2 = mpost2 - mfix2;
mag_sled = mpost3 - mfix3;

if(mag_sled <= 0.0)
        sled_dir = 'R';
else
        sled_dir = 'L';
end

if(((mag_deg1 >= 0.0)&(sled_profile >= 0.0))|((mag_deg1 <= 0.0)&(sled_profile <=
0.0)))
         direction1 = 'C';
else
  direction1 = 'I';
end
if(mag_deg2 >= 0.0)
          direction2 = 'R';
else
  direction2 = 'L';
end

clear fix_regions post_regions xfix xpost xfix2 xpost2 xfix3 xpost3
clear mpost mpost2 mpost3
clear i m n y
return;
```

```
%*********************************************************************
%file_specs
%
%Written by David Balkwill 7/1/91
%Modified by Karla Polutchko 5/28/92
%
%*********************************************************************

data_path = ['KP4:KAP_temp'];   %check this
stat_path = ['KP4:sled_stats:'];

Data_File = '#.MAT';

%Ensure that colon is last character in path name, for Mac convention
if (data_path(length(data_path)) ~= ':')
   data_path = [data_path,':'];
end
```

```
%*************************************************************************
%file_name
%
%Written by David Balkwill 9/26/90
%modified by Karla Polutchko 5/28/92
%
%returns the input file name, given the file spec and run code
%
%*************************************************************************

function in_file = file_name(file_spec,code)

in_file = file_spec;
l=length(in_file);

i=1;
while(i<=l)
        if(in_file(i) == '#'
        break;
        end
  i=i+1;
end

if(i==l)
        in_file = [in_file(1:l-1),code];
elseif(i<l)
  in_file = [in_file(1:i-1),code,in_file(i+1:l)];
end

%make sure ther are no blank spaces in the file name
l = length(in_file);
i=1;
while(i<=1)
  if(in_file(i) == ' ')
    in_file = [in_file(1:i-1),in_file(i+1:l)];
    l=l-1;
  else
    i = i+1;
  end
end

clear i l
return;
```

```
%************************************************************
%Adaptation
%
%This script was written to analyze the frequency
%components of the joystick signal of the subject during
%the linear adaptation paradigm
%
%************************************************************
file_specs
code = input('Enter First Run Code: ','s');
data_file = file_name(Data_File, code);
eval(['load ',data_path,data_file]);

joy_stick = ADCData(:,2);
clear ADCData

l = length(joy_stick);
if(l >= 49152)
        last = 65536;
   final_freq = 200;
else
        last = 32768;
   final_freq = 100;
end

Y=fft(joy_stick,last);
Pyy=Y.*conj(Y);
frequency = 200/last*(0:last-1);
title('Subject KJ: Adaptation Power Spectral Density')
subplot(221)
plot(frequency(1:final_freq),Pyy(1:final_freq))
xlabel('Frequency (Hz)')
eval(['save ',stat_path,code,'.PSD Pyy frequency']);
clear joy_stick l Y frequency last final_freq code Pyy

code = input('Enter Second Run Code: ','s');
data_file = file_name(Data_File, code);
eval(['load ',data_path,data_file]);

joy_stick=ADCData(:,2);
clear ADCData

l = length(joy_stick);
if(l >= 49152)
        last = 65536;
   final_freq = 200;
else
        last = 32768;
   final_freq = 100;
end

Y=fft(joy_stick,last);
Pyy=Y.*conj(Y);
```

```
frequency = 200/last*(0:last-1);
subplot(222)
plot(frequency(1:final_freq),Pyy(1:final_freq))
xlabel('Frequency (Hz)')

eval(['save ',stat_path,code,'.PSD Pyy frequency']);
clear joy_stick l Y frequency last final_freq Pyy

code = input('Enter Third Run Code: ','s');
data_file = file_name(Data_File, code);
eval(['load ',data_path,data_file]);

joy_stick=ADCData(:,2);
clear ADCData

l = length(joy_stick);
if(l >= 49152)
        last = 65536;
   final_freq = 200;
else
        last = 32768;
   final_freq = 100;
end

Y=fft(joy_stick,last);
Pyy=Y.*conj(Y);
frequency = 200/last*(0:last-1);
subplot(223)
plot(frequency(1:final_freq),Pyy(1:final_freq))
xlabel('Frequency (Hz)')

eval(['save ',stat_path,code,'.PSD Pyy frequency']);
clear joy_stick l Y frequency last final_freq Pyy

code = input('Enter Fourth Run Code: ','s');
data_file = file_name(Data_File, code);
eval(['load ',data_path,data_file]);

joy_stick=ADCData(:,2);
clear ADCData

l = length(joy_stick);
if(l >= 49152)
        last = 65536;
   final_freq = 200;
else
        last = 32768;
   final_freq = 100;
end

Y=fft(joy_stick,last);
Pyy=Y.*conj(Y);
frequency = 200/last*(0:last-1);
subplot(224)
```

```
plot(frequency(1:final_freq),Pyy(1:final_freq))
xlabel('Frequency (Hz)')

eval(['save ',stat_path,code,'.PSD Pyy frequency']);
clear joy_stick l Y frequency last final_freq Pyy
```

APPENDIX G: SLED TRAJECTORY GENERATORS

This appendix contains the programs written in C++ which generate different sled trajectories. The sled program was written by Mr. Bob Grimes of Payload Systems, Inc. The following trajectory generators were developed and implemented by the author of this thesis to expand the kinds of motion the sled was capable of. The list below gives the name of the file that generates the trajectory (.CPP) and its associated header file (.HPP) which defines the global variables, and gives a brief description of the trajectory form.

Squaretg (.CPP and .HPP): Generates a square acceleration wave (step of acceleration). The user inputs the acceleration of the step (G) and the frequency of the signal (1/time). The sled accelerates for one third of the trial duration, accelerates in the opposite direction (decelerates) for two thirds of the trial duration, and then accelerates again to bring the sled back to the center of the track.

Newsqrtg (.CPP and .HPP): Generates a step of acceleration similar to *Squaretg*, but uses two different accelerations for the initial step and the step to return the sled back to the center of the track. Since we are primarily interested in the response to the first step of acceleration, the remainder of the trial can be at a higher acceleration to return the subject to the center of the track more quickly. The user inputs the acceleration of the signal, the duration of the signal, and the return acceleration.

Velstptg (.CPP and .HPP): Generates a step of velocity. The user inputs the magnitude of the desired velocity, the duration of the signal, and the acceleration used to ramp up to the desired velocity.

Steptg (.CPP and .HPP): Generates a damped-position step (single cycle of sine acceleration). The user inputs the acceleration (G) and frequency (1/time) of the sinusoid. This is the trajectory generator used for the Hidden Target Pursuit experiments described in this thesis.

Similar trajectory generators were written by the author, but not included here, for the auxiliary channel of the controller. This allows any other instrumentation that is to be controlled by the sled computer to move in similar motion profiles as the sled. The names of the C++ files for the auxiliary channel are Auxstptg (.CPP and .HPP) and Auxsqrtg (.CPP and .HPP).

```
////////////////////////////////////////////////////////////////////////
// Title:   Sled - Functions
// Author:  Karla A. Polutchko
// Date:    December, 1991
// $Revision:  1.0  $
//
// Contents
//
// Description
//
// Copyright (C) 1991 Payload Systems Inc.  All Rights Reserved
////////////////////////////////////////////////////////////////////////
// $Log:  C:/ey1/sled/vcs/squaretg.cpv  $
//
//   Rev 1.0   16 Nov 1991 19:17:40   rsg
// Bug fixes for bugs encountered during Zinc switch
//
//   Rev 1.9.1.4   28 May 1991 14:29:30   rsg
// Incremental updates.
//
//   Rev 1.9.1.3   21 May 1991 09:12:46   rsg
// Incremental updates.
//
//   Rev 1.9.1.2   15 May 1991 18:07:00   rsg
// Incremental updates.
//
//   Rev 1.9.1.1   13 May 1991 16:03:38   rsg
// Debugged trajectory generators.
//
//   Rev 1.9.1.0   08 May 1991 13:04:14   rsg
// Incremental updates.
//
//   Rev 1.9   27 Apr 1991 13:00:28   rsg
// Incremental updates.
//
//   Rev 1.8   24 Apr 1991 13:33:24   rsg
// Incremental updates.
//
//   Rev 1.7   24 Apr 1991 08:15:30   rsg
// Incremental updates.
//
//   Rev 1.6   22 Apr 1991 08:38:00   rsg
// Incremental updates.
//
//   Rev 1.5   09 Apr 1991 14:56:04   rsg
// Deleted derivation of AbstractTG from UIW_WINDOW.
//
//   Rev 1.4   09 Apr 1991 10:23:52   rsg
// Documentation fixups.
//
//   Rev 1.3   09 Apr 1991 09:34:04   rsg
// Documentation update.
//
//   Rev 1.2   09 Apr 1991 08:51:24   rsg
```

```
// Incremental update.
////////////////////////////////////////////////////////////////////////

// Interface Dependencies ----------------------------------------------

#ifndef  SQUARETG_HPP
#include "squaretg.hpp"
#endif

// End Interface Dependencies ------------------------------------------

// Implementation Dependencies -----------------------------------------

#ifndef __MATH_H
#include <math.h>
#endif

#ifndef __STDIO_H
#include <stdio.h>
#endif

#ifndef __STRING_H
#include <string.h>
#endif

#ifndef  DISPVARS_HPP
#include "dispvars.hpp"
#endif

#ifndef  SLEDCONV_HPP
#include "sledconv.hpp"
#endif

#ifndef  TRAJEDIT_HPP
#include "trajedit.hpp"
#endif

// End Implementation Dependencies -------------------------------------

class SquareEditForm : public TrajEditForm {
public:
        SquareEditForm(SquareTG *traj,int rate,int flag);

        static int validateAccel(void *item, int ccode);
        static int validateFrequency(void *item, int ccode);
        static int validateHalfCycles(void *item, int ccode);

private:
        int doValidateAccel(void *item, int ccode);
        int doValidateFrequency(void *item, int ccode);
        int doValidateHalfCycles(void *item, int ccode);
        };

SquareEditForm::SquareEditForm(SquareTG *traj,int rate,int flag) :
```

```
                TrajEditForm(traj,rate,3,3,36,7,flag,0) {
        }

int SquareEditForm::validateAccel(void *item,int ccode) {
        UIW_NUMBER *number = (UIW_NUMBER *)item;
        return (((SquareEditForm *)number->parent)->doValidateAccel(item, ccode));
        }

int SquareEditForm::doValidateAccel(void *item, int ccode) {
        if (ccode == S_CURRENT)
                return (0);

        UIW_NUMBER *field = (UIW_NUMBER *)item;
        float value = *(float *)field->DataGet();
        SquareEditForm *me = (SquareEditForm *)(((UIW_NUMBER *)item)->parent);
        SquareTG *mine = (SquareTG *)me->myTraj;
        float max;

        if (mine->verifyAcceleration(max)) {
                _errorSystem->ReportError(field->windowManager, -1,
                        "%f is not valid.  The absolute value must be greater than 0.0, but"
                        " less than %f", value,accelToG(max));
                return (-1);
                }
        else
                return 0;
        }

int SquareEditForm::validateFrequency(void *item,int ccode) {
        UIW_NUMBER *number = (UIW_NUMBER *)item;
        return (((SquareEditForm *)number->parent)->doValidateFrequency(item, ccode));
        }

int SquareEditForm::doValidateFrequency(void *item,int ccode) {
        if (ccode == S_CURRENT)
                return (0);

        UIW_NUMBER *field = (UIW_NUMBER *)item;
        float value = *(float *)field->DataGet();
        SquareEditForm *me = (SquareEditForm *)(((UIW_NUMBER *)item)->parent);
        SquareTG *mine = (SquareTG *)me->myTraj;
        float min;


        if (mine->verifyFrequency(min)) {
                _errorSystem->ReportError(field->windowManager, -1,
                        "%f is not valid.  The value must be greater than %f, but less than"
                        " %f", value,min,getMaximumFrequency());
                return (-1);
                }
        else
                return 0;
        }
```

```
int SquareEditForm::validateHalfCycles(void *item,int ccode) {
        UIW_NUMBER *number = (UIW_NUMBER *)item;
        return (((SquareEditForm *)number->parent)->doValidateHalfCycles(item, ccode));
        }

int SquareEditForm::doValidateHalfCycles(void *item,int ccode) {
        if (ccode == S_CURRENT)
                return (0);

        UIW_NUMBER *field = (UIW_NUMBER *)item;
        int value = *(int *)field->DataGet();

        if (value >= 0 && value < 100)
                return 0;
        else {
                _errorSystem->ReportError(field->windowManager, 0,
                        "%d is not valid.  The value must be at least 0, but less than 100",
                        value,100);
                return (-1);
                }
        }


SquareTG::SquareTG() : AbstractTG() {
        strcpy(myName,"Square");
        frequency = 1.0;
        amplitude = 0.0;
        acceleration = 0.1;
        rampHalfCycles = 2;
        validAxis = Sled;
        }

SquareTG::~SquareTG() {
        }

int SquareTG::readHeader(const char *filename) {
        FILE *f;

        // First, read the data of our ancestor(s).
        if (AbstractTG::readHeader(filename))
                return 1;

        // Open the file for reading. Note that an existing file is assumed.
        f = fopen(filename,"rb");

        // Seek past our ancestor(s) data. Note the true data size of the our
        // ancestor(s) is two less that the size of our immediate ancestor.
        fseek(f,sizeof(AbstractTG)-2,SEEK_SET);

        // Read our portion of the header. To do this, we must find our data,
        // which is located after our ancestor. The size to read is the
        // difference between our size and that of our ancestor.
        char *ptr = (char *)this;
        ptr += sizeof(AbstractTG);
```

```
	int size = sizeof(SquareTG)-sizeof(AbstractTG);
	fread(ptr,size,1,f);

	// Close the file
	fclose(f);
	return 0;
	}

void SquareTG::writeHeader(const char *filename) {
	FILE *f;

	// First, write the data of our ancestor(s).
	AbstractTG::writeHeader(filename);

	// Open the file for writing. Note that an existing file is assumed.
	f = fopen(filename,"rb+");

	// Seek past our ancestor(s) data. Note the true data size of the our
	// ancestor(s) is two less that the size of our immediate ancestor.
	fseek(f,sizeof(AbstractTG)-2,SEEK_SET);

	// Write our portion of the header. To do this, we must find our data,
	// which is located after our ancestor. The size to write is the
	// difference between our size and that of our ancestor.
	char *ptr = (char *)this;
	ptr += sizeof(AbstractTG);
	int size = sizeof(SquareTG)-sizeof(AbstractTG);
	fwrite(ptr,size,1,f);

	// Close the file
  fclose(f);
	}

int SquareTG::verifyFrequency(float &min) {
	min = sqrt(fabs(gToAccel(acceleration)/(32*(getTrackLength()-0.1))));

	if (frequency < min || frequency > getMaximumFrequency())
		return 1;// Invalid.
	else
		return 0;// Okay
	}

int SquareTG::verifyAcceleration(float &max) {
	max = (getTrackLength()-0.1)*32*frequency*frequency;

	if (max > getMaximumAccel())
		max = getMaximumAccel();

	if (fabs(acceleration) == 0.0 || fabs(acceleration) > accelToG(max))
		return 1;// Invalid.
	else
		return 0;// Okay.
	}
```

```
int SquareTG::verifyParameters() {
        int error = 0;

        float temp;
        error = verifyAcceleration(temp);
        error += verifyFrequency(temp);

        if (rampHalfCycles < 0)
                error += 1;

        // Calculate our derived parameters.
        if (!error) {
                amplitude = gToAccel(acceleration);

                numberCommands[0] = (long)(0.5 + rampHalfCycles*commandRate/(2*frequency));
                numberCommands[1] = (long)(commandRate/frequency + 0.5);
                numberCommands[2] = numberCommands[0];
                }
        else {
                amplitude = 0.0;
                numberCommands[0] = numberCommands[1] = numberCommands[2] = 0;
                }
        return error;
        }

float SquareTG::generateCommand(int phase,long index) {
        float velocity;

        if ((1.0*index)/commandRate <= 1/(4*frequency))
                velocity = (amplitude*index)/commandRate;
        else if ((1.0*index)/commandRate <= 3/(4*frequency))
                velocity = amplitude/(4*frequency) -
                                        ((1.0*index)/commandRate -
(1.0/(4*frequency)))*amplitude;
        else
                velocity = (-amplitude/(4*frequency)) +
                                        ((1.0*index)/commandRate - (3/(4*frequency)))*amplitude;

        switch (phase) {
                case 0:
                        // Note that while rampHalfCycles may be zero, the following division
                        // will not be called, because numberCommands[0] will also be 0, and
                        // thus this function won't be called. The same applies in case 2.
                        velocity = (velocity*index)/numberCommands[phase];
                        if (rampHalfCycles & 1)
                                velocity = -velocity;
                        return velocity;
                case 1:
                        return velocity;
                case 2:
                        velocity -= (velocity*index)/numberCommands[phase];
                        return velocity;
                }
        }
```

```
void SquareTG::getParameters(int rate,int modal) {
        commandRate = rate;

        // Create an edit form.
        SquareEditForm *form = new SquareEditForm(this,rate,modal);

        *form
                + new UIW_BORDER
                + new UIW_TITLE(myName)
                + new UIW_SYSTEM_BUTTON
                + new UIW_PROMPT(2,1,"Acceleration (g)",WOF_NO_FLAGS)
                + new UIW_NUMBER(22,1,10,&acceleration,NULL,NMF_NO_FLAGS,

WOF_AUTO_CLEAR|WOF_NO_ALLOCATE_DATA|WOF_BORDER,
                                                SquareEditForm::validateAccel)
                + new UIW_PROMPT(2,2,"Frequency (Hz)",WOF_NO_FLAGS)
                + new UIW_NUMBER(18,2,10,&frequency,NULL,NMF_NO_FLAGS,

WOF_AUTO_CLEAR|WOF_NO_ALLOCATE_DATA|WOF_BORDER,
                                                SquareEditForm::validateFrequency)
                + new UIW_PROMPT(2,3,"Ramp 1/2 cycles",WOF_NO_FLAGS)
                + new UIW_NUMBER(18,3,5,&rampHalfCycles,NULL,NMF_NO_FLAGS,

WOF_AUTO_CLEAR|WOF_NO_ALLOCATE_DATA|WOF_BORDER,
                                                SquareEditForm::validateHalfCycles)
                + new UIW_BUTTON(16,4,4,"Ok",BTF_NO_FLAGS,WOF_BORDER,
                                                SquareEditForm::generateFunction);

        // Give it to the window manager.
        *_windowManager + form;
        }

void SquareTG::getHeaderDisplaySize(UI_REGION& size) {
        AbstractTG::getHeaderDisplaySize(size);
        if (size.right < 72)
                size.right = 72;
        size.bottom += 3;
        }

void SquareTG::displayHeader(UIW_WINDOW *window,int& left, int& top) {
        AbstractTG::displayHeader(window,left,top);
        *window
                + new UIW_PROMPT(left,top+1,"Acceleration (g)",WOF_NO_FLAGS)
                + new UIW_NUMBER(left+17,top+1,10,&acceleration,NULL,NMF_NO_FLAGS,

WOF_NON_SELECTABLE|WOF_BORDER)
                + new UIW_PROMPT(left,top+2,"Frequency (Hz)",WOF_NO_FLAGS)
                + new UIW_NUMBER(left+17,top+2,10,&frequency,NULL,NMF_NO_FLAGS,

WOF_NON_SELECTABLE|WOF_BORDER)
                + new UIW_PROMPT(left+29,top+1,"Amplitude (m/s)",WOF_NO_FLAGS)
                + new UIW_NUMBER(left+45,top+1,10,&amplitude,NULL,NMF_NO_FLAGS,
```

```
WOF_NON_SELECTABLE|WOF_BORDER)
                + new UIW_PROMPT(left+29,top+2,"Ramp 1/2 cycles",WOF_NO_FLAGS)
                + new UIW_NUMBER(left+45,top+2,5,&rampHalfCycles,NULL,NMF_NO_FLAGS,

WOF_NON_SELECTABLE|WOF_BORDER);

        top += 3;
        }

void SquareTG::dumpHeader(char *name,FILE *f) {
        AbstractTG::dumpHeader(name,f);
        fprintf(f,"Acceleration: %6.3f g    Frequency: %7.4f Hz\n",acceleration,
                                frequency);
        fprintf(f,"Amplitude:    %6.3f m/s  Ramp 1/2 Cycles: %d\n\n",amplitude,
                        rampHalfCycles);
        }
```

```
////////////////////////////////////////////////////////////////////////////
// Title:   Sled - Functions
// Author:  Karla A. Polutchko
// Date:    December, 1991
// $Revision:   1.0  $
//
// Contents
//
// Description
//
// Copyright (C) 1991 Payload Systems Inc.  All Rights Reserved
////////////////////////////////////////////////////////////////////////////
// $Log:   C:/ey1/sled/vcs/squaretg.hpv  $
//
//   Rev 1.0   16 Nov 1991 19:17:44   rsg
// Bug fixes for bugs encountered during Zinc switch
//
//   Rev 1.7.1.2   28 May 1991 14:30:00   rsg
// Incremental updates.
//
//   Rev 1.7.1.1   13 May 1991 16:03:54   rsg
// Debugged trajectory generators.
//
//   Rev 1.7.1.0   08 May 1991 13:05:10   rsg
// Incremental updates.
//
//   Rev 1.7   24 Apr 1991 13:33:34   rsg
// Incremental updates.
//
//   Rev 1.6   24 Apr 1991 08:16:58   rsg
// Incremental updates.
//
//   Rev 1.5   22 Apr 1991 08:39:28   rsg
// Incremental updates.
//
//   Rev 1.4   09 Apr 1991 14:56:58   rsg
// Deleted derivation of AbstractTG from UIW_WINDOW.
//
//   Rev 1.3   09 Apr 1991 10:28:54   rsg
// Documentation fixups.
//
//   Rev 1.2   09 Apr 1991 09:31:36   rsg
// Documentation update.
//
//   Rev 1.1   09 Apr 1991 08:54:26   rsg
// Incremental update.
////////////////////////////////////////////////////////////////////////////

#ifndef  SQUARETG_HPP
#define  SQUARETG_HPP

// Interface Dependencies -------------------------------------------------

#ifndef   UI_WIN_HPP
```

```
#include <ui_win.hpp>
#endif

#ifndef __STDIO_H
#include <stdio.h>
#endif

#ifndef  ABSTRAJG_HPP
#include "abstrajg.hpp"
#endif

// End Interface Dependencies ------------------------------------------------

// Implementation Dependencies -----------------------------------------------

// End Implementation Dependencies -------------------------------------------

class SquareTG : public AbstractTG {
public:
        SquareTG();
        ~SquareTG();

        AbstractTG *dup() { return new SquareTG(); }

        int readHeader(const char *filename);
        void writeHeader(const char *filename);

        void dumpHeader(char *name,FILE *f);

        float generateCommand(long index);
        void generateTrajectory(const char *filename);

        void getParameters(int rate,int modal);

        void getHeaderDisplaySize(UI_REGION& size);
        void displayHeader(UIW_WINDOW *window,int& left, int& top);

        float generateCommand(int phase,long index);

        int verifyAcceleration(float &max);
        int verifyFrequency(float &min);
        int verifyParameters();

        int getWidth();// { return 36; }
        int getHeight();// { return 8; }

        float frequency;
        float acceleration;
        float amplitude;
        int rampHalfCycles;
        };
#endif
```

```
////////////////////////////////////////////////////////////////////////
// Title:   Sled - Functions
// Author:  Karla A. Polutchko
// Date:    January 13, 1993
// $Revision:  1.0  $
//
// Contents
//
// Description
//
// Copyright (C) 1991 Payload Systems Inc.  All Rights Reserved
////////////////////////////////////////////////////////////////////////
// $Log:  C:/ey1/sled/vcs/newsqrtg.cpv  $
//
//   Rev 1.0   16 Nov 1991 19:17:40   rsg
// Bug fixes for bugs encountered during Zinc switch
//
//   Rev 1.9.1.4   28 May 1991 14:29:30   rsg
// Incremental updates.
//
//   Rev 1.9.1.3   21 May 1991 09:12:46   rsg
// Incremental updates.
//
//   Rev 1.9.1.2   15 May 1991 18:07:00   rsg
// Incremental updates.
//
//   Rev 1.9.1.1   13 May 1991 16:03:38   rsg
// Debugged trajectory generators.
//
//   Rev 1.9.1.0   08 May 1991 13:04:14   rsg
// Incremental updates.
//
//   Rev 1.9   27 Apr 1991 13:00:28   rsg
// Incremental updates.
//
//   Rev 1.8   24 Apr 1991 13:33:24   rsg
// Incremental updates.
//
//   Rev 1.7   24 Apr 1991 08:15:30   rsg
// Incremental updates.
//
//   Rev 1.6   22 Apr 1991 08:38:00   rsg
// Incremental updates.
//
//   Rev 1.5   09 Apr 1991 14:56:04   rsg
// Deleted derivation of AbstractTG from UIW_WINDOW.
//
//   Rev 1.4   09 Apr 1991 10:23:52   rsg
// Documentation fixups.
//
//   Rev 1.3   09 Apr 1991 09:34:04   rsg
// Documentation update.
//
//   Rev 1.2   09 Apr 1991 08:51:24   rsg
```

```
// Incremental update.
////////////////////////////////////////////////////////////////////////

// Interface Dependencies ----------------------------------------------

#ifndef  NEWSQRTG_HPP
#include "newsqrtg.hpp"
#endif

// End Interface Dependencies ------------------------------------------

// Implementation Dependencies -----------------------------------------

#ifndef __MATH_H
#include <math.h>
#endif

#ifndef __STDIO_H
#include <stdio.h>
#endif

#ifndef __STRING_H
#include <string.h>
#endif

#ifndef  DISPVARS_HPP
#include "dispvars.hpp"
#endif

#ifndef  SLEDCONV_HPP
#include "sledconv.hpp"
#endif

#ifndef  TRAJEDIT_HPP
#include "trajedit.hpp"
#endif

// End Implementation Dependencies -------------------------------------

class NewsqrEditForm : public TrajEditForm {
public:
        NewsqrEditForm(NewsqrTG *traj,int rate,int flag);

        static int validateAccel(void *item, int ccode);
        static int validateAccel2(void *item, int ccode);
        static int validateFrequency(void *item, int ccode);
        static int validateSignalDuration(void *item, int ccode);
        static int validateHalfCycles(void *item, int ccode);

private:
        int doValidateAccel(void *item, int ccode);
        int doValidateAccel2(void *item, int ccode);
        int doValidateFrequency(void *item, int ccode);
        int doValidateSignalDuration(void *item, int ccode);
```

```
        int doValidateHalfCycles(void *item, int ccode);
        };

NewsqrEditForm::NewsqrEditForm(NewsqrTG *traj,int rate,int flag) :
                TrajEditForm(traj,rate,3,3,40,9,flag,0) {
        }

int NewsqrEditForm::validateAccel(void *item,int ccode) {
        UIW_NUMBER *number = (UIW_NUMBER *)item;
        return (((NewsqrEditForm *)number->parent)->doValidateAccel(item, ccode));
        }

int NewsqrEditForm::doValidateAccel(void *item, int ccode) {
        if (ccode == S_CURRENT)
                return (0);

        UIW_NUMBER *field = (UIW_NUMBER *)item;
        float value = *(float *)field->DataGet();
        NewsqrEditForm *me = (NewsqrEditForm *)(((UIW_NUMBER *)item)->parent);
        NewsqrTG *mine = (NewsqrTG *)me->myTraj;
        float max;

        if (mine->verifyAcceleration(max)) {
                _errorSystem->ReportError(field->windowManager, -1,
                        "%f is not valid.  The absolute value must be greater than 0.0, but"
                        " less than %f", value,accelToG(max));
                return (-1);
                }
        else
                return 0;
        }

int NewsqrEditForm::validateAccel2(void *item,int ccode) {
        UIW_NUMBER *number = (UIW_NUMBER *)item;
        return (((NewsqrEditForm *)number->parent)->doValidateAccel2(item, ccode));
        }

int NewsqrEditForm::doValidateAccel2(void *item, int ccode) {
        if (ccode == S_CURRENT)
                return (0);

        UIW_NUMBER *field = (UIW_NUMBER *)item;
        float value = *(float *)field->DataGet();
        NewsqrEditForm *me = (NewsqrEditForm *)(((UIW_NUMBER *)item)->parent);
        NewsqrTG *mine = (NewsqrTG *)me->myTraj;
        float max;

        if (mine->verifyAcceleration2(max)) {
                _errorSystem->ReportError(field->windowManager, -1,
                        "%f is not valid.  The absolute value must be greater than 0.0, but"
                        " less than %f", value,accelToG(max));
                return (-1);
                }
        else
```

```
                return 0;
        }

int NewsqrEditForm::validateFrequency(void *item,int ccode) {
        UIW_NUMBER *number = (UIW_NUMBER *)item;
        return (((NewsqrEditForm *)number->parent)->doValidateFrequency(item, ccode));
        }

int NewsqrEditForm::doValidateFrequency(void *item,int ccode) {
        if (ccode == S_CURRENT)
                return (0);

        UIW_NUMBER *field = (UIW_NUMBER *)item;
        float value = *(float *)field->DataGet();
        NewsqrEditForm *me = (NewsqrEditForm *)(((UIW_NUMBER *)item)->parent);
        NewsqrTG *mine = (NewsqrTG *)me->myTraj;
        float min;


        if (mine->verifyFrequency(min)) {
                _errorSystem->ReportError(field->windowManager, -1,
                        "%f is not valid.  The value must be greater than %f, but less than"
                        " %f", value,min,getMaximumFrequency());
                return (-1);
                }
        else
                return 0;
        }

int NewsqrEditForm::validateSignalDuration(void *item,int ccode) {
        UIW_NUMBER *number = (UIW_NUMBER *)item;
        return (((NewsqrEditForm *)number->parent)->doValidateSignalDuration(item, ccode));
        }

int NewsqrEditForm::doValidateSignalDuration(void *item,int ccode) {
        if (ccode == S_CURRENT)
                return (0);

        UIW_NUMBER *field = (UIW_NUMBER *)item;
        float value = *(float *)field->DataGet();
        NewsqrEditForm *me = (NewsqrEditForm *)(((UIW_NUMBER *)item)->parent);
        NewsqrTG *mine = (NewsqrTG *)me->myTraj;
  float max2;

        if (mine->verifySignalDuration(max2)) {
                _errorSystem->ReportError(field->windowManager, -1,
                        "%f is not valid.  The value must be greater than %f, but less than"
      " %f", value,0.0,max2);
                return -1;
                }
        else
                return 0;
        }
```

```
int NewsqrEditForm::validateHalfCycles(void *item,int ccode) {
        UIW_NUMBER *number = (UIW_NUMBER *)item;
        return (((NewsqrEditForm *)number->parent)->doValidateHalfCycles(item, ccode));
        }

int NewsqrEditForm::doValidateHalfCycles(void *item,int ccode) {
        if (ccode == S_CURRENT)
                return (0);

        UIW_NUMBER *field = (UIW_NUMBER *)item;
        int value = *(int *)field->DataGet();

        if (value >= 0 && value < 100)
                return 0;
        else {
                _errorSystem->ReportError(field->windowManager, 0,
                        "%d is not valid.  The value must be at least 0, but less than 100",
                        value,100);
                return (-1);
                }
        }


NewsqrTG::NewsqrTG() : AbstractTG() {
        strcpy(myName,"New Square");
        amplitude = 0.0;
        acceleration = 0.010;
        acceleration2 = .082;
        signalDuration = 2.5;
        rampHalfCycles = 0;
        validAxis = Sled;

// Calculate the duration (frequency) of the whole trial
    long k;
    float totalDuration;
                amplitude = gToAccel(acceleration);
                if (amplitude > 0.0)
                        amplitude2 = gToAccel(acceleration2);
                else
                        amplitude2 = -gToAccel(acceleration2);

                t1 = signalDuration;

                // Calculate position when velocity is zero at end of 1/2 cycle...
                posFinal = 0.0;
                float command = 0.0;
                long numComm = 0.0;

                t2 = amplitude*t1/amplitude2;
                numComm = (long)(commandRate*(t1 + t2) + 0.5);
                for (k = 0; k < numComm; k++) {
                        if ((1.0*k)/commandRate <= t1)
                                command = (amplitude*k)/commandRate;
                        else if ((1.0*k)/commandRate <= (t1 + t2))
```

```
                        command = amplitude*t1 - ((1.0*k)/commandRate - t1)*amplitude2;

                    posFinal += command/commandRate;
                    }

            t3 = sqrt(4.0*posFinal/amplitude2);
    totalDuration = t1 + t2 + t3;
    frequency = 1.0/(totalDuration);

        }

NewsqrTG::~NewsqrTG() {
        }

int NewsqrTG::readHeader(const char *filename) {
        FILE *f;

        // First, read the data of our ancestor(s).
        if (AbstractTG::readHeader(filename))
                return 1;

        // Open the file for reading. Note that an existing file is assumed.
        f = fopen(filename,"rb");

        // Seek past our ancestor(s) data. Note the true data size of the our
        // ancestor(s) is two less that the size of our immediate ancestor.
        fseek(f,sizeof(AbstractTG)-2,SEEK_SET);

        // Read our portion of the header. To do this, we must find our data,
        // which is located after our ancestor. The size to read is the
        // difference between our size and that of our ancestor.
        char *ptr = (char *)this;
        ptr += sizeof(AbstractTG);
        int size = sizeof(NewsqrTG)-sizeof(AbstractTG);
        fread(ptr,size,1,f);

        // Close the file
        fclose(f);
        return 0;
        }

void NewsqrTG::writeHeader(const char *filename) {
        FILE *f;

        // First, write the data of our ancestor(s).
        AbstractTG::writeHeader(filename);

        // Open the file for writing. Note that an existing file is assumed.
        f = fopen(filename,"rb+");

        // Seek past our ancestor(s) data. Note the true data size of the our
        // ancestor(s) is two less that the size of our immediate ancestor.
        fseek(f,sizeof(AbstractTG)-2,SEEK_SET);
```

```
        // Write our portion of the header. To do this, we must find our data,
        // which is located after our ancestor. The size to write is the
        // difference between our size and that of our ancestor.
        char *ptr = (char *)this;
        ptr += sizeof(AbstractTG);
        int size = sizeof(NewsqrTG)-sizeof(AbstractTG);
        fwrite(ptr,size,1,f);

        // Close the file
        fclose(f);
        }

int NewsqrTG::verifyFrequency(float &min) {
        min = sqrt(fabs(gToAccel(acceleration)/(32*(getTrackLength()-0.1))));
                if (frequency < min || frequency > getMaximumFrequency())
                return 1;// Invalid.
        else
                return 0;// Okay
        }

int NewsqrTG::verifySignalDuration(float &max2) {
  max2 = 1.0/sqrt(fabs(gToAccel(acceleration)/(32*(getTrackLength()-0.1))));
        if (signalDuration < 0.0 || signalDuration > max2)
                return 1;// Invalid.
        else
                return 0;// Okay
        }

int NewsqrTG::verifyAcceleration(float &max) {
        max = (getTrackLength()-0.1)*32*frequency*frequency;

        if (max > getMaximumAccel())
                max = getMaximumAccel();

        if (fabs(acceleration) == 0.0 || fabs(acceleration) > accelToG(max))
                return 1;// Invalid.
        else
                return 0;// Okay.
        }

int NewsqrTG::verifyAcceleration2(float &max) {
        if (fabs(acceleration2) == 0.0 || fabs(acceleration2) > accelToG(max))
                return 1;// Invalid.
        else
                return 0;// Okay.
        }

int NewsqrTG::verifyParameters() {
        int error = 0;
        long k;

        float temp;
        error = verifyAcceleration(temp);
  error += verifyAcceleration2(temp);
```

```
        error += verifyFrequency(temp);
        error += verifySignalDuration(temp);

        if (rampHalfCycles < 0)
                error += 1;

        // Calculate our derived parameters.
        if (!error) {

                amplitude = gToAccel(acceleration);
                if (amplitude > 0.0)
                        amplitude2 = gToAccel(acceleration2);
                else
                        amplitude2 = -gToAccel(acceleration2);

                t1 = signalDuration;

                // Calculate position when velocity is zero at end of 1/2 cycle...
                posFinal = 0.0;
                float command = 0.0;
                long numComm = 0.0;

                t2 = amplitude*t1/amplitude2;
                numComm = (long)(commandRate*(t1 + t2) + 0.5);
                for (k = 0; k < numComm; k++) {
                        if ((1.0*k)/commandRate <= t1)
                                command = (amplitude*k)/commandRate;
                        else if ((1.0*k)/commandRate <= (t1 + t2))
                                command = amplitude*t1 - ((1.0*k)/commandRate - t1)*amplitude2;

                        posFinal += command/commandRate;
                        }

                t3 = sqrt(4.0*posFinal/amplitude2);

                numberCommands[0] = (long)(0.5 + rampHalfCycles*commandRate/(2*frequency));
                numberCommands[1] = (long)((commandRate*(t1 + t2 + t3)) + 0.5);
                numberCommands[2] = numberCommands[0];
        }
        else {
                amplitude = 0.0;
                amplitude2 = 0.0;
                numberCommands[0] = numberCommands[1] = numberCommands[2] = 0;
                }
        return error;
        }

float NewsqrTG::generateCommand(int phase,long index) {
        float velocity = 0.0;

        if ((1.0*index)/commandRate <= t1)
                velocity = (amplitude*index)/commandRate;
        else if ((1.0*index)/commandRate <= t1 + t2 + t3/2.0)
                velocity = amplitude*t1 - ((1.0*index)/commandRate - t1)*amplitude2;
```

```
        else if ((1.0*index)/commandRate <= t1 + t2 + t3)
                velocity = -amplitude2*(t3/2.0) + ((1.0*index)/commandRate - (t1 + t2 +
t3/2.0))*amplitude2;

        return velocity;
        }

void NewsqrTG::getParametersDisplaySize(UI_REGION& size) {
        if (size.right < 45)
                size.right = 45;
        size.bottom += 5;
        }


void NewsqrTG::getParameters(int rate,int modal) {
        commandRate = rate;

        // Create an edit form.
        NewsqrEditForm *form = new NewsqrEditForm(this,rate,modal);

        *form
                + new UIW_BORDER
                + new UIW_TITLE(myName)
                + new UIW_SYSTEM_BUTTON
                + new UIW_PROMPT(2,1,"Signal Acceleration (g)",WOF_NO_FLAGS)
                + new UIW_NUMBER(28,1,10,&acceleration,NULL,NMF_NO_FLAGS,

WOF_AUTO_CLEAR|WOF_NO_ALLOCATE_DATA|WOF_BORDER,
                                                        NewsqrEditForm::validateAccel)
                + new UIW_PROMPT(2,2,"Return Acceleration (g)",WOF_NO_FLAGS)
                + new UIW_NUMBER(28,2,10,&acceleration2,NULL,NMF_NO_FLAGS,

WOF_AUTO_CLEAR|WOF_NO_ALLOCATE_DATA|WOF_BORDER,
                                                        NewsqrEditForm::validateAccel)
                + new UIW_PROMPT(2,3,"Signal Duration (s)",WOF_NO_FLAGS)
                + new UIW_NUMBER(28,3,10,&signalDuration,NULL,NMF_NO_FLAGS,

WOF_AUTO_CLEAR|WOF_NO_ALLOCATE_DATA|WOF_BORDER,
                                                        NewsqrEditForm::validateSignalDuration)
                + new UIW_PROMPT(2,4,"Ramp 1/2 cycles",WOF_NO_FLAGS)
                + new UIW_NUMBER(28,4,10,&rampHalfCycles,NULL,NMF_NO_FLAGS,

WOF_AUTO_CLEAR|WOF_NO_ALLOCATE_DATA|WOF_BORDER,
                                                        NewsqrEditForm::validateHalfCycles)
                + new UIW_BUTTON(18,5,4,"Ok",BTF_NO_FLAGS,WOF_BORDER,
                                                        NewsqrEditForm::generateFunction);

        // Give it to the window manager.
        *_windowManager + form;
        }

void NewsqrTG::getHeaderDisplaySize(UI_REGION& size) {
        AbstractTG::getHeaderDisplaySize(size);
        if (size.right < 72)
```

```
            size.right = 72;
        size.bottom += 5;
        }

void NewsqrTG::displayHeader(UIW_WINDOW *window,int& left, int& top) {
        AbstractTG::displayHeader(window,left,top);
        *window
                + new UIW_PROMPT(left,top+1,"Signal Acceleration (g)",WOF_NO_FLAGS)
                + new UIW_NUMBER(left+17,top+1,10,&acceleration,NULL,NMF_NO_FLAGS,

WOF_NON_SELECTABLE|WOF_BORDER)
                + new UIW_PROMPT(left+29,top+1,"Return Acceleration (g)",WOF_NO_FLAGS)
                + new UIW_NUMBER(left+45,top+1,10,&acceleration2,NULL,NMF_NO_FLAGS,

WOF_NON_SELECTABLE|WOF_BORDER)
                + new UIW_PROMPT(left,top+2,"Signal Duration (s)",WOF_NO_FLAGS)
                + new UIW_NUMBER(left+17,top+2,10,&signalDuration,NULL,NMF_NO_FLAGS,

WOF_NON_SELECTABLE|WOF_BORDER)
                + new UIW_PROMPT(left+29,top+2,"Signal Displacement (m)",WOF_NO_FLAGS)
                + new UIW_NUMBER(left+45,top+2,10,&posFinal,NULL,NMF_NO_FLAGS,

WOF_NON_SELECTABLE|WOF_BORDER)
                + new UIW_PROMPT(left,top+3,"Amplitude (m/s)",WOF_NO_FLAGS)
                + new UIW_NUMBER(left+17,top+3,10,&amplitude,NULL,NMF_NO_FLAGS,

WOF_NON_SELECTABLE|WOF_BORDER);

        top += 3;

        }

void NewsqrTG::dumpHeader(char *name,FILE *f) {
        AbstractTG::dumpHeader(name,f);
        fprintf(f,"Acceleration: %6.3f g    Signal Duration: %6.3f s\n",acceleration,
                                signalDuration);
        fprintf(f,"Amplitude:   %6.3f m/s  Ramp 1/2 Cycles: %d\n\n",amplitude,
                        rampHalfCycles);
  fprintf(f,"Signal Displacement: %6.3f m",posFinal);
        }
```

```
////////////////////////////////////////////////////////////////////////
// Title:   Sled - Functions
// Author:  Karla A. Polutchko
// Date:    April, 1993
// $Revision:   1.0  $
//
// Contents
//
// Description
//
// Copyright (C) 1991 Payload Systems Inc.  All Rights Reserved
////////////////////////////////////////////////////////////////////////
// $Log:   C:/ey1/sled/vcs/newsqrtg.hpv  $
//
//   Rev 1.0   16 Nov 1991 19:17:44   rsg
// Bug fixes for bugs encountered during Zinc switch
//
//   Rev 1.7.1.2   28 May 1991 14:30:00   rsg
// Incremental updates.
//
//   Rev 1.7.1.1   13 May 1991 16:03:54   rsg
// Debugged trajectory generators.
//
//   Rev 1.7.1.0   08 May 1991 13:05:10   rsg
// Incremental updates.
//
//   Rev 1.7   24 Apr 1991 13:33:34   rsg
// Incremental updates.
//
//   Rev 1.6   24 Apr 1991 08:16:58   rsg
// Incremental updates.
//
//   Rev 1.5   22 Apr 1991 08:39:28   rsg
// Incremental updates.
//
//   Rev 1.4   09 Apr 1991 14:56:58   rsg
// Deleted derivation of AbstractTG from UIW_WINDOW.
//
//   Rev 1.3   09 Apr 1991 10:28:54   rsg
// Documentation fixups.
//
//   Rev 1.2   09 Apr 1991 09:31:36   rsg
// Documentation update.
//
//   Rev 1.1   09 Apr 1991 08:54:26   rsg
// Incremental update.
////////////////////////////////////////////////////////////////////////

#ifndef  NEWSQRTG_HPP
#define  NEWSQRTG_HPP

// Interface Dependencies -------------------------------------------------

#ifndef   UI_WIN_HPP
```

```
#include <ui_win.hpp>
#endif

#ifndef __STDIO_H
#include <stdio.h>
#endif

#ifndef  ABSTRAJG_HPP
#include "abstrajg.hpp"
#endif

// End Interface Dependencies ----------------------------------------------

// Implementation Dependencies ---------------------------------------------

// End Implementation Dependencies -----------------------------------------

class NewsqrTG : public AbstractTG {
public:
        NewsqrTG();
        ~NewsqrTG();

        AbstractTG *dup() { return new NewsqrTG(); }

        int readHeader(const char *filename);
        void writeHeader(const char *filename);

        void dumpHeader(char *name,FILE *f);

        float generateCommand(long index);
        void generateTrajectory(const char *filename);

        void getParametersDisplaySize(UI_REGION& size);
        void getParameters(int rate,int modal);

        void getHeaderDisplaySize(UI_REGION& size);
        void displayHeader(UIW_WINDOW *window,int& left, int& top);

        float generateCommand(int phase,long index);

        int verifyAcceleration(float &max);
        int verifyAcceleration2(float &max);
        int verifyFrequency(float &min);
        int verifySignalDuration(float &max2);
        int verifyParameters();

        int getWidth();// { return 36; }
        int getHeight();// { return 11; }

        float frequency;
        float signalDuration;
        float t1;
        float t2;
        float t3;
```

```
        double acceleration;
        double acceleration2;
        float amplitude;
        float amplitude2;
        int rampHalfCycles;
        float posFinal;
        };
#endif
```

```
////////////////////////////////////////////////////////////////////////////
// Title:   Sled - Functions
// Author:  Karla A. Polutchko
// Date:    April, 1993
// $Revision:   1.0  $
//
// Contents
//
// Description
//
// Copyright (C) 1991 Payload Systems Inc.  All Rights Reserved
////////////////////////////////////////////////////////////////////////////
// $Log:   C:/ey1/sled/vcs/velstptg.cpv  $
//
//   Rev 1.0   16 Nov 1991 19:17:40   rsg
// Bug fixes for bugs encountered during Zinc switch
//
//   Rev 1.9.1.4   28 May 1991 14:29:30   rsg
// Incremental updates.
//
//   Rev 1.9.1.3   21 May 1991 09:12:46   rsg
// Incremental updates.
//
//   Rev 1.9.1.2   15 May 1991 18:07:00   rsg
// Incremental updates.
//
//   Rev 1.9.1.1   13 May 1991 16:03:38   rsg
// Debugged trajectory generators.
//
//   Rev 1.9.1.0   08 May 1991 13:04:14   rsg
// Incremental updates.
//
//   Rev 1.9   27 Apr 1991 13:00:28   rsg
// Incremental updates.
//
//   Rev 1.8   24 Apr 1991 13:33:24   rsg
// Incremental updates.
//
//   Rev 1.7   24 Apr 1991 08:15:30   rsg
// Incremental updates.
//
//   Rev 1.6   22 Apr 1991 08:38:00   rsg
// Incremental updates.
//
//   Rev 1.5   09 Apr 1991 14:56:04   rsg
// Deleted derivation of AbstractTG from UIW_WINDOW.
//
//   Rev 1.4   09 Apr 1991 10:23:52   rsg
// Documentation fixups.
//
//   Rev 1.3   09 Apr 1991 09:34:04   rsg
// Documentation update.
//
```

```
//   Rev 1.2   09 Apr 1991 08:51:24   rsg
// Incremental update.
////////////////////////////////////////////////////////////////////////

// Interface Dependencies -------------------------------------------------

#ifndef  VELSTPTG_HPP
#include "velstptg.hpp"
#endif

// End Interface Dependencies ---------------------------------------------

// Implementation Dependencies --------------------------------------------

#ifndef __MATH_H
#include <math.h>
#endif

#ifndef __STDIO_H
#include <stdio.h>
#endif

#ifndef __STRING_H
#include <string.h>
#endif

#ifndef  DISPVARS_HPP
#include "dispvars.hpp"
#endif

#ifndef  SLEDCONV_HPP
#include "sledconv.hpp"
#endif

#ifndef  TRAJEDIT_HPP
#include "trajedit.hpp"
#endif

// End Implementation Dependencies ----------------------------------------

class VelstpEditForm : public TrajEditForm {
public:
        VelstpEditForm(VelstpTG *traj,int rate,int flag);

        static int validateAccel(void *item, int ccode);
        static int validatessVelocity(void *item, int ccode);
        static int validateDuration(void *item, int ccode);

private:
        int doValidateAccel(void *item, int ccode);
        int doValidatessVelocity(void *item, int ccode);
        int doValidateDuration(void *item, int ccode);
        };
```

```
VelstpEditForm::VelstpEditForm(VelstpTG *traj,int rate,int flag) :
        TrajEditForm(traj,rate,3,3,40,7,flag,0) {
    }

int VelstpEditForm::validateAccel(void *item,int ccode) {
    UIW_NUMBER *number = (UIW_NUMBER *)item;
    return (((VelstpEditForm *)number->parent)->doValidateAccel(item, ccode));
    }

int VelstpEditForm::doValidateAccel(void *item, int ccode) {
    if (ccode == S_CURRENT)
        return (0);

    UIW_NUMBER *field = (UIW_NUMBER *)item;
    float value = *(float *)field->DataGet();
    VelstpEditForm *me = (VelstpEditForm *)(((UIW_NUMBER *)item)->parent);
    VelstpTG *mine = (VelstpTG *)me->myTraj;
    float max;

    if (mine->verifyAcceleration(max)) {
        _errorSystem->ReportError(field->windowManager, -1,
            "%f is not valid.  The absolute value must be greater than 0.0, but"
            " less than %f", value,accelToG(max));
        return (-1);
        }
    else
        return 0;
    }

int VelstpEditForm::validatessVelocity(void *item,int ccode) {
    UIW_NUMBER *number = (UIW_NUMBER *)item;
    return (((VelstpEditForm *)number->parent)->doValidatessVelocity(item, ccode));
    }

int VelstpEditForm::doValidatessVelocity(void *item, int ccode) {

    if (ccode == S_CURRENT)
        return (0);

    UIW_NUMBER *field = (UIW_NUMBER *)item;
    float value = *(float *)field->DataGet();
    VelstpEditForm *me = (VelstpEditForm *)(((UIW_NUMBER *)item)->parent);
    VelstpTG *mine = (VelstpTG *)me->myTraj;
    float max;

    if (mine->verifyssVelocity(max)) {
        _errorSystem->ReportError(field->windowManager, -1,
            "%f is not valid.  The absolute value must be greater than 0.0, but"
            " less than %f", value,max);
        return (-1);
        }
    else
        return 0;
    }
```

```
int VelstpEditForm::validateDuration(void *item,int ccode) {
        UIW_NUMBER *number = (UIW_NUMBER *)item;
        return (((VelstpEditForm *)number->parent)->doValidateDuration(item, ccode));
        }
int VelstpEditForm::doValidateDuration(void *item,int ccode) {
        if (ccode == S_CURRENT)
                return (0);

        UIW_NUMBER *field = (UIW_NUMBER *)item;
        float value = *(float *)field->DataGet();
        VelstpEditForm *me = (VelstpEditForm *)(((UIW_NUMBER *)item)->parent);
        VelstpTG *mine = (VelstpTG *)me->myTraj;

        if (mine->verifyDuration()) {
                _errorSystem->ReportError(field->windowManager, -1,
                        "%f is not valid.  The value must be greater than %f", value,0.0);
                return -1;
                }
        else
                return 0;
        }


VelstpTG::VelstpTG() : AbstractTG() {
        strcpy(myName,"Velocity Step");
        ssVelocity = 0.0;
        acceleration = 0.010;
        duration = 0.0;
  rampHalfCycles = 0;
        validAxis = Sled;
        }

VelstpTG::~VelstpTG() {
        }

int VelstpTG::readHeader(const char *filename) {
        FILE *f;

        // First, read the data of our ancestor(s).
        if (AbstractTG::readHeader(filename))
                return 1;

        // Open the file for reading. Note that an existing file is assumed.
        f = fopen(filename,"rb");

        // Seek past our ancestor(s) data. Note the true data size of the our
        // ancestor(s) is two less that the size of our immediate ancestor.
        fseek(f,sizeof(AbstractTG)-2,SEEK_SET);

        // Read our portion of the header. To do this, we must find our data,
        // which is located after our ancestor. The size to read is the
        // difference between our size and that of our ancestor.
```

```
	char *ptr = (char *)this;
	ptr += sizeof(AbstractTG);
	int size = sizeof(VelstpTG)-sizeof(AbstractTG);
	fread(ptr,size,1,f);

	// Close the file
	fclose(f);
	return 0;
	}

void VelstpTG::writeHeader(const char *filename) {
	FILE *f;

	// First, write the data of our ancestor(s).
	AbstractTG::writeHeader(filename);

	// Open the file for writing. Note that an existing file is assumed.
	f = fopen(filename,"rb+");

	// Seek past our ancestor(s) data. Note the true data size of the our
	// ancestor(s) is two less that the size of our immediate ancestor.
	fseek(f,sizeof(AbstractTG)-2,SEEK_SET);

	// Write our portion of the header. To do this, we must find our data,
	// which is located after our ancestor. The size to write is the
	// difference between our size and that of our ancestor.
	char *ptr = (char *)this;
	ptr += sizeof(AbstractTG);
	int size = sizeof(VelstpTG)-sizeof(AbstractTG);
	fwrite(ptr,size,1,f);
	// Close the file
	fclose(f);
	}

int VelstpTG::verifyDuration() {

	if (duration < 0.0)
		return 1;// Invalid.
	else
		return 0;// Okay
	}

int VelstpTG::verifyssVelocity(float &max) {

	max = sqrt((fabs(gToAccel(acceleration)))*(getTrackLength()-0.1));
		if (ssVelocity > max || ssVelocity > getMaximumVelocity())
		return 1;// Invalid.
	else
		return 0;// Okay
	}


int VelstpTG::verifyAcceleration(float &max) {
  max = getMaximumAccel();
```

```
        if (fabs(acceleration) == 0.0 || fabs(acceleration) > accelToG(max))
                return 1;// Invalid.
        else
                return 0;// Okay.
        }


int VelstpTG::verifyParameters() {
        int error = 0;

        float temp;
        error = verifyAcceleration(temp);
  error += verifyssVelocity(temp);
        error += verifyDuration();

  if ((ssVelocity*duration + ssVelocity*ssVelocity/fabs(gToAccel(acceleration))) >
(getTrackLength()-0.1))
    error += 1;
  tramp = ssVelocity/fabs(gToAccel(acceleration));

  if ((1/(4*tramp + 2*duration)) > getMaximumFrequency())
    error += 1;

        // Calculate our derived parameters.
        if (!error) {

                amplitude = gToAccel(acceleration);
    index1 = (tramp + duration)*commandRate;
    index2 = (3*tramp + 2*duration)*commandRate;

                numberCommands[0] = 0.0;
                numberCommands[1] = (long)((commandRate*(4*tramp + 2*duration)) + 0.5);
                numberCommands[2] = numberCommands[0];
    }

        else {
                amplitude = 0.0;
                numberCommands[0] = numberCommands[1] = numberCommands[2] = 0;
                }
        return error;
        }

float VelstpTG::generateCommand(int phase,long index) {
        float velocity = 0.0;

        if ((1.0*index)/commandRate <= tramp)
                velocity = (amplitude*index)/commandRate;
        else if ((1.0*index)/commandRate <= (tramp + duration))
                velocity = amplitude/fabs(amplitude)*ssVelocity;
        else if ((1.0*index)/commandRate <= (3*tramp + duration))
                velocity = amplitude/(fabs(amplitude))*ssVelocity -amplitude*(index -
index1)/commandRate;
  else if ((1.0*index)/commandRate <= (3*tramp + 2*duration))
    velocity = -amplitude/fabs(amplitude)*ssVelocity;
```

```
  else if ((1.0*index)/commandRate <= (4*tramp + 2*duration))
    velocity = -amplitude/(fabs(amplitude))*ssVelocity + amplitude*(index - index2)/commandRate;

        return velocity;
        }

void VelstpTG::getParametersDisplaySize(UI_REGION& size) {
        if (size.right < 45)
                size.right = 45;
        size.bottom += 5;
        }


void VelstpTG::getParameters(int rate,int modal) {
        commandRate = rate;

        // Create an edit form.
        VelstpEditForm *form = new VelstpEditForm(this,rate,modal);

        *form
                + new UIW_BORDER
                + new UIW_TITLE(myName)
                + new UIW_SYSTEM_BUTTON
                + new UIW_PROMPT(2,1,"Acceleration (g)",WOF_NO_FLAGS)
                + new UIW_NUMBER(30,1,8,&acceleration,NULL,NMF_NO_FLAGS,

WOF_AUTO_CLEAR|WOF_NO_ALLOCATE_DATA|WOF_BORDER,
                                                VelstpEditForm::validateAccel)
                + new UIW_PROMPT(2,2,"Steady State Velocity (m/s)",WOF_NO_FLAGS)
                + new UIW_NUMBER(30,2,8,&ssVelocity,NULL,NMF_NO_FLAGS,

WOF_AUTO_CLEAR|WOF_NO_ALLOCATE_DATA|WOF_BORDER,
                                                VelstpEditForm::validatessVelocity)
                + new UIW_PROMPT(2,3,"Steady State Duration (sec)",WOF_NO_FLAGS)
                + new UIW_NUMBER(30,3,8,&duration,NULL,NMF_NO_FLAGS,

WOF_AUTO_CLEAR|WOF_NO_ALLOCATE_DATA|WOF_BORDER,
                                                VelstpEditForm::validateDuration)
                + new UIW_BUTTON(18,4,4,"Ok",BTF_NO_FLAGS,WOF_BORDER,
                                                VelstpEditForm::generateFunction);

        // Give it to the window manager.
        *_windowManager + form;
        }

void VelstpTG::getHeaderDisplaySize(UI_REGION& size) {
        AbstractTG::getHeaderDisplaySize(size);
        if (size.right < 72)
                size.right = 72;
        size.bottom += 5;
        }

void VelstpTG::displayHeader(UIW_WINDOW *window,int& left, int& top) {
        AbstractTG::displayHeader(window,left,top);
```

```
        *window
                + new UIW_PROMPT(left,top+1,"Acceleration (g)",WOF_NO_FLAGS)
                + new UIW_NUMBER(left+25,top+1,10,&acceleration,NULL,NMF_NO _FLAGS,

WOF_NON_SELECTABLE|WOF_BORDER)
                + new UIW_PROMPT(left,top+2,"Steady State Velocity (m/s)",WOF_NO_FLAGS)
                + new UIW_NUMBER(left+25,top+2,10,&ssVelocity,NULL,NMF_NO_F LAGS,

WOF_NON_SELECTABLE|WOF_BORDER)
                + new UIW_PROMPT(left,top+3,"Duration (s)",WOF_NO_FLAGS)
                + new UIW_NUMBER(left+25,top+3,10,&duration,NULL,NMF_NO_FL AGS,

WOF_NON_SELECTABLE|WOF_BORDER)
                + new UIW_PROMPT(left,top+4,"Ramp Duration (s)",WOF_NO_FLAGS)
                + new UIW_NUMBER(left+25,top+4,10,&tramp,NULL,NMF_NO_FLAG S,

WOF_NON_SELECTABLE|WOF_BORDER);

        top += 3;

        }

void VelstpTG::dumpHeader(char *name,FILE *f) {
        AbstractTG::dumpHeader(name,f);
        fprintf(f,"Acceleration: %6.3f g    Velocity: %7.4f Hz\n",acceleration,
                                ssVelocity);
        fprintf(f,"Amplitude:   %6.3f m/s  Ramp 1/2 Cycles: %d\n\n",amplitude,
                        rampHalfCycles);
        }
```

```
////////////////////////////////////////////////////////////////////////
// Title:   Sled - Functions
// Author:  Karla A. Polutchko
// Date:    April, 1993
// $Revision:  1.0  $
//
// Contents
//
// Description
//
// Copyright (C) 1991 Payload Systems Inc.  All Rights Reserved
////////////////////////////////////////////////////////////////////////
// $Log:  C:/ey1/sled/vcs/velstptg.hpv  $
//
//   Rev 1.0   16 Nov 1991 19:17:44   rsg
// Bug fixes for bugs encountered during Zinc switch
//
//   Rev 1.7.1.2   28 May 1991 14:30:00   rsg
// Incremental updates.
//
//   Rev 1.7.1.1   13 May 1991 16:03:54   rsg
// Debugged trajectory generators.
//
//   Rev 1.7.1.0   08 May 1991 13:05:10   rsg
// Incremental updates.
//
//   Rev 1.7   24 Apr 1991 13:33:34   rsg
// Incremental updates.
//
//   Rev 1.6   24 Apr 1991 08:16:58   rsg
// Incremental updates.
//
//   Rev 1.5   22 Apr 1991 08:39:28   rsg
// Incremental updates.
//
//   Rev 1.4   09 Apr 1991 14:56:58   rsg
// Deleted derivation of AbstractTG from UIW_WINDOW.
//
//   Rev 1.3   09 Apr 1991 10:28:54   rsg
// Documentation fixups.
//
//   Rev 1.2   09 Apr 1991 09:31:36   rsg
// Documentation update.
//
//   Rev 1.1   09 Apr 1991 08:54:26   rsg
// Incremental update.
////////////////////////////////////////////////////////////////////////

#ifndef  VELSTPTG_HPP
#define  VELSTPTG_HPP

// Interface Dependencies -------------------------------------------------

#ifndef   UI_WIN_HPP
```

```
#include <ui_win.hpp>
#endif

#ifndef __STDIO_H
#include <stdio.h>
#endif

#ifndef  ABSTRAJG_HPP
#include "abstrajg.hpp"
#endif

// End Interface Dependencies ----------------------------------------------

// Implementation Dependencies ---------------------------------------------

// End Implementation Dependencies -----------------------------------------

class VelstpTG : public AbstractTG {
public:
        VelstpTG();
        ~VelstpTG();

        AbstractTG *dup() { return new VelstpTG(); }

        int readHeader(const char *filename);
        void writeHeader(const char *filename);

        void dumpHeader(char *name,FILE *f);

        float generateCommand(long index);
        void generateTrajectory(const char *filename);

        void getParametersDisplaySize(UI_REGION& size);
        void getParameters(int rate,int modal);

        void getHeaderDisplaySize(UI_REGION& size);
        void displayHeader(UIW_WINDOW *window,int& left, int& top);

        float generateCommand(int phase,long index);

        int verifyAcceleration(float &max);
        int verifyssVelocity(float &max);
        int verifyDuration();
        int verifyParameters();

        int getWidth();// { return 36; }
        int getHeight();// { return 11; }


        float ssVelocity;
  float duration;
        float acceleration;
        float amplitude;
  float tramp;
```

```
    float rampHalfCycles;
    long index1;
    long index2;
        };
#endif
```

```
////////////////////////////////////////////////////////////////////////
// Title:   Sled - Functions
// Author:  Karla Polutchko
// Date:    November, 1991
// $Revision:   1.0  $
//
// Contents
//
// Description
//
// Copyright (C) 1991 Payload Systems Inc.  All Rights Reserved
////////////////////////////////////////////////////////////////////////
// $Log:   C:/ey1/sled/vcs/steptg.cpv  $
//
//   Rev 1.0   16 Nov 1991 19:17:50   rsg
// Bug fixes for bugs encountered during Zinc switch
////////////////////////////////////////////////////////////////////////

// Interface Dependencies -------------------------------------------------

#ifndef  STEPTG_HPP
#include "steptg.hpp"
#endif

// End Interface Dependencies ---------------------------------------------

// Implementation Dependencies --------------------------------------------

#ifndef __MATH_H
#include <math.h>
#endif

#ifndef __STDIO_H
#include <stdio.h>
#endif

#ifndef __STRING_H
#include <string.h>
#endif

#ifndef  DISPVARS_HPP
#include "dispvars.hpp"
#endif

#ifndef  SLEDCONV_HPP
#include "sledconv.hpp"
#endif

#ifndef  TRAJEDIT_HPP
#include "trajedit.hpp"
#endif

// End Implementation Dependencies ----------------------------------------
```

```
class StepEditForm : public TrajEditForm {
public:
        StepEditForm(StepTG *traj,int rate,int flag);

        static int validateAccel(void *item, int ccode);
        static int validateFrequency(void *item, int ccode);
        static int validateHalfCycles(void *item, int ccode);

private:
        int doValidateAccel(void *item, int ccode);
        int doValidateFrequency(void *item, int ccode);
        int doValidateHalfCycles(void *item, int ccode);
        };

StepEditForm::StepEditForm(StepTG *traj,int rate,int flag) :
                TrajEditForm(traj,rate,3,3,36,7,flag,0) {
        }

int StepEditForm::validateAccel(void *item,int ccode) {
        UIW_NUMBER *number = (UIW_NUMBER *)item;
        return (((StepEditForm *)number->parent)->doValidateAccel(item, ccode));
        }

int StepEditForm::doValidateAccel(void *item, int ccode) {
        if (ccode == S_CURRENT)
                return (0);

        UIW_NUMBER *field = (UIW_NUMBER *)item;
        float value = *(float *)field->DataGet();
        StepEditForm *me = (StepEditForm *)(((UIW_NUMBER *)item)->parent);
        StepTG *mine = (StepTG *)me->myTraj;
        float max;

        if (mine->verifyAcceleration(max)) {
                _errorSystem->ReportError(field->windowManager, -1,
                        "%f is not valid.  The absolute value must be greater than 0.0, but"
                        " less than %f", value,accelToG(max));
                return (-1);
                }
        else
                return 0;
        }

int StepEditForm::validateFrequency(void *item,int ccode) {
        UIW_NUMBER *number = (UIW_NUMBER *)item;
        return (((StepEditForm *)number->parent)->doValidateFrequency(item, ccode));
        }

int StepEditForm::doValidateFrequency(void *item,int ccode) {
        if (ccode == S_CURRENT)
                return (0);

        UIW_NUMBER *field = (UIW_NUMBER *)item;
        float value = *(float *)field->DataGet();
```

```
        StepEditForm *me = (StepEditForm *)(((UIW_NUMBER *)item)->parent);
        StepTG *mine = (StepTG *)me->myTraj;
        float min;


        if (mine->verifyFrequency(min)) {
                _errorSystem->ReportError(field->windowManager, -1,
                        "%f is not valid.  The value must be greater than %f, but less than"
                        " %f", value,min,getMaximumFrequency());
                return (-1);
                }
        else
                return 0;
        }

int StepEditForm::validateHalfCycles(void *item,int ccode) {
        UIW_NUMBER *number = (UIW_NUMBER *)item;
        return (((StepEditForm *)number->parent)->doValidateHalfCycles(item, ccode));
        }

int StepEditForm::doValidateHalfCycles(void *item,int ccode) {
        if (ccode == S_CURRENT)
                return (0);

        UIW_NUMBER *field = (UIW_NUMBER *)item;
        int value = *(int *)field->DataGet();

        if (value >= 0 && value < 100)
                return 0;
        else {
                _errorSystem->ReportError(field->windowManager, 0,
                        "%d is not valid.  The value must be at least 0, but less than 100",
                        value,100);
                return (-1);
                }
        }


StepTG::StepTG() : AbstractTG() {
        strcpy(myName,"Damped Step");
        frequency = 1.0;
        amplitude = 0.0;
        acceleration = 0.1;
        rampHalfCycles = 0;
        validAxis = Sled;
        }

StepTG::~StepTG() {
        }

int StepTG::readHeader(const char *filename) {
        FILE *f;

        // First, read the data of our ancestor(s).
```

```
        if (AbstractTG::readHeader(filename))
                return 1;

        // Open the file for reading. Note that an existing file is assumed.
        f = fopen(filename,"rb");

        // Seek past our ancestor(s) data. Note the true data size of the our
        // ancestor(s) is two less that the size of our immediate ancestor.
        fseek(f,sizeof(AbstractTG)-2,SEEK_SET);

        // Read our portion of the header. To do this, we must find our data,
        // which is located after our ancestor. The size to read is the
        // difference between our size and that of our ancestor.
        char *ptr = (char *)this;
        ptr += sizeof(AbstractTG);
        int size = sizeof(StepTG)-sizeof(AbstractTG);
        fread(ptr,size,1,f);

        // Close the file
        fclose(f);
        return 0;
        }

void StepTG::writeHeader(const char *filename) {
        FILE *f;

        // First, write the data of our ancestor(s).
        AbstractTG::writeHeader(filename);

        // Open the file for writing. Note that an existing file is assumed.
        f = fopen(filename,"rb+");

        // Seek past our ancestor(s) data. Note the true data size of the our
        // ancestor(s) is two less that the size of our immediate ancestor.
        fseek(f,sizeof(AbstractTG)-2,SEEK_SET);

        // Write our portion of the header. To do this, we must find our data,
        // which is located after our ancestor. The size to write is the
        // difference between our size and that of our ancestor.
        char *ptr = (char *)this;
        ptr += sizeof(AbstractTG);
        int size = sizeof(StepTG)-sizeof(AbstractTG);
        fwrite(ptr,size,1,f);
        // Close the file
  fclose(f);
        }

int StepTG::verifyFrequency(float &min) {
        min = sqrt(fabs(gToAccel(acceleration))/(4*PI*(getTrackLength()-0.1)) );

        if (frequency < min || frequency > getMaximumFrequency())
                return 1;// Invalid.
        else
                return 0;// Okay
```

```
	}

int StepTG::verifyAcceleration(float &max) {
	max = (getTrackLength()-0.1)*4*PI*frequency*frequency;

	if (max > getMaximumAccel())
		max = getMaximumAccel();

	if (fabs(acceleration) == 0.0 || fabs(acceleration) > accelToG(max))
		return 1;// Invalid.
	else
		return 0;// Okay.
	}

int StepTG::verifyParameters() {
	int error = 0;

	float temp;
	error = verifyAcceleration(temp);
	error += verifyFrequency(temp);

	if (rampHalfCycles < 0)
		error += 1;

	// Calculate our derived parameters.
	if (!error) {
		amplitude = gToAccel(acceleration)/(2*PI*frequency);

		numberCommands[0] = (long)(0.5 +

	rampHalfCycles*commandRate/(2*frequency));
		numberCommands[1] = (long)(commandRate/frequency + 0.5);
		numberCommands[2] = numberCommands[0];
		}
	else {
		amplitude = 0.0;
		numberCommands[0] = numberCommands[1] = numberCommands[2] = 0;
		}
	return error;
	}

float StepTG::generateCommand(int phase,long index) {
//	float velocity = amplitude*(1-cos(index*2*PI*frequency/commandRate));
//	switch (phase) {
//		case 0:
//			// Note that while rampHalfCycles may be zero, the following division
//			// will not be called, because numberCommands[0] will also be 0, and
//			// thus this function won't be called. The same applies in case 2.
//			velocity = (velocity*index)/numberCommands[phase];
//			if (rampHalfCycles & 1)
//				velocity = -velocity;
//			return velocity;
//		case 1:
//			return velocity;
```

```
//                  case 2:
//                          velocity -= (velocity*index)/numberCommands[phase];
//                          return velocity;
//    }

        if (phase != 1)
                return 0.0;
        else
                return amplitude*(1-cos(index*2*PI/numberCommands[1]));
        }

void StepTG::getParameters(int rate,int modal) {
        commandRate = rate;

        // Create an edit form.
        StepEditForm *form = new StepEditForm(this,rate,modal);

        *form
                + new UIW_BORDER
                + new UIW_TITLE(myName)
                + new UIW_SYSTEM_BUTTON
                + new UIW_PROMPT(2,1,"Acceleration (g)",WOF_NO_FLAGS)
                + new UIW_NUMBER(22,1,10,&acceleration,NULL,NMF_NO_FLAGS,

WOF_AUTO_CLEAR|WOF_NO_ALLOCATE_DATA|WOF_BORDER,
                                                        StepEditForm::validateAccel)
                + new UIW_PROMPT(2,2,"Frequency (Hz)",WOF_NO_FLAGS)
                + new UIW_NUMBER(18,2,10,&frequency,NULL,NMF_NO_FLAGS,

WOF_AUTO_CLEAR|WOF_NO_ALLOCATE_DATA|WOF_BORDER,
                                                        StepEditForm::validateFrequency)
                + new UIW_PROMPT(2,3,"Ramp 1/2 cycles",WOF_NO_FLAGS)
                + new UIW_NUMBER(18,3,5,&rampHalfCycles,NULL,NMF_NO_FLAGS,

WOF_AUTO_CLEAR|WOF_NO_ALLOCATE_DATA|WOF_BORDER,
                                                        StepEditForm::validateHalfCycles)
                + new UIW_BUTTON(16,4,4,"Ok",BTF_NO_FLAGS,WOF_BORDER,
                                                        StepEditForm::generateFunction);

        // Give it to the window manager.
        *_windowManager + form;
        }

void StepTG::getHeaderDisplaySize(UI_REGION& size) {
        AbstractTG::getHeaderDisplaySize(size);
        if (size.right < 72)
                size.right = 72;
        size.bottom += 3;
        }

void StepTG::displayHeader(UIW_WINDOW *window,int& left, int& top) {
        AbstractTG::displayHeader(window,left,top);
        *window
                + new UIW_PROMPT(left,top+1,"Acceleration (g)",WOF_NO_FLAGS)
```

```
                + new UIW_NUMBER(left+17,top+1,10,&acceleration,NULL,NMF_NO _FLAGS,

WOF_NON_SELECTABLE|WOF_BORDER)
                + new UIW_PROMPT(left,top+2,"Frequency (Hz)",WOF_NO_FLAGS)
                + new UIW_NUMBER(left+17,top+2,10,&frequency,NULL,NMF_NO_F LAGS,

WOF_NON_SELECTABLE|WOF_BORDER)
                + new UIW_PROMPT(left+29,top+1,"Amplitude (m/s)",WOF_NO_FLAGS)
                + new UIW_NUMBER(left+45,top+1,10,&amplitude,NULL,NMF_NO_F LAGS,

WOF_NON_SELECTABLE|WOF_BORDER)
                + new UIW_PROMPT(left+29,top+2,"Ramp 1/2 cycles",WOF_NO_FLAGS)
                + new UIW_NUMBER(left+45,top+2,5,&rampHalfCycles,NULL,NMF_ NO_FLAGS,

WOF_NON_SELECTABLE|WOF_BORDER);

        top += 3;
        }

void StepTG::dumpHeader(char *name,FILE *f) {
        AbstractTG::dumpHeader(name,f);
        fprintf(f,"Acceleration: %6.3f g    Frequency: %7.4f Hz\n",acceleration,
                                frequency);
        fprintf(f,"Amplitude:    %6.3f m/s  Ramp 1/2 Cycles: %d\n\n",amplitude,
                        rampHalfCycles);
        }
```

```
////////////////////////////////////////////////////////////////////////
// Title:   Sled - Functions
// Author:  Karla Polutchko
// Date:    November, 1991
// $Revision:   1.0  $
//
// Contents
//
// Description
//
// Copyright (C) 1991 Payload Systems Inc.  All Rights Reserved
////////////////////////////////////////////////////////////////////////
// $Log:   C:/ey1/sled/vcs/steptg.hpv  $
//
//   Rev 1.0   16 Nov 1991 19:17:54   rsg
// Bug fixes for bugs encountered during Zinc switch
//
//   Rev 1.7.1.2   28 May 1991 14:30:00   rsg
// Incremental updates.
//
//   Rev 1.7.1.1   13 May 1991 16:03:54   rsg
// Debugged trajectory generators.
//
//   Rev 1.7.1.0   08 May 1991 13:05:10   rsg
// Incremental updates.
//
//   Rev 1.7   24 Apr 1991 13:33:34   rsg
// Incremental updates.
//
//   Rev 1.6   24 Apr 1991 08:16:58   rsg
// Incremental updates.
//
//   Rev 1.5   22 Apr 1991 08:39:28   rsg
// Incremental updates.
//
//   Rev 1.4   09 Apr 1991 14:56:58   rsg
// Deleted derivation of AbstractTG from UIW_WINDOW.
//
//   Rev 1.3   09 Apr 1991 10:28:54   rsg
// Documentation fixups.
//
//   Rev 1.2   09 Apr 1991 09:31:36   rsg
// Documentation update.
//
//   Rev 1.1   09 Apr 1991 08:54:26   rsg
// Incremental update.
////////////////////////////////////////////////////////////////////////

#ifndef  STEPTG_HPP
#define  STEPTG_HPP

// Interface Dependencies -------------------------------------------------

#ifndef   UI_WIN_HPP
```

```
#include <ui_win.hpp>
#endif

#ifndef __STDIO_H
#include <stdio.h>
#endif

#ifndef  ABSTRAJG_HPP
#include "abstrajg.hpp"
#endif

// End Interface Dependencies ----------------------------------------------

// Implementation Dependencies ---------------------------------------------

// End Implementation Dependencies -----------------------------------------

class StepTG : public AbstractTG {
public:
        StepTG();
        ~StepTG();

        AbstractTG *dup() { return new StepTG(); }

        int readHeader(const char *filename);
        void writeHeader(const char *filename);

        void dumpHeader(char *name,FILE *f);

        float generateCommand(long index);
        void generateTrajectory(const char *filename);

        void getParameters(int rate,int modal);

        void getHeaderDisplaySize(UI_REGION& size);
        void displayHeader(UIW_WINDOW *window,int& left, int& top);

        float generateCommand(int phase,long index);

        int verifyAcceleration(float &max);
        int verifyFrequency(float &min);
        int verifyParameters();

        int getWidth();// { return 36; }
        int getHeight();// { return 8; }

        float frequency;
        float acceleration;
        float amplitude;
        int rampHalfCycles;
        };
#endif
```

APPENDIX H: HUMAN USE DOCUMENTATION

This appendix contains the informed consent statement that was signed by each subject prior to any testing.

INFORMED CONSENT STATEMENT

You have been asked to participate in an experiment aimed at better understanding the workings of the inner ear and the eyes. Your participation is purely voluntary and you are free to withdraw at any time. In the experiment, you will be seated and strapped into a linear acceleration device (sled) either in the upright or supine position and asked to look straight ahead. The sled may or may not move. You may be asked to look at a moving display and you may be asked to indicate your perception of movement. At the end of the experiment, you may be asked to discuss how you perceived various stages of the experiment.

Please feel free to ask any questions you care to about the experiment. When the sled is moving, you can stop it at any time by pushing the "panic button". If at any time, you experience any discomfort or have any misgivings about continuing the experiment, we ask that you tell us - we will stop the test at any time you like.

Your eye movements will be measured using soft contact lens search coils, the most accurate method available today. The cornea of your eye will be anaesthetized using eye drops. The anesthetic used is Proparacain. If you have any allergies to this anesthetic, you should withdraw from participation in this experiment. The lens, in which a tiny search coil is embedded, will be applied to your eye. This will be worn for no longer than thirty minutes. Before application and after removal, your eyes will be examined by an optometrist to rule out any possible corneal abrasion. There is a less than one percent chance that the wearing of the soft contact lens may cause a slight corneal abrasion. If this does occur, a prophylactic antibiotic and covering will be applied overnight. Finally, we may also video your eye movements, using a small video camera with a low level light source.

"In the unlikely event of injury resulting from participation in this research, I understand that medical treatment will be available from the MIT Medical Department, including first aid, emergency treatment and follow-up care as needed, and that my insurance carrier may be billed for the cost of such treatment. However, no compensation can be provided for medical care apart from the foregoing. I further understand that making such medical treatment available, or providing it, does not imply that such injury is the investigator's fault. I also understand that by my participation in this study I am not waiving any of my legal rights (for more information, call the Institute's Insurance and Legal Affairs Office at 253-2822). I understand that I may also contact the Chairman of the Committee on the Use of Humans as Experimental Subjects, Dr. H. Walter Jones (MIT E23-389, 253-6787), "

I have been informed as to the procedures and purpose of this experiment and agree to participate.

Signed:_____

Date:_____

Witness:_____